

# Targeting pro-survival cell signaling pathways in multiple myeloma

personalized treatment for newly-diagnosed  
and relapsed-refractory patients

Ingrid Spaan





# **Targeting pro-survival cell signaling pathways in multiple myeloma**

personalized treatment for newly-diagnosed and relapsed-refractory patients

**Ingrid Spaan**

Targeting pro-survival cell signaling pathways in multiple myeloma,  
personalized treatment for newly-diagnosed and relapsed-refractory patients

Thesis with a summary in Dutch, Utrecht University

© Ingrid Spaan, 2022

The copyrights of published articles have been transferred to the respective journals. No part of this thesis may be reproduced, stored in a retrieval system, or transmitted in any other form or by any means, without permission of the author.

ISBN: 978-94-6458-127-0

Cover and layout design: Publiss | [www.publiss.nl](http://www.publiss.nl)

Printed by: Ridderprint | [www.ridderprint.nl](http://www.ridderprint.nl)

Printing of this thesis was financially supported by Infection & Immunity Utrecht.



# **Targeting pro-survival cell signaling pathways in multiple myeloma**

personalized treatment for newly-diagnosed  
and relapsed-refractory patients

## **Signaleringscascades die celoverleving bevorderen als therapeutisch target in multipel myeloom**

behandeling op maat voor nieuw-gediagnosticeerde  
en recidiverend-refractaire ziekte

(met een samenvatting in het Nederlands)

### **Proefschrift**

ter verkrijging van de graad van doctor aan de  
Universiteit Utrecht op gezag van de  
rector magnificus, prof.dr. H.R.B.M. Kummeling,  
ingevolge het besluit van het college voor promoties  
in het openbaar te verdedigen op

donderdag 28 april 2022 des middags te 12.15 uur

door

### **Ingrid Spaan**

geboren op 24 mei 1990  
te Doetinchem

**Promotoren:**

Prof. dr. M.C. Minnema

Prof. dr. M.M. Maurice

**Copromotoren:**

Dr. V. Peperzak

Dr. R.A.P. Raijmakers

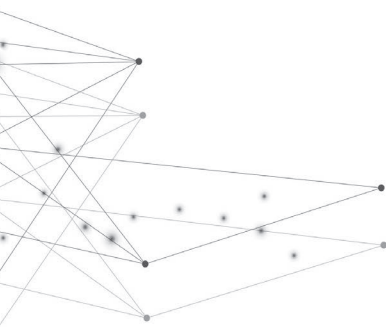
# TABLE OF CONTENTS

<b>Chapter 1</b>	General introduction and thesis outline	7
<b>Chapter 2</b>	From MGUS to multiple myeloma, a paradigm for clonal evolution of premalignant cells	21
<b>Chapter 3</b>	Wnt signaling in multiple myeloma: a central player in disease with therapeutic potential	41
<b>Chapter 4</b>	Dual targeting of Wnt signaling promotes cell death of primary multiple myeloma cells by inhibition of the unfolded protein response pathway	79
<b>Chapter 5</b>	Direct P70S6K1 inhibition to replace dexamethasone in synergistic combination with MCL-1 inhibition in multiple myeloma	97
<b>Chapter 6</b>	Multiple myeloma relapse is associated with increased NF $\kappa$ B pathway activity and upregulation of the pro-survival BCL-2 protein BFL-1	141
<b>Chapter 7</b>	Bortezomib resistance in multiple myeloma is independent of PIM kinases	163
<b>Chapter 8</b>	Targeting pro-survival cell signaling pathways as personalized treatment for multiple myeloma: summary and future perspectives	181
<b>Appendices</b>	Nederlandse samenvatting (summary in Dutch)	198
	Dankwoord (acknowledgements)	205
	Curriculum vitae	210
	List of publications	211



# Chapter one

General introduction  
and thesis outline



# 1 | CELL SIGNALING PATHWAYS - COMMUNICATION IS KEY

Cell signaling is the molecular mechanism by which cells communicate. It allows cells to perceive and relay information, generally coming from signals of the extracellular environment, and to respond to this information by modifying their cellular physiology [1]. All core cellular processes are regulated by signaling pathways, including cell growth and metabolism, proliferation, differentiation, migration, and programmed cell death. In healthy multicellular organisms, these pathways culminate to ensure proper organization of cells into complex tissues during development, and to maintain tissue homeostasis during adult life [2]. Deregulation of cell signaling pathways can disturb this balance and is associated with diverse human pathologies. For example, insufficient cell proliferation can lead to loss of tissue integrity and contribute to degenerative diseases and aging, while unrestrained cell proliferation increases the risk of cancer [3,4].

## 1.1 | Cell signals to convey information

Cell signaling pathways can be categorized based on the main process they affect, and include developmental pathways (e.g. Wnt signaling), growth factor pathways (e.g. PI3K-Akt signaling), immune pathways (e.g. NF $\kappa$ B signaling), and hormonal nuclear receptor pathways [5]. In healthy cells, activation of signaling pathways is usually initiated by signals, which can be of diverse composition and include proteins (e.g. cytokines, chemokines, and growth factors), small molecules like lipids (e.g. steroid hormones), and dissolved gasses (e.g. NO) [6]. The majority of cells are capable of both receiving signals and emitting signals by exocytosis into the extracellular environment. Some signals, including hormones, are soluble and can operate over long distances in the body by endocrine signaling (Figure 1). But in most instances signals act locally, and can influence neighboring cells by paracrine signaling, or directly affect the cells that produced the signal by means of autocrine signaling [6].

## 1.2 | Signal transduction cascades – receive, transduce, adapt

Signals are capable of activating cell signaling cascades in the target cell, by binding as a ligand to their cognate receptor (Figure 2). Most signals are hydrophilic and bind to receptors that are present on external target cell surfaces. Only a few signals, like steroid hormones, are hydrophobic and small enough to diffuse over the target cell plasma membrane and bind to intracellular receptors [6]. Ligand binding induces a conformational change in the receptor, resulting in activation of

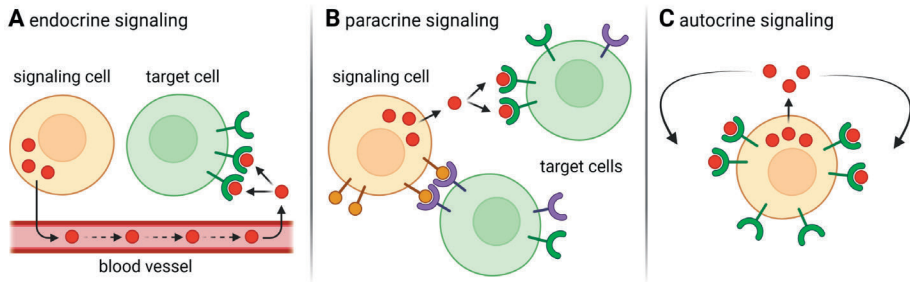


**Figure 1 | Cells communicate via endocrine, paracrine, and autocrine cell signaling.** Cells use different forms of signaling for their communication. This communication starts by the signaling cells, which emit signals into the extracellular environment. When these signals bind to a receptor, the information is received by target cells. (A) In endocrine signaling, small soluble signals can travel over long distances in the body to reach target cells, for example by traveling via the bloodstream. (B) In paracrine signaling, signaling cells use soluble or membrane-bound signals to communicate with neighboring cells. (C) Alternatively, signaling cells can respond to their own emitted signals via autocrine signaling.

its signal transduction capacity [7]. Cell surface receptors can be categorized based on their mechanism of signal transduction. G-protein-coupled receptors and receptor tyrosine kinases are present on the majority of cells, and use intracellular molecules for subsequent signal transduction. These molecules comprise small second messengers and large intracellular signaling proteins that relay signals into the cells [8,9].

Intracellular signal transduction pathways are not just simple mechanisms by which signals are passed on straightforward into target cells. Instead, they are complex functional networks that can amplify signals, transduce the type of signaling, integrate signals coming from multiple signaling pathways, or, the other way around, spread signals from one to multiple signal transduction cascades [10]. The mechanism by which many of these intracellular signaling proteins function, resembles that of a molecular switch; in most instances, when a signal is received the protein switches “on” to a conformational active state, until it is switched “off” again to a conformational inactive state [7]. Proteins that act like molecular switches often cycle between their “on” and “off” conformation through phosphorylation (Figure 3). Active protein kinases phosphorylate these target switches by adding phosphate groups, and thereby induce a conformational change that, in most instances, results in activation of the target. Protein phosphatases remove the added phosphate groups, and thereby reset the target switch to its original status [11]. The majority of kinases recognize and phosphorylate serine and threonine target motifs, and are therefore referred to as serine/threonine kinases.

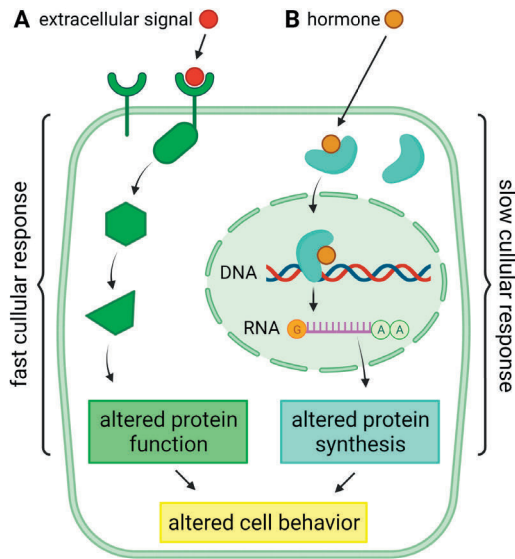


**Figure 2 | Signal transduction cascades adapt target cell behavior in response to cell signals.** Signal transduction cascades are activated when a cell signal binds to their cognate receptor at the target cells. (A) Extracellular signals bind to transmembrane receptors. The resulting conformational change in the receptor intracellular domain leads to activation of the downstream signaling cascade. If the appropriate signal response only requires adaptation of proteins that are already present in the cell, the cellular response can be accomplished within seconds to minutes after receiving the signal. (B) A subset of small hydrophobic signals, like hormones, diffuse over the target cell plasma membrane and bind to intracellular receptors. These receptors shuttle from the cytosol to the nucleus where they bind to the DNA of target genes. This DNA is transcribed to RNA, which forms the blueprint for synthesis of new proteins. The cascade from cell signal to protein synthesis takes multiple hours. Ultimately, both altered protein function and altered protein synthesis result in altered cell behavior.

Effector molecules form the final stages of signal transduction pathways and are the proteins that alter target cell behavior in response to the received signal. Depending on the type of signal and the response that is required, effects on cell behavior can be accomplished within seconds or after several hours [12]. For example, adaptation of cell motility usually requires direct alterations of proteins that are present in the cell, and can therefore be fast [13]. More intricate processes like cell division require changes in gene expression by transcription factors, and therefore take more time [14]. In adult homeostasis, effects of cell signaling are usually transient. Cell signaling intermediates are often subjected to continuous turnover, meaning that their activity will decrease shortly after the initiation signal fades. In highly regulated pathways, signaling cascades typically activate one or multiple negative feedback loops to ensure a short-lived response [15].



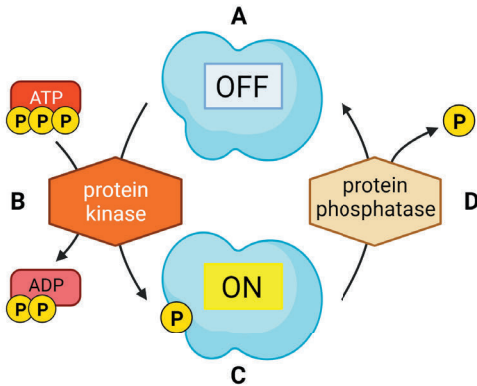


**Figure 3 | Cell signaling cascades are managed by protein kinases and protein phosphatases.** The intracellular signaling proteins that are responsible for relay of the cell signal into target cells are often regulated by phosphorylation. (A) When there is no signal present, the target protein is not phosphorylated and is stable in its inactive conformation. (B) When a signal activates the cascade, an activated upstream protein kinase phosphorylates the target protein. ATP is used as a source of phosphate groups by the kinase, and is converted to ADP in the process. (C) Phosphorylation results in an activating conformational change of the target protein, and thereby switches the target protein on. (D) When the signaling cascade becomes inactive, a protein phosphatase removes the phosphate group of the target protein, and the target protein switches back to its inactive conformation as in A. Although not shown, a subset of intracellular signaling proteins are inhibited by phosphorylation, and activated by dephosphorylation.

### 1.3 | Cell signaling determines cell fate

In complex organisms like humans, cells are subjected to a myriad of signals in all sorts of combinations. Still, cells should respond in a selective way that is appropriate for the specific cell type they belong to. How cells respond to these signals depends on many different factors, including the presence and cellular localization of receptors and signaling mediators, concentrations of activating and/or inhibitory signals, the target genes that are regulated by transcription factors, epigenetics, and cross-talk between multiple cell signaling pathways. Ultimately, all this information is integrated and determines cell fate [16]. For the majority of human cells, a specific combination of survival signals and an appropriate pro-survival response is required to maintain cell viability. Deprivation of pro-survival signaling can activate the cell's suicide program, called intrinsic apoptosis [17].

## **2 | CELL SIGNALING PATHWAYS IN CANCER – OPPORTUNITIES FOR TARGETING**

In healthy multicellular organisms, cells use signaling pathways to communicate and coordinate their behavior. This means that they grow, divide, differentiate, rest, and die as needed to serve the best interest of the organism. After differentiation, highly specialized cells permanently stop dividing. In tissues that are subjected to continuous cell turnover (e.g. the epithelial lining of the intestines, and the white blood cells of the hematopoietic system), a pool of stem and precursor cells is available to continuously replenish the required cell types. All these cells are continuously subjected to events that damage their DNA, and this damaged DNA can be passed on to their progeny by means of cell division. If the damaged DNA affects genomic regions that encode for genes, or regions that (in)directly regulate gene expression, this can result in altered cell behavior and thereby threaten organismal homeostasis. Therefore, cells are equipped with signaling pathways that act as safety mechanisms. These cell signaling pathways can sense DNA damage and halt cell cycle to repair it, or ensure that cells permanently stop dividing by inducing cellular senescence or by committing suicide via apoptosis, when the DNA damage cannot be fixed. This intrinsic safety mechanism is complemented by an extrinsic anti-cancer mechanism, called cancer immune surveillance. This refers to the process in which cells of the immune system continuously scan the organism for malignant cells, and eliminate these cancerous cells, for example by inducing cell death, to prevent cancer outgrowth [18].

### **2.1 | Tumorigenesis and hallmarks of cancer**

Cancer cells do no longer follow the critically defined rules to cooperate, but compete for survival; they reproduce uncontrollably and spread beyond their boundaries to invade the territory of other cells and tissues. The transformation of a healthy cell into a malignant cancer cell is a multi-step process that is referred to as tumorigenesis [19]. During these successive steps, cells acquire DNA damage that can vary from single point mutations to gains or losses of complete chromosomes. If these genetic lesions provide a selective advantage, it will promote tumorigenic behavior of the cell and its descendants, and thereby facilitate progressive outgrowth and dominance of this malignant cell clone (Figure 4) [20]. The initial genetic lesions that drive tumorigenesis and facilitate uncontrollable growth of cancer cells, frequently activate oncogenes or inhibit tumor-suppressor genes [21]. The process is accelerated by the genomic instability that cancer cells typically

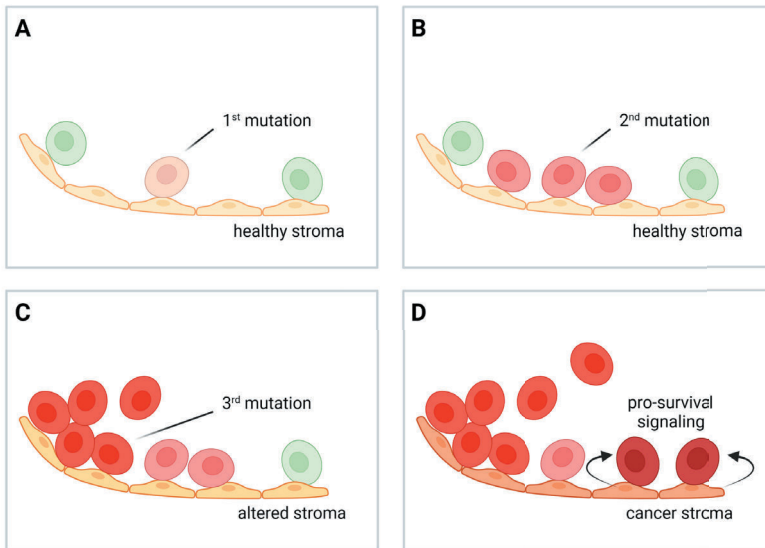


**Figure 4 | Tumorigenesis is a multi-step process driven by clonal evolution.** The transformation from a healthy to a malignant cell requires multiple rounds of genetic mutation and clonal selection. (A) The first mutation that marks the onset of tumorigenesis often results in activation of an oncogene or suppression of a tumor-suppressor gene, and thereby provides an advantage for the mutated cell. (B) This mutated cell divides more rapidly or survives more readily and thereby gives rise to a clone of cells. At some point, one of the descendants of the first clone acquires a second mutation that confers an extra advantage. (C) The descending cells with 2 tumor-promoting mutations divide and/or survive more readily than the surrounding healthy cells and the cells with only 1 tumor-promoting mutation, and thereby give rise to a larger second clone of malignant cells. (D) When tumorigenesis continues, the malignant cells start to infiltrate into the surrounding cell and tissue territories, and oppress other cells. Malignant cells also intensify their interaction with the cancer cell microenvironment, including the stromal cells. These cells provide additional pro-survival signals that make the malignant cells thrive.

acquire during tumorigenesis. By compromising the signaling systems that sense and repair DNA damage and/or by preventing cells to become senescent or undergo apoptosis in response to unreparable DNA damage, the cancer cell mutability is increased [22].

The alterations in cell physiology that mark the progression to malignancy are summarized as the hallmarks of cancer. These hallmarks comprise sustained proliferative signaling, evasion of growth suppressors, enabling replicative immortality, resistance to cell death, inducing angiogenesis, activation of invasion and metastasis, deregulation of cellular energetics, avoiding immune destruction, genome instability and mutation, and tumor-promoting inflammation [23]. These

hallmarks are not solely acquired by genetic lesions resulting in altered cell-autonomous behavior, but are also facilitated by the cancer cell microenvironment. Non-malignant cells in this microenvironment can be instructed by the cancer cells to facilitate its pro-tumorigenic behavior. For example, by secreting signals that stimulate growth of the cancer cells, or by providing a niche that protect cancer cells from elimination by drugs or by cells of the immune system [24].

## **2.2 | Targeted therapy and small-molecule inhibitors**

Irrespective whether cancer cell behavior is initiated by intrinsic genetic lesions and/or by interactions with the extrinsic microenvironment, the resulting effects on cancer cell physiology are induced by modulation of the cell signaling pathways that normally ensure homeostasis [25]. In fact, many mediators of cell signaling pathways have been identified because their function was frequently altered in cancer cells. These affected mechanisms include increased availability of signaling ligands, receptor overexpression or mutation, increased or permanent activation of protein kinases, altered gene regulatory protein activity, and inhibition of negative feedback loops. The observation that cancer cells alter specific cell signaling pathways, and rely or become addicted to those active pathways for survival, formed the basis for development of targeted therapy [26]. By specifically interfering with those mechanisms, targeted therapy aims to potently affect malignant cells, while sparing healthy cells. This should result in less off-target toxicity, compared to the systemic side-effects induced by conventional chemotherapy [27].

Targeted drugs can be categorized based on their size (Figure 5). Macro-molecules include monoclonal antibodies and antibody-drug conjugates which bind to targets on external cell surfaces (e.g. the extracellular domains of cell surface receptors). In contrast, small-molecule inhibitors penetrate the cells to target intracellular cell signaling mediators [28]. Inhibition of intracellular signaling mediators by small-molecules can be accomplished via multiple mechanisms. For enzymatic proteins, including kinases, these mechanisms include competitive binding to the ATP-binding pocket, or binding of the small-molecule to the allosteric pocket to directly inhibit enzymatic activity [29]. Alternatively, small-molecules can bind to a hydrophobic pocket to induce a conformational change or to directly inhibit protein-protein interactions [30]. The tyrosine kinase inhibitor imatinib/Gleevec was the first small-molecule targeted therapy approved by the US Food and Drug Administration (FDA) in 2001 [31]. Since then, at least 89 small molecules have been approved as targeted anti-cancer drugs, and a multitude of small-molecule inhibitors are in clinical trials, representing the major shift in anti-cancer treatment that took place during the past two decades [32].

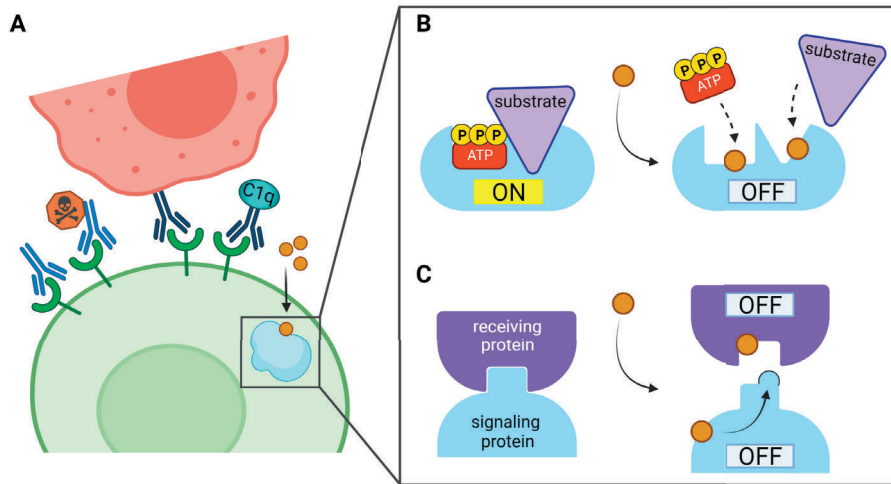


**Figure 5 | Targeted therapy of cancer cells.** The development of targeted drugs significantly improved cancer treatment options during the last two decades. (A) Target therapies can consist of macro-molecules, like monoclonal antibodies, that can bind to any antigen present on the external cell surface, for example receptor extracellular domains. From left to right: 1, the antibody can directly induce cell death of the cancer cell by blocking the availability of pro-survival signaling receptors; 2, the antibody can be coupled to a toxin to create an antibody-drug conjugate that potentiates cell death induction; 3, with its Fc-tail, the antibody can recruit immune cells that subsequently kill the cancer cell by direct or indirect mechanisms; 4, alternatively, the antibody F- tail can activate the complement system to induce immune-mediated cell death; 5, small-molecule inhibitors diffuse over the target cell plasma membrane to inhibit intracellular signaling proteins. (B) When the small-molecule target is an enzyme, the enzymatic function can be inhibited by binding to the ATP pocket, or by directly interfering with the substrate-binding site. (C) Small-molecules can also disrupt protein-protein interactions by inducing a conformational change in one of the interaction partners, or by directly interfering with the protein-binding pocket.

### 3 | SCOPE AND OUTLINE OF THIS THESIS

The translational research described in this thesis focuses on pro-survival cell signaling pathways as therapeutic targets for personalized treatment of newly-diagnosed and relapsed-refractory multiple myeloma patients. Multiple myeloma (MM) is a plasma cell malignancy of which curative treatment is frequently hampered by drug toxicity, development of drug resistance, and relapse of refractory disease. The aim of this research is to identify which pro-survival cell signaling pathways are active in MM, and if these pro-survival pathways can be targeted by currently available drugs to improve therapeutic options. Additional research included in this thesis was performed to determine if and how cell signaling pathways are altered by current standard-of-care treatments, if potential therapy-induced alterations of pro-survival cell signaling pathways contribute to

the development of drug resistance, and if targeting of these pro-survival pathways is a potential strategy to overcome drug resistance in MM.

**Chapter 2** introduces the stepwise transformation of a healthy plasma cell, via the pre-malignant MGUS phase, to the overt malignancy MM. This process is dependent on both the acquisition of genomic lesions and the development of a permissive bone marrow microenvironment. This review summarizes the molecular processes underlying MM tumorigenesis, including the cell signaling pathways that are affected, and the implications of clonal evolution.

The Wnt pathway is one of cell signaling pathways that is affected in MM pathogenesis. **Chapter 3** reviews the relevance of deregulated Wnt signaling in MM by summarizing the effects of Wnt signaling on osteolytic bone disease, and by discussing recent studies that shed light on the role of intrinsic Wnt signaling for survival of MM plasma cells. Based on this literature study, I hypothesize that targeting of pro-survival Wnt signaling has therapeutic potential for MM. This hypothesis is addressed in **chapter 4**, in which the effects of combined canonical and non-canonical Wnt pathway inhibition in cell lines and primary patient samples of MM is studied.

Pro-survival cell signaling pathways can be specifically targeted by small-molecule inhibitors, but can also be affected as part of the mechanism-of-action of conventional drugs. **Chapter 5** unravels the molecular mechanism by which the standard-of-care glucocorticoid dexamethasone inhibits pro-survival signaling, and that underlies its synergistic drug effect with the novel pro-apoptotic MCL-1 inhibitor. A subgroup of MM patients is ineligible or insensitive to dexamethasone, due to toxicity and drug resistance. Therefore, the replacement of dexamethasone by a more targeted small-molecule inhibitor of the pro-survival pathway is assessed, to induce apoptosis of MM plasma cells in combination with MCL-1 inhibition.

Although the combination of conventional therapy and novel agents improved MM treatment, the majority of patients suffer from disease relapse and become refractory to therapy. In **chapter 6**, a novel computational model is used to study if MM disease relapse is associated with altered pro-survival cell signaling that could form a potential target for therapy. This research is extended in **chapter 7**, in which we study MM cell lines that are either sensitive or resistant to standard-of-care proteasome inhibitors. The aim is to identify pro-survival cell signaling pathways that are affected by proteasome inhibition, and to assess if these pathways can be targeted to re-sensitize resistant cells to therapy.

In **chapter 8**, I summarize the main results and insights obtained during these studies, and discuss the future perspectives of targeting pro-survival cell signaling pathways as personalized treatment for MM.

## REFERENCES

1. Iqbal, J.; Sun, L.; Zaidi, M. Complexity in signal transduction. *Ann N Y Acad Sci* 2010, *1192*, 238-244, doi:10.1111/j.1749-6632.2010.05388.x.
2. Mian, I.S.; Rose, C. Communication theory and multicellular biology. *Integr Biol (Camb)* 2011, *3*, 350-367, doi:10.1039/c0ib00117a.
3. Carlson, M.E.; Silva, H.S.; Conboy, I.M. Aging of signal transduction pathways, and pathology. *Exp Cell Res* 2008, *314*, 1951-1961, doi:10.1016/j.yexcr.2008.03.017.
4. Sever, R.; Brugge, J.S. Signal transduction in cancer. *Cold Spring Harb Perspect Med* 2015, *5*, doi:10.1101/cshperspect.a006098.
5. van de Stolpe, A.; Holtzer, L.; van Ooijen, H.; Inda, M.A.; Verhaegh, W. Enabling precision medicine by unravelling disease pathophysiology: quantifying signal transduction pathway activity across cell and tissue types. *Sci Rep* 2019, *9*, 1603, doi:10.1038/s41598-018-38179-x.
6. Nair, A.; Chauhan, P.; Saha, B.; Kubatzky, K.F. Conceptual Evolution of Cell Signaling. *Int J Mol Sci* 2019, *20*, doi:10.3390/ijms20133292.
7. Tompa, P. The principle of conformational signaling. *Chem Soc Rev* 2016, *45*, 4252-4284, doi:10.1039/c6cs00011h.
8. Hilger, D.; Masureel, M.; Kobilka, B.K. Structure and dynamics of GPCR signaling complexes. *Nat Struct Mol Biol* 2018, *25*, 4-12, doi:10.1038/s41594-017-0011-7.
9. Trenker, R.; Jura, N. Receptor tyrosine kinase activation: From the ligand perspective. *Curr Opin Cell Biol* 2020, *63*, 174-185, doi:10.1016/jceb.2020.01.016.
10. Kholodenko, B.N. Cell-signalling dynamics in time and space. *Nat Rev Mol Cell Biol* 2006, *7*, 165-176, doi:10.1038/nrm1838.
11. Gelens, L.; Qian, J.; Bollen, M.; Saurin, A.T. The Importance of Kinase-Phosphatase Integration: Lessons from Mitosis. *Trends Cell Biol* 2018, *28*, 6-21, doi:10.1016/j.tcb.2017.09.005.
12. Di-Bella, J.P.; Colman-Lerner, A.; Ventura, A.C. Properties of cell signaling pathways and gene expression systems operating far from steady-state. *Sci Rep* 2018, *8*, 17035, doi:10.1038/s41598-018-34766-0.
13. Devreotes, P.; Horwitz, A.R. Signaling networks that regulate cell migration. *Cold Spring Harb Perspect Biol* 2015, *7*, a005959, doi:10.1101/cshperspect.a005959.
14. Liu, Y.; Chen, S.; Wang, S.; Soares, F.; Fischer, M.; Meng, F.; Du, Z.; Lin, C.; Meyer, C.; DeCaprio, J.A.; et al. Transcriptional landscape of the human cell cycle. *Proc Natl Acad Sci U S A* 2017, *114*, 3473-3478, doi:10.1073/pnas.1617636114.
15. Lemmon, M.A.; Freed, D.M.; Schlessinger, J.; Kiyatkin, A. The Dark Side of Cell Signaling: Positive Roles for Negative Regulators. *Cell* 2016, *164*, 1172-1184, doi:10.1016/j.cell.2016.02.047.
16. Pawson, C.T.; Scott, J.D. Signal integration through blending, bolstering and bifurcating of intracellular information. *Nat Struct Mol Biol* 2010, *17*, 653-658, doi:10.1038/nsmb.1843.
17. Kearney, C.J.; Martin, S.J. Competition for growth factors: a lot more death with a little less Aktion. *Cell Death Differ* 2013, *20*, 1291-1292, doi:10.1038/cdd.2013.99.



18. Vesely, M.D.; Kershaw, M.H.; Schreiber, R.D.; Smyth, M.J. Natural innate and adaptive immunity to cancer. *Annu Rev Immunol* 2011, 29, 235-271, doi:10.1146/annurev-immunol-031210-101324.
19. Hanahan, D.; Weinberg, R.A. The hallmarks of cancer. *Cell* 2000, 100, 57-70, doi:10.1016/s0092-8674(00)81683-9.
20. Greaves, M.; Maley, C.C. Clonal evolution in cancer. *Nature* 2012, 481, 306-313, doi:10.1038/nature10762.
21. Vogelstein, B.; Papadopoulos, N.; Velculescu, V.E.; Zhou, S.; Diaz, L.A., Jr.; Kinzler, K.W. Cancer genome landscapes. *Science* 2013, 339, 1546-1558, doi:10.1126/science.1235122.
22. Kloeber, J.A.; Lou, Z. Critical DNA damaging pathways in tumorigenesis. *Semin Cancer Biol* 2021, doi:10.1016/j.semcancer.2021.04.012.
23. Hanahan, D.; Weinberg, R.A. Hallmarks of cancer: the next generation. *Cell* 2011, 144, 646-674, doi:10.1016/j.cell.2011.02.013.
24. Whiteside, T.L. The tumor microenvironment and its role in promoting tumor growth. *Oncogene* 2008, 27, 5904-5912, doi:10.1038/onc.2008.271.
25. Martin, G.S. Cell signaling and cancer. *Cancer Cell* 2003, 4, 167-174, doi:10.1016/s1535-6108(03)00216-2.
26. Vivanco, I. Targeting molecular addictions in cancer. *Br J Cancer* 2014, 111, 2033-2038, doi:10.1038/bjc.2014.461.
27. Bedard, P.L.; Hyman, D.M.; Davids, M.S.; Siu, L.L. Small molecules, big impact: 20 years of targeted therapy in oncology. *Lancet* 2020, 395, 1078-1088, doi:10.1016/s0140-6736(20)30164-1.
28. Lee, Y.T.; Tan, Y.J.; Oon, C.E. Molecular targeted therapy: Treating cancer with specificity. *Eur J Pharmacol* 2018, 834, 188-196, doi:10.1016/j.ejphar.2018.07.034.
29. Wu, P.; Nielsen, T.E.; Clausen, M.H. Small-molecule kinase inhibitors: an analysis of FDA-approved drugs. *Drug Discov Today* 2016, 21, 5-10, doi:10.1016/j.drudis.2015.07.008.
30. Arkin, M.R.; Tang, Y.; Wells, J.A. Small-molecule inhibitors of protein-protein interactions: progressing toward the reality. *Chem Biol* 2014, 21, 1102-1114, doi:10.1016/j.chembiol.2014.09.001.
31. Savage, D.G.; Antman, K.H. Imatinib mesylate--a new oral targeted therapy. *N Engl J Med* 2002, 346, 683-693, doi:10.1056/NEJMra013339.
32. Zhong, L.; Li, Y.; Xiong, L.; Wang, W.; Wu, M.; Yuan, T.; Yang, W.; Tian, C.; Miao, Z.; Wang, T.; et al. Small molecules in targeted cancer therapy: advances, challenges, and future perspectives. *Signal Transduct Target Ther* 2021, 6, 201, doi:10.1038/s41392-021-00572-w.



# Chapter two

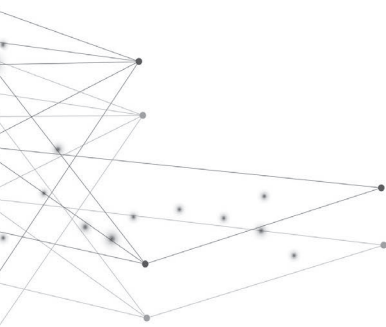
## From MGUS to multiple myeloma, a paradigm for clonal evolution of premalignant cells

Niels van Nieuwenhuijzen<sup>1,2</sup>, Ingrid Spaan<sup>1</sup>  
Reinier Raymakers<sup>2</sup>, and Victor Peperzak<sup>1</sup>

<sup>1</sup> Laboratory of Translational Immunology,  
University Medical Center Utrecht,  
Utrecht, the Netherlands

<sup>2</sup> Department of Hematology,  
University Medical Center Utrecht,  
Utrecht, the Netherlands

*Cancer Research, 2018; 78(10):2449*



## ABSTRACT

Multiple myeloma (MM) is a treatable, but incurable, malignancy of plasma cells (PC) in the bone marrow (BM). It represents the final stage in a continuum of PC dyscrasias and is consistently preceded by a premalignant phase termed monoclonal gammopathy of undetermined significance (MGUS). The existence of this well-defined premalignant phase provides the opportunity to study clonal evolution of a premalignant condition into overt cancer. Unravelling the mechanisms of malignant transformation of PC could enable early identification of MGUS patients at high risk of progression and may point to novel therapeutic targets, thereby possibly delaying or preventing malignant transformation. The MGUS-to-MM progression requires multiple genomic events and the establishment of a permissive BM microenvironment, although it is generally not clear if the various microenvironmental events are causes or consequences of disease progression. Advances in gene-sequencing techniques and the use of serial paired analyses have allowed for a more specific identification of driver lesions. The challenge in cancer biology is to identify and target those lesions that confer selective advantage and thereby drive evolution of a premalignant clone. Here, we review recent advances in the understanding of malignant transformation of MGUS to MM.

## 1 | INTRODUCTION

Multiple myeloma (MM) is a malignant growth of clonal plasma cells (PC) primarily located in the bone marrow (BM) and is the second most common hematological malignancy [1]. Survival improved with the introduction of immunomodulatory drugs and proteasome inhibitors in the previous decade, but the current 5-year survival rate does not exceed 50% [2]. MM represents the most important clinical manifestation in a spectrum of PC dyscrasias and it is unique in that it is consistently preceded by a premalignant phase, termed monoclonal gammopathy of undetermined significance (MGUS) [3,4]. MGUS is defined as the presence of monoclonal immunoglobulin (Ig) in blood or urine (M protein), less than 10% clonal PC in the BM and the absence of myeloma-related end-organ damage [4,5]. MGUS is found in 3% of the population above the age of 50 and its prevalence increases with age [5]. The rate of progression from MGUS to MM is approximately 1% of patients per year, which means that the majority of MGUS patients are never diagnosed nor progress to a symptomatic malignancy [3,5]. Some patients develop an intermediate disease stage between MGUS and MM, termed smoldering multiple myeloma (SMM). SMM patients have an M protein level of more than

30 grams per liter and over 10% clonal PC in the BM, but are asymptomatic with regard to myeloma-related end-organ damage. 10% of SMM patients progress to MM during the first five years after diagnosis, after which the rate of progression declines [6]. In the final stages of the disease MM cells can acquire the ability to grow outside the BM, which is referred to as extramedullary MM or PC leukemia (Figure 1).

Malignant transformation of a healthy cell into a cancer cell is a multistep and multifaceted process. Advances in cancer biology have stipulated that tumors are genetically heterogeneous and that clonal evolution drives tumor progression [7]. The existence of a well-defined clinical spectrum of premalignant states that defines MM provides the rare opportunity to study premalignant cells in their clonal evolution, much like the progression of colorectal adenomas into colorectal carcinomas has served as a model for the malignant transformation of epithelial cells [8]. However, predicting progression of MGUS/SMM to MM remains a challenge. Unravelling the mechanisms of malignant transformation of PC might enable early identification of MGUS patients at a high risk of progression and may point to novel early and more precise therapeutic targets. Here, we review recent advances in the understanding of MGUS-to-MM progression, as these represent two ends on the spectrum between a benign premalignant condition and an overt cancer. We show that multiple mechanisms of MGUS-to-MM progression are universal principles in malignant evolution.

## 2 | FROM PLASMA CELL TO MGUS

MGUS is believed to arise from post-germinal center (GC) PC that have regained their capacity for proliferation. Two mostly non-overlapping modes of pathogenesis can be discriminated that are thought to initiate PC proliferation. First, approximately half of both MGUS and MM cases are hyperdiploid, usually with extra copies of the odd-numbered chromosomes (typically 3,5,7,9,11,15,19,21) [9]. Second, most non-hyperdiploid MGUS/MM cases are characterized by a primary translocation involving the Ig heavy-chain gene at 14q32 [4,10]. The majority of translocations go by unnoticed, except when an oncogene is juxtaposed near the potent Ig-enhancers, most often involving cyclin D genes, *MAF* transcription factors, or *NSD2/FGFR3* [10]. Less than 10% of patients are non-hyperdiploid and are negative for known translocations [11]. Dysregulation of the G1/S cell cycle transition via overexpression of a cyclin D gene is present in both hyperdiploid and non-hyperdiploid MM and is thought to be a common and early initiating event in MM pathogenesis [12]. Overexpression of cyclin D genes has been reported in various

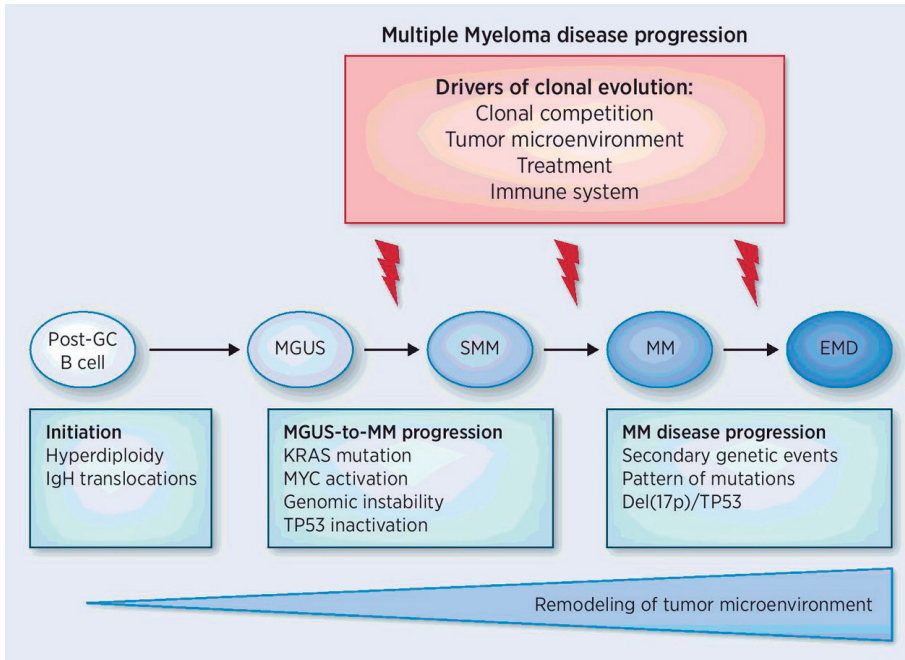


**Figure 1 | Clonal evolution of plasma cell dyscrasias.** The malignant transformation of a post-germinal center B cell or plasma cell into monoclonal gammopathy of undetermined significance (MGUS) and subsequently multiple myeloma (MM) requires both an initiating event and multiple secondary genetic events. Initiating events are broadly subdivided into IgH-translocations or hyperdiploidy. Copy-number variants, mutations and epigenetic changes are secondary genetic events that characterize progression. In the continuum of disease stages, genetic lesions accumulate in the tumor clone. Progression of MGUS to MM is promoted by a remodeling of the bone marrow microenvironment. Clonal evolution is driven by clonal competition, the tumor microenvironment, immune cells and therapy regimens. SMM, smoldering multiple myeloma; EMD, extramedullary disease.

solid tumors, including breast cancer and melanoma, but overexpression is especially implicated in the pathogenesis of lymphomas and is for example considered to be the molecular hallmark of mantle cell lymphoma [13,14].

Since the development of tumors generally requires multiple hits, overexpression of cyclin D alone, either due to hyperdiploidy or IgH translocations, is not sufficient for progression from MGUS to MM [4]. However, these primary genetic events in myelomagenesis do have prognostic relevance upon diagnosis of MM. Generally, hyperdiploid MM is associated with a better prognosis than MM with a primary Ig translocation. Translocations  $t(14;16)$  and  $t(4;14)$  especially confer a high risk of fulminant disease (Table 1). Within the premalignant PC clone, secondary translocations, copy-number variants (CNVs), oncogenic mutations, epigenetic

alterations and microenvironmental changes drive clonal evolution from MGUS to MM. Together, primary and secondary events produce the cancer phenotype and are implicated in a differential disease course, prognosis and therapy response [4].

**Table 1 | Intrinsic drivers of malignant progression from MGUS-to-MM and their prognosis in MM.**

Type of event	Potential oncogenes	Frequency in MGUS (%)	Frequency in MM (%)	Prognosis in newly-diagnosed MM
<b>Initiating events</b>				
t(11;14)	<i>CCND1</i>	12	19	+
t(12;14)	<i>CCND2</i>	<1	<1	0
t(6;14)	<i>CCND3</i>	0	1	0
t(14;16)	<i>MAF</i>	3	4	-
t(14;20)	<i>MAFB</i>	3	1	*
t(4;14)	<i>NSD2/FGFR3</i>	9	13	-
hyperdiploidy	°	50	55	+
<b>Secondary cytogenetic aberrations</b>				
Amp 1q	<i>CKS1B, ILF2</i>	25	50	-
Del(1p)	<i>CDKN2C, FAM46C</i>	6	40	-
Del(13)	<i>RB1</i>	30 <sup>†</sup>	70	‡
Del(17p)	<i>TP53</i>	1	12	-
translocations 8q24	<i>MYC</i>	3-4	20	-
<b>Oncogenic pathways</b>				
MAPK activation	<i>NRAS</i>	36	33	
	<i>KRAS</i>	<1	33	
	<i>BRAF</i>	27	19	
MYC dysregulation	<i>MYC</i>	<1	67	-
Constitutive NFκB activation	<i>TRAF6, CYLD</i>	<1	20	

\* t(14;20) is associated with poor prognosis in MM, but correlates with quiescence in MGUS. ° The exact oncogenic mechanism of hyperdiploidy remains to be elucidated, but cyclin D1 is consistently overexpressed. † The frequency of del(13) in MGUS is dependent on concomitant presence of specific primary IgH translocations. It is high in patients with t(4;14), t(14;16), and t(14;20), but low in t(11;14) and t(6;14). ‡ The prognosis of del(13) depends on the presence of specific IgH translocations. - denotes a negative impact on survival, + denotes a positive impact on survival and 0 denotes no reported impact on survival. Source references: [18, 36, 37, 41, 46].

### 3 | COPY-NUMBER VARIANTS

The number of mutations in cancer varies from only several to many hundreds, whereby a hematopoietic malignancy generally has less mutations than a solid tumor. Most of the genetic events that are present in cancer are neutral mutations that have arisen from genetic instability – so-called passenger lesions. The challenge is to identify and consequently target those genetic changes that confer a selective advantage to the cancer clone and thereby drive malignant evolution. A genetic event is considered a driver lesion when (i) its associated gene(s) are recognized to play a role in malignant pathophysiology, (ii) the lesion itself has been associated with clonal expansion and (iii) the frequency of the event exceeds the normal background mutation rate [15]. Results from knockdown and overexpression studies of genes in animal and *in vitro* models confer extra weight to the status of potential driver lesions. Most of the studies discussed here compare genetics of PC from healthy donors and MGUS, SMM or MM patients, occasionally accompanied by animal studies. A more reliable method to identify driver lesions is the use of sequential, paired MGUS-MM or SMM-MM samples from the same patient that has progressed from one disease stage to another. We have tried to include these studies when possible, however the number of completed studies and included patients is limited. In addition, MGUS and SMM patients are often pooled. The advent of liquid biopsies will allow for more convenient sequential sampling in the near future [16].

Variations of gene copy numbers are common to both solid and hematological cancers and are believed to contribute to tumor growth. Examining several thousand cancer copy-number profiles revealed 158 regions of somatic CNVs that are altered at significant frequency across multiple cancer types [17]. CNVs are more frequently found in MM than MGUS and there is a greater median number of CNVs in each MM versus MGUS patient [18]. Although CNVs can be merely passenger events, some of them have an effect on MGUS progression and MM prognosis [11]. In addition, sequential sequencing of MGUS/SMM patients that progressed to MM and MGUS/SMM patients that did not progress to MM within follow-up, revealed a greater number of CNVs at baseline in patients that progressed to MM [19]. Consistently, loss-of-heterozygosity was much more frequent at baseline in patients that were about to progress. This study suggests that the degree of genomic instability is a driver of MGUS-to-MM progression itself. CNVs are generally more frequent in patients with non-hyperdiploid MM, contributing to the worse prognosis of these patients [11].

Amplification of the chromosomal region 1q21 is the most common chromosomal gain reported in MM, often occurring concomitantly with the deletion of 1p.



Gain of 1q21 is more frequent in MM (40%) than in MGUS (25%) (Table 1) [18]. It is associated with a higher risk of progression to MM in MGUS patients and with a poor prognosis in MM patients [11]. Similarly, the transformation from a myeloproliferative neoplasm to acute myeloid leukemia is associated with amplification of chromosome 1q [20]. Remarkably, 30% of the GEP-70 gene set that has been shown to predict high-risk disease in MM maps to chromosome 1 [21]. Despite its high prevalence and relation with high-risk disease, the oncogenes on 1q21 responsible for malignant transformation are subject to debate. *CKS1B* was originally proposed to be involved in disease progression, although a more recent study found no association between *CKS1B* expression and clinical parameters [22]. Recently, *ILF2* was identified as a potential oncogene in 1q21 amplification [23]. *ILF2* is involved in DNA damage repair and its overexpression enables genomic instability, thereby enhancing MM cell survival and drug resistance. In line, inhibition of *ILF2* resulted in an increased frequency of apoptosis in MM cells with a 1q21 amplification, designating *ILF2* as potential therapeutic target [23]. In addition, multiple other candidates are located on 1q21 that may contribute to disease progression, including *MCL1* and *IL6R* that are both known to play a role in MM cell survival [4].

The frequency of 1p deletions in MM is approximately 30%, opposed to only 6% in MGUS (Table 1) [18]. A majority of patients have interstitial deletions, but removal of the entire short arm has also been observed. Two tumor suppressor genes linked to the pathogenesis of del(1p) are *CDKN2C* and *FAM46C* [24]. Deletion of 1p32.3 (*CDKN2C*) increases from MGUS (5%) to MM (15%) and is associated with adverse overall survival [25]. 1p12 (*FAM46C*) was found to be deleted in 19% of MM patients and also confers an impaired risk of survival. Its frequency of deletion in MGUS is unknown [24].

Half of MM patients show loss of the complete chromosome 13, but it is more common in non-hyperdiploid MM (66%) than in hyperdiploid MM (34%) (Table 1) [26]. Its frequency in MGUS is dependent on the concomitant presence of specific IgH-translocations. Del(13) is almost equally frequent in MGUS and MM with t(4;14) and t(14;16) translocations, suggesting that it is an early event in these patients [26]. In contrast, del(13) is practically absent in MGUS with t(6;14) and t(11;14) translocations but common in MM patients carrying either translocation (40% and 67%, respectively), implicating del(13) in MGUS-to-MM progression [26]. The retinoblastoma (*RB1*) tumor suppressor gene is located on chromosome 13. Inactivation of *RB1* is associated with both initiation and progression of many solid and hematopoietic cancers, including the progression to invasive growth in prostate and bladder cancer and the progression to a blast crisis in chronic myeloid leukemia [27]. Experiments demonstrated that complete loss of *RB1* increased

proliferation in both MM cell lines and murine GC B cells, but was unable to initiate malignant transformation by itself [28]. Therefore, loss-of-heterozygosity of *RB1* in case of del(13) could potentially contribute to MGUS-to-MM progression, although other genes located on chromosome 13 may also be involved.

Deletions of the short arm of chromosome 17 are uncommon in MGUS, but 12% prevalence was reported in untreated MM (Table 1) [18]. Multiple studies have confirmed that del(17p) in MM is associated with extramedullary disease and with very poor prognosis [11]. The prototypical tumor suppressor gene *TP53* is located on the short arm of chromosome 17 and functions to halt cell-cycle progression and/or induce apoptosis in case of intracellular stress following DNA damage. Additionally, more recent studies have recognized that p53 modulates its tumor suppressing effects via other mechanisms, including regulation of metabolism and autophagy [29]. Approximately half of all malignancies are affected by a *TP53* mutation, making it the most common genetic change in human cancers [29]. Mutations of *TP53* have been reported in 37% of MM patients with del(17p), but are absent in cases without the deletion. This suggests that haploinsufficiency of *TP53* may be important for disease progression directly, or that it increases the probability for loss or mutation of the remaining allele [30].

## 4 | RECURRENT MUTATIONS AND CELL SIGNALING PATHWAYS

With the advent of gene expression profiling (GEP), molecular subclasses were described for breast cancer based on distinctive interpatient expression of gene clusters. Subsequently, molecular subgroups were recognized in other cancers, including MM [31]. These molecular subgroups of MM were found to be already present in MGUS [32], which is in line with the finding that genetic differences between MGUS and MM are smaller than the differential gene expression between healthy PC and MGUS cells [33]. Similarly, serial whole-exome sequencing (WES) analyses of paired MGUS-MM or SMM-MM samples demonstrated that most somatic mutations are present before the onset of clinical MM [19,34,35]. Nevertheless, the genetic complexity increases as MGUS progresses to MM and the mutational load itself is associated with poor prognosis [36,37]. Eight driver genes that are recurrently mutated on progression from MGUS to MM have been identified using next-generation sequencing (NGS): *KRAS*, *NRAS*, *BRAF*, *TP53*, *CCND1*, *FAM46C*, *IRF4* and *LTB* [37]. A study using WES reported the additional involvement of *HIST1H1E* and *EGR1*, confirming the genetic heterogeneity of driver genes in MM [36]. These results correspond with studies showing that all tumors have a variable and increasing clonal heterogeneity during development [7]. In contrast, a more

recent study does mention that most frequent mutations including *NRAS*, *KRAS* and *HIS1TH1E* in MM are in fact already present in MGUS [35]. Oddly, in 20% of MM patients no mutations in any of the aforementioned driver genes were found, suggesting that currently unknown mechanisms play a role in MM pathogenesis in these patients [37]. Recent WES studies of paired MGUS-MM or SMM-MM patient samples confirmed the widespread intraclonal heterogeneity of MM [38]. In 10 patients, 82 different genes were gained or lost during progression of MGUS to MM. Beyond the previously identified driver genes, further potential genetic events of MGUS-to-MM progression that were identified in this study include *ICAM5*, *DUSP27*, *HERPUD1*, *NOD2* and *TOP2A* [38]. Surprisingly, the comparison of samples from MGUS/SMM patients that progressed to MM with samples from patients that did not progress revealed no difference in mutational load [19]. Additionally, de novo acquired mutations at progression to MM were rare in studies using paired SMM-MM samples specifically [34,35]. Although preliminary, these results indicate that the specific pattern of mutations drives MM disease progression, especially from SMM to MM. However, it needs to be mentioned that purification of PC using markers CD138 (and CD38) in abovementioned studies does not discriminate between healthy and (pre)malignant PC. Since healthy PC can constitute up to 2% of total leukocytes in the BM and MGUS never exceeds 10% there can be a substantial contamination of healthy PC in the MGUS fraction.

An important feature of malignant cells is their acquired independence from mitogenic signaling for cell proliferation, which is often achieved by constitutive activation of one of the cell signaling pathways. Whole-genome sequencing studies showed that 40-60% of MM patients have mutations in genes involved in the MAPK-pathway, making it the most frequently mutated pathway in MM [37]. Recent studies using NGS have shown that RAS protein family mutations accumulate during disease progression, which is in line with earlier GEP results that demonstrated increased expression of RAS proteins in MM compared to healthy PC. *NRAS* and *BRAF* mutations that result in their constitutive activation are found in both MGUS and MM cells, while for *KRAS* this is only the case in MM cells. Interestingly, it was reported that only *KRAS* mutations are associated with downstream pathway activation in MM, while *NRAS* mutations were not (Table 1) [39]. These findings with respect to the MAPK-pathway were recently confirmed by the aforementioned paired MGUS-MM WES. Combined, these results suggest a critical role for MAPK-pathway signaling – and specifically *KRAS* – in MGUS-to-MM progression.

Expression of *MYC* induces pleiotropic downstream effects that drive cell proliferation and is under strict regulation in healthy cells. The activation of *MYC* in cancer generally results from either constitutive activation of one of the

pathways regulating *MYC* expression, or through chromosomal amplifications or translocations, where the latter is more commonly seen in hematopoietic malignancies [40]. *MYC* rearrangements involving chromosome 8q24 were detected by FISH in 3% of MGUS and 15% of newly diagnosed MM patients, although a more recent study using comparative genomic hybridization found these rearrangements in almost 50% of MM cases [41]. GEP of *MYC* showed *MYC* activation in the majority of MM (67%), while little to no activation was demonstrated in healthy controls and MGUS (Table 1) [42]. Transgenic mice with constitutive overexpression of *MYC* in B cells develop post-GC PC tumors similar to human MM [42]. Suppression of the *MYC*-activating LIN28B/let-7 axis significantly reduced tumor growth and prolonged survival in a xenograft mouse model, thereby exposing a novel therapeutic target [43]. Most *MYC*-driven MM mouse models are generated on the C57BL/6 genetic background and *MYC* activation is generally believed to be less important in mice with a different genetic background. Nevertheless, enforced expression of *MYC*, together with IL-6, does result in the outgrowth of malignant PC in BALB/c mice [44]. However, it is questionable whether the level of *MYC* expression in these mouse models is comparable to the level of *MYC* expressed in MGUS/MM patients.

The NF- $\kappa$ B pathway regulates expression of many genes involved in inflammatory and immune responses. NF- $\kappa$ B activation in cancer is common and can result either from intrinsic mutations of NF- $\kappa$ B pathway-related genes or from extrinsic signals from the tumor microenvironment. Intrinsic activation is more commonly found in hematopoietic cancers, whereas activation of NF- $\kappa$ B by the microenvironment is required as an anti-apoptotic survival factor for various types of solid cancers that arise from chronic inflammation [45]. Ordinarily, the NF- $\kappa$ B pathway is activated by extrinsic signals from BM stromal cells in healthy PC, MGUS and most MM cells. However, 17% of untreated MM have mutations that constitutively activate part of the NF $\kappa$ B pathway (Table 1) [46]. Intrinsic activation of NF- $\kappa$ B makes MM cells less dependent on the BM microenvironment and thereby facilitates extramedullary progression. A recent study demonstrated that TRAF6, implicated in regulating NF $\kappa$ B and MAPK signaling, is significantly overexpressed in patients with active MM compared to MGUS [47]. Inhibition of TRAF6 using a TRAF6 dominant-negative peptide decreased NF- $\kappa$ B-related signaling, induced apoptosis of MM cells and reduced MM growth [47].

Transcriptional silencing of genes by DNA methylation is an important epigenetic method to regulate gene expression. Alterations in DNA methylation profiles are known to affect oncogenic pathways and are thought to play a role in tumorigenesis. Genome-wide hypomethylation was found to occur at the transition from MGUS to MM, accompanied by hypermethylation of specific tumor suppressor genes [48]. This aberrant methylation profile was shown to be a universal characteristic

for many types of cancer [49]. Global hypomethylation is believed to result in genomic instability and thereby facilitates chromosomal rearrangements, while hypermethylation of tumor suppressor genes has been associated with aberrant activation of Wnt and JAK/STAT3 signaling pathways in MM [50]. One study reported that methylation status regulates expression of only a few genes, challenging clinical relevance of DNA methylation in MM [51]. However, another study has shown that changes in methylation status of 195 tumor suppressor genes are significantly associated with adverse survival [52].

## 5 | CLINICAL PREDICTORS OF PROGRESSION

A number of clinical risk factors are recognized that allow stratification of the risk of MGUS-to-MM progression. These parameters do not provide an account for underlying causes of malignant progression, but have proven useful for predicting risk of progression in individual patients [53]. Important and easy to determine parameters are based on the size of the MGUS clone: both the percentage of BM PC and the baseline level and rate of increased serum M-protein level predict progression to MM [54,55]. Further risk factors include the heavy-chain isotype – whereby the risk of progression is most prevalent for IgD and greater for IgA/IgM MGUS than for IgG MGUS –, serum free light-chain (FLC) ratio, detection of focal lesions by MRI, and Bence Jones proteinuria [53]. Combining these parameters has led to the development of models predicting progression of MGUS to MM. The first model that was proposed uses the M-protein level, heavy-chain isotype and serum FLC ratio to stratify MGUS patients in four groups from low-risk to high-risk of progression over a 20-year disease course [56]. Two other models are based on the percentage of aberrant PC in the BM and either DNA aneuploidy or development of M-protein level, both stratifying MGUS patients in three risk groups at 5 and 7 years after diagnosis, respectively [54,57]. Similar models to predict risk of progression have been developed for SMM [32].

Many of the genetic events that have been discussed above impart an influence on an MGUS patient's risk of progression to MM (Figure 1). It was found that the aforementioned GEP-70 gene set not only predicts high-risk disease in MM, but also independently signifies a higher risk of MGUS-to-MM progression [32]. The combination of conventional clinical risk factors with genomic predictors of progression, such as the GEP-70 risk score, was used to identify new subsets of high-risk SMM patients that require earlier therapy [32]. Incorporation of genomic data in prediction models of MGUS progression should lead to more accurate stratification of high-risk MGUS patients in the near future. This may allow for specific and early treatment and may thereby delay or prevent clonal evolution of a premalignant lesion.

## 6 | TUMOR MICROENVIRONMENT IN MALIGNANT PROGRESSION

It has become increasingly clear that reciprocal interaction between tumor cells and the tumor microenvironment plays an essential role in the development of cancer [7]. In solid tumors, the establishment of tumor-associated stroma facilitates not only tumor growth and progression, but also invasive and metastatic growth [58]. Similar to healthy PC, MM cells initially depend on signals from the BM microenvironment for their survival [4]. Intricate interactions between MM cells and cells from the BM microenvironment play an important role in MM proliferation, survival, migration and drug resistance [4,59]. The nature and relevance of the microenvironment in MM has been described extensively elsewhere, including the important role of bone and immune cells in MM pathophysiology [60,61]. This is nicely illustrated by recent studies where MGUS cells were shown capable of progressive growth in mouse models, and that immune surveillance and extrinsic restraints from the endosteal niche are involved in MGUS dormancy [62,63]. Here, we will primarily discuss differences that have been found in BM stroma when comparing MGUS and MM patients. It is believed that malignant evolution of MGUS is mediated by structural and functional alterations of the tumor-associated stromal cells, making the BM microenvironment an active participant in malignant transformation and thus an interesting target for therapy in early disease stages [4,59-61,64] (Figure 1).

Tumor-associated stromal cells are active participants in structural and functional remodeling and constitutive activation of angiogenesis in a cancer microenvironment [58]. Endothelial cells (EC) in the microenvironment of solid tumors overexpress genes related to the extracellular matrix (ECM), proliferation, migration, and especially angiogenesis [58]. Similarly, GEP of BM EC in MGUS and MM patients revealed differential expression of 22 genes involved in resistance to apoptosis, ECM formation, bone remodeling, cell adhesion and angiogenesis, and thus implicates a functional transformation of BM EC in MGUS-to-MM progression [65].

A proteomic analysis of fibroblast-like cells and ECM demonstrated that ECM-proteins, ECM-receptors, and ECM-modulating enzymes are progressively up-regulated from MGUS to MM [59]. Two proteins, Annexin A2 (ANXA2) and Galectin-2 (LGALS2), were identified in the BM ECM of MM but were absent in BM from healthy donors or MGUS patients [59]. Remarkably, high expression of these proteins was associated with decreased overall survival, suggesting that remodeling of BM ECM contributes to a permissive tumor microenvironment [59].

Angiogenesis results in tumor growth via increased blood flow and a greater supply of nutrients to tumor cells and is widely recognized as vital to cancer progression [58]. Angiogenesis in the BM microenvironment was shown to increase during progression from MGUS to MM and is associated with poor prognosis and therapy resistance [66]. Endothelial progenitor cells (EPC) mediate angiogenesis in the BM microenvironment. It has been shown that levels of circulating EPC are significantly higher in MM compared to healthy subjects and MGUS patients [64]. Targeting EPC with a VEGFR2 antibody in mice effectively delayed MM growth only during early disease progression. Additionally, the BM microvessel density (MVD) in mice with spontaneous MM was twice as high as in mice with MGUS and strongly correlated with the level of monoclonal Ig in blood [67]. In line with these findings it was found that MVD in BM of MGUS patients who showed progression to MM at follow-up significantly increased compared to MVD of patients with MGUS that remained quiescent [67]. Since the FDA-approval of bevacizumab in 2004 many angiogenesis inhibitors, alone or in combination with other drugs, have been introduced for the treatment of a range of tumors. However, anti-angiogenic therapy, monotherapy especially, proves not to be as effective as was predicted [68]. Aforementioned results illustrate the need to further investigate anti-angiogenic drugs during early stages of malignant transformation.

## 7 | CONCLUDING REMARKS

The 5-year survival rate of MM patients does not exceed 50%, notwithstanding recent therapeutic advances [2]. Treatment of MGUS patients before progression to MM is currently not considered beneficial. The high degree of genetic and molecular heterogeneity makes it difficult to identify those patients who are at imminent risk of progression and to decide on a choice of therapy that outweighs the risks and costs. In an ongoing phase I clinical trial high-risk MGUS patients are being treated with anti-CD38 monoclonal antibody daratumumab, which, in contrast to chemotherapy, is believed to be non-mutagenic [69]. Further delineating the molecular mechanisms that drive malignant transformation may allow for a more precise definition of high-risk MGUS and may lead to prevention or delay of MM development by targeting specific signaling pathways involved in disease progression. The efficacy of targeting actionable mutations is hindered by clonal heterogeneity, highlighting further difficulties in finding appropriate therapeutic regimens.

Existence of the well-defined spectrum of disease stages that marks MM allows for research on the transformation of premalignant cells. Sequential paired MGUS-MM sequencing is an elegant method to study the genetics of MGUS-to-

MM progression and should become more convenient with liquid biopsies in the near future, yielding more precise data on the link between genomic events and malignant evolution [16]. Ideally, this could be extended to monitoring virtually any premalignant lesion in its progression towards overt cancer. Simultaneously, there is a need to further characterize remodeling events of the tumor microenvironment during early stages of cancer. Novel and precise targeting of the BM microenvironment in MGUS should abrogate the effect of stromal cells on tumor growth, survival and resistance to therapy, thereby preventing progression from MGUS to MM. Rapid advances of genomic techniques to study premalignant cells in their progression should enable identification and subsequent targeting of driver events during clonal evolution in MM and cancer in general.

## **ACKNOWLEDGEMENTS**

This work was supported by a Bas Mulder Award from the Dutch Cancer Foundation (KWF)/Alpe d'HuZes foundation (Number UU 2015-7663) to V. Peperzak and a project grant from the Dutch Cancer Foundation (KWF)/Alpe d'HuZes foundation (Number 11108) to V. Peperzak.



## REFERENCES

1. Siegel RL, Miller KD, Jemal A. Cancer Statistics, 2017. *CA Cancer J Clin.* 2017;67(1):7-30.
2. Howlader N, Noone A, Krapcho M, et al. SEER Cancer Statistics Review, 1975-2013, National Cancer Institute. Bethesda, MD. In:2016.
3. Landgren O, Kyle RA, Pfeiffer RM, et al. Monoclonal gammopathy of undetermined significance (MGUS) consistently precedes multiple myeloma: a prospective study. *Blood.* 2009;113(22):5412-5417.
4. Pawlyn C, Morgan GJ. Evolutionary biology of high-risk multiple myeloma. *Nat Rev Cancer.* 2017;17(9):543-556.
5. Kyle RA, Therneau TM, Rajkumar SV, et al. Prevalence of monoclonal gammopathy of undetermined significance. *N Engl J Med.* 2006;354(13):1362-1369.
6. Kyle RA, Remstein ED, Therneau TM, et al. Clinical course and prognosis of smoldering (asymptomatic) multiple myeloma. *N Engl J Med.* 2007;356(25):2582-2590.
7. Gupta RG, Somer RA. Intratumor Heterogeneity: Novel Approaches for Resolving Genomic Architecture and Clonal Evolution. *Mol Cancer Res.* 2017.
8. Strum WB. Colorectal Adenomas. *N Engl J Med.* 2016;375(4):389-390.
9. Smadja NV, Fruchart C, Isnard F, et al. Chromosomal analysis in multiple myeloma: cytogenetic evidence of two different diseases. *Leukemia.* 1998;12(6):960-969.
10. Fonseca R, Debes-Marun CS, Picken EB, et al. The recurrent IgH translocations are highly associated with nonhyperdiploid variant multiple myeloma. *Blood.* 2003;102(7):2562-2567.
11. Rajan AM, Rajkumar SV. Interpretation of cytogenetic results in multiple myeloma for clinical practice. *Blood Cancer J.* 2015;5:e365.
12. Bergsagel PL, Kuehl WM, Zhan F, Sawyer J, Barlogie B, Shaughnessy J. Cyclin D dysregulation: an early and unifying pathogenic event in multiple myeloma. *Blood.* 2005;106(1):296-303.
13. Vose JM. Mantle cell lymphoma: 2015 update on diagnosis, risk-stratification, and clinical management. *Am J Hematol.* 2015;90(8):739-745.
14. Musgrove EA, Caldon CE, Barraclough J, Stone A, Sutherland RL. Cyclin D as a therapeutic target in cancer. *Nat Rev Cancer.* 2011;11(8):558-572.
15. Greaves M, Maley CC. Clonal evolution in cancer. *Nature.* 2012;481(7381):306-313.
16. Mishima Y, Paiva B, Shi J, et al. The Mutational Landscape of Circulating Tumor Cells in Multiple Myeloma. *Cell Rep.* 2017;19(1):218-224.
17. Beroukhi R, Mermel CH, Porter D, et al. The landscape of somatic copy-number alteration across human cancers. *Nature.* 2010;463(7283):899-905.
18. Mikulasova A, Smetana J, Wayhelova M, et al. Genomewide profiling of copy-number alteration in monoclonal gammopathy of undetermined significance. *Eur J Haematol.* 2016;97(6):568-575.
19. Zhao S, Choi M, Heuck C, et al. Serial exome analysis of disease progression in premalignant gammopathies. *Leukemia.* 2014;28(7):1548-1552.
20. Spivak JL. Myeloproliferative Neoplasms. *N Engl J Med.* 2017;376(22):2168-2181.

21. Shaughnessy JD, Zhan F, Burington BE, et al. A validated gene expression model of high-risk multiple myeloma is defined by deregulated expression of genes mapping to chromosome 1. *Blood*. 2007;109(6):2276-2284.
22. Stella F, Pedrazzini E, Baialardo E, Fantl DB, Schutz N, Slavutsky I. Quantitative analysis of CKS1B mRNA expression and copy number gain in patients with plasma cell disorders. *Blood Cells Mol Dis*. 2014;53(3):110-117.
23. Marchesini M, Ogoti Y, Fiorini E, et al. ILF2 Is a Regulator of RNA Splicing and DNA Damage Response in 1q21-Amplified Multiple Myeloma. *Cancer Cell*. 2017.
24. Boyd KD, Ross FM, Walker BA, et al. Mapping of chromosome 1p deletions in myeloma identifies FAM46C at 1p12 and CDKN2C at 1p32.3 as being genes in regions associated with adverse survival. *Clin Cancer Res*. 2011;17(24):7776-7784.
25. Leone PE, Walker BA, Jenner MW, et al. Deletions of CDKN2C in multiple myeloma: biological and clinical implications. *Clin Cancer Res*. 2008;14(19):6033-6041.
26. Chiecchio L, Dagrada GP, Ibrahim AH, et al. Timing of acquisition of deletion 13 in plasma cell dyscrasias is dependent on genetic context. *Haematologica*. 2009;94(12):1708-1713.
27. Burkhart DL, Sage J. Cellular mechanisms of tumour suppression by the retinoblastoma gene. *Nat Rev Cancer*. 2008;8(9):671-682.
28. He Z, O'Neal J, Wilson WC, et al. Deletion of Rb1 induces both hyperproliferation and cell death in murine germinal center B cells. *Exp Hematol*. 2016;44(3):161-165.e164.
29. Duffy MJ, Synnott NC, Crown J. Mutant p53 as a target for cancer treatment. *Eur J Cancer*. 2017;83:258-265.
30. Lodé L, Eveillard M, Trichet V, et al. Mutations in TP53 are exclusively associated with del(17p) in multiple myeloma. *Haematologica*. 2010;95(11):1973-1976.
31. Zhan F, Huang Y, Colla S, et al. The molecular classification of multiple myeloma. *Blood*. 2006;108(6):2020-2028.
32. Dhodapkar MV, Sexton R, Waheed S, et al. Clinical, genomic, and imaging predictors of myeloma progression from asymptomatic monoclonal gammopathies (SWOG S0120). *Blood*. 2014;123(1):78-85.
33. Davies FE, Dring AM, Li C, et al. Insights into the multistep transformation of MGUS to myeloma using microarray expression analysis. *Blood*. 2003;102(13):4504-4511.
34. Walker BA, Wardell CP, Melchor L, et al. Intraclonal heterogeneity is a critical early event in the development of myeloma and precedes the development of clinical symptoms. *Leukemia*. 2014;28(2):384-390.
35. Seckinger A, Jauch A, Emde M, et al. Asymptomatic Multiple Myeloma - Background of Progression, Evolution, and Prognosis. *Blood*. 2016;128(22):235.
36. Mikulasova A, Wardell CP, Murison A, et al. Somatic mutation spectrum in monoclonal gammopathy of undetermined significance indicates a less complex genomic landscape compared to multiple myeloma. *Haematologica*. 2017.
37. Rossi A, Voigtlaender M, Janjetovic S, et al. Mutational landscape reflects the biological continuum of plasma cell dyscrasias. *Blood Cancer J*. 2017;7(2):e537.
38. Dutta AK, Grady JP, Hewett DR, Bik To L, Fink L, Zannettino ACW. Whole Exome Sequencing of Paired MGUS/SMM to MM Patients Reveals Novel Subclonal Tumour Evolution Models in Disease Progression of Multiple Myeloma. *Blood*. 2017;130(Suppl 1):391.

39. Xu J, Pfarr N, Endris V, et al. Molecular signaling in multiple myeloma: association of RAS/RAF mutations and MEK/ERK pathway activation. *Oncogenesis*. 2017;6(5):e337.
40. Meyer N, Penn LZ. Reflecting on 25 years with MYC. *Nat Rev Cancer*. 2008;8(12):976-990.
41. Affer M, Chesi M, Chen WD, et al. Promiscuous MYC locus rearrangements hijack enhancers but mostly super-enhancers to dysregulate MYC expression in multiple myeloma. *Leukemia*. 2014;28(8):1725-1735.
42. Chesi M, Robbiani DF, Sebag M, et al. AID-dependent activation of a MYC transgene induces multiple myeloma in a conditional mouse model of post-germinal center malignancies. *Cancer Cell*. 2008;13(2):167-180.
43. Manier S, Powers JT, Sacco A, et al. The LIN28B/let-7 axis is a novel therapeutic pathway in multiple myeloma. *Leukemia*. 2017;31(4):853-860.
44. Rutsch S, Neppalli VT, Shin DM, et al. IL-6 and MYC collaborate in plasma cell tumor formation in mice. *Blood*. 2010;115(9):1746-1754.
45. Hoesel B, Schmid JA. The complexity of NF- $\kappa$ B signaling in inflammation and cancer. *Mol Cancer*. 2013;12:86.
46. Demchenko YN, Glebov OK, Zingone A, Keats JJ, Bergsagel PL, Kuehl WM. Classical and/or alternative NF-kappaB pathway activation in multiple myeloma. *Blood*. 2010;115(17):3541-3552.
47. Chen H, Li M, Sanchez E, et al. Combined TRAF6 Targeting and Proteasome Blockade Has Anti-myeloma and Anti-Bone Resorptive Effects. *Mol Cancer Res*. 2017;15(5):598-609.
48. Walker BA, Wardell CP, Chiecchio L, et al. Aberrant global methylation patterns affect the molecular pathogenesis and prognosis of multiple myeloma. *Blood*. 2011;117(2):553-562.
49. Wilson AS, Power BE, Molloy PL. DNA hypomethylation and human diseases. *Biochim Biophys Acta*. 2007;1775(1):138-162.
50. Dimopoulos K, Gimsing P, Grønbaek K. The role of epigenetics in the biology of multiple myeloma. *Blood Cancer J*. 2014;4:e207.
51. Jung S, Kim S, Gale M, et al. DNA methylation in multiple myeloma is weakly associated with gene transcription. *PLoS One*. 2012;7(12):e52626.
52. Kaiser MF, Johnson DC, Wu P, et al. Global methylation analysis identifies prognostically important epigenetically inactivated tumor suppressor genes in multiple myeloma. *Blood*. 2013;122(2):219-226.
53. van de Donk NW, Mutis T, Poddighe PJ, Lokhorst HM, Zweegman S. Diagnosis, risk stratification and management of monoclonal gammopathy of undetermined significance and smoldering multiple myeloma. *Int J Lab Hematol*. 2016;38 Suppl 1:110-122.
54. Pérez-Persona E, Vidrales MB, Mateo G, et al. New criteria to identify risk of progression in monoclonal gammopathy of uncertain significance and smoldering multiple myeloma based on multiparameter flow cytometry analysis of bone marrow plasma cells. *Blood*. 2007;110(7):2586-2592.
55. Rosiñol L, Cibeira MT, Montoto S, et al. Monoclonal gammopathy of undetermined significance: predictors of malignant transformation and recognition of an evolving type characterized by a progressive increase in M protein size. *Mayo Clin Proc*. 2007;82(4):428-434.

56. Rajkumar SV, Kyle RA, Therneau TM, et al. Serum free light chain ratio is an independent risk factor for progression in monoclonal gammopathy of undetermined significance. *Blood*. 2005;106(3):812-817.
57. Pérez-Persona E, Mateo G, García-Sanz R, et al. Risk of progression in smouldering myeloma and monoclonal gammopathies of unknown significance: comparative analysis of the evolution of monoclonal component and multiparameter flow cytometry of bone marrow plasma cells. *Br J Haematol*. 2010;148(1):110-114.
58. Quail DF, Joyce JA. Microenvironmental regulation of tumor progression and metastasis. *Nat Med*. 2013;19(11):1423-1437.
59. Glavey SV, Naba A, Manier S, et al. Proteomic characterization of human multiple myeloma bone marrow extracellular matrix. *Leukemia*. 2017.
60. Bianchi G, Munshi NC. Pathogenesis beyond the cancer clone(s) in multiple myeloma. *Blood*. 2015;125(20):3049-3058.
61. Ghobrial IM, Detappe A, Anderson KC, Steensma DP. The bone-marrow niche in MDS and MGUS: implications for AML and MM. *Nat Rev Clin Oncol*. 2018.
62. Das R, Strowig T, Verma R, et al. Microenvironment-dependent growth of preneoplastic and malignant plasma cells in humanized mice. *Nat Med*. 2016;22(11):1351-1357.
63. Lawson MA, McDonald MM, Kovacic N, et al. Osteoclasts control reactivation of dormant myeloma cells by remodelling the endosteal niche. *Nat Commun*. 2015;6:8983.
64. Moschetta M, Mishima Y, Kawano Y, et al. Targeting vasculogenesis to prevent progression in multiple myeloma. *Leukemia*. 2016;30(5):1103-1115.
65. Ria R, Todoerti K, Berardi S, et al. Gene expression profiling of bone marrow endothelial cells in patients with multiple myeloma. *Clin Cancer Res*. 2009;15(17):5369-5378.
66. Rajkumar SV, Mesa RA, Fonseca R, et al. Bone marrow angiogenesis in 400 patients with monoclonal gammopathy of undetermined significance, multiple myeloma, and primary amyloidosis. *Clin Cancer Res*. 2002;8(7):2210-2216.
67. Calcinotto A, Ponzoni M, Ria R, et al. Modifications of the mouse bone marrow microenvironment favor angiogenesis and correlate with disease progression from asymptomatic to symptomatic multiple myeloma. *Oncoimmunology*. 2015;4(6):e1008850.
68. Rajabi M, Mousa SA. The Role of Angiogenesis in Cancer Treatment. *Biomedicines*. 2017;5(2).
69. Study of the CD38 Antibody Daratumumab in Patients With High-Risk MGUS and Low-Risk Smoldering Multiple Myeloma. In:2017.





# Chapter three

## Wnt signaling in multiple myeloma: a central player in disease with therapeutic potential

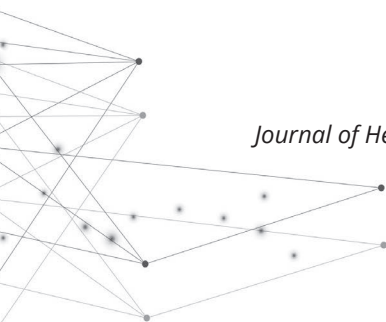
Ingrid Spaan<sup>1</sup>, Reinier Raymakers<sup>2</sup>,  
Anja van de Stolpe<sup>3</sup>, and Victor Peperzak<sup>1</sup>

<sup>1</sup> Laboratory of Translational Immunology,  
University Medical Center Utrecht,  
Utrecht, the Netherlands

<sup>2</sup> Department of Hematology,  
University Medical Center Utrecht,  
Utrecht, the Netherlands

<sup>3</sup> Precision Diagnostics, Philips Research,  
Eindhoven, the Netherlands

*Journal of Hematology & Oncology, 2018; 11(1):679*



## ABSTRACT

Multiple myeloma is the second most frequent hematological malignancy in the western world and remains incurable, predominantly due to acquired drug resistance and disease relapse. The highly conserved Wnt signal transduction pathway, which plays a key role in regulating cellular processes of proliferation, differentiation, migration and stem cell self-renewal, is associated with multiple aspects of disease. Bone homeostasis is severely disturbed by Wnt antagonists that are secreted by the malignant plasma cells in the bone marrow. In the vast majority of patients this results in osteolytic bone disease, which is associated with bone pain and pathological fractures and was reported to facilitate disease progression. More recently, cumulative evidence also indicates the importance of intrinsic Wnt signaling in the survival of multiple myeloma cells. However, Wnt pathway-activating gene mutations could not be identified. The search for factors or processes responsible for Wnt pathway activation currently focuses on aberrant ligand levels in the bone marrow microenvironment, increased expression of Wnt transcriptional co-factors and associated micro-RNA's and disturbed epigenetics and post-translational modification processes. Furthermore, Wnt pathway activation is associated with acquired cell adhesion-mediated resistance of multiple myeloma cells to conventional drug therapies, including doxorubicin and lenalidomide. In this review we present an overview of the relevance of Wnt signaling in multiple myeloma and highlight the Wnt pathway as a potential therapeutic target for this disease.

## 1 | BACKGROUND

Multiple myeloma (MM) is a neoplastic disorder that is characterized by the infiltration and clonal proliferation of antibody-secreting post-germinal center plasma cells (PCs) in the bone marrow (BM). It is the second most frequent hematological malignancy, accounting for approximately 10% of all hematological cancers, and particularly affects the elderly with a median age at diagnosis of 69 years [1, 2]. MM is typically preceded by a pre-malignant state, which is referred to as monoclonal gammopathy of undetermined significance (MGUS). It is estimated that approximately 3-4% of the population above the age of 50 acquire this condition, but risk of progressing to MM is limited to 0.5-1% per year [3]. When detected monoclonal protein is accompanied by a clonal BM PC count exceeding 10% the diagnosis MM is set [3]. Intramedullary MM may first present in an asymptomatic phase, often referred to as smoldering myeloma (SMM), but progression to active disease is significant within the first five years after onset



[4]. Active disease is characterized by myeloma-related end organ failure and includes renal insufficiency, anemia, bone disease and subsequent hypercalcemia as a result of the excess bone resorption [5]. Especially the presence of osteolytic bone disease, which develops in 80-90% of patients, is a major disease burden and often results in severe bone pain and detrimental pathological fractures [6]. Development of novel pharmaceutical agents has resulted in major advances in the treatment of MM in the last two decades [7]. In particular co-treatment strategies of immune-modulatory drugs, proteasome inhibitors, conventional chemotherapy and recently also monoclonal antibodies resulted in substantial progression in treatment outcome. However, despite the improvements in patient survival rates and quality of life, MM remains an incurable disease, with a current median survival of six to seven years [2].

The Wnt signal transduction pathway is a highly evolutionary conserved and pleiotropic cell-to-cell communication route that regulates cellular processes including proliferation, differentiation and fate determination. During embryogenesis it functions as a concentration-dependent and long-range morphogen in establishing body axis formation [8]. In mature organisms Wnt signaling is predominantly known for its role in the regulation of tissue-specific stem cell populations, thereby maintaining adult tissue homeostasis [9]. This has been confirmed in colon epithelium and skin tissue and has now also been reported in the hematopoietic stem cells (HSCs) that give rise to all blood cell lineages [10]. Deregulation of the Wnt pathway is associated with diverse human pathologies, cancer in particular. Although it was primarily recognized for its role in colorectal cancers, many more malignancies have been linked to aberrant Wnt pathway activation. Mutations in crucial Wnt signaling components, including Apc, Axin,  $\beta$ -catenin and Wnt ligands themselves have been reported in gastrointestinal cancers [11], pancreatic ductal adenocarcinoma [12], melanoma [13], lung cancer [14], cervical cancer [15], mammary carcinoma [16], prostate cancer [17] and tumors of the central nervous system [18], and result in hyperactivation of the Wnt pathway, ultimately increasing proliferation of malignant cells. Besides its reported role in the initiation and development of these solid tumors there is now an increasing body of evidence that indicates involvement of Wnt signaling in hematological malignancies as well, including leukemias and MM [19].

The relevance of Wnt signaling in MM was first acknowledged for its regulating role in bone homeostasis. Wnt signaling tightly controls the balance between bone-forming osteoblasts and bone-resorbing osteoclasts, both by direct and indirect mechanisms [20]. Malignant PCs in MM severely disturb this system by secretion of Wnt antagonists in the BM microenvironment. This skews the balance towards osteogenic bone resorption and results in development of the characteristic

osteolytic bone lesions [21]. In this process, a plethora of growth factors that were embedded in the bone matrix are released, which subsequently enhance MM cell growth and survival [22]. This coupled interaction essentially creates a vicious cycle of destructive bone disease and MM disease progression.

In recent years more emphasis was put on the biological significance of active Wnt signaling intrinsic in MM malignant PCs. Human multiple myeloma cell lines (HMCLs) were found to express multiple Wnt receptors, co-receptors and downstream pathway mediators that stabilized in response to ligand-mediated pathway activation [23]. Furthermore, HMCLs as well as primary PC isolates from MM patients overexpress the transcriptional co-activator  $\beta$ -catenin, including the active non-phosphorylated variant which is key to Wnt target gene transcription upon pathway activation [24]. The biological consequence of active Wnt signaling in these cells remains a point of discussion however. Multiple *in vitro* and *in vivo* studies used various approaches to either activate or inhibit Wnt signaling in MM cells and reported contradictory results on cell proliferation, morphology and disease progression. Also, the mechanistic role of pathway activation remains elusive, since no mutations in the genes of any of the major pathway mediators, including APC, Axin and  $\beta$ -catenin itself, could be detected [24]. Current research focuses on aberrant levels of ligands in the BM microenvironment, increased expression of transcriptional co-factors, including BCL9 and associated micro-RNA's, as well as disturbed epigenetics and post-translational modification processes including sumoylation, as factors contributing to malignant Wnt signaling in MM.

In addition to canonical  $\beta$ -catenin mediated transcriptional effects, Wnt signaling can also affect cell morphology, migration and adhesion in a more direct way via the non-canonical Wnt/planar cell polarity (PCP) pathway. By acting on the small GTPases that regulate cytoskeleton formation, Wnt signaling can increase adhesion of malignant PCs to BM stromal cells and thereby enhance drug resistance [25]. The acquisition of resistance to conventional therapies in disease relapse is an emerging clinical problem. Targeting the Wnt pathway could therefore be an interesting new avenue in the treatment of MM.

Here we present a complete overview of the relevance of Wnt signaling in MM. We summarize the role of Wnt signaling in MM bone disease, discuss the relevant studies performed in the context of intrinsic Wnt signaling in MM pathogenesis, both focusing on the biological significance as well as mechanisms responsible for signaling activation, and highlight the role of Wnt signaling in drug resistance and its potential as a therapeutic target in the treatment of MM.

## 2 | THE WNT SIGNALING PATHWAY

The Wnt family currently consists of 19 secreted lipid-modified glycoproteins that can signal through one or more of the Wnt signal transduction pathways and can do so in a paracrine or autocrine fashion. They exhibit unique expression patterns and developmental functions, but were previously classified based on their ability to induce transformation of the epithelial cell line C57MG. Highly transforming members are thought to signal mainly through the  $\beta$ -catenin dependent canonical Wnt pathway and include Wnt1, Wnt2, Wnt3 and Wnt3a, while the non-transforming members Wnt4, Wnt5a, Wnt5b and Wnt7b were reported to have no effects on transformation and are likely to signal towards the non-canonical Wnt pathways. Several additional Wnts including Wnt6 and Wnt7a do not belong to these categories and are classified as intermediate transforming members, resulting in weak morphological changes [26]. There is only very little information about the structure of Wnts, since they are by nature difficult to synthesize in a recombinant setting, insoluble and problematically complex to purify. Only in 2012, researchers succeeded in elucidating the X-ray crystal structure of *Xenopus laevis* XWnt8 [27]. Human Wnts are all very similar in size, between 39 and 46 kDa, and all contain 22 to 24 highly conserved cysteine residues that determine protein folding. All Wnt ligands go through an extensive process of post-translational modification before they become secreted. Both transforming and non-transforming members become glycosylated in the endoplasmic reticulum (ER), however, glycosylation of both Wnt1 and Wnt5a were reported to be indispensable for their functions [28]. In the ER, Wnts also become acylated. The membrane-bound O-acetyltransferase Porcupine catalyzes the addition of palmitoleate groups to the conserved cysteine residues, which were found to be essential for progression of Wnts through the secretory pathway. Also Wnt signaling capacity is diminished in absence of palmitoylation, most likely because these acyl groups mediate the interaction of the ligands with its receptors [29]. Additional post-translational modifications have been reported in very specific subgroups of Wnt ligands and include GPI anchorage to Wnt1 and Wnt3a and tyrosine sulfation of Wnt5a and Wnt11 [30]. Since Wnt proteins are so hydrophobic, they are mainly associated with the plasma membrane and extracellular matrix (ECM) [19]. Incorporation of Wnt ligands in membrane enclosed vesicles, including exosomes, ensures adequate transport over larger distances of extracellular space [31].

The canonical Wnt signaling pathway all revolves around the transcriptional co-activator  $\beta$ -catenin. When the Wnt pathway is inactive, continuously synthesized  $\beta$ -catenin is eliminated by a cytosolic destruction complex consisting of the scaffold proteins APC and Axin1 and the kinases GSK3 and CK1 (Figure 1A). This destruction

complex phosphorylates  $\beta$ -catenin at specific and highly conserved serine and threonine residues, thereby marking it for ubiquitination by the E3 ligase  $\beta$ -TrCP and subsequent proteasomal degradation [32]. Wnt signaling is activated upon binding of a Wnt ligand to its cognate receptor complex, consisting of the seven-span transmembrane protein frizzled (Fzd), of which ten isoforms are identified, and its co-receptors LRP5 and LRP6. Upon activation, the receptor complex recruits the effector protein dishevelled (Dvl) to the plasma membrane, which is thought to result in subsequent recruitment of Axin1-GSK3, thereby disrupting the cytosolic destruction complex (Figure 1B) [33]. Consequently,  $\beta$ -catenin is no longer phosphorylated and degraded but stabilized in the cytoplasm and able to translocate to the nucleus. Upon association with the basal transcriptional machinery and co-factors including pygopus and BCL9,  $\beta$ -catenin binds to members of the LEF/TCF family of transcription factors [34]. In this way,  $\beta$ -catenin facilitates transcription of Wnt target genes. These include cell cycle regulators like *CCND1* (encoding cyclinD1) and *MYC* and the survival molecule *BIRC5*, which translates into the inhibitor-of-apoptosis family member survivin. Survivin is overexpressed in a subset of MM patients and is correlated with multidrug resistance [35]. Also *AXIN2*, a structural and functional homolog of Axin1, is transcribed upon  $\beta$ -catenin-LEF/TCF mediated transcription and thereby initiates a negative feedback loop upon canonical Wnt pathway activation [36].

In contrast to the canonical pathway,  $\beta$ -catenin-independent non-canonical Wnt pathways signal through the Fzd receptor without the need of the LRP co-receptor. Instead, association with other transmembrane proteins, including the receptor tyrosine kinases Ryk and Ror, has been reported. Multiple Wnt ligands including Wnt5a and Wnt11 are capable of doing so [37]. By recruiting Dvl these Wnts can activate multiple signaling cascades, which are vastly intertwined. In the Wnt/PCP pathway recruitment of Dvl results in activation of the small GTPases RhoA, Rac and Cdc42, which actively rearrange the cell's cytoskeleton and control cell polarity and motility (Figure 1C) [38]. Additionally, RhoA and Rac are capable of activating Jun kinase (JNK), which can induce activation of AP1- and NFAT-mediated transcriptional programs [37]. In the Wnt/Ca<sup>2+</sup> pathway similar recruitment of Dvl results in activation of heterotrimeric G-proteins, which ultimately induce a calcium flux into the cytosol (Figure 1D). Calcium-dependent signaling molecules such as PKC, camKII and CaN subsequently become activated and influence a wide variety of signaling cascades, reliant on the cellular context [38]. Like JNK, both PKC and CamKII are capable of inducing NFAT-mediated transcription by facilitating its nuclear translocation [37].

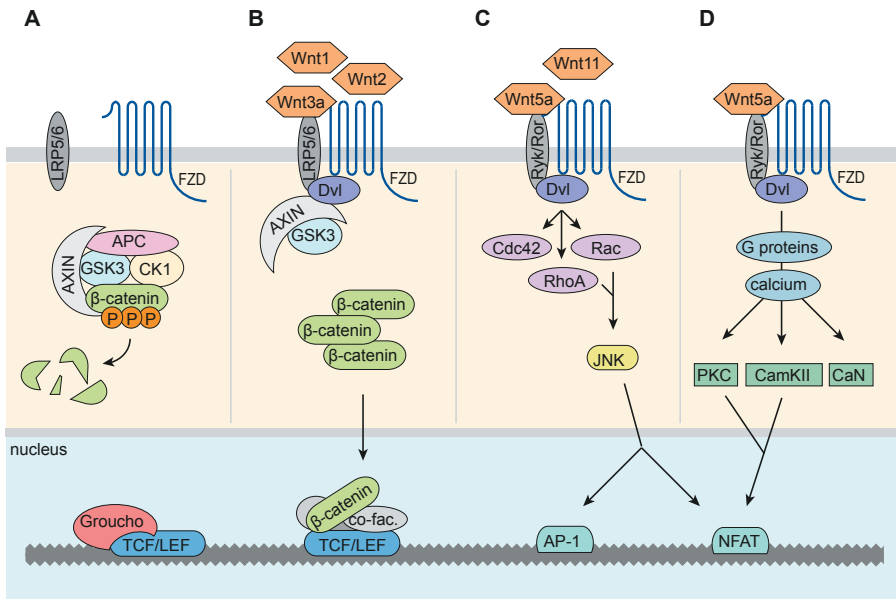


**Figure 1 | Schematic depiction of the canonical and non-canonical Wnt pathways.** (A) When the canonical Wnt pathway is inactive, a cytosolic destruction complex consisting of Axin, APC, GSK3 and CK1 is formed. By phosphorylating  $\beta$ -catenin, this complex marks  $\beta$ -catenin for ubiquitination and subsequent degradation by the proteasome. The Wnt transcription factors TCF/LEF remain repressed by Groucho. (B) Upon binding of a canonical Wnt ligand to the Fzd receptor and LRP5/6 co-receptor, the canonical pathway becomes activated. Dvl is recruited to the receptor complex and subsequently recruits Axin-GSK3, thereby disrupting the destruction complex. Cytosolic levels of  $\beta$ -catenin stabilize and translocate to the nucleus. Here,  $\beta$ -catenin associates with the transcriptional machinery, transcriptional co-factors, and binds to TCF/LEF. This allows for active transcription of Wnt target genes. (C/D) Non-canonical Wnt ligands bind to Fzd and other transmembrane proteins such as Ryk and Ror, resulting in the recruitment of Dvl. (C) In the PCP pathway, this can result in activation of the small GTPases RhoA, Rac, and CDC42, which influence cytoskeleton function. RhoA and Rac can also activate JNK, and subsequent AP-1 and NFAT-mediated transcriptional programs. (D) In the  $\text{Ca}^{2+}$  pathway, Dvl activates heterotrimeric G proteins, resulting in a cytosolic calcium flux. This activates calcium-dependent signaling molecules including PKC, CamKII and CaN. Both PKC and CamKII can also promote NFAT transcriptional activity.

The cellular outcome of active Wnt signaling is dictated by many factors, including the type(s) of Wnts present, as well as the receptor and co-receptor it engages with. Following the classification of Wnt ligands also Fzd receptors were divided into separate groups based on their ability to activate either canonical or non-canonical Wnt pathways upon overexpression [39]. However, from a biological standpoint these classification systems provide only limited information. The classical transforming Wnt3a is also capable of stabilizing  $\beta$ -catenin via non-canonical Rho [40], while the notorious non-canonical Wnt5a is able to activate the

$\beta$ -catenin-driven canonical Wnt pathway in the presence of Fzd5 in *Xenopus laevis* overexpression studies [41]. Many additional levels of regulation affect which downstream signaling cascades become activated. Varying concentrations of Wnt ligands in the microenvironment can induce differential target gene transcription. This is a direct consequence of the fact that Wnts create gradients to function as morphogens during embryonic development [9]. Expression of intracellular pathway mediators, including basal levels of  $\beta$ -catenin and differentially expressed isoforms of the LEF/TCF transcription factors, can also influence Wnt signaling and can even result in distinct cellular outcomes in identical Wnt ligand and receptor conditions [42]. Furthermore, the Wnt pathway can be associated with, and influenced by, other cell signaling pathways, including the PI3K/Akt, FGF, Notch and Hedgehog signaling pathways [43]. In addition, a growing list of Wnt antagonists are currently being identified. Extracellular inhibitors comprise soluble secreted Fzd-related proteins (sFRP)1-5 that act as decoy receptors by directly binding to extracellular Wnts, resulting in a concentration-dependent downregulation of general Wnt pathway activation. This in contrast to Dkk1-4, which specifically antagonizes canonical Wnt signaling by binding to extracellular subregions of the LRP co-receptors. Other extracellular antagonists are Wnt inhibitory factor 1 (WIF1) and the bone-specific Wnt inhibitor SOST/sclerostin [44]. The best characterized intracellular Wnt pathway inhibitor is ICAT, which inhibits the interaction between  $\beta$ -catenin and the transcriptional complex members LEF/TCF and p300 [45]. All these different levels of control combined ensure tight regulation of the potent Wnt signal transduction pathway.

### **3 | WNT SIGNALING IN MULTIPLE MYELOMA BONE DISEASE**

MM cells preferentially home to the BM as their host organ, which is a very active site of Wnt signaling. The BM is a soft, well vascularized and highly spatially organized tissue that harbors a diverse cellular content consisting of bone-forming osteoblasts and bone-resorbing osteoclasts, BM adipocytes, endothelial cells, BM stromal cells, mesenchymal stem cells (MSC) and HSC [46]. The latter two stem cell populations reside in specific BM niches, where their stemness potential is tightly regulated by distinct niche signaling pathways that allegedly includes canonical Wnt signaling [47]. Furthermore, the BM hosts a wide variety of innate and adaptive immune cells including macrophages, neutrophils and diverse B and T cell populations. All these cells are joint by an extensive network of ECM proteins and fluid, which contain a variety of growth factors and cytokines [48]. Many of the cells present in the BM produce a range of Wnts, both of the canonical and non-

canonical branches. MSC do not only rely on intrinsic Wnt signaling to maintain their stem cell features, they also secrete Wnt ligands, including Wnt2, Wnt4, Wnt5a, Wnt11 and Wnt16 [49]. Additional major sources of Wnts are endothelial cells and BM stromal cells. Several immune cells were also shown to be able to contribute to Wnt signaling, including monocytes, dendritic cells and macrophages [50]. When located in the BM, T cells also express the canonical ligand Wnt10b, which is positively associated with bone formation [51]. Additionally, cells of the osteoblast and osteoclast lineages themselves secrete Wnt5 and Wnt10b that function as part of their intercellular communication pathways [52, 53].

### 3.1 | Wnt signaling is a master regulator of bone homeostasis

MM cells interrupt Wnt signaling in the BM and thereby severely disturb bone homeostasis. Essentially, bone metabolism is controlled by three cell types: osteoblasts, osteocytes and osteoclasts. Osteoblasts are derived from pluripotent MSCs, which also produce fibroblasts, chondrocytes, myoblasts and adipocytes. Wnt signaling has a major impact on this differentiation process by directing MSC differentiation away from the chondrocytic and adipocytic lineages, towards differentiation into osteoblasts [54]. Additionally, Wnt signaling was proven to promote survival of these osteoblasts, at least partly via signaling through the Src/ERK and PI3K/Akt pathways [55]. Mature osteoblasts reside in specific niches that are separated from the rest of the BM by a single layer of bone-lining canopy cells [56]. The osteoblasts are responsible for the formation of new bone tissue during the continuous bone modeling and remodeling processes and do so by secreting bone matrix components, including collagen, and regulating mineralization of the bone tissue [56]. During this process they can become embedded in the bone tissue, which promotes their terminal differentiation into osteocytes.

Osteocytes comprise approximately 95% of all cells present in the bone matrix and are the only cell type identified in bone that possess a significantly active intrinsic canonical Wnt signaling pathway [57]. Within the mineralized matrix they influence bone formation by secreting the Wnt antagonist SOST/Sclerostin [58]. These factors diffuse from the osteocyte lacuna, via a canalicular network, to the bone surface, where they inhibit osteoblastic activity [57]. The main function of osteocytes is to regulate bone mass in the context of mechanical loading. As a result of the mechanotransduction pathway, significant mechanical stress directly leads to a downregulation of Wnt inhibitor secretion levels and a subsequent gain in bone mass to maintain skeletal integrity [59].

Osteoclasts are the natural counterpart of osteoblasts and facilitate the process of bone remodeling by resorbing bone tissue. They do so by secreting lytic enzymes

that degrade the bone matrix [60]. Osteoclasts arise from monocyte/macrophage hematopoietic precursor cells that reach the BM via the vasculature [56]. Fusion of multiple of these cells results in the characteristic multinucleated cells. However, for osteoclasts to become fully differentiated, several osteoblast-secreted factors including RANKL are required [61]. Like osteoblasts, osteoclasts and their precursors are influenced by Wnt signaling. However, the biological consequences of Wnt signaling are rather complex, since Wnt ligands were found to stimulate early steps of osteoclastogenesis, while inhibiting the final differentiation stages [62].

In healthy human adults bone remodeling is executed to replenish old bone, strengthen bone tissue in response to physical stress, or at sites of injury. Osteoclasts resorb the compromised bone tissue, after which adjacent cells, and presumably also tissue specific macrophages called osteomacs, clean the affected surface. The osteoclasts then recruit and stimulate osteoblasts to form new bone tissue in order to fill the created space. To balance bone resorption with equal bone formation, osteoblast and osteoclast activity is matched, which is referred to as coupling (Figure 2, black arrows) [56]. The Wnt signaling pathway is found to be directly involved in this coupling mechanism. Bone forming osteoblasts secrete non-canonical Wnt5a, which is a ligand for the Fzd-Ror2 and Fzd-Ryk receptor complexes that are present on the cell surface of osteoclast precursors. Subsequent activation of the downstream signaling cascade stimulates differentiation into more mature bone resorbing osteoclasts [52, 63]. These osteoclasts in turn express multiple factors, including chemoattractants that recruit osteoblast precursors to the site of bone remodeling, and Wnt10b that stimulates bone formation, creating an ingenious feedback/feedforward loop of bone remodeling [53]. Besides these direct effects, Wnt signaling also plays a more indirect role in bone remodeling by influencing the RANK/RANKL/OPG signaling axis; one of the best characterized coupling routes [64]. The receptor RANK, which is present on the plasma membrane of osteoclasts, can be activated by binding of its cognate ligand RANKL that is predominantly expressed by osteoblasts. In addition, osteoblasts are also capable of secreting the natural decoy receptor OPG, which competes with RANK for the binding of RANKL. The balance between RANKL and OPG determines the level of signal transduction and thereby regulates osteoclast activation [65]. Both RANKL and OPG were shown to be direct Wnt target genes in osteoblasts. Increased Wnt signaling is associated with high secretion levels of OPG, but negatively regulates RANKL expression, which subsequently results in impaired osteoclastogenesis [66, 67].



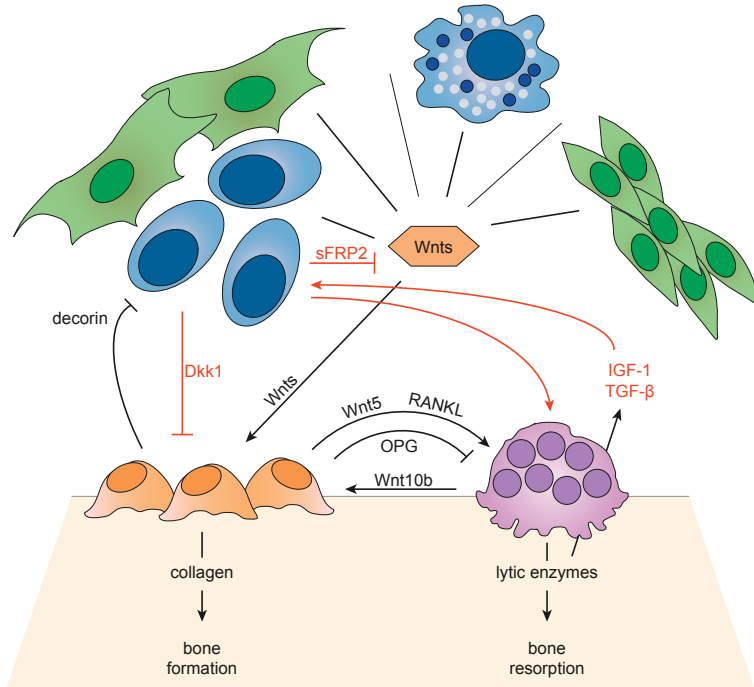


**Figure 2 | Bone homeostasis and multiple myeloma-induced osteolytic bone disease.**

(In black) In the BM, Wnt ligands are expressed by MSCs, endothelial cells, BM stromal cells, immune cells including macrophages and dendritic cells, osteoblasts and osteoclast. Wnts promote differentiation of MSCs toward the osteoblastic lineage, stimulate osteoblast proliferation, and promote osteoblast survival. Osteoblasts regulate osteoclast activity by secreting the antagonistic molecules RANKL and OPG, and Wnt5. Osteoclasts also regulate osteoblast function by secreting Wnt10b. Through this system, osteoblast and osteoclast activity is coupled and bone homeostasis is maintained. Osteoblasts also inhibit MM cell growth by expressing decorin. (In red) MM cells promote osteoclast function by secreting RANKL. Osteoclasts stimulate MM cells by secreting IL-6 and Annexin II. Enhanced bone resorption also leads to increased IGF-1 and TGF- $\beta$  levels. MM cells also inhibit osteoblasts by secreting Wnt inhibitors sFRP2 and Dkk1. This disrupts the osteoblast-osteoclast balance and bone homeostasis and leads to osteolytic bone disease.

### 3.2 | Multiple myeloma cells disrupt bone homeostasis by interfering with Wnt signaling

Like their benign counterparts, malignant PCs in MM express high levels of CXCR4 on their cell surface in order to home the BM [68]. Here, they adhere to BM stromal cells, that create a permissive environment by expressing adhesion molecules and secreting an array of growth factors, chemokines and other molecules [69]. By this direct cell-to-cell contact MM cells also instruct BM stromal cells to produce high levels of osteoclastogenic stimuli, including RANKL, to augment bone resorption [70]. More importantly, BM infiltration allows MM cells to exert their effects on

osteoblasts and osteoclasts in a more direct fashion, which ultimately facilitates tumor progression (Figure 2, red arrows).

MM bone disease is characterized by both an increase in osteoclast activity, as well as a decrease in the number of osteoblasts. Osteoclastogenesis is stimulated in a direct fashion by the expression and secretion of osteoclast-activating factors such as RANKL by MM cells themselves, resulting in increased bone resorption [71]. As a consequence of bone resorption, a plethora of immobilized growth factors, including insulin-like growth factor and TGF- $\beta$  [6], as well as calcium and ECM proteins, are released from the bone matrix. All these factors contribute to MM cell growth and survival [48]. Subsequent disease progression then results in an additional gain in bone tissue lysis, giving rise to a vicious cycle. In addition, osteoclasts themselves also secrete multiple factors to sustain MM cells, including the growth factor IL6 and survival factors BAFF and APRIL, and are believed to promote angiogenesis by secreting the pro-angiogenic factor osteopontin [72, 73]. Besides increased osteoclastogenesis, MM cells also reduce the number and activity of osteoblasts [64]. This not only enhances osteolytic bone disease by preventing new bone formation; osteoblasts were found to reduce MM cell growth, i.a. by producing a proteoglycan called decorin that was reported to induce apoptosis of MM cells [74].

Presumably the most important mechanism by which MM cells promote an osteoblast/osteoclast disbalance is by attenuating active canonical Wnt signaling. MM cells, but not PCs isolated from MGUS patients, were found to express high levels of the canonical Wnt inhibitor Dkk1. Mouse model studies had previously shown that Dkk1 plays a crucial role in bone homeostasis. Overexpression of Dkk1 resulted in a decrease in bone mass, leading to osteopenia, while increased bone formation and bone mass was observed in single allele Dkk1 knockout mice [75]. The increased level of Dkk1 present in serum of MM patients was found to correlate with the presence and extend of bone lesions [76]. *In vitro*, serum of MM patients was shown to inhibit osteoblast differentiation, which could be restored by the addition of a Dkk1 neutralizing antibody [76]. In a more recent study, Yaccoby *et al.* used the murine SCID-rab model, in which mouse BM is substituted by rabbit BM through subcutaneous implantation of rabbit bone, to study the effects of Dkk1. Treatment with an anti-Dkk1 antibody, after engraftment of Dkk1 expressing primary MM cells, resulted in a reduced number of osteoclasts, enhanced number of osteoblasts, decreased bone resorption and a subsequent decrease in tumor burden [77]. Edwards *et al.* reported similar results when C57BL/KaLwRij mice were intravenously inoculated with murine 5TGM1 MM cells, after which Wnt signaling was activated by treatment with the potent GSK3 inhibitor lithium chloride (LiCl). Although tumor burden in the BM was reduced, increased tumor growth was

observed when the 5TGM1 cells were engrafted subcutaneously [78]. Qiang *et al.* showed that SCID-hu mice, which are comparable to the SCID-rab model but transplanted with human fetal bone, could be engrafted with the HMCL NCI-H929, which was stably transfected with either Wnt3a or empty vector control. Also in this model, increased osteoblast/osteoclast ratios were reported, accompanied by a reduction in tumor burden. In addition, recombinant Wnt3a treatment of SCID-hu mice carrying primary MM cells resulted in attenuation of bone resorption and MM cell growth [79]. These findings combined have culminated in clinical testing of the human neutralizing anti-Dkk1 monoclonal antibody BHQ880. Results from the phase 1b study, in which 28 patients with relapsed or refractory MM were enrolled, showed a general trend towards increased bone mass over time, particularly in the spine [80]. In 2013, a phase 2 study in SMM patients with high risk of disease progression was completed and also in this study evidence of anabolic bone activity in a subset of patients was reported [81].

Although the effects of Dkk1 secretion on MM pathogenesis are most extensively characterized, MM cells have additionally been proven to express the Wnt antagonists sFRP2, sFRP3 and SOST/Sclerostin. Serum levels of these Wnt inhibitors also correlate with the extent of MM bone disease [46]. Interestingly, *in vitro* treatment of osteoblasts with sFRP2 resulted in impaired differentiation capacity of these cells, similar to what was observed for Dkk1 [82]. Additional studies are required to elucidate the exact effects of these antagonists on MM pathogenesis.

## 4 | INTRINSIC WNT SIGNALING IN MULTIPLE MYELOMA CELLS

In recent years, several studies were published indicating that MM cells do not only disturb Wnt signaling in the BM by secreting Wnt antagonists, but also have the potential of an active intrinsic canonical Wnt signaling pathway. This was first evidenced by Qiang *et al.*, who reported that HMCLs can express up to nine isoforms of the Fzd receptor that are co-expressed with the canonical co-receptor LRP6 and in most instances also LRP5 [23]. Although this was only studied on the mRNA level, treatment of these cell lines with Wnt ligand was found to stabilize transcriptionally active  $\beta$ -catenin, suggesting that these receptors were also functionally active [23]. In a similar study, the same HMCLs were found to also produce a range of Wnt ligands [83]. The presence of Fzd1, Fzd6, Fzd7, Wnt5A and Wnt11 was later confirmed in a panel of primary PC samples isolated from MM patients and suggests that MM cells can stimulate their Wnt signaling pathway in an autocrine fashion [84]. However, since this analysis was also performed on

the mRNA level, it is difficult to estimate how the subsequent protein Wnt ligand concentrations would relate to Wnts produced by other cells in the BM.

The presence of an active intrinsic Wnt signaling pathway in MM cells was proven to be quite specific for malignant PCs. According to current hypotheses, the canonical Wnt signaling pathway is active in B cells during early stages of development, but is terminated upon expression of IgM by immature B cells [85]. In accordance with this model, several malignant mature B cell lines only expressed high levels of Fzd3 and did not show any expression of LRP5 or LRP6 [23]. This suggests that the final maturation step of activated mature B cells towards PCs, which is accompanied by extensive genetic rearrangements, could be essential for the cells to be able to reactivate the canonical Wnt signaling pathway during malignant transformation.

#### **4.1 | Wnt signaling is indispensable for normal B cell development**

B cells, like all cells from the blood lineage, arise from multipotent HSCs that have the ability of self-renewal, as well as the ability to differentiate into more committed precursor cells through a processes referred to as asymmetric cell division. Optimal regulation of these processes is required in order to maintain tissue homeostasis and to prevent depletion of the stem cell pool. Therefore, HSCs reside in specific BM stem cell niches, where their fate is tightly regulated by several distinct microenvironmental cell signaling pathways [85]. The exact role of Wnt signaling in this system is still under debate. The presence of an active canonical Wnt pathway in HSC *in vivo* was first confirmed by Reya *et al.* in 2003 [86]. However, several subsequent studies reported opposite results on the effect of Wnt signaling on the processes of HSC self-renewal and the capacity to reconstitute upon transplantation [87, 88]. Recent evidence now suggests that these contradictory observations result from differences in signaling levels. As Wnts function as morphogens and are normally present in concentration gradients within tissues, varying signaling levels can have differential cellular outcomes [89]. By introducing several distinct mutations in the APC gene in a conditional mouse model, Luis *et al.* were able to create a gradient of five different Wnt signaling levels. The results showed that a mild two-fold increase in Wnt signaling level enhances HSC function through a six-fold increase in repopulation capacity upon transplantation. This is in contrast with intermediate or higher Wnt signaling levels, which completely impaired HSC self-renewal potential [89]. This data, in combination with a previously published study that revealed that a nearly complete blockage of the Wnt pathway in Wnt3a-deficient mice is detrimental for HSC function, highlights the complexity of Wnt signaling in this system [90].

In contrast to HSC biology, the role of canonical Wnt signaling in subsequent early stages of B cell development was more robustly established (Figure 3). Already in 2000, Reya *et al.* reported that expression of LEF1 is confined to precursor B cells, pro-B cells and IgM-negative pre-B cells [91]. Canonical Wnt signaling at these stages is thought to solely occur through the LEF1 isoform of the TCF/LEF family, since TCF members are the commitment factor for T cell development and are therefore expected to be specifically downregulated during B cell development [92]. Analysis of LEF1 knockout mice revealed an up to eight-fold decrease in the number of pre-B and pro-B cells, accompanied by an increase in apoptotic cell numbers, which could be partly rescued by treatment with the GSK3 inhibitor LiCl. In addition, *in vitro* stimulation of isolated LEF1 knockout pro-B cells with Wnt3a-conditioned medium only resulted in stabilization of free  $\beta$ -catenin, while this was accompanied by cell cycle activation and proliferation in wild-type pro-B cells [91]. Similar findings were reported by Ranheim *et al.*, who utilized a Fzd9 knockout mouse model to study the effects of canonical Wnt signaling on B cell development. Fzd9 was found to be exclusively expressed in pro-B cells and large pre-B cells. Knockdown of Fzd9 resulted in a depletion of developing B cells, which was most pronounced in the large pre-B cell population [93].

Although both abovementioned studies suggest that canonical Wnt signaling is terminated when the final major round of pre-B cell division is completed, Yu *et al.* found evidence that canonical Wnt signaling is also required for normal PC function.

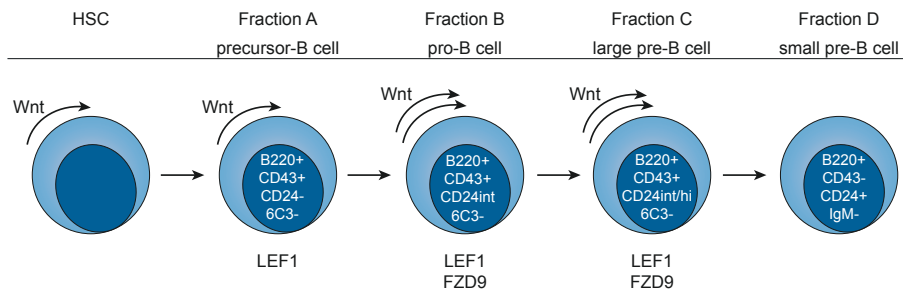


**Figure 3 | Wnt signaling in hematopoietic stem cells and early B cell development.**

Wnt signaling is essential for HSC self-renewal capacity and is also active in precursor cells from fraction A. Fraction B pro-B cells, that undergo IgH rearrangement, have an active Wnt pathway and express high levels of LEF1 and Fzd9. Also large pre-B cells from fraction C, that greatly expand their population, express LEF1 and Fzd9 and have an active Wnt pathway. Small pre-B cells from fraction D stop proliferating and start rearranging IgL genes. Upon expression of IgM, Wnt pathway activity is expected to be terminated.

When  $\beta$ -catenin was specifically deleted in the B cell lineage in a conditional mouse model, a small but significant reduction in PC generation was observed upon stimulation with bacterial LPS. Further analysis showed that the reduction in PC formation was accompanied by decreased expression levels of the transcription factors Blimp-1 and IRF-4, which are both essential for PC differentiation [94].

## **4.2 | Activation of Wnt signaling in multiple myeloma cells is facilitated by multiple processes**

With previous studies taken into account, one could state that canonical Wnt signaling is of importance during many of the major proliferative stages in the development and activation of B cells: HSC self-renewal, population expansion of developing B lymphocytes and PC generation upon antigenic stimulation of mature B cells. From this perspective, (re)activation of the canonical Wnt pathway in MM cells, which evidently have an active cell cycle, seems intuitive. In addition, aberrant Wnt pathway activation is very often implicated in cancer. This accounts for solid tumors, as well as different types of leukemia [10, 19]. Indeed, Derksen *et al.* showed that both HMCLs and primary PC isolates from MM patients overexpress  $\beta$ -catenin, including the transcriptionally active subset. This is in contrast to mature B cells, memory B cells and healthy PC populations [24]. However, it currently remains unclear what drives activation of the intrinsic Wnt/ $\beta$ -catenin pathway in MM cells. Extensive sequencing experiments did not reveal any detectable mutations in the major Wnt pathway mediators, including  $\beta$ -catenin itself (encoded by *CTNNB1*), *AXIN1*, or the tumor suppressor *APC*, as is normally observed in canonical Wnt-driven tumors like colon cancer [8].

First studies indicated a role for BCL9 in the activation of intrinsic Wnt signaling in MM. The *BCL9* gene, which is located on the frequently amplified 1q chromosomal region, was first identified in B-cell acute lymphoblastic leukemia as a result of the t(1;14) translocation [95]. The nuclear protein was shown to be an important co-factor for transmission of downstream Wnt signaling by facilitating effective  $\beta$ -catenin-LEF/TCF cooperation [96]. Mani *et al.* reported that BCL9 transcript levels were specifically enhanced in a subset of HMCLs and primary PC samples from MM patients, compared to normal PCs. This was accompanied by a perinuclear localization of  $\beta$ -catenin, enhanced transcriptional activation and an increase in cell proliferation, migration and invasion. Furthermore, murine xenograft models transplanted with the HMCL MM1.s in which BCL9 was knocked down by shRNA, showed reduced tumor burden, decreased metastasis and prolonged survival compared to shRNA control mice [97]. A follow-up study in 2014 identified the oncogenic BCL9 as a direct target of the tumor suppressor microRNA miR-30-5p. Levels of miR-30s are downregulated in a large subset of MM PC samples, which

is thought to result from adhesive interactions of MM cells to BM stromal cells, and is inversely correlated with BCL9 expression. Ectopic expression of miR-30c in malignant PCs was associated with reduced levels of BCL9 mRNA and BCL9 protein and decreased Wnt target gene transcription, as was assessed by functional promoter-reporter assay and CD44 and Axin2 mRNA levels. Furthermore, HMCLsNCI-H929 and OPM1 overexpressing miR-30c showed a clear reduction in cell proliferation, migration and invasion, accompanied by a mild increase in the number of apoptotic cells. In addition, miR-30c, as well as a miR-30mix could resensitize the NCI-H929 cells to dexamethasone treatment, thereby revealing great therapeutic potential. These results were validated *in vivo* by the use of murine xenograft models [98].

Several studies also suggested a role for dysregulated post-translational modification of Wnt pathway mediators in aberrant intrinsic Wnt pathway activation in MM cells. In 2015, Huang *et al.* reported that  $\beta$ -catenin is subject to sumoylation [99]. Previous studies already indicated that SUMO protein expression levels are upregulated in carcinogenic cellular processes, including oxidative stress and apoptosis [100]. Furthermore, sumoylation is known to be aberrantly activated in a large subset of MM patients and hyperactive sumoylation is correlated with adverse patient prognosis [101]. By siRNA-mediated downregulation of the effector protein SUMO-1, Huang *et al.* were able to interfere with the sumoylation process in MM cells *in vitro*. This resulted in a proteasome-mediated downregulation of  $\beta$ -catenin protein levels, which was accompanied by a reduction in canonical Wnt signaling and decreased expression of Wnt target genes. Combined, this results in increased numbers of apoptotic cells and subsequent growth inhibition of HMCLs [99].

Aberrant epigenetics were suggested to be responsible for intrinsic Wnt pathway activation in MM cells by Chim *et al.*, who analyzed DNA methylation of CpG islands, indicative of transcriptional repression and subsequent gene silencing, in the promoter regions of the Wnt antagonists WIF1, Dkk3, APC and sFRP1, sFRP2, sFRP4 and sFRP5. Of the 50 MM patients enrolled in this study, 42% showed abnormal methylation of at least one of these genes. Within this group, more than two-thirds of the patients even showed methylation of two or more inhibitors. This is in contrast to healthy PC control samples, in which no methylation of any of these genes was detected [102].

Very recently, van Andel *et al.* proposed two additional mechanisms for Wnt/ $\beta$ -catenin activation in MM cells. The first hypothesis concerns the loss of the tumor suppressor deubiquitinating enzyme CYLD, which is a known negative regulator of NF $\kappa$ B, TGF $\beta$  and Notch signaling [103-105]. A previous study by Tauriello

*et al.* already reported that loss of CYLD results in hyperubiquitination of Dvl, thereby augmenting active complex formation at the plasma membrane upon Wnt stimulation and enhanced downstream  $\beta$ -catenin signaling levels [106]. The current study reports highly variable CYLD levels in both HMCLs and primary PC isolates from MM patients and correlates loss of CYLD, either by mutation or complete deletion of the locus, to MGUS progression and poor clinical prognosis in MM patients. Loss of CYLD in HMCLs was found to enhance  $\beta$ -catenin stabilization and localization to the nucleus, increase  $\beta$ -catenin-LEF/TCF reporter activity and enhance MM cell growth and survival. Overall, loss of CYLD was associated with a Wnt-signaling gene expression signature [107]. Another study published by Van Andel *et al.* in 2017 put more focus on the role of the BM microenvironment as a supportive niche for MM development. Numerous previous studies already showed the presence of R-spondins in the BM microenvironment, which are essential factors for osteoblastogenesis and thereby play an important role in bone development and homeostasis [108]. R-spondins are Wnt/ $\beta$ -catenin agonists and function by binding to their cognate receptors LGR4, LGR5 and LGR6 at the plasma membrane and subsequently regulate Wnt (co)-receptor turnover dynamics via the E3 ubiquitin ligases Rnf43 and Znf3 [109]. The current study revealed aberrant expression of LGR4 in the majority of HMCLs, as well as primary PC isolates from MM patients. Interestingly, LGR4 overexpression is at least partially regulated via STAT-3 signaling, which in turn is mediated by IL-6, another cytokine that is vastly present in the BM microenvironment of MM patients. Simultaneous stimulation of LGR4-positive HMCLs with Wnt ligand and R-spondin resulted in a major increase in LRP6 phosphorylation,  $\beta$ -catenin stabilization and translocation to the nucleus, activation of a Wnt reporter construct and an increase in MM cell proliferation, while the LGR-4 negative HMCL L363 did not show this. Stimulation with R-spondin alone did not result in Wnt pathway activation in the majority of cell lines [110]. This underlines the fact that aberrant R-spondin-LGR signaling only causes Wnt hypersensitivity in the context of an already active Wnt pathway, and not as a primary pathway activation event. In a very recent follow-up study Ren *et al.* indicated an important role for the heparan sulfate proteoglycan syndecan-1 in MM Wnt signaling activation. Syndecan-1 is an ECM-related transmembrane protein that is expressed by malignant PCs and to a lesser extent healthy PCs as well. It has previously been shown to be important for the connection between PCs and the BM microenvironment and furthermore impacts MM cell growth and survival [111]. In this study Ren *et al.* showed that the heparan sulfate chains that decorate syndecan-1 are able to bind Wnt ligands, as well as R-spondin, and thereby facilitates active and efficient Wnt-receptor complex formation on the MM plasma membrane. Knockdown of the enzyme responsible for functional syndecan-1 assembly was found to result in a reduction of Wnt signaling and impaired cell growth of a panel of HMCLs [112].



### 4.3 | Intrinsic canonical Wnt signaling is crucial for multiple myeloma cell survival

Besides the controversial mechanism that is responsible for activation of the canonical Wnt pathway in MM cells, there are some additional observations that remain unclear. Although Derksen *et al.* showed that MM PCs have an aberrantly active Wnt pathway due to  $\beta$ -catenin overexpression, signal transduction in response to Wnt ligands remained functional. Additional stimulation by Wnt3a-conditioned medium, purified Wnt3a, treatment with LiCl, or ectopic expression of constitutively active  $\beta$ -catenin, all resulted in a further two to four-fold increase in proliferation of HMCLs [24]. MM cells thus still respond to Wnt ligands, irrespective of an already constitutive active pathway. However, it is not clear if stimulation occurs in a paracrine fashion, as a result of microenvironment-derived Wnts, or in an autocrine fashion by the canonical ligands that are expressed by MM cells themselves, or combinations thereof.

The major topic for discussion, however, concerns the biological consequences of intrinsic canonical Wnt signaling in MM. In 2003, Qiang *et al.* reported that Wnt pathway stimulation of HMCLs by Wnt3a-conditioned medium resulted in activation of the canonical Wnt pathway. This was demonstrated by increased levels and activation of Dvl2 and Dvl3, cellular stabilization of transcriptionally active  $\beta$ -catenin and an approximate six-fold increase in Wnt activity using a TopFlash reporter assay that is indicative of TCF/LEF-mediated transcription. However, they did not report an effect on the level of cell proliferation. Instead, major morphological changes were observed: the MM cells acquired a fibroblast-like phenotype, started to become adherent and developed filopodia-like protrusions [23]. This was in strong contrast to what was published by Derksen *et al.* in 2004. Here, stimulation of the Wnt pathway by purified Wnt3a, subsequent stabilization of transcriptionally active  $\beta$ -catenin and increased TopFlash reporter activity was accompanied by a two to four-fold increase in cell proliferation. In this study, no morphological changes of MM cells were reported [24]. Interestingly, both authors included NCI-H929 in their panel of HMCLs, so these contradictory results cannot be explained by a differential use of cell lines. However, it is known that the exact cellular outcome of Wnt signaling is influenced by many additional factors, including the level of Wnt ligands present like was observed for HSC self-renewal capacity. Especially in the case of Wnt-conditioned medium, the actual concentration of Wnt ligand is difficult to determine. In 2007, in accordance with the last study, Sukhdeo *et al.* reported that termination of Wnt/ $\beta$ -catenin signaling inhibited MM cell proliferation. By treating HMCLs with the small molecular compound PKF115-584, which interferes with the transcriptionally active  $\beta$ -catenin-TCF/LEF complex, cell cycle arrest in the G1 phase was induced. This resulted in increased levels of

cleaved caspases 3, 8, and 9 and a subsequent gain in the number of apoptotic cells [84].

Since all previous observations are based on *in vitro* experiments, several independent research groups used genetically engineered mouse models to gain more insight into the *in vivo* mechanism of action. Both Yaccoby *et al.* and Qiang *et al.* reported a reduction in MM tumor growth upon forced activation of the Wnt signaling pathway. Yaccoby *et al.* used the SCID-rab model and, upon transplantation with primary MM cells, treated these mice with antibodies to neutralize the canonical Wnt inhibitor Dkk1. This resulted in a general reduction of MM tumor burden [77]. In a slightly different approach, Qiang *et al.* stably transduced the HMCLNCI-H929 with a Wnt3a expression construct. Although subsequent stabilization of  $\beta$ -catenin was confirmed, this again did not result in increased cell growth *in vitro* or *in vivo* upon subcutaneous transplantation into SCID mice [79]. Edwards *et al.* used the C57BL/KaLwRij model, which was engrafted with murine 5TGM1 MM cell line, followed by treatment with the GSK3 inhibitor LiCl to stimulate canonical Wnt signaling. This resulted in a decrease in tumor burden in bone, but concurrently resulted in increased tumor growth when MM cells were inoculated subcutaneously. Furthermore, expression of dominant negative TCF4 did not affect the LiCl-induced reduction in tumor burden in bone [78]. This suggests that the reported observations might result from interference with molecular processes distinct from canonical Wnt signaling, which seems plausible since GSK3 is involved in many additional cellular processes. More recently, two similar studies that address Wnt signaling in MM mouse models were published by Dutta-Simmons *et al.* and Ashihara *et al.*, that used a rather different approach. Instead of enforcing active Wnt signaling, the canonical pathway was inhibited by specific knockdown of  $\beta$ -catenin. The first study used a shRNA-mediated approach for efficient knockdown of  $\beta$ -catenin. After the *in vitro* observation that treatment with Wnt3a-conditioned medium enhanced cell proliferation in HMCLs,  $\beta$ -catenin knockdown was found to greatly reduce this effect. When these MM cells were intravenously injected into NOD/SCID mice, the  $\beta$ -catenin knockdown group showed a mean survival of 94 days, versus 25 days for control mice that were treated with a scrambled shRNA. In addition, the experimental group showed a significant reduction in tumor burden with less tumor nodules in the BM, as well as a dramatic decrease in the occurrence of metastasis compared to control mice [113]. A similar trend was reported by Ashihara *et al.*, who subcutaneously inoculated BALB/c albino nude mice with HMCLs. After 3-4 weeks, mice were injected around the site of active tumor development with either  $\beta$ -catenin siRNA or a control scrambled siRNA. Efficient  $\beta$ -catenin knockdown on the protein level was found to be correlated with significantly reduced MM tumor volume. This was

accompanied by decreased expression levels of the direct  $\beta$ -catenin target c-Myc and increased levels of cleaved caspase 3 [114].

Although the additional use of *in vivo* mouse models could not elucidate the exact molecular mechanism of Wnt signaling or its relevance for tumor growth, these studies, when combined with *in vitro* data, did reveal an interesting trend. Extra stimulation of the Wnt pathway did not confer a growth advantage for MM *per se*. However, almost complete termination of canonical Wnt signaling, either by knockdown of  $\beta$ -catenin or disruption of the transcriptionally active  $\beta$ -catenin-TCF/LEF complex, induced MM cell apoptosis and significantly reduced tumor growth. This is similar to what was observed for Wnt signaling in HSC biology and could be the direct result of essential growth factor deprivation.

The ultimate purpose of the canonical Wnt/ $\beta$ -catenin pathway is to activate transcription of Wnt target genes. *In vitro*, this process is studied by the TopFlash reporter assay, in which the cells are transfected with a promoter-reporter construct that contains multiple Wnt responsive elements (WRE) followed by the sequence encoding the luciferase enzyme. After addition of substrate, the amount of measurable product formed by the enzyme reflects the level of Wnt/ $\beta$ -catenin transcriptional activity. Some studies additionally analyze expression levels of up to three Wnt target genes, often including *MYC*, *CD44* and *CCND1*. Although these are all direct Wnt target genes, *MYC* and *CD44* are both a-specific, since their activity is incorporated in and influenced by many other cell signaling pathways [115, 116]. Additionally, in MM *CCND1* is not an ideal candidate, since upregulation of this gene is very often observed, either due to gene duplication or chromosomal translocations involving the cyclin-D locus [117]. When Wnt target gene activation upon stimulation of MM cells with Wnt3a was studied on a larger scale by microarray, no significant increase in the expression level of the Wnt target gene panel was observed [64]. One explanation for this observation is that Wnt/ $\beta$ -catenin-mediated transcription in MM cells is thought to occur solely through LEF1 of the TCF/LEF family. The *LEF1* gene is however quite distinct from the TCF genes. Whereas all TCFs are able to produce an "E" tail isoform at their carboxyl terminus, the *LEF1* gene does not encode such a tail at all. This "E" tail, which encodes a DNA-binding domain and a region that facilitates interaction with p300, was shown to be essential for the regulation of multiple Wnt target genes. The TopFlash reporter, with the multimerized WREs, is however so optimally constructed that reporter activation is tail-independent [118]. This could at least partially explain why a positive TopFlash assay is not necessarily accompanied by robust Wnt target gene expression upon Wnt stimulation. However, Sukhdeo *et al.* showed that several HMCLs additionally express TCF-4, further complicating the matter [84]. Another explanation could be that almost all Wnt target genes

are identified from studies performed in colon cancer. The intestine, as well as the skin, is a site of very active canonical Wnt signaling by nature. These levels are more modest in mammary tissue and the central nervous system, but even lower in the hematopoietic system [89]. Since the concentration of Wnt ligands at least partially determine which Wnt target genes are transcribed, it could very well be that canonical Wnt signaling in MM does result in active transcription, but that these Wnt target genes have not yet been identified because they differ from the Wnt target genes that are activated in colon tissue. Of note, also no Wnt target genes have yet been identified in developing B cells, which also have an active canonical Wnt signaling pathway. Furthermore, MM cells are derived from the hematopoietic lineage and therefore genes which are present in epithelial tissues, including Wnt target genes, could be epigenetically silenced.

#### **4.4 | Active Wnt signaling in multiple myeloma cells promotes drug resistance**

Besides the possible effects of Wnt signaling on MM cell proliferation and subsequent MM disease progression, two studies suggest a role for Wnt in cell adhesion-mediated drug resistance (CAM-DR) of MM. Qiang *et al.* already reported that Wnt ligands can induce migration and invasion of MM cells by activating the non-canonical Wnt pathway mediators RhoA and PKC [83]. In 2007, Kobune *et al.* followed up on this study by showing that levels of Wnt3 ligand, produced in an autocrine fashion by the HMCLs, positively correlated with adhesive properties of MM cells to BM stromal cells *in vitro*. This finding was accompanied by stabilization of  $\beta$ -catenin protein levels and activation of RhoA [25]. It is generally accepted that MM cell adhesion to BM stromal cells does not only contribute to MM bone disease, but also plays a critical role in CAM-DR [119]. In accordance with this hypothesis, Kobune *et al.* reported that the level of Wnt3-mediated MM cell adhesion negatively correlated with the degree of drug sensitivity of MM cells to doxorubicin. Furthermore, Wnt pathway inhibition by treatment with the Wnt antagonist sFRP1, siRNA-mediated knockdown of Wnt3 ligand, or inhibition of the effector RhoA kinase ROCK by Y27632, rescued MM cell sensitivity to doxorubicin [25]. In 2011, Bjorklund *et al.* reported that long term exposure of HMCLs to lenalidomide increased the level of drug resistance to lenalidomide up to 2500-fold. Extensive analyses showed that this was accompanied by an up to 20-fold increase in  $\beta$ -catenin protein levels, a significant gain in TopFlash reporter activity and enhanced expression of the Wnt target genes cyclin-D1 and c-Myc. This was found to result from a general suppression of CK1 $\alpha$ , one of the members of the  $\beta$ -catenin destruction complex, and inactivation of GSK3 $\alpha/\beta$  due to increased phosphorylation of inhibitory residues. Additional treatment with recombinant

Wnt3a ligand resulted in an even further increase of MM lenalidomide resistance, while shRNA-mediated knockdown of  $\beta$ -catenin greatly rescued drug sensitivity [120]. More recently, a follow-up study by the same group was published in which they identified the direct Wnt target gene CD44 as the downstream effector molecule of Wnt-mediated lenalidomide resistance in MM. This hyaluronan-binding protein was found to be overexpressed by lenalidomide-resistant HMCLs *in vitro*, and these cells showed increased adhesive potential to BM stromal cells, indicative for CAM-DR. Inhibition of CD44 reduced the adhesive properties of MM cells and rescued sensitivity to lenalidomide, reflected by an increase in apoptotic cell numbers. Interestingly, *in vitro* treatment of lenalidomide-resistant HMCLs with the pharmaceutical agent ATRA resulted in decreased  $\beta$ -catenin mRNA and protein, as well as downregulated CD44 transcription and expression. In addition, the combinatorial treatment of ATRA with lenalidomide in NOD/SCID mice that were subcutaneously engrafted with lenalidomide-resistant HMCLs, resulted in significant reduction of tumor growth and a trend towards increased survival. Also in primary PC isolates from lenalidomide-treated MM patients with relapsed or refractory disease, this combinatorial treatment of ATRA with lenalidomide showed a clear reduction in MM cell viability [121].

## 5 | THE WNT PATHWAY AS A POTENTIAL THERAPEUTIC TARGET IN MULTIPLE MYELOMA

It seems counterintuitive that MM cells require an active intrinsic canonical Wnt pathway to maintain cell survival and tumor growth, but at the same time also upregulate the canonical Wnt inhibitor Dkk1. However, Dkk1 was found to be a direct gene target of canonical Wnt signaling as well and could therefore function in a negative feedback loop, like is established for Axin2 [122]. In this perspective, Dkk1 could be acknowledged as a tumor suppressor protein. Indeed, Dkk1 expression was found to be high in early stages of active MM, but was lower or even undetectable in a subset of patients with advanced disease. This was found to be the direct result of acquired CpG island promoter methylation and resulted in increased intrinsic Wnt signaling activity in MM cells [123]. Targeting the Wnt pathway could therefore be an interesting new avenue to treat MM: 1) it could increase apoptosis of MM cells and thereby decrease tumor growth; 2) it could reduce Dkk1 levels secreted by MM cells and thereby reduce osteolytic bone disease and subsequent bone-related symptoms; 3) it could reduce MM acquired CAM-DR and thereby increase the response to established treatment regimens.

Although Wnt signaling is extensively studied and its role in malignancies is well established, biologicals targeting this cascade have not yet entered the standard-

of-care procedures. This is primarily due to concerns about drug safety, as Wnt signaling is required for stem cell maintenance and tissue homeostasis during the complete course of adult life [124]. However, also the complexity of the pathway, its subtle regulation and cellular outcome makes it difficult to develop a successful strategy. Levels of  $\beta$ -catenin are not just under control of the Wnt-Fzd-LRP-Dvl axis, but are also regulated by alternative pathways, including HGF-Met, prostaglandin PGE<sub>2</sub>-EP<sub>2/4</sub> and estrogen E<sub>2</sub>-ER $\alpha$  [125-127]. Environmental factors such as hypoxia and glucose levels were also shown to affect  $\beta$ -catenin activation [128, 129]. In addition,  $\beta$ -catenin not only facilitates the transcription of Wnt target genes by association with the LEF/TCF family members, but also co-operates with FOXO, multiple SOX transcription factors and SMADs to regulate cellular functions [130-132].

## 5.1 | Molecular Wnt pathway inhibitors in the clinic

Despite the aforementioned challenges, many compounds that modulate Wnt pathway activity have been identified and developed in the past decade and some have now made it to the first phases of clinical trials. The compounds LGK974 and ETC-159, also referred to as ETC-1922159, are small molecules that block the secretion of Wnt ligands by inhibition of porcupine. This membrane-bound O-acetyltransferase is required for Wnt palmitoylation, which is an essential step in ligand secretion [133]. Both drugs were initially identified by screening large libraries of small molecule compounds. Testing of LGK974 *in vitro* showed that this drug blocks secretion of all canonical Wnt ligands, inhibits Wnt-driven phosphorylation and activation of LRP6 and reduces Wnt target gene expression as assessed by Axin2 mRNA levels in a large panel of human head and neck cancer cell lines. Additional *in vivo* experiments in a Wnt-driven murine tumor model showed significant tumor reduction upon treatment with a well-tolerated dose of LGK974 [134]. Similar results were obtained for ETC-159. *In vivo* experiments showed that this orally-available drug reduces tumor growth in a Wnt-sensitive murine mammary cancer model, accompanied by a reduction in nuclear  $\beta$ -catenin levels and decreased expression of Wnt target genes, including Axin2 [135]. Both LGK974 and ETC-159 are now in phase I clinical trials for advanced Wnt sensitive solid tumors.

For the antibody-based inhibitor OPM-54F28 the first dose-escalating phase I clinical trial in solid tumors has been completed in 2016. OPM-54F28 consists of the cysteine-rich domain of Fzd8 fused to the IgG1 Fc region and thereby acts as a decoy receptor for extracellular Wnt ligands. Also for this compound, efficacy was validated in a Wnt-sensitive murine cancer model and additional *in vivo* data showed synergy in combination with the chemotherapeutic agent gemcitabine.

Furthermore, a reduction in the cancer stem cell population was reported [136]. Currently, three phase I clinical trials are ongoing in which OPM-54F28 is combined with standard-of-care drugs for hepatocellular, ovarian and (advanced) pancreatic cancer.

Several monoclonal antibody therapies that directly target the membrane-bound receptor complex have also been developed. OMP-18R5, also referred to as vantictumab, binds to a conserved epitope of the canonical Fzd1, Fzd2, Fzd5, Fzd7 and Fzd8 receptors. Binding studies showed that this blocks the binding of Wnt3a to the extracellular domain of Fzd5, which subsequently leads to inhibition of downstream Wnt/ $\beta$ -catenin signaling. Treatment of human solid tumor xenografts in mice showed a clear reduction in tumor growth in a subset of the tumors and also reported significant synergistic effects in combination with standard chemotherapeutic agents, including taxol and gemcitabine [137]. Three phase I clinical trials are currently testing this compound in combination with standard-of-care chemotherapy in advanced solid tumors.

Most compounds developed to inhibit canonical Wnt signaling function by interfering with the downstream  $\beta$ -catenin-LEF/TCF complex [138]. One of the most successful agents in this category are the  $\beta$ -catenin-LEF/TCF antagonists PKF115-584 and the structurally-related small molecule inhibitor CGP049090. These natural compounds of fungal origin were first identified by a high-throughput ELISA-based screen. Although the exact molecular mechanism of Wnt interference has yet to be established, both compounds were found to reduce  $\beta$ -catenin immunoprecipitation efficiency and also inhibited the  $\beta$ -catenin-APC complex, suggesting a direct binding affinity for  $\beta$ -catenin [139]. PKF115-584 was also thoroughly characterized in a pre-clinical MM study by Sukhdeo *et al.* This compound was found to reduce  $\beta$ -catenin-LEF/TCF transcriptional activity and Wnt target gene expression, disrupts cell proliferation and induces cytotoxicity in HMCLs and primary PC isolates of MM patients. Additional *in vivo* data reported a decrease in tumor growth and prolonged survival in a murine xenograft model using a HMCL [84]. Although many  $\beta$ -catenin-LEF/TCF antagonists have proven to be successful in pre-clinical research, most of them have not yet entered clinical trials. The small molecule inhibitor PRI-724, which blocks the transcriptional co-factor CBP, is an exception. Although therapeutic specificity could be questioned, pre-clinical studies and a dose escalating phase I clinical trial in advanced/metastatic pancreatic cancer did not show major adverse events at a therapeutic dosage [140]. In 2015, a phase I/II clinical trial of PRI-724 in acute myeloid leukemia and chronic myeloid leukemia was completed. No study results have been published yet.



It is yet too early to determine which strategy of inhibiting Wnt signaling in cancer patients will be most successful and targeting the Wnt signaling pathway for the treatment of MM is still at the preclinical stage. Multiple studies have been published in the last years suggesting a range of molecules that inhibit Wnt signaling in MM, either as a single agent or in combination with currently used therapies. An example is the  $\beta$ -catenin inhibitor BC2059 that was shown to induce apoptosis of HMCLs, even in the presence of the protective feeder cell line HS5. Apoptosis of malignant PCs from relapsed and/or refractory MM patients induced by BC2059 was reported to be synergistically enhanced when combined with the proteasome inhibitor Bortezomib. Furthermore, NOD/SCID/gamma mice transplanted with HMCL U266 intravenously, that were treated with BC2059 showed an impaired tumor burden and an increased survival when compared to the vehicle control [141]. In addition, drugs that have been approved by the US Food and Drug Administration for the treatment of other diseases have been reported as candidates for treatment of MM. Pyrvinium pamoate (PP) is an oral anthelmintic drug that was recently reported to inhibit Wnt signaling through activation of the destruction complex member CK1 $\alpha$ , thereby diminishing active  $\beta$ -catenin levels. Treatment of both the HMCL RPMI-8226 as well as primary MM cells with PP resulted in an increase in apoptosis. Combinatorial treatment with Bortezomib was also reported in this study to result in a synergistic effect on MM cell viability [142]. Although the results of these and many other studies are hopeful, challenges for moving these drugs towards treatment of MM lie ahead. As discussed previously, the Wnt pathway has an important role in keeping adult tissue homeostasis by regulating multiple stem cell populations. Long-term Wnt blockage could very well result in disruption of these processes and ultimately lead to severe side effects. In addition, resistance to Wnt inhibiting agents should also be taken into account. Whereas treatment with monoclonal antibodies can result in the occurrence of drug resistance due to downregulation of the target from the MM cell membrane, treatment of the Wnt pathway at a more downstream level can put extensive selective pressure on cells. This has indeed been described for the colorectal cancer cell line VACO6, which harbors a constitutively active Wnt pathway due to translocation of R-spondin3, resulting in a *PTPRK(e1)-RSPO3(e2)* fusion. Although clear sensitivity to the Porcupine inhibitor LGK974 was observed *in vitro* and *in vivo* in a murine xenograft model, long-term treatment led to the emergence of a resistant population. This resistant population was characterized by two novel frame-shift deletions in *AXIN1*, resulting in protein loss [143]. Although no mutations in Wnt pathway components in MM have been reported, treatment of the active Wnt signaling pathway can thus result in emergence of such mutations. This stresses the need for further research in order to determine specificity and safety of targeting the Wnt pathway in the treatment of MM.



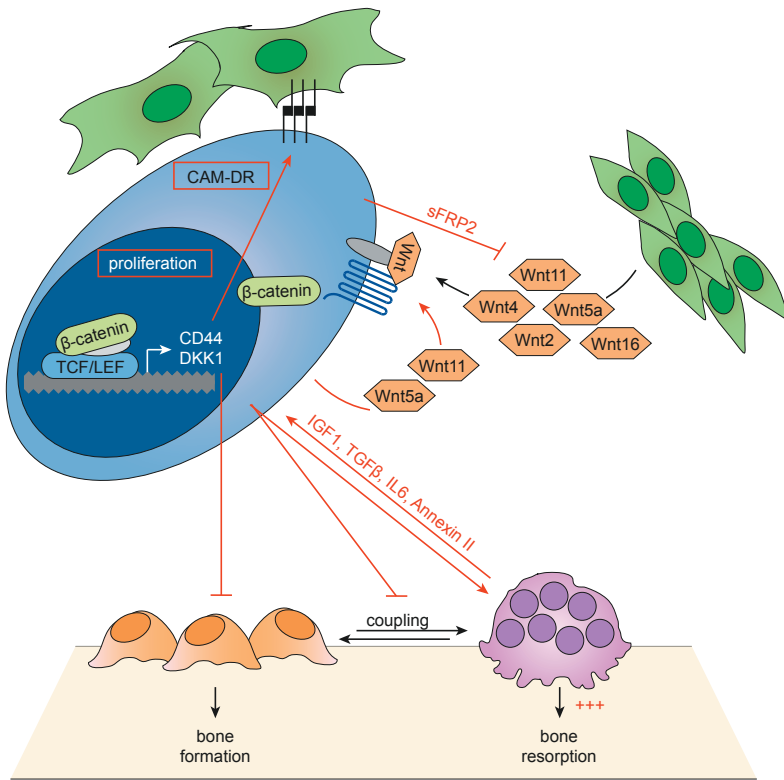


**Figure 4 | The Wnt signaling pathway is a central player in MM.** MM cells have an active intrinsic Wnt pathway. This can be stimulated by Wnt ligands produced by BM cells including MSC, or in an autocrine fashion via at least Wnt5a and Wnt11. Canonical Wnt pathway activation via Fzd1, Fzd6, or Fzd7 leads to active LEF/TCF mediated transcription of Wnt target genes that promote tumor growth. The transcribed Wnt antagonist Dkk1 is secreted into the BM microenvironment and inhibits osteoblast proliferation, differentiation and survival. Combined with stimulation of osteoclast activity, this results in disruption of bone homeostasis and increased osteolytic bone resorption. The growth factors IGF-1 and TGF- $\beta$  that are released from the bone matrix, together with osteoclast-secreted factors IL-6 and Annexin II, further stimulate MM cells. Expression of the Wnt target gene CD44, together with stimulation of the non-canonical Wnt pathways, stimulate adhesive properties of MM cells to BM stromal cells. This induces cell adhesion-mediated resistance of MM cells to conventional drug therapies.

## 6 | CONCLUSION

The Wnt signaling pathway is implicated in multiple aspects of MM disease (Figure 4). By secreting Wnt antagonists including Dkk1, MM cells disturb the balance between bone-forming osteoblasts and bone-resorbing osteoclast. The subsequent disruption of bone homeostasis results in the development of

osteolytic bone lesion. This does not only provide the MM cells with a direct and indirect growth advantage, resulting in tumor progression, but also causes MM patients to suffer from bone pain and pathologic fractures. Intrinsic canonical Wnt/ $\beta$ -catenin signaling has been reported to promote MM cell survival and thereby establishes disease progression. This is at least partially achieved via autocrine stimulation. In addition, both canonical and non-canonical Wnt signaling pathways are associated with acquired drug resistance. This is most likely mediated by adhesive properties of MM cells to BM stromal cells. The acquisition of MM resistance to conventional therapies is an emerging clinical problem and negatively influences patient outcome. Targeting the Wnt pathway could therefore be an interesting new avenue to treat MM. It would increase apoptosis of MM cells and as such decrease tumor growth, it would reduce secretion of Dkk1 in the BM microenvironment and thereby restrict osteolytic bone disease, and it would reduce CAM-DR in MM and thereby facilitate a more successful and prolonged response to already established drug treatment options.

## **ACKNOWLEDGEMENTS**

This work was supported in part by a Bas Mulder Award from the Dutch Cancer Foundation (KWF)/Alped'HuZes foundation (No. UU 2015-7663) and a project grant from the Dutch Cancer Foundation (KWF)/Alped'HuZes foundation (No. 11108).

## REFERENCES

1. Kumar SK, Rajkumar V, Kyle RA, van Duin M, Sonneveld P, Mateos MV, et al. Multiple myeloma. *Nat Rev Dis Primers*. 2017;3:17046.
2. Rollig C, Knop S, Bornhauser M. Multiple myeloma. *Lancet*. 2015;385(9983):2197-2208.
3. Rajkumar SV, Dimopoulos MA, Palumbo A, Blade J, Merlini G, Mateos MV, et al. International Myeloma Working Group updated criteria for the diagnosis of multiple myeloma. *Lancet Oncol*. 2014;15(12):e538-48.
4. Kyle RA, Remstein ED, Therneau TM, Dispenzieri A, Kurtin PJ, Hodnefield JM, et al. Clinical course and prognosis of smoldering (asymptomatic) multiple myeloma. *N Engl J Med*. 2007;356(25):2582-2590.
5. Palumbo A, Anderson K. Multiple myeloma. *N Engl J Med*. 2011;364(11):1046-1060.
6. Silbermann R, Roodman GD. Myeloma bone disease: Pathophysiology and management. *J Bone Oncol*. 2013;2(2):59-69.
7. Pawlyn C, Morgan GJ. Evolutionary biology of high-risk multiple myeloma. *Nat Rev Cancer*. 2017;17(9):543-556.
8. Logan CY, Nusse R. The Wnt signaling pathway in development and disease. *Annu Rev Cell Dev Biol*. 2004;20:781-810.
9. Nusse R, Fuerer C, Ching W, Harnish K, Logan C, Zeng A, et al. Wnt signaling and stem cell control. *Cold Spring Harb Symp Quant Biol*. 2008;73:59-66.
10. Clevers H. Wnt/beta-catenin signaling in development and disease. *Cell*. 2006;127(3):469-480.
11. Flanagan DJ, Austin CR, Vincan E, Pheffe TJ. Wnt Signalling in Gastrointestinal Epithelial Stem Cells. *Genes (Basel)*. 2018;9(4):10.3390/genes9040178.
12. Zhang Y, Morris JP, Ath, Yan W, Schofield HK, Gurney A, Simeone DM, et al. Canonical wnt signaling is required for pancreatic carcinogenesis. *Cancer Res*. 2013;73(15):4909-4922.
13. Kovacs D, Migliano E, Muscardin L, Silipo V, Catricala C, Picardo M, et al. The role of Wnt/beta-catenin signaling pathway in melanoma epithelial-to-mesenchymal-like switching: evidences from patients-derived cell lines. *Oncotarget*. 2016;7(28):43295-43314.
14. Rapp J, Jaromi L, Kvell K, Miskei G, Pongracz JE. WNT signaling - lung cancer is no exception. *Respir Res*. 2017;18(1):167-017-0650-6.
15. Yang M, Wang M, Li X, Xie Y, Xia X, Tian J, et al. Wnt signaling in cervical cancer? *J Cancer*. 2018;9(7):1277-1286.
16. Yu QC, Verheyen EM, Zeng YA. Mammary Development and Breast Cancer: A Wnt Perspective. *Cancers (Basel)*. 2016;8(7):10.3390/cancers8070065.
17. Murillo-Garzon V, Kypta R. WNT signalling in prostate cancer. *Nat Rev Urol*. 2017;14(11):683-696.
18. McCord M, Mukouyama YS, Gilbert MR, Jackson S. Targeting WNT Signaling for Multifaceted Glioblastoma Therapy. *Front Cell Neurosci*. 2017;11:318.
19. Tiemessen MM, Staal FJ. Wnt signaling in leukemias and myeloma: T-cell factors are in control. *Future Oncol*. 2013;9(11):1757-1772.
20. Baron R, Kneissel M. WNT signaling in bone homeostasis and disease: from human mutations to treatments. *Nat Med*. 2013;19(2):179-192.

21. Edwards CM, Zhuang J, Mundy GR. The pathogenesis of the bone disease of multiple myeloma. *Bone*. 2008;42(6):1007-1013.
22. Fowler JA, Edwards CM, Croucher PI. Tumor-host cell interactions in the bone disease of myeloma. *Bone*. 2011;48(1):121-128.
23. Qiang YW, Endo Y, Rubin JS, Rudikoff S. Wnt signaling in B-cell neoplasia. *Oncogene*. 2003;22(10):1536-1545.
24. Derksen PW, Tjin E, Meijer HP, Klok MD, MacGillavry HD, van Oers MH, et al. Illegitimate WNT signaling promotes proliferation of multiple myeloma cells. *Proc Natl Acad Sci U S A*. 2004;101(16):6122-6127.
25. Kobune M, Chiba H, Kato J, Kato K, Nakamura K, Kawano Y, et al. Wnt3/RhoA/ROCK signaling pathway is involved in adhesion-mediated drug resistance of multiple myeloma in an autocrine mechanism. *Mol Cancer Ther*. 2007;6(6):1774-1784.
26. Shimizu H, Julius MA, Giarre M, Zheng Z, Brown AM, Kitajewski J. Transformation by Wnt family proteins correlates with regulation of beta-catenin. *Cell Growth Differ*. 1997;8(12):1349-1358.
27. Janda CY, Waghray D, Levin AM, Thomas C, Garcia KC. Structural basis of Wnt recognition by Frizzled. *Science*. 2012;337(6090):59-64.
28. Kikuchi A, Yamamoto H, Kishida S. Multiplicity of the interactions of Wnt proteins and their receptors. *Cell Signal*. 2007;19(4):659-671.
29. Nile AH, Hannoush RN. Fatty acylation of Wnt proteins. *Nat Chem Biol*. 2016;12(2):60-69.
30. Langton PF, Kakugawa S, Vincent JP. Making, Exporting, and Modulating Wnts. *Trends Cell Biol*. 2016;26(10):756-765.
31. Gross JC, Chaudhary V, Bartscherer K, Boutros M. Active Wnt proteins are secreted on exosomes. *Nat Cell Biol*. 2012;14(10):1036-1045.
32. Kimelman D, Xu W. Beta-Catenin Destruction Complex: Insights and Questions from a Structural Perspective. *Oncogene*. 2006;25(57):7482-7491.
33. Zeng X, Huang H, Tamai K, Zhang X, Harada Y, Yokota C, et al. Initiation of Wnt signaling: control of Wnt coreceptor Lrp6 phosphorylation/activation via frizzled, dishevelled and axin functions. *Development*. 2008;135(2):367-375.
34. Stadel R, Hoffmans R, Basler K. Transcription under the control of nuclear Arm/beta-catenin. *Curr Biol*. 2006;16(10):R378-85.
35. Hua Y, White-Gilbertson S, Kellner J, Rachidi S, Usmani SZ, Chiosis G, et al. Molecular chaperone gp96 is a novel therapeutic target of multiple myeloma. *Clin Cancer Res*. 2013;19(22):6242-6251.
36. Leung JY, Kolligs FT, Wu R, Zhai Y, Kuick R, Hanash S, et al. Activation of AXIN2 expression by beta-catenin-T cell factor. A feedback repressor pathway regulating Wnt signaling. *J Biol Chem*. 2002;277(24):21657-21665.
37. Anastas JN, Moon RT. WNT signalling pathways as therapeutic targets in cancer. *Nat Rev Cancer*. 2013;13(1):11-26.
38. Camilli TC, Weeraratna AT. Striking the target in Wnt-y conditions: intervening in Wnt signaling during cancer progression. *Biochem Pharmacol*. 2010;80(5):702-711.
39. Miller JR. The Wnts. *Genome Biol*. 2002;3(1):REVIEWS3001.
40. Kishida S, Yamamoto H, Kikuchi A. Wnt-3a and Dvl induce neurite retraction by activating Rho-associated kinase. *Mol Cell Biol*. 2004;24(10):4487-4501.

41. He X, Saint-Jeannet JP, Wang Y, Nathans J, Dawid I, Varmus H. A member of the Frizzled protein family mediating axis induction by Wnt-5A. *Science*. 1997;275(5306):1652-1654.
42. Weerkamp F, Baert MR, Naber BA, Koster EE, de Haas EF, Atkuri KR, et al. Wnt signaling in the thymus is regulated by differential expression of intracellular signaling molecules. *Proc Natl Acad Sci U S A*. 2006;103(9):3322-3326.
43. Katoh M. Networking of WNT, FGF, Notch, BMP, and Hedgehog signaling pathways during carcinogenesis. *Stem Cell Rev*. 2007;3(1):30-38.
44. Kawano Y, Kypta R. Secreted antagonists of the Wnt signalling pathway. *J Cell Sci*. 2003;116(Pt 13):2627-2634.
45. Daniels DL, Weis WI. ICAT inhibits beta-catenin binding to Tcf/Lef-family transcription factors and the general coactivator p300 using independent structural modules. *Mol Cell*. 2002;10(3):573-584.
46. Gooding S, Edwards CM. New approaches to targeting the bone marrow microenvironment in multiple myeloma. *Curr Opin Pharmacol*. 2016;28:43-49.
47. Van Den Berg DJ, Sharma AK, Bruno E, Hoffman R. Role of members of the Wnt gene family in human hematopoiesis. *Blood*. 1998;92(9):3189-3202.
48. Fairfield H, Falank C, Avery L, Reagan MR. Multiple myeloma in the marrow: pathogenesis and treatments. *Ann N Y Acad Sci*. 2016;1364(1):32-51.
49. Ling L, Nurcombe V, Cool SM. Wnt signaling controls the fate of mesenchymal stem cells. *Gene*. 2009;433(1-2):1-7.
50. Staal FJ, Luis TC, Tiemessen MM. WNT signalling in the immune system: WNT is spreading its wings. *Nat Rev Immunol*. 2008;8(8):581-593.
51. Terauchi M, Li JY, Bedi B, Baek KH, Tawfeek H, Galley S, et al. T lymphocytes amplify the anabolic activity of parathyroid hormone through Wnt10b signaling. *Cell Metab*. 2009;10(3):229-240.
52. Maeda K, Kobayashi Y, Udagawa N, Uehara S, Ishihara A, Mizoguchi T, et al. Wnt5a-Ror2 signaling between osteoblast-lineage cells and osteoclast precursors enhances osteoclastogenesis. *Nat Med*. 2012;18(3):405-412.
53. Pederson L, Ruan M, Westendorf JJ, Khosla S, Oursler MJ. Regulation of bone formation by osteoclasts involves Wnt/BMP signaling and the chemokine sphingosine-1-phosphate. *Proc Natl Acad Sci U S A*. 2008;105(52):20764-20769.
54. Bennett CN, Longo KA, Wright WS, Suva LJ, Lane TF, Hankenson KD, et al. Regulation of osteoblastogenesis and bone mass by Wnt10b. *Proc Natl Acad Sci U S A*. 2005;102(9):3324-3329.
55. Almeida M, Han L, Bellido T, Manolagas SC, Kousteni S. Wnt proteins prevent apoptosis of both uncommitted osteoblast progenitors and differentiated osteoblasts by beta-catenin-dependent and -independent signaling cascades involving Src/ERK and phosphatidylinositol 3-kinase/AKT. *J Biol Chem*. 2005;280(50):41342-41351.
56. Sims NA, Martin TJ. Coupling the activities of bone formation and resorption: a multitude of signals within the basic multicellular unit. *Bonekey Rep*. 2014;3:481.
57. Dallas SL, Prideaux M, Bonewald LF. The osteocyte: an endocrine cell ... and more. *Endocr Rev*. 2013;34(5):658-690.

58. Poole KE, van Bezooijen RL, Loveridge N, Hamersma H, Papapoulos SE, Lowik CW, et al. Sclerostin is a delayed secreted product of osteocytes that inhibits bone formation. *FASEB J*. 2005;19(13):1842-1844.
59. Bonewald LF, Johnson ML. Osteocytes, mechanosensing and Wnt signaling. *Bone*. 2008;42(4):606-615.
60. Boyle WJ, Simonet WS, Lacey DL. Osteoclast differentiation and activation. *Nature*. 2003;423(6937):337-342.
61. Suda T, Takahashi N, Udagawa N, Jimi E, Gillespie MT, Martin TJ. Modulation of osteoclast differentiation and function by the new members of the tumor necrosis factor receptor and ligand families. *Endocr Rev*. 1999;20(3):345-357.
62. Wei W, Zeve D, Suh JM, Wang X, Du Y, Zerwekh JE, et al. Biphasic and dosage-dependent regulation of osteoclastogenesis by beta-catenin. *Mol Cell Biol*. 2011;31(23):4706-4719.
63. Santiago F, Oguma J, Brown AM, Laurence J. Noncanonical Wnt signaling promotes osteoclast differentiation and is facilitated by the human immunodeficiency virus protease inhibitor ritonavir. *Biochem Biophys Res Commun*. 2012;417(1):223-230.
64. Qiang Y, Rudikoff S. Wnt signaling pathways in multiple myeloma. Multiple Myeloma: Symptoms, Diagnosis and Treatment. New York: *Nova Science Publishers*. 2010;:51-75.
65. Silva I, Branco JC. Rank/Rankl/opg: literature review. *Acta Reumatol Port*. 2011;36(3):209-218.
66. Glass DA, 2nd, Bialek P, Ahn JD, Starbuck M, Patel MS, Clevers H, et al. Canonical Wnt signaling in differentiated osteoblasts controls osteoclast differentiation. *Dev Cell*. 2005;8(5):751-764.
67. Holmen SL, Zylstra CR, Mukherjee A, Sigler RE, Faugere MC, Bouxsein ML, et al. Essential role of beta-catenin in postnatal bone acquisition. *J Biol Chem*. 2005;280(22):21162-21168.
68. Alsayed Y, Ngo H, Runnels J, Leleu X, Singha UK, Pitsillides CM, et al. Mechanisms of regulation of CXCR4/SDF-1 (CXCL12)-dependent migration and homing in multiple myeloma. *Blood*. 2007;109(7):2708-2717.
69. Urashima M, Chauhan D, Uchiyama H, Freeman GJ, Anderson KC. CD40 ligand triggered interleukin-6 secretion in multiple myeloma. *Blood*. 1995;85(7):1903-1912.
70. Giuliani N, Bataille R, Mancini C, Lazzaretti M, Barille S. Myeloma cells induce imbalance in the osteoprotegerin/osteoprotegerin ligand system in the human bone marrow environment. *Blood*. 2001;98(13):3527-3533.
71. Callander NS, Roodman GD. Myeloma bone disease. *Semin Hematol*. 2001;38(3):276-285.
72. Abe M, Hiura K, Wilde J, Shioyasono A, Moriyama K, Hashimoto T, et al. Osteoclasts enhance myeloma cell growth and survival via cell-cell contact: a vicious cycle between bone destruction and myeloma expansion. *Blood*. 2004;104(8):2484-2491.
73. Abe M, Kido S, Hiasa M, Nakano A, Oda A, Amou H, et al. BAFF and APRIL as osteoclast-derived survival factors for myeloma cells: a rationale for TACI-Fc treatment in patients with multiple myeloma. *Leukemia*. 2006;20(7):1313-1315.
74. Li X, Pennisi A, Yaccoby S. Role of decorin in the antimyeloma effects of osteoblasts. *Blood*. 2008;112(1):159-168.

75. Morvan F, Boulukos K, Clement-Lacroix P, Roman Roman S, Suc-Royer I, Vayssiere B, et al. Deletion of a single allele of the Dkk1 gene leads to an increase in bone formation and bone mass. *J Bone Miner Res.* 2006;21(6):934-945.
76. Tian E, Zhan F, Walker R, Rasmussen E, Ma Y, Barlogie B, et al. The role of the Wnt-signaling antagonist DKK1 in the development of osteolytic lesions in multiple myeloma. *N Engl J Med.* 2003;349(26):2483-2494.
77. Yaccoby S, Ling W, Zhan F, Walker R, Barlogie B, Shaughnessy JD Jr. Antibody-based inhibition of DKK1 suppresses tumor-induced bone resorption and multiple myeloma growth in vivo. *Blood.* 2007;109(5):2106-2111.
78. Edwards CM, Edwards JR, Lwin ST, Esparza J, Oyajobi BO, McCluskey B, et al. Increasing Wnt signaling in the bone marrow microenvironment inhibits the development of myeloma bone disease and reduces tumor burden in bone in vivo. *Blood.* 2008;111(5):2833-2842.
79. Qiang YW, Shaughnessy JD Jr, Yaccoby S. Wnt3a signaling within bone inhibits multiple myeloma bone disease and tumor growth. *Blood.* 2008;112(2):374-382.
80. Iyer SP, Beck JT, Stewart AK, Shah J, Kelly KR, Isaacs R, et al. A Phase IB multicentre dose-determination study of BHQ880 in combination with anti-myeloma therapy and zoledronic acid in patients with relapsed or refractory multiple myeloma and prior skeletal-related events. *Br J Haematol.* 2014;167(3):366-375.
81. Munshi NC, Abonour R, Beck JT, Bensinger W, Facon T, Stockerl-Goldstein K, et al. Early Evidence of Anabolic Bone Activity of BHQ880, a Fully Human Anti-DKK1 Neutralizing Antibody: Results of a Phase 2 Study in Previously Untreated Patients with Smoldering Multiple Myeloma At Risk for Progression. *Blood.* 2012;120
82. Oshima T, Abe M, Asano J, Hara T, Kitazoe K, Sekimoto E, et al. Myeloma cells suppress bone formation by secreting a soluble Wnt inhibitor, sFRP-2. *Blood.* 2005;106(9):3160-3165.
83. Qiang YW, Walsh K, Yao L, Kedei N, Blumberg PM, Rubin JS, et al. Wnts induce migration and invasion of myeloma plasma cells. *Blood.* 2005;106(5):1786-1793.
84. Sukhdeo K, Mani M, Zhang Y, Dutta J, Yasui H, Rooney MD, et al. Targeting the beta-catenin/TCF transcriptional complex in the treatment of multiple myeloma. *Proc Natl Acad Sci U S A.* 2007;104(18):7516-7521.
85. Staal FJ, Clevers HC. WNT signalling and haematopoiesis: a WNT-WNT situation. *Nat Rev Immunol.* 2005;5(1):21-30.
86. Reya T, Duncan AW, Ailles L, Domen J, Scherer DC, Willert K, et al. A role for Wnt signalling in self-renewal of haematopoietic stem cells. *Nature.* 2003;423(6938):409-414.
87. Kirstetter P, Anderson K, Porse BT, Jacobsen SE, Nerlov C. Activation of the canonical Wnt pathway leads to loss of hematopoietic stem cell repopulation and multilineage differentiation block. *Nat Immunol.* 2006;7(10):1048-1056.
88. Scheller M, Huelsken J, Rosenbauer F, Taketo MM, Birchmeier W, Tenen DG, et al. Hematopoietic stem cell and multilineage defects generated by constitutive beta-catenin activation. *Nat Immunol.* 2006;7(10):1037-1047.
89. Luis TC, Ichii M, Brugman MH, Kincade P, Staal FJ. Wnt signaling strength regulates normal hematopoiesis and its deregulation is involved in leukemia development. *Leukemia.* 2012;26(3):414-421.

90. Luis TC, Naber BA, Fibbe WE, van Dongen JJ, Staal FJ. Wnt3a nonredundantly controls hematopoietic stem cell function and its deficiency results in complete absence of canonical Wnt signaling. *Blood*. 2010;116(3):496-497.
91. Reya T, O'Riordan M, Okamura R, Devaney E, Willert K, Nusse R, et al. Wnt signaling regulates B lymphocyte proliferation through a LEF-1 dependent mechanism. *Immunity*. 2000;13(1):15-24.
92. Qiang YW, Rudikoff S. Wnt signaling in B and T lymphocytes. *Front Biosci*. 2004;9:1000-1010.
93. Ranheim EA, Kwan HC, Reya T, Wang YK, Weissman IL, Francke U. Frizzled 9 knock-out mice have abnormal B-cell development. *Blood*. 2005;105(6):2487-2494.
94. Yu Q, Quinn WJ, 3rd, Salay T, Crowley JE, Cancro MP, Sen JM. Role of beta-catenin in B cell development and function. *J Immunol*. 2008;181(6):3777-3783.
95. Willis TG, Zalberg IR, Coignet LJ, Wlodarska I, Stul M, Jadayel DM, et al. Molecular cloning of translocation t(1;14)(q21;q32) defines a novel gene (BCL9) at chromosome 1q21. *Blood*. 1998;91(6):1873-1881.
96. Kramps T, Peter O, Brunner E, Nellen D, Froesch B, Chatterjee S, et al. Wnt/wingless signaling requires BCL9/legless-mediated recruitment of pygopus to the nuclear beta-catenin-TCF complex. *Cell*. 2002;109(1):47-60.
97. Mani M, Carrasco DE, Zhang Y, Takada K, Gatt ME, Dutta-Simmons J, et al. BCL9 promotes tumor progression by conferring enhanced proliferative, metastatic, and angiogenic properties to cancer cells. *Cancer Res*. 2009;69(19):7577-7586.
98. Zhao JJ, Lin J, Zhu D, Wang X, Brooks D, Chen M, et al. miR-30-5p functions as a tumor suppressor and novel therapeutic tool by targeting the oncogenic Wnt/beta-catenin/BCL9 pathway. *Cancer Res*. 2014;74(6):1801-1813.
99. Huang HJ, Zhou LL, Fu WJ, Zhang CY, Jiang H, Du J, et al. beta-catenin SUMOylation is involved in the dysregulated proliferation of myeloma cells. *Am J Cancer Res*. 2014;5(1):309-320.
100. Bettermann K, Benesch M, Weis S, Haybaeck J. SUMOylation in carcinogenesis. *Cancer Lett*. 2012;316(2):113-125.
101. Driscoll JJ, Pelluru D, Lefkimmatis K, Fulciniti M, Prabhala RH, Greipp PR, et al. The sumoylation pathway is dysregulated in multiple myeloma and is associated with adverse patient outcome. *Blood*. 2010;115(14):2827-2834.
102. Chim CS, Pang R, Fung TK, Choi CL, Liang R. Epigenetic dysregulation of Wnt signaling pathway in multiple myeloma. *Leukemia*. 2007;21(12):2527-2536.
103. Kovalenko A, Chable-Bessia C, Cantarella G, Israel A, Wallach D, Courtois G. The tumour suppressor CYLD negatively regulates NF-kappaB signalling by deubiquitination. *Nature*. 2003;424(6950):801-805.
104. Lim JH, Jono H, Komatsu K, Woo CH, Lee J, Miyata M, et al. CYLD negatively regulates transforming growth factor-beta-signalling via deubiquitinating Akt. *Nat Commun*. 2012;3:771.
105. Rajan N, Elliott RJ, Smith A, Sinclair N, Swift S, Lord CJ, et al. The cylindromatosis gene product, CYLD, interacts with MIB2 to regulate notch signalling. *Oncotarget*. 2014;5(23):12126-12140.



106. Tauriello DV, Haegebarth A, Kuper I, Edelmann MJ, Henraat M, Canninga-van Dijk MR, et al. Loss of the tumor suppressor CYLD enhances Wnt/beta-catenin signaling through K63-linked ubiquitination of Dvl. *Mol Cell*. 2010;37(5):607-619.
107. van Andel H, Kocemba KA, de Haan-Kramer A, Mellink CH, Piwowar M, Broijl A, et al. Loss of CYLD expression unleashes Wnt signaling in multiple myeloma and is associated with aggressive disease. *Oncogene*. 2017;36(15):2105-2115.
108. Shi GX, Zheng XF, Zhu C, Li B, Wang YR, Jiang SD, et al. Evidence of the Role of R-Spondin 1 and Its Receptor Lgr4 in the Transmission of Mechanical Stimuli to Biological Signals for Bone Formation. *Int J Mol Sci*. 2017;18(3):10.3390/ijms18030564.
109. de Lau W, Peng WC, Gros P, Clevers H. The R-spondin/Lgr5/Rnf43 module: regulator of Wnt signal strength. *Genes Dev*. 2014;28(4):305-316.
110. van Andel H, Ren Z, Koopmans I, Joosten SP, Kocemba KA, de Lau W, et al. Aberrantly expressed LGR4 empowers Wnt signaling in multiple myeloma by hijacking osteoblast-derived R-spondins. *Proc Natl Acad Sci U S A*. 2017;114(2):376-381.
111. Reijmers RM, Groen RW, Rozemuller H, Kuil A, de Haan-Kramer A, Csikos T, et al. Targeting EXT1 reveals a crucial role for heparan sulfate in the growth of multiple myeloma. *Blood*. 2010;115(3):601-604.
112. Ren Z, van Andel H, de Lau W, Hartholt RB, Maurice MM, Clevers H, et al. Syndecan-1 promotes Wnt/beta-catenin signaling in multiple myeloma by presenting Wnts and R-spondins. *Blood*. 2017;Epub ahead of print(blood-2017-07-797050)
113. Dutta-Simmons J, Zhang Y, Gorgun G, Gatt M, Mani M, Hideshima T, et al. Aurora kinase A is a target of Wnt/beta-catenin involved in multiple myeloma disease progression. *Blood*. 2009;114(13):2699-2708.
114. Ashihara E, Kawata E, Nakagawa Y, Shimazaki C, Kuroda J, Taniguchi K, et al. beta-catenin small interfering RNA successfully suppressed progression of multiple myeloma in a mouse model. *Clin Cancer Res*. 2009;15(8):2731-2738.
115. Kumar D, Sharma N, Giri R. Therapeutic Interventions of Cancers Using Intrinsically Disordered Proteins as Drug Targets: c-Myc as Model System. *Cancer Inform*. 2017;16:1176935117699408.
116. Bourguignon LY. Matrix Hyaluronan Promotes Specific MicroRNA Upregulation Leading to Drug Resistance and Tumor Progression. *Int J Mol Sci*. 2016;17(4):517.
117. Furukawa Y, Kikuchi J. Molecular pathogenesis of multiple myeloma. *Int J Clin Oncol*. 2015;20(3):413-422.
118. Arce L, Yokoyama NN, Waterman ML. Diversity of LEF/TCF action in development and disease. *Oncogene*. 2006;25(57):7492-7504.
119. Di Marzo L, Desantis V, Solimando AG, Ruggieri S, Annese T, Nico B, et al. Microenvironment drug resistance in multiple myeloma: emerging new players. *Oncotarget*. 2016;7(37):60698-60711.
120. Bjorklund CC, Ma W, Wang ZQ, Davis RE, Kuhn DJ, Kornblau SM, et al. Evidence of a role for activation of Wnt/beta-catenin signaling in the resistance of plasma cells to lenalidomide. *J Biol Chem*. 2011;286(13):11009-11020.
121. Bjorklund CC, Baladandayuthapani V, Lin HY, Jones RJ, Kuitatse I, Wang H, et al. Evidence of a role for CD44 and cell adhesion in mediating resistance to lenalidomide in multiple myeloma: therapeutic implications. *Leukemia*. 2014;28(2):373-383.

122. Niida A, Hiroko T, Kasai M, Furukawa Y, Nakamura Y, Suzuki Y, et al. DKK1, a negative regulator of Wnt signaling, is a target of the beta-catenin/TCF pathway. *Oncogene*. 2004;23(52):8520-8526.
123. Kocemba KA, Groen RW, van Andel H, Kersten MJ, Mahtouk K, Spaargaren M, et al. Transcriptional silencing of the Wnt-antagonist DKK1 by promoter methylation is associated with enhanced Wnt signaling in advanced multiple myeloma. *PLoS One*. 2012;7(2):e30359.
124. Kahn M. Can we safely target the WNT pathway? *Nat Rev Drug Discov*. 2014;13(7):513-532.
125. Previdi S, Maroni P, Matteucci E, Brogginini M, Bendinelli P, Desiderio MA. Interaction between human-breast cancer metastasis and bone microenvironment through activated hepatocyte growth factor/Met and beta-catenin/Wnt pathways. *Eur J Cancer*. 2010;46(9):1679-1691.
126. Fujino H, West KA, Regan JW. Phosphorylation of glycogen synthase kinase-3 and stimulation of T-cell factor signaling following activation of EP2 and EP4 prostanoid receptors by prostaglandin E2. *J Biol Chem*. 2002;277(4):2614-2619.
127. Kim RY, Yang HJ, Song YM, Kim IS, Hwang SJ. Estrogen Modulates Bone Morphogenetic Protein-Induced Sclerostin Expression Through the Wnt Signaling Pathway. *Tissue Eng Part A*. 2015;21(13-14):2076-2088.
128. Xu W, Zhou W, Cheng M, Wang J, Liu Z, He S, et al. Hypoxia activates Wnt/beta-catenin signaling by regulating the expression of BCL9 in human hepatocellular carcinoma. *Sci Rep*. 2017;7:40446.
129. Chocarro-Calvo A, Garcia-Martinez JM, Ardila-Gonzalez S, De la Vieja A, Garcia-Jimenez C. Glucose-induced beta-catenin acetylation enhances Wnt signaling in cancer. *Mol Cell*. 2013;49(3):474-486.
130. Essers MA, de Vries-Smits LM, Barker N, Polderman PE, Burgering BM, Korswagen HC. Functional interaction between beta-catenin and FOXO in oxidative stress signaling. *Science*. 2005;308(5725):1181-1184.
131. Bernard P, Harley VR. Acquisition of SOX transcription factor specificity through protein-protein interaction, modulation of Wnt signalling and post-translational modification. *Int J Biochem Cell Biol*. 2010;42(3):400-410.
132. Nishita M, Hashimoto MK, Ogata S, Laurent MN, Ueno N, Shibuya H, et al. Interaction between Wnt and TGF-beta signalling pathways during formation of Spemann's organizer. *Nature*. 2000;403(6771):781-785.
133. Herr P, Hausmann G, Basler K. WNT secretion and signalling in human disease. *Trends Mol Med*. 2012;18(8):483-493.
134. Liu J, Pan S, Hsieh MH, Ng N, Sun F, Wang T, et al. Targeting Wnt-driven cancer through the inhibition of Porcupine by LGK974. *Proc Natl Acad Sci U S A*. 2013;110(50):20224-20229.
135. Madan B, Ke Z, Harmston N, Ho SY, Frois AO, Alam J, et al. Wnt addiction of genetically defined cancers reversed by PORCN inhibition. *Oncogene*. 2016;35(17):2197-2207.
136. Le PN, McDermott JD, Jimeno A. Targeting the Wnt pathway in human cancers: therapeutic targeting with a focus on OMP-54F28. *Pharmacol Ther*. 2015;146:1-11.

137. Gurney A, Axelrod F, Bond CJ, Cain J, Chartier C, Donigan L, et al. Wnt pathway inhibition via the targeting of Frizzled receptors results in decreased growth and tumorigenicity of human tumors. *Proc Natl Acad Sci U S A*. 2012;109(29):11717-11722.
138. Katoh M, Katoh M. Molecular genetics and targeted therapy of WNT-related human diseases (Review). *Int J Mol Med*. 2017;
139. Lepourcelet M, Chen YN, France DS, Wang H, Crews P, Petersen F, et al. Small-molecule antagonists of the oncogenic Tcf/beta-catenin protein complex. *Cancer Cell*. 2004;5(1):91-102.
140. Lenz HJ, Kahn M. Safely targeting cancer stem cells via selective catenin coactivator antagonism. *Cancer Sci*. 2014;105(9):1087-1092.
141. Sawidou I, Khong T, Cuddihy A, McLean C, Horrigan S, Spencer A. beta-Catenin Inhibitor BC2059 Is Efficacious as Monotherapy or in Combination with Proteasome Inhibitor Bortezomib in Multiple Myeloma. *Mol Cancer Ther*. 2017;16(9):1765-1778.
142. Xu F, Zhu Y, Lu Y, Yu Z, Zhong J, Li Y, et al. Anthelmintic pyrvinium pamoate blocks Wnt/beta-catenin and induces apoptosis in multiple myeloma cells. *Oncol Lett*. 2018;15(4):5871-5878.
143. Picco G, Petti C, Centonze A, Torchiario E, Crisafulli G, Novara L, et al. Loss of AXIN1 drives acquired resistance to WNT pathway blockade in colorectal cancer cells carrying RSPO3 fusions. *EMBO Mol Med*. 2017;9(3):293-303.



# Chapter four

## Dual targeting of Wnt signaling promotes cell death of primary multiple myeloma cells by inhibition of the unfolded protein response pathway

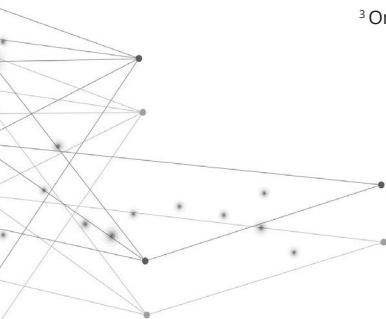
Ingrid Spaan<sup>1</sup>, Niels van Nieuwenhuijzen<sup>1,2</sup>,  
Madelon Maurice<sup>3</sup>, Monique Minnema<sup>2</sup>,  
Reinier Raymakers<sup>2</sup>, and Victor Peperzak

<sup>1</sup> Laboratory of Translational Immunology,  
University Medical Center Utrecht,  
Utrecht, the Netherlands

<sup>2</sup> Department of Hematology,  
University Medical Center Utrecht,  
Utrecht, the Netherlands

<sup>3</sup> Oncode Institute and Department of Cell Biology,  
University Medical Center Utrecht,  
Utrecht, the Netherlands

*Manuscript in preparation*



## ABSTRACT

Multiple myeloma (MM) is a neoplasm of clonal plasma cells that, despite many treatment options, remains incurable due to development of therapy resistance and relapse of disease. Aberrant Wnt signaling is key to MM. In addition to its well described role in osteolytic bone disease, Wnt signaling activity was reported to be intrinsic in MM cells. The biological significance of this intrinsic Wnt signaling, however, remains a point of debate; multiple studies using MM cell lines *in vitro* and in mouse models reported contradictory effects on cell proliferation and disease progression. As an increasing number of Wnt-modulating agents are entering clinical trials for solid tumors and leukemia, we aimed to provide clarity concerning the relevance of Wnt signaling in MM and the therapeutic potential of targeting this pro-survival pathway. For the first time, we assessed the effects of two established Wnt pathway inhibitors on primary human MM cells, isolated from bone marrow (BM) aspirates. We demonstrate that Wnt targeting by dual inhibition of tankyrase and porcupine promotes cell death of primary MM cells by inhibition of the unfolded protein response pathway.

## 1 | INTRODUCTION

The Wnt signal transduction pathway is one of the main regulators of cell growth, and essential for both embryonic development and adult tissue homeostasis [1]. During canonical Wnt signaling, Wnt ligands bind and activate Frizzled receptors and LRP5/6 co-receptors to recruit components of the  $\beta$ -catenin destruction complex. Subsequent inhibition of destruction complex activity results in stabilization of non-phosphorylated  $\beta$ -catenin which, upon nuclear translocation, associates with LEF/TCF to activate transcription of Wnt target genes [2]. In addition, multiple Wnt ligands can activate  $\beta$ -catenin-independent Wnt pathways, that are activated via Frizzled and alternative Wnt receptors Ror and Ryk. This non-canonical Wnt signaling can control cell motility and polarity, and activate JNK and calcium-dependent signaling pathways [2].

Dysregulation of the Wnt pathway is causative for many types of carcinomas [1], but is also associated with leukemia and MM [3]. Human myeloma cell lines (HMCL) express mRNA encoding for multiple Frizzled and LRP isoforms and Wnt ligands [4,5]. HMCL stimulation with Wnt ligand results in upregulation of pathway mediators, stabilization of  $\beta$ -catenin, and transcriptional Wnt-reporter activation [4,5]. Aforementioned studies, however, reported contradictory results on the biological consequence of this Wnt signaling. Reported *in vitro* responses to Wnt stimulation varied between increased cell proliferation [4], and stable proliferation

with altered cell morphology [5]. Stimulation of Wnt signaling in MM cells engrafted in mouse models resulted in reduced tumor burden in bone without effects on subcutaneous growth [6], while a second study reported increased subcutaneous growth [7]. In addition to the results in this last study, Wnt inhibition did not affect Wnt-induced reduction in bone tumor burden [7], while two other studies reported decreased tumor burden [8,9], and improved survival after knockdown of  $\beta$ -catenin [9]. The opposing biological responses can be attributed to many different factors, including (non)-canonical signaling activity and the chosen model system [2]. To obtain a better understanding of the biological consequence of intrinsic Wnt signaling in MM cells, we made use of primary MM cells to stimulate and inhibit Wnt pathway activity.

## 2 | RESULTS AND DISCUSSION

MM is characterized by extensive inter- and intra-patient heterogeneity, mainly due to the complex clonal evolution that is required for malignant transformation [10]. In this study we included MM patients with varying clinical characteristics and cytogenetics (Supplemental Table 1). The mononuclear cells, that were isolated from BM biopsies at diagnosis, contained MM cell percentages varying between 10-60%. Since primary MM cells lack essential growth factors outside their BM microenvironment, the cells were cultured in the continuous presence of growth factors IL-6 and APRIL.

Canonical Wnt signaling can be stimulated with Wnt3a ligand conditioned medium (WCM). In HMCL MM1.s and L363, exposure to WCM resulted in stabilization of  $\beta$ -catenin protein expression and transcriptional Wnt-reporter activation (Supplemental Figure 1A-B). For a subset of primary samples (MM1-3), IL-6 and APRIL was not sufficient to maintain MM cell viability for the culture period of 14 days. However, supplementation with WCM promoted viability of MM cells (Figure 1A-B) and resulted in a significant increase in the number of viable MM cells at day 14 (Figure 1C). For the remainder of primary samples (MM4-7), MM cell viability did not reduce during the 14 days of culture, and these cells did not benefit from extra WCM supplementation (Supplemental Figure 1C). This indicates that canonical Wnt stimulation increases survival of low-viability primary MM cells.

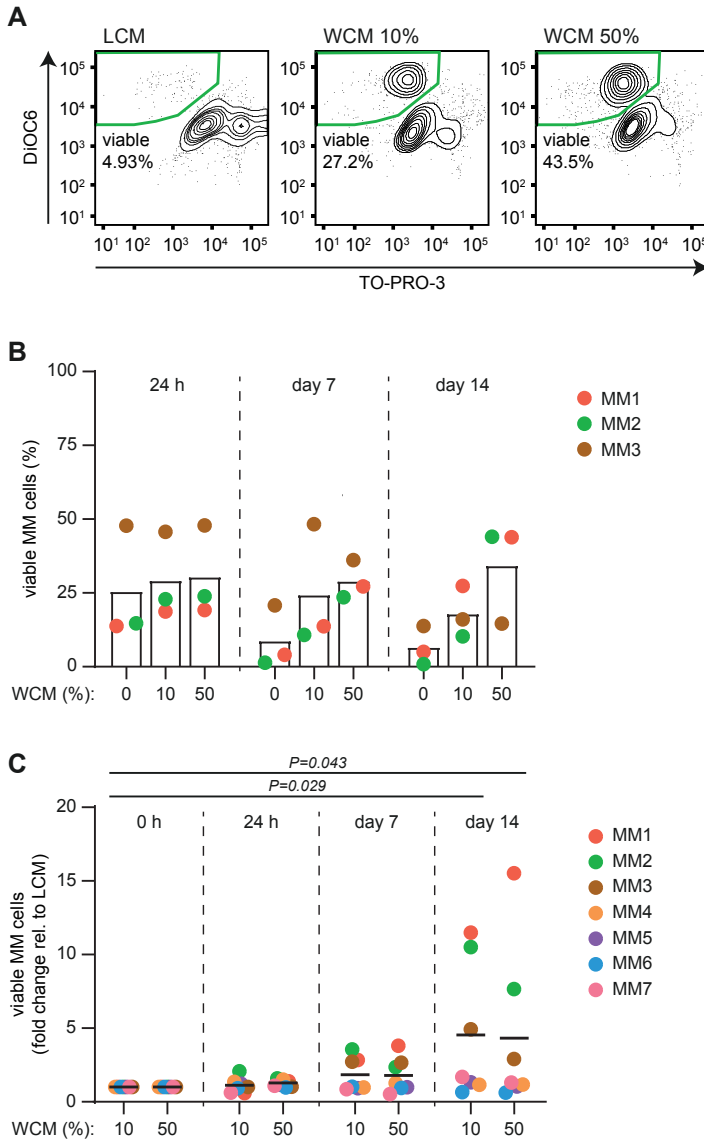


**Figure 1 | Canonical Wnt pathway stimulation increases survival of low-viability primary multiple myeloma cells.** (A) Representative flow cytometry analysis plots of a low-viability MM sample. Viability of CD38<sup>+</sup> primary MM cells was assessed after 14 days of exposure to the indicated concentrations of Wnt3a conditioned medium (WCM) or L-cell control medium (LCM), in the presence of IL-6 and APRIL. Gates represent viable (DiOC6<sup>+</sup>/TO-PRO-3<sup>-</sup>) cells. (B) Percentage of viability in CD38<sup>+</sup> primary MM cells of low-viability MM samples. Viable cells were identified as DiOC6<sup>+</sup>/TO-PRO-3<sup>-</sup> by flow cytometry after 24 hours,



7 days, and 14 days of exposure to indicated concentrations of WCM, in the presence of IL-6 and APRIL. Bars represent the mean of the 3 included low-viability MM samples. (C) Absolute viable CD38<sup>+</sup> primary MM cells, represented as fold-change relative to LCM-treated control cells per timepoint, after 24 hours, 7 days, and 14 days of exposure to indicated concentrations of WCM, in the presence of IL-6 and APRIL. Viable cells were identified as DiOC6<sup>+</sup>/TO-PRO-3<sup>-</sup> and cell counts were determined using flow cytometry beads. Solid lines indicate the mean of the 3 included low-viability and 4 included high-viability samples. Statistical significance was determined by two-way ANOVA using Sidak correction for multiple testing.

Blocking of aberrant Wnt signaling has been a focus of anti-cancer therapy development for the last decades, but has been hampered by the limited number of pathway mediators susceptible to small-molecule interference [1]. An indirect, but successful, approach to inhibit canonical Wnt signaling was found in tankyrase inhibition (TNKSi) by XAV939. TNKSi promotes degradation of  $\beta$ -catenin due to stabilization of Axin, which is the concentration-limiting component of the  $\beta$ -catenin destruction complex [11]. Inhibition of porcupine, an enzyme required for the secretion of all human Wnt ligands, by porcupine inhibitor (PORCi) C59 also reduced Wnt signaling both *in vitro* and in a mouse model [12]. We tested the functionality of these two Wnt inhibitors on HMCL by assessing  $\beta$ -catenin protein expression. WCM-induced stabilization of  $\beta$ -catenin was significantly blocked by TNKSi in both HMCL (Figure 2A and Supplemental Figure 2A). Exposure to PORCi also significantly reduced endogenous  $\beta$ -catenin in MM1.s, but not L363 cells (Figure 2B and Supplemental Figure 2B). This indicates a potential autocrine Wnt signaling loop in MM1.s cells.

To test if the TNKSi and PORCi effects on  $\beta$ -catenin expression are accompanied by a downstream biological response on cell growth in these HMCL, we assessed both short-term effects on cell death, as well as altered proliferation during long-term treatment. Single TNKSi exposure did not impact cell viability, while single PORCi exposure resulted in an induction of apoptosis of 29.1% in MM1.s and 18.6% in L363 at 72 hours (Figure 2C). The combination of both inhibitors induced a more potent effect on cell death, especially in MM1.s with a maximum of 57.3% specific apoptosis at 72 hours. The observed apoptosis at this condition was significantly higher than expected from an additive drug response, indicating synergy between both Wnt inhibitors in MM1.s (Supplemental Figure 2C). In addition to a direct effect on cell death, Wnt inhibition may also decrease cell division. We therefore assessed numbers of viable MM cells during long-term cultures in the presence of TNKSi and PORCi. Exposure to single PORCi or combinations of PORCi and TNKSi significantly reduced viable cell numbers in MM1.s at 3 and 7 days of culture (Figure 2D and Supplemental Figure 2D). At day 7, L363 only showed a significant reduction of viable cells at the highest drug dose combination. At 10 days of culture, single TNKSi and PORCi at the highest dosages, and all

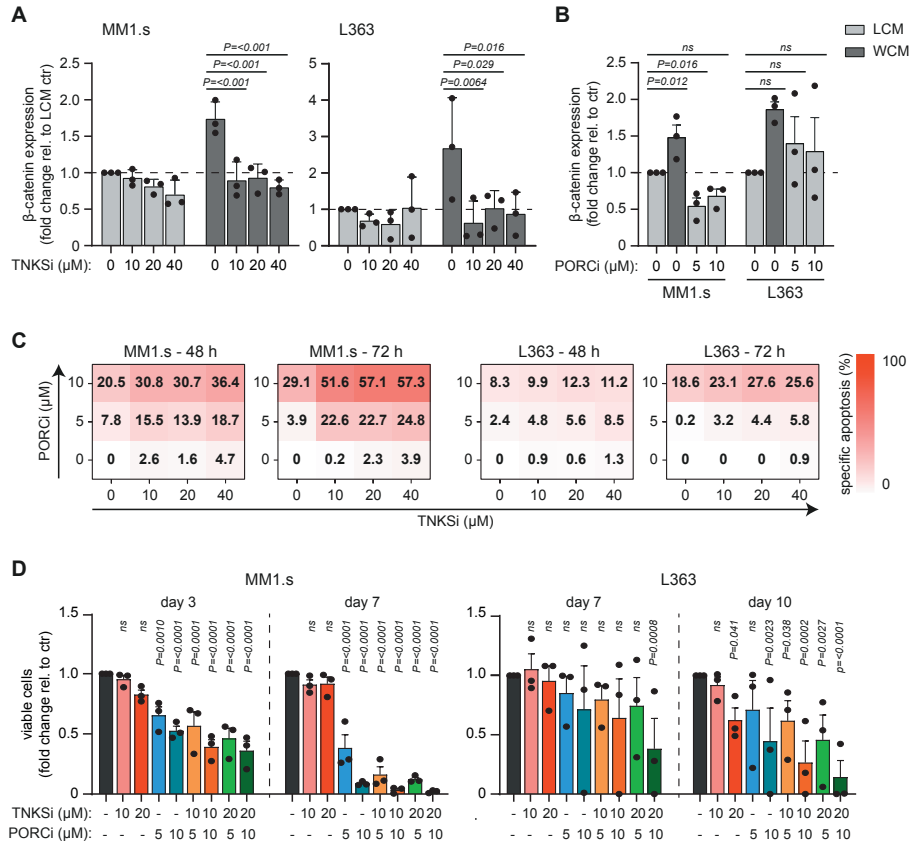


**Figure 2 | Small molecule inhibitors of tankyrase and porcupine inhibit Wnt signaling and reduce cell growth in multiple myeloma cell lines.** (A) Quantification of  $\beta$ -catenin protein expression as assessed by western blot in HMCL MM1.s and L363, after overnight exposure to increasing concentrations of tankyrase inhibitor (TNKSi) XAV939, in the presence of Wnt3a conditioned medium (WCM) or L-cell control medium (LCM). Bars show the mean of 3 individual experiments as fold change to untreated LCM control cells, indicated by the dashed lines. Error bars represent the standard error of the mean, and statistical significance was determined by two-way ANOVA using Sidak correction for multiple testing. (B) Quantification of  $\beta$ -catenin protein expression as assessed by western blot in MM1.s and L363, after overnight exposure to increasing concentrations of porcupine inhibitor (PORCi) C59 in the presence of LCM, or WCM as a positive control. Bars show the mean of 3 individual experiments as fold change to untreated LCM control cells, indicated by the dashed lines. Error bars represent the standard error of the mean, and statistical significance was determined by one-way ANOVA using Dunnett correction for multiple testing. (C) Heatmaps showing specific apoptosis in MM1.s and L363 induced by serial dilution of TNKSi and PORCi, individual or combined. Viable cells were determined by flow cytometry as DiOC6<sup>+</sup>/TO-PRO-3<sup>-</sup> and analyzed after 48 and 72 hours of drug exposure. Values represent the mean of 3 individual experiments. (D) Absolute viable cells, represented as fold-change relative to untreated control cells per timepoint, after long-term culture in the presence of TNKSi and PORCi, individual or combined. Viable cells were identified as TO-PRO-3<sup>-</sup>, cell counts were determined using flow cytometry beads, and were analyzed after 3 and 7 days of exposure

for MM1.s, and 7 and 10 days of exposure for L363. Bars show the mean of 3 individual experiments, error bars represent the standard error of the mean, and statistical significance was determined by two-way ANOVA using Sidak correction for multiple testing; ns, not significant.

combinations of TNKSi with PORCi, were sufficient to significantly reduce viable cell numbers in L363. Since in L363 single PORCi exposure did not affect  $\beta$ -catenin expression (Figure 2B), this suggests a potential role for non-canonical Wnt signaling in this HMCL. Combined, these results show that TNKSi and PORCi, and especially the combination of both inhibitors, significantly impact cell growth in HMCL. These results are accompanied by a significant reduction in transcriptional Wnt-reporter activity (Supplemental Figure 2E).

Previous studies have shown that the biological consequences of Wnt pathway alteration in MM cell lines is dependent on the context of the model system. We therefore verified the biological response to TNKSi and PORCi in primary MM cells. Exposure to TNKSi significantly reduced viable MM cells at 24 hours and 7 days of culture (Figure 3A). However, the responses varied between 5.0-fold decrease in MM7 and 1.4-fold increase in MM13. This variation in response was also observed after 7 days of culture with PORCi, ranging between a complete reduction in MM1 and a 1.5-fold increase in MM12 (Figure 3B). The variability in response observed in primary MM samples seems to resemble the variable results obtained in MM cell lines. This indicates that the MM clones differ in their dependency on (non)-canonical Wnt ligands, which are either the result of autocrine stimulation or, in the case of primary cells, can be secreted by additional mononuclear cells that are present in the BM aspirate.

In an attempt to minimize the variability in responses, we tested the combinatorial effect of both inhibitors on MM cell viability in a subset of primary samples. Seven days exposure to the combination of TNKSi and PORCi resulted in a significant decrease of viable MM cells, with all samples showing a reduction compared to control (Figure 3C-D). This decrease in viable cell numbers was accompanied by a significant reduction in the average MM cell viability at 72 hours, and at day 7 with a reduction from 70.2% in control cells to 32.5% in cells treated with the inhibitor combination (Figure 3E). To elucidate the mechanism underlying this combinatorial TNKSi-PORCi effect, the MM cells from samples MM09-MM13 were subjected to single cell RNA sequencing after 72 hours of exposure to the inhibitor combination or control. Clustering of the transcriptome by tSNE analysis showed that the samples cluster individually, with sample MM12 divided over clusters 1 and 5 (Figure 4-B). Only in cluster 2, corresponding to sample MM09, treated versus control cells grouped separately within the cluster (Supplemental Figure 3A). Analysis of treated and

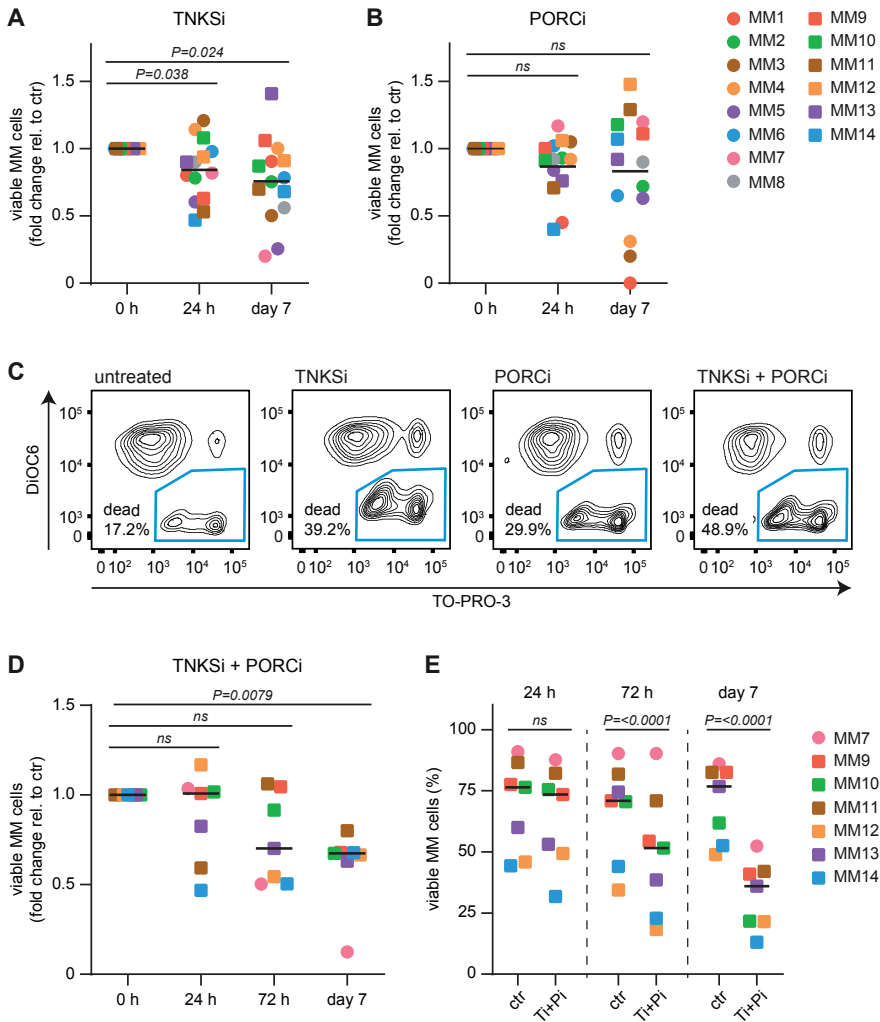


**Figure 3 | Wnt targeting by dual tankyrase and porcupine inhibition promotes cell death of primary multiple myeloma cells.** Absolute viable CD38<sup>+</sup> primary MM cells, represented as fold-change relative to untreated control cells per timepoint, after 24 hours and 7 days of exposure to (A) 20  $\mu$ M tankyrase inhibitor (TNKSi) XAV939, or (B) 5  $\mu$ M porcupine inhibitor (PORCi) C59. Both drug treatments were performed in the presence of IL-6 and APRIL. Viable cells were identified as DiOC6<sup>+</sup>/TO-PRO-3<sup>-</sup> and cell counts were determined using flow cytometry beads. Solid lines indicate the mean of the 14 included MM samples. Statistical significance was determined by one-way ANOVA using Dunnett correction for multiple testing. (C) Flow cytometry analysis plots of viability in CD38<sup>+</sup> cells of a primary MM sample after 72 hours of exposure to 20  $\mu$ M TNKSi, 5  $\mu$ M PORCi, and the combination thereof, or untreated control cells, in the presence of IL-6 and APRIL. Gates represent dead (DiOC6<sup>-</sup>/TO-PRO-3<sup>+</sup>) cells. (D) Absolute viable CD38<sup>+</sup> primary MM cells, represented as fold-change relative to untreated control cells per timepoint, after 24 hours, 72 hours, and 7 days

of exposure to the combination of 20  $\mu\text{M}$  TNKSi and 5  $\mu\text{M}$  PORCi, in the presence of IL-6 and APRIL. Viable cells were identified as DiOC6<sup>+</sup>/TO-PRO-3<sup>-</sup> and cell counts were determined using flow cytometry beads. Solid lines indicate the mean of the 7 included MM samples. Statistical significance was determined by one-way ANOVA using Dunnett correction for multiple testing. (E) Percentage of viability of CD38<sup>+</sup> primary MM cells after 24 hours, 72 hours, and 7 days of exposure to the combination of 20  $\mu\text{M}$  TNKSi and 5  $\mu\text{M}$  PORCi, or untreated control cells, in the presence of IL-6 and APRIL. Viable cells were identified as DiOC6<sup>+</sup>/TO-PRO-3 by flow cytometry. Solid lines indicate the mean of the 7 included MM samples. Statistical significance was determined by two-way ANOVA using Sidak correction for multiple testing. ns, not significant.

control cells of the combined samples, identified 153 differentially expressed genes with an adjusted P-value of  $<0.01$  (Figure 4C). Top hits, including XBP1, MZB1, SEC61G, and HSP90B1 (Figure 4D) are all associated with the unfolded protein response (UPR) pathway, and were also significantly reduced in the treated MM cells of individual samples MM09, MM12, and MM13, compared to untreated control cells (Supplemental Figure 3B). As the UPR pathway is crucial for cellular functionality of both healthy and malignant plasma cells, due to their high antibody production load [13], we hypothesize that inhibition of the UPR is the mechanism underlying apoptosis of primary MM cells by dual tankyrase and porcupine inhibition.

### 3 | CONCLUSION

In conclusion, the current study shows that tankyrase and porcupine inhibition, two established methods to block the Wnt pathway, reduces Wnt signaling in HMCL, and promotes cell death of HMCL and primary MM cells by inhibition of the UPR. As the UPR is crucial for cellular functionality of both healthy and malignant plasma cells, we hypothesize that inhibition of the UPR by TNKSi and PORCi, in combination with standard-of-care proteasome inhibitors like bortezomib, will have therapeutic potential and could be a new avenue in the treatment of MM.

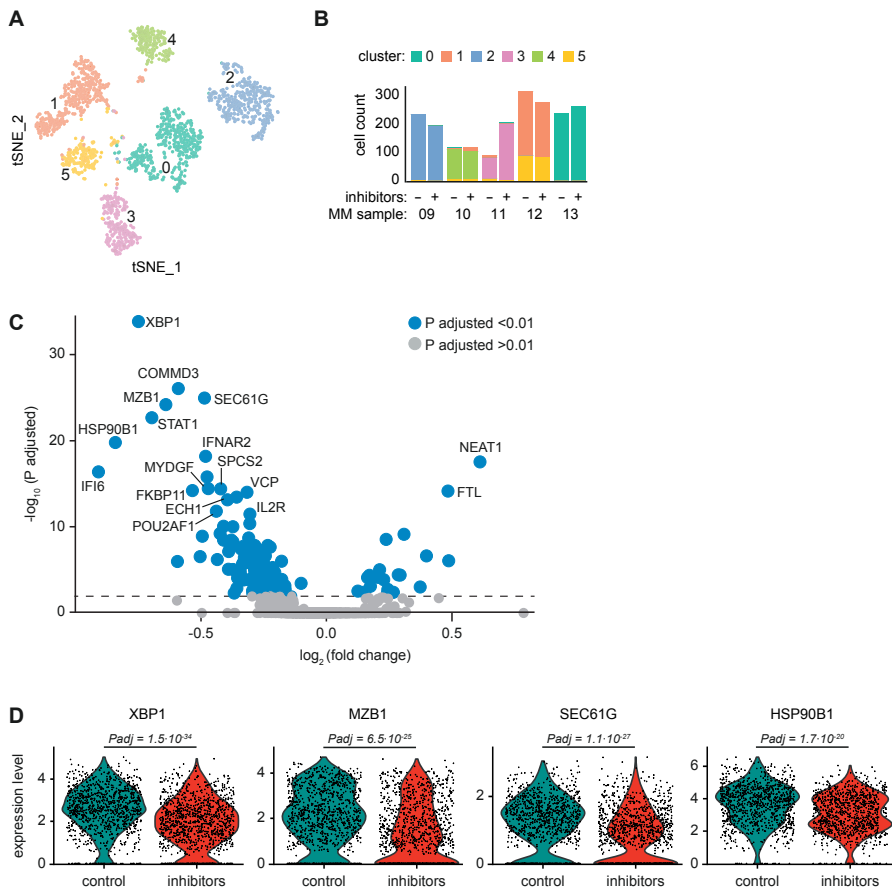


**Figure 4 | Dual tankyrase and porcupine targeting in primary multiple myeloma cells inhibits the unfolded protein response pathway.** Transcriptome analysis by single-cell RNA sequencing of viable CD38<sup>+</sup> CD138<sup>+</sup> primary MM cells of samples MM09-MM13 after 72 hours of exposure to a combination of 20  $\mu\text{M}$  tankyrase inhibitor XAV939 and 5  $\mu\text{M}$  porcupine inhibitor C59, or untreated control cells, in the presence of IL-6 and APRIL. (A) Dimensionality reduction and clustering of transcriptome analysis by tSNE, and (B) cluster distribution of the individual MM samples. The 6 clusters are denoted by digits 0-5 and corresponding colors. (C) Volcano plot of genes differentially expressed (DE) between MM cells exposed to the inhibitor combination versus control. Blue datapoints indicate significant DE genes with an adjusted P-value <0.01, grey datapoints indicate not-significant DE genes with an adjusted P-value >0.01. The top 17 DE have been annotated with their corresponding gene name. (D) Violin plots showing expression of mediators of the unfolded protein response pathway: XBP1, MZB1, SEC61G, and HSP90B1, in MM cells exposed to control or the inhibitor combination. Individual datapoints represent the sequenced single cells, and the adjusted P-value is annotated as Padj, for which <0.01 is considered statistically significant.

## **ACKNOWLEDGEMENTS**

The authors would like to thank the support facilities of the University Medical Center Utrecht and the Dutch Parelsnoer Institute for providing primary patient samples. We are grateful to Ingrid Jordens for providing the tankyrase and porcupine inhibitors, and discussion and feedback on this manuscript. We thank Hans Clevers for providing Wnt reporter constructs. This work was supported in part by a Bas Mulder Award from the Dutch Cancer Foundation (KWF)/Alped'HuZes foundation (No. UU 2015-7663) to VP, and a project grant from the Dutch Cancer Foundation (KWF)/Alped'HuZes foundation (No. 11108) to VP.

## REFERENCES

1. Nusse, R.; Clevers, H. Wnt/ $\beta$ -Catenin Signaling, Disease, and Emerging Therapeutic Modalities. *Cell* 2017, *169*, 985-999.
2. Spaan, I.; Raymakers, R.A.; van de Stolpe, A.; Peperzak, V. Wnt signaling in multiple myeloma: a central player in disease with therapeutic potential. *J Hematol Oncol* 2018, *11*, 67.
3. Tiemessen, M.M.; Staal, F.J. Wnt signaling in leukemias and myeloma: T-cell factors are in control. *Future Oncol* 2013, *9*, 1757-1772.
4. Derksen, P.W.; Tjin, E.; Meijer, H.P.; Klok, M.D.; MacGillavry, H.D.; van Oers, M.H.; Lokhorst, H.M.; Bloem, A.C.; Clevers, H.; Nusse, R.; et al. Illegitimate WNT signaling promotes proliferation of multiple myeloma cells. *Proc Natl Acad Sci U S A* 2004, *101*, 6122-6127.
5. Qiang, Y.W.; Endo, Y.; Rubin, J.S.; Rudikoff, S. Wnt signaling in B-cell neoplasia. *Oncogene* 2003, *22*, 1536-1545.
6. Qiang, Y.W.; Shaughnessy, J.D., Jr.; Yaccoby, S. Wnt3a signaling within bone inhibits multiple myeloma bone disease and tumor growth. *Blood* 2008, *112*, 374-382.
7. Edwards, C.M.; Edwards, J.R.; Lwin, S.T.; Esparza, J.; Oyajobi, B.O.; McCluskey, B.; Munoz, S.; Grubbs, B.; Mundy, G.R. Increasing Wnt signaling in the bone marrow microenvironment inhibits the development of myeloma bone disease and reduces tumor burden in bone in vivo. *Blood* 2008, *111*, 2833-2842.
8. Ashihara, E.; Kawata, E.; Nakagawa, Y.; Shimazaki, C.; Kuroda, J.; Taniguchi, K.; Uchiyama, H.; Tanaka, R.; Yokota, A.; Takeuchi, M.; et al. beta-catenin small interfering RNA successfully suppressed progression of multiple myeloma in a mouse model. *Clin Cancer Res* 2009, *15*, 2731-2738.
9. Dutta-Simmons, J.; Zhang, Y.; Gorgun, G.; Gatt, M.; Mani, M.; Hideshima, T.; Takada, K.; Carlson, N.E.; Carrasco, D.E.; Tai, Y.T.; et al. Aurora kinase A is a target of Wnt/beta-catenin involved in multiple myeloma disease progression. *Blood* 2009, *114*, 2699-2708.
10. van Nieuwenhuijzen, N.; Spaan, I.; Raymakers, R.; Peperzak, V. From MGUS to Multiple Myeloma, a Paradigm for Clonal Evolution of Premalignant Cells. *Cancer Res* 2018, *78*, 2449-2456.
11. Huang, S.M.; Mishina, Y.M.; Liu, S.; Cheung, A.; Stegmeier, F.; Michaud, G.A.; Charlat, O.; Wiellette, E.; Zhang, Y.; Wiessner, S.; et al. Tankyrase inhibition stabilizes axin and antagonizes Wnt signalling. *Nature* 2009, *461*, 614-620.
12. Proffitt, K.D.; Madan, B.; Ke, Z.; Pendharkar, V.; Ding, L.; Lee, M.A.; Hannoush, R.N.; Virshup, D.M. Pharmacological inhibition of the Wnt acyltransferase PORCN prevents growth of WNT-driven mammary cancer. *Cancer Res* 2013, *73*, 502-507.
13. Vincenz, L.; Jäger, R.; O'Dwyer, M.; Samali, A. Endoplasmic reticulum stress and the unfolded protein response: targeting the Achilles heel of multiple myeloma. *Mol Cancer Ther* 2013, *12*, 831-843.



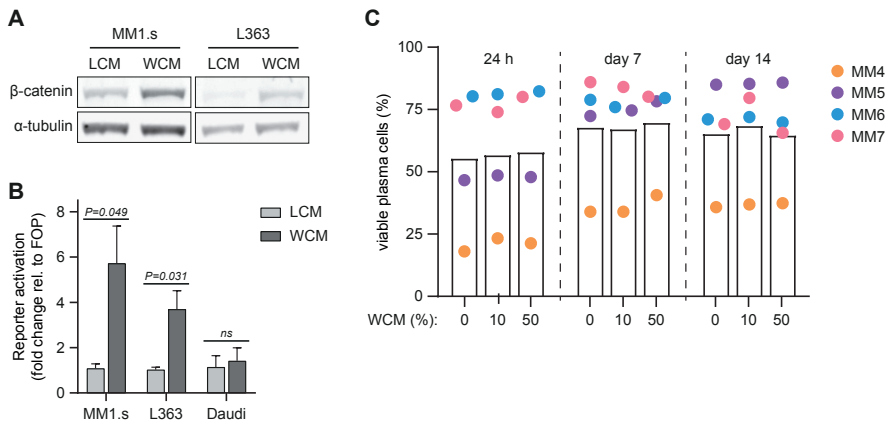
## SUPPLEMENTAL TABLES

**Supplemental Table 1 | Overview of clinical characteristics and cytogenetics of the 14 MM patients included in the study.**

Sample	Age, y	Sex	IgH type	IgL type	ISS	cytogenetics		
						HD	amp/del	translocations
MM1	66	F	IgA	κ	1	yes	no	no
MM2	66	M	IgG+IgA	κ	1	yes	13q-,16q-	no
MM3	74	M	IgA	κ	1	yes	13q-	no
MM4	74	M	no	κ	3	nd	nd	nd
MM5	38	M	IgG	κ	2	yes	no	no
MM6	64	M	IgG	κ	1	yes	no	no
MM7	68	M	nd	λ	1	no	no	no
MM8	60	M	IgG	κ	3	yes	no	no
MM9	51	M	IgG	κ	3	no	13q-	t(14;16)
MM10	80	M	IgA	κ	2	yes	no	no
MM11	74	F	IgA	λ	1	yes	13q-	no
MM12	80	F	IgA	κ	2	no	13q-	t(11;14)
MM13	63	M	IgG	κ	2	no	1q+	t(11;14)
MM14	60	M	IgG	κ	SMM	no	no	t(11;14)

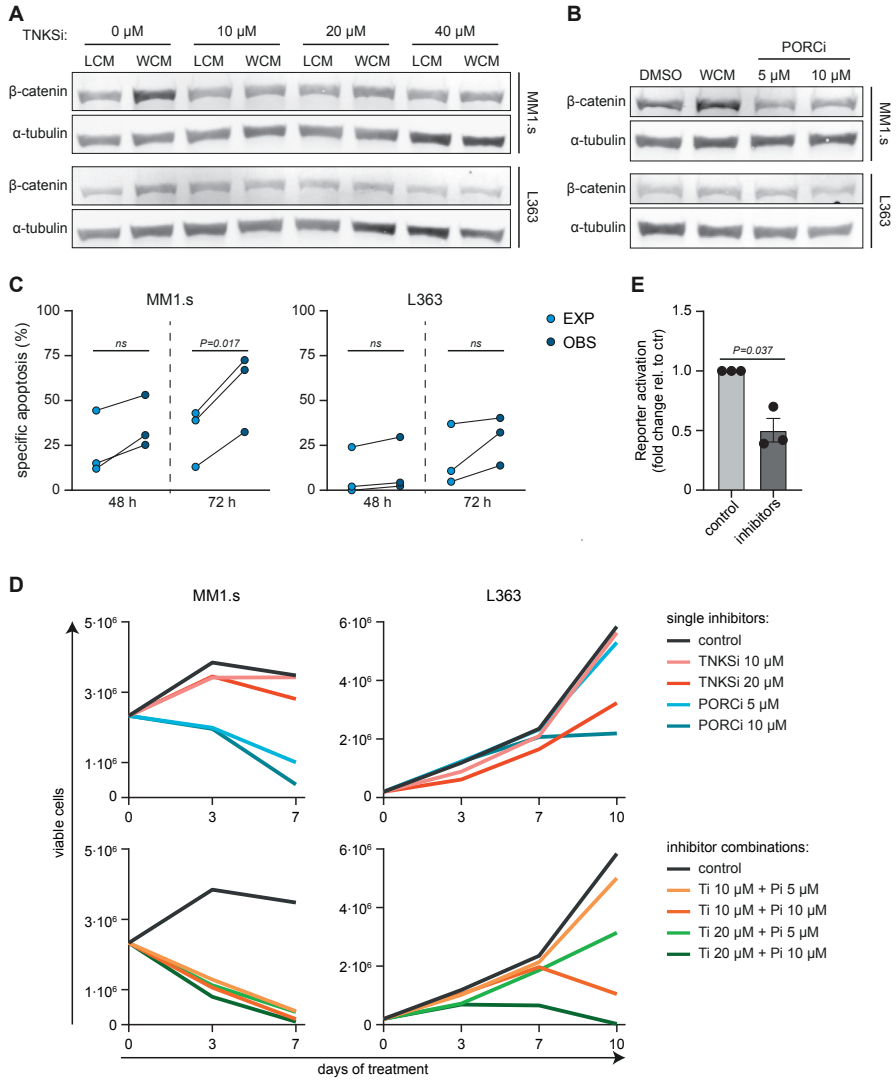
MM: multiple myeloma; y: years; F: female; M: male; IgH: immunoglobulin heavy chain; IgL immunoglobulin light chain; ISS: international staging system; SMM: smoldering multiple myeloma; HD: hyperdiploidy; amp: amplifications; del: deletions; nd : not determined

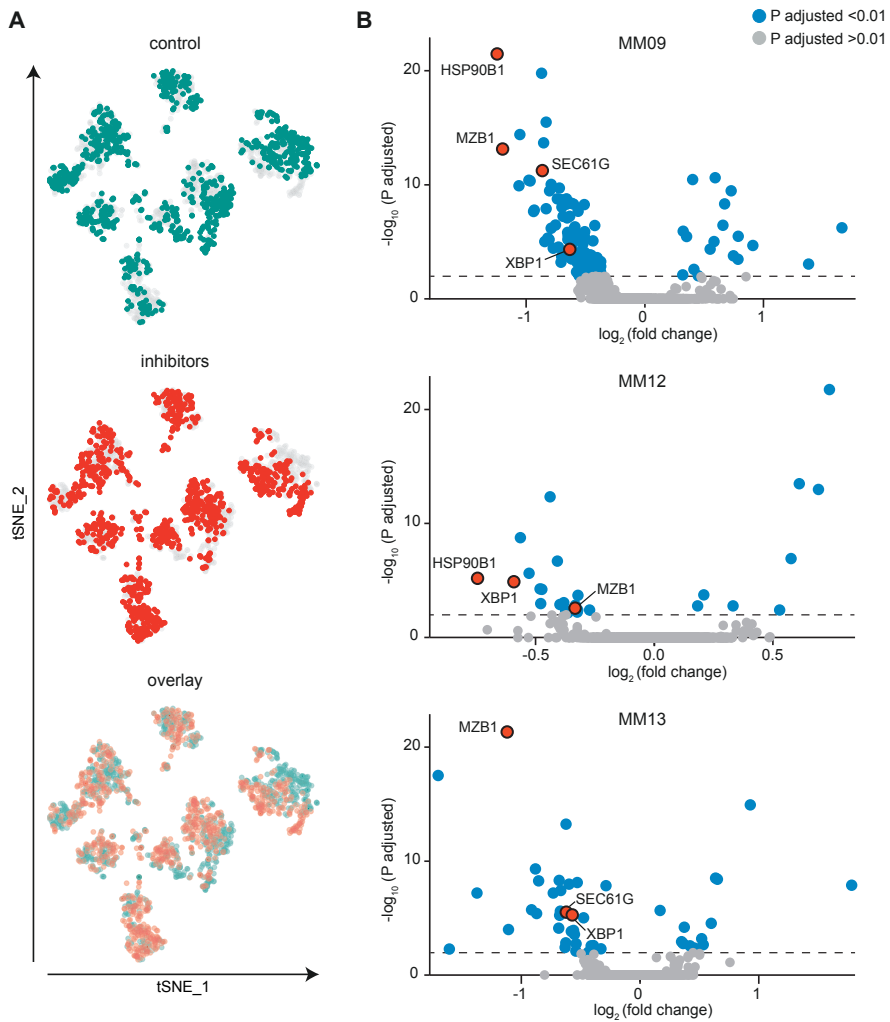
## SUPPLEMENTAL FIGURES



**Supplemental Figure 1 | Wnt3a conditioned medium activates canonical Wnt signaling, but is not required for survival of high-viability primary multiple myeloma cells.** (A) Representative western blot showing  $\beta$ -catenin protein expression in HMCL MM1.s and L363 after overnight exposure to 50% Wnt3a conditioned medium (WCM) or 50% L-cell control medium (LCM). Alpha-tubulin was used as a loading control. (B) Transcriptional Wnt reporter activity as determined by TopFlash after overnight exposure to 50% WCM or 50% LCM. Data is normalized to internal Renilla control and shown as fold change to FOP negative control. Bars show the mean of 3 individual experiments, error bars represent the standard error of the mean, and statistical significance was determined by Student t-test; ns, not significant. (C) Percentage of viability of CD38<sup>+</sup> primary MM cells after 24 hours, 7 days, and 14 days of exposure to indicated concentrations of WCM, in the presence of IL-6 and APRIL. Viable cells were identified as DiOC6<sup>+</sup>/TO-PRO-3<sup>-</sup> by flow cytometry. Bars represent the mean of the 4 included high-viability MM samples.

**► Supplemental Figure 2 | Small molecule inhibitors of tankyrase and porcupine inhibit Wnt signaling and reduce cell growth in multiple myeloma cell lines.** (A) Representative western blot showing  $\beta$ -catenin protein expression in HMCL MM1.s and L363 after overnight exposure to indicated concentrations of tankyrase inhibitor (TNKSi) XAV939, in the presence of 50% Wnt3a conditioned medium (WCM) or 50% L-cell control medium (LCM). Alpha-tubulin was used as a loading control. (B) Representative western blot showing  $\beta$ -catenin protein expression in HMCL MM1.s and L363 after overnight exposure to indicated concentrations of porcupine inhibitor (PORCi) C59, in the presence of 50% LCM, or 50% WCM as positive control. Alpha-tubulin was used as a loading control. (C) Plots comparing observed (OBS) specific apoptosis to hypothetical expected (EXP) specific apoptosis that assumes an additive effect of the combination of 40  $\mu$ M TNKSi and 10  $\mu$ M PORCi. The 3 connected datapoints show the data obtained from 3 individual experiments. Statistical analysis was performed by Student t-test; ns, not significant. (D) Representative growth curves showing absolute viable cells of MM1.s and L363 after 3 - 10 days of culture in the presence of indicated concentrations of TNKSi, PORCi, or untreated control. Viable cells were identified as TO-PRO-3<sup>-</sup>, and cell counts were determined using flow cytometry beads. (E) Transcriptional Wnt reporter activity as determined by TopFlash after 12 - 24 hours of exposure to the combination of 20  $\mu$ M TNKSi and 5  $\mu$ M PORCi in MM1.s. Data is normalized to internal Renilla and FOP negative control, and shown as fold change to untreated control cells. Bars show the mean of 3 individual experiments, error bars represent the standard error of the mean, and statistical significance was determined by Student t-test.





**Supplemental Figure 3 | Dual tankyrase and porcupine targeting in primary multiple myeloma cells inhibits the unfolded protein response pathway.** Transcriptome analysis by single-cell RNA sequencing of viable CD38+ CD138+ primary MM cells of samples MM09-MM13 after 72 hours of exposure to a combination of 20  $\mu\text{M}$  tankyrase inhibitor XAV939 and 5  $\mu\text{M}$  porcupine inhibitor C59, or untreated control cells, in the presence of IL-6 and APRIL. (A) Dimensionality reduction and clustering of transcriptome analysis by tSNE, as shown in Figure 4A, of control MM cells (N = 1001), MM cells exposed to the inhibitor combination (N = 1066), and overlay of the two groups. (B) Volcano plots of genes differentially expressed (DE) between MM cells exposed to the inhibitor combination versus control, of samples MM09, MM12, and MM13. Blue datapoints indicate significant DE genes with an adjusted P-value < 0.01, grey datapoints indicate not-significant DE genes with an adjusted P-value > 0.01. The mediators of the unfolded protein response pathway: XBP1, MZB1, SEC61G, and HSP90B1, are annotated and indicated by the red datapoints.

Dual targeting of Wnt signaling promotes cell death of pMM cells by inhibition of the UPR pathway.

---



# Chapter five

## Direct P70S6K1 inhibition to replace dexamethasone in synergistic combination with MCL-1 inhibition in multiple myeloma

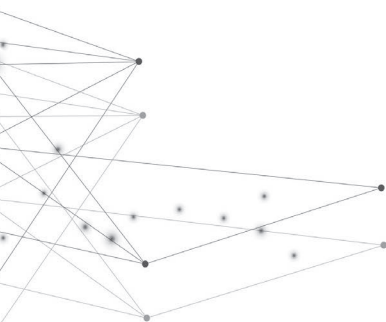
Ingrid Spaan<sup>1</sup>, Laura Timmerman<sup>1</sup>, Thomas Kimman<sup>1</sup>,  
Anne Slomp<sup>1</sup>, Marta Cuenca<sup>1</sup>, Niels van Nieuwenhuijzen<sup>1,2</sup>,  
Laura Moesbergen<sup>1</sup>, Monique Minnema<sup>2</sup>,  
Reinier Raymakers<sup>2</sup>, and Victor Peperzak<sup>1</sup>

<sup>1</sup> Laboratory of Translational Immunology,  
University Medical Center Utrecht,  
Utrecht, the Netherlands

<sup>2</sup> Department of Hematology,  
University Medical Center Utrecht,  
Utrecht, the Netherlands

*Blood Advances*, 2021; 5(12):2596

5



## ABSTRACT

Novel combination therapies have markedly improved the lifespan of multiple myeloma (MM) patients, but drug resistance and disease relapse remain major clinical problems. Dexamethasone and other glucocorticoids are a cornerstone of conventional and new combination therapies for MM, although their use is accompanied by serious side-effects. We aimed to uncover drug combinations that act in synergy and as such allow reduced dosing while remaining effective. Dexamethasone and the MCL-1 inhibitor S63845 (MCL-1i) proved the most potent combination in our lethality screen and induced apoptosis of human myeloma cell lines (HMCLs) that was 50% higher compared to an additive drug effect. Kinome analysis of dexamethasone-treated HMCLs revealed a reduction in serine/threonine peptide phosphorylation, which was predicted to result from reduced Akt activity. Biochemical techniques showed no dexamethasone-induced effects on FOXO or GSK3, but did demonstrate a 50% reduction in P70S6K phosphorylation, downstream of the Akt-mTORC1 axis. Replacing dexamethasone by the P70S6K1 isoform-specific inhibitor PF-4708671 (S6K1i) showed similar and statistically significant synergistic apoptosis of HMCLs in combination with MCL-1i. Interestingly, apoptosis induced by the P70S6K1i and MCL-1i combination was more-than-additive in all 9 primary MM samples tested, while this effect was observed for 6 out of 9 samples with the dexamethasone and MCL-1i combination. Toxicity on stem and progenitor cell subsets remained minimal. Combined, our results show a strong rationale for combination treatments using P70S6K inhibitor in MM. Direct and specific inhibition of P70S6K may also provide a solution for patients ineligible or insensitive to dexamethasone or other glucocorticoids.

## 1 | INTRODUCTION

Despite the development of increasingly effective therapies in the last decades, multiple myeloma (MM) is still considered to be incurable, characterized by acquired drug resistance and relapse of disease [1]. One mechanism by which MM cells circumvent cell death is resistance against the intrinsic apoptosis pathway, in which the BCL-2 family of pro-survival proteins, including BCL-2, MCL-1 and BCL-XL, play an important role [2]. By binding and sequestering pro-apoptotic BH3-only proteins, e.g. BIM, or apoptotic effectors BAX/BAK, the BCL-2 proteins regulate the balance between apoptosis and cell survival [3]. Overexpression of pro-survival proteins, in particular MCL-1, is common in MM and associated with disease relapse and impaired patient survival [4]. This resulted in development of BCL-2 homology domain 3 (BH3)-mimetics that inhibit BCL-2 family proteins



and thereby overcome intrinsic apoptosis resistance [5]. Multiple BH3-mimetics, including the specific MCL-1 inhibitor S63845, are currently being tested in clinical trials for MM [6]. Even though MCL-1 inhibitors show potent single-agent activity, recent *in vitro* studies reported that combinations with dexamethasone resulted in synergistic apoptosis of MM cells [7,8].

Dexamethasone is a synthetic glucocorticoid (GC) that forms an integral component of conventional and new combination therapies for both newly diagnosed and relapsed-refractory (RR) MM patients [5,9]. Binding of GCs to the glucocorticoid receptor (GR) alters the cells transcriptional program either directly by binding to glucocorticoid responsive elements (GRE) in the DNA, or indirectly by interacting with other transcription factors, such as NFκB [10]. Synthetic GCs are widely recognized for their significant anti-inflammatory, immune-suppressive and cytotoxic effects [11]. Although the precise molecular mechanisms remain unclear, treatment of MM cells with single-agent dexamethasone results in intrinsic apoptosis activation [12]. Its effectiveness, however, is accompanied by serious side-effects including muscle weakness, increased infection rate, cardiovascular problems, hyperglycemia, mental health problems, osteoporosis, respiratory problems and fatigue [13]. This makes administration of dexamethasone challenging; dose reduction is required in many patients, especially the elderly and more fragile patients, thereby limiting its potential [14]. As an alternative, dexamethasone might be replaced by the synthetic GC prednisone, which is often better tolerated [15,16].

The PI3K-Akt pathway is the most frequently activated signal transduction pathway in human cancers and also plays a crucial role in MM [17,18]. Akt is the central signaling node in this pathway and mainly acts through regulation of three key downstream mediators: FOXO, GSK3 and mTORC1 [19]. By doing so it regulates multiple cellular processes, including cell growth, survival and apoptosis [20]. The family of FOXO transcription factors control a diverse set of target genes, including (pro-)apoptotic mediators such as BIM [21]. The kinase GSK3 phosphorylates a plethora of proliferation mediators and pro-survival substrates, including MCL-1, thereby marking them for inactivation and/or proteasomal degradation [22]. Upon phosphorylation Akt can inhibit FOXO and GSK3 activity, but also activate mTORC1, resulting in activation of the two mTORC1 targets 4E-BP1 and P70S6K [23]. Although primarily known for its role in metabolism and cell growth, the mTORC1-P70S6K axis has a pleiotropic function in regulation of cell survival and apoptosis [24].

The continued efforts to improve MM treatment has resulted in the development of many new agents, including the BH3-mimetics [25]. However, there is an unmet

need for a strategy to rationally combine these new agents with current standard-of-care therapies to reach synergistic effects that allow for reduced dosing and toxicity. In this study we perform a small-scale lethality screen to test for synergistic effects between novel and conventional MM drugs. We report the highest synergy for the combination of dexamethasone and MCL-1 inhibitor S63845 (MCL-1i) and reveal the molecular mechanism underlying this synergistic combination. These results provide a strong rationale to replace dexamethasone by the P70S6K1 isoform inhibitor PF-4708671 (S6K1i) to induce synergistic apoptosis of MM with the advantage to reduce the vast amount of side-effects experienced with GCs.

## **2 | METHODS**

### **2.1 | Cell culture and chemicals**

The human multiple myeloma cell lines (HMCLs) MM1.s, OPM-2 and L363 were cultured in RPMI 1640 GlutaMAX HEPES (Life Technologies), supplemented with 10% fetal bovine serum (FBS; Biowest) and 100 µg/ml penicillin-streptomycin (Life Technologies). MS-5 feeder cells (DSMZ) were cultured in MEM $\alpha$  (Life Technologies), supplemented with 10% FBS, 2 mM L-glutamine (Life Technologies) and 100 µg/ml penicillin-streptomycin. All cells were maintained at 37 °C and 5% CO<sub>2</sub>. An overview of all drugs incorporated in this study, including titrations, can be found in Supplemental Table 1 and Supplemental Figure 1, respectively.

### **2.2 | MM patient samples**

Frozen vials with mononuclear cells (MNC) isolated from bone marrow (BM) aspirates of newly diagnosed MM patients were requested from the “Parelsnoer” Institute biobank. All samples were obtained after written informed consent and protocols were approved by the local ethics committee of the Utrecht University Medical Center and contributing partners of the Dutch “Parelsnoer Project”. An overview of clinical characteristics and cytogenetics can be found in Supplemental Table 2. Primary MM cells were cultured on near-confluent monolayers of MS-5 feeder cells as previously described [26]. For flow cytometric analysis primary MM cells were discriminated by positive surface staining using CD38-PerCP.CY5.5 monoclonal antibody (Biolegend).

## 2.3 | Healthy donor primary cells

CD34<sup>+</sup> stem and progenitor cells were isolated from umbilical cord blood as previously described [27]. In short, MNC were isolated using Ficoll-Paque and CD34<sup>+</sup> cells were isolated using magnetic bead separation (Miltenyi Biotec) resulting in a 80-95% pure population. CD34<sup>+</sup> cells were cultured in X-VIVO 15 (Lonza), supplemented with 50 ng/ml Flt3L, 50 ng/ml SCF, 20 ng/ml IL-3 and 20 ng/ml IL-6 (all Miltenyi). For flow cytometric analysis CD34<sup>+</sup> cells were discriminated by monoclonal antibody CD34-FITC (BD Biosciences).

Endothelial progenitor cells (EPC) were isolated from cord blood MNC as previously described and cultured in EGM-2 medium (Lonza), supplemented with 10% FBS, SingleQuot kit (Lonza), and 100 µg/ml penicillin-streptomycin on collagen-I (BD Biosciences) coated surfaces [28]. Multipotent mesenchymal stem cells (MSC) were isolated from MNC of healthy donor BM aspirates as previously described and cultured in MEMα, supplemented with 10% FBS, 0.2 mM L-ascorbic acid 2-phosphate (Sigma Aldrich) and 100 µg/ml penicillin-streptomycin [28]. All samples were obtained after informed consent and protocols were approved by the local ethics committee of the Utrecht University Medical Center.

## 2.4 | Preclinical 3D MM model

MSC, EPC and OPM-2 cells were combined in a 3D co-culture using growth-factor reduced Matrigel 50% (Corning) in a 4:1:1 cellular ratio, respectively, containing equal ratios of culture medium as previously described by Braham *et al.* [28]. To discriminate the three cell populations, OPM-2 cells were labeled with CellTrace-violet (Invitrogen) and EPC with Vybrant DiO (ThermoFisher Scientific).

## 2.5 | Apoptosis assays

Cell viability of HMCLs, primary MM cells, CD34<sup>+</sup> cells, MSC and EPC was determined after 48 hours of drug exposure by staining with 15 nM DiOC6 (Thermo Fisher Scientific) and/or 20 nM TO-PRO-3 (Thermo Fisher Scientific) unless stated otherwise and measured by flow cytometry (FACS Canto II, BD Biosciences) using FACSDiva software (BD Biosciences). Data was analyzed using FlowJo software (BD). Specific apoptosis was calculated by relating the reduced percentage of viable cells (DiOC6<sup>+</sup>/TO-PRO-3<sup>-</sup>) upon drug exposure to the percentage of viable control cells, as follows:  $([\% \text{ cell death in treated cells} - \% \text{ cell death in control}] / \% \text{ viable cells control}) \times 100\%$ . The drug combination effects were determined by comparing observed (OBS) specific apoptosis to hypothetical expected (EXP) specific apoptosis that assumes an additive effect of the two combined drugs. This was

calculated as previously published by Nijhof *et al.*:  $[(\text{apoptosis drug A} + \text{apoptosis drug B}) - (\text{apoptosis drug A} \times \text{apoptosis drug B})]$  [29]. Synergy was assessed using isobolograms. All drug combinations that caused 50% specific apoptosis ( $IC_{50}$ ) or 25% specific apoptosis ( $IC_{25}$ ) were included to create isobolograms. Combination indexes (CIs) were calculated using the Chou-Talalay method [30].

## 2.6 | Kinome analysis

For kinomic profiling HMCLs were lysed in M-PER mammalian protein extraction reagent (Thermo Fisher Scientific) containing Halt protease and Halt phosphatase inhibitor cocktails (Thermo Fisher Scientific). Analysis of serine/threonine kinase (STK) activity was performed using the high-throughput peptide microarray system of the PamStation 12 platform (PamGene), according to the manufacturer's instructions. Initial sample and array processing and image captures were performed using Evolve software (PamGene). Raw data processing, quantification and statistical analysis of peptide phosphorylation was performed using BioNavigator software (PamGene). Prediction of upstream kinases was performed on peptides with dexamethasone-induced statistically significant altered phosphorylation using the Kinexus Kinase Predictor ([www.phosphonet.ca](http://www.phosphonet.ca)) and identified by scoring kinase prevalence in the top10 list per peptide.

## 2.7 | SDS-PAGE, immunoblotting and antibodies

Total cell lysates were prepared in lysis buffer containing 1% NP-40. Cytosolic and nuclear fractions were separated by subsequent exposure to lysis buffer containing 0.1% NP-40 (cytosolic fraction), 1% NP-40, and RIPA lysis buffer in combination with mechanical disruption (nuclear fraction). Proteins were separated using mini-protean TGX (Bio-Rad) SDS-PAGE electrophoresis and transferred to low-fluorescence PVDF membranes (Bio-Rad). An overview of all primary antibodies incorporated in this study can be found in Supplemental Table 3. Detection was performed using secondary antibodies goat-anti-mouse 680RD and goat-anti-rabbit 800CW (LI-COR Biosciences) and infra-red imaging (Odyssey Sa, LI-COR Biosciences). Image capture was performed using Image Studio software (LI-COR). Image processing and quantification was performed using ImageJ2 (Fiji) software.

## 2.8 | ImageStream flow cytometry

HMCLs were fixed by 4% PFA, permeabilized using 100% ice-cold methanol and incubated with rabbit anti-FOXO1, rabbit anti-FOXO3a, or an equal antibody concentration of rabbit IgG isotype control (R&D systems). Subsequently, cells were incubated with FITC-conjugated goat-anti-rabbit (Jackson ImmunoResearch) in 1% BSA. For nuclear staining, DRAQ5 (1  $\mu$ M; BioLegend) was added directly

before sample analysis. Flow cytometry was performed on an ImageStreamX MKII (Amnis, Luminex). Bright-field and immunofluorescent images were captured at 60x magnification using Inspire software (Amnis, Luminex). Per sample 20,000 cells were analyzed and selected for round, single cells in focus. The Similarity feature of Ideas analysis software (Amnis, Luminex) was used to determine nuclear localization of FOXO.

## 2.9 | Intracellular staining flow cytometry

HMCL fixation, permeabilization and antibody incubation were performed as described for ImageStream flow cytometry, using rabbit anti-pS6 Ser235/236, rabbit anti-pS6 Ser240/244, rabbit IgG isotype control and FITC-conjugated goat-anti-rabbit.

## 2.10 | Statistical analysis

Data bars are represented as mean and error bars indicate standard error of the mean. Data of synergy experiments visualized as heatmaps show the mean of 3 individual experiments. Datapoints of experiments comparing EXP and OBS specific apoptosis are obtained from the same 3 individual experiments. Statistical analysis was performed using GraphPad Prism8 (GraphPad software Inc.). Sets of 2 groups were compared using paired *t*-tests and comparison of 3 groups was performed by 2-way ANOVA using Sidak correction for multiple comparison. For all tests a *p*-value of  $< 0.05$  was considered statistically significant.

# 3 | RESULTS

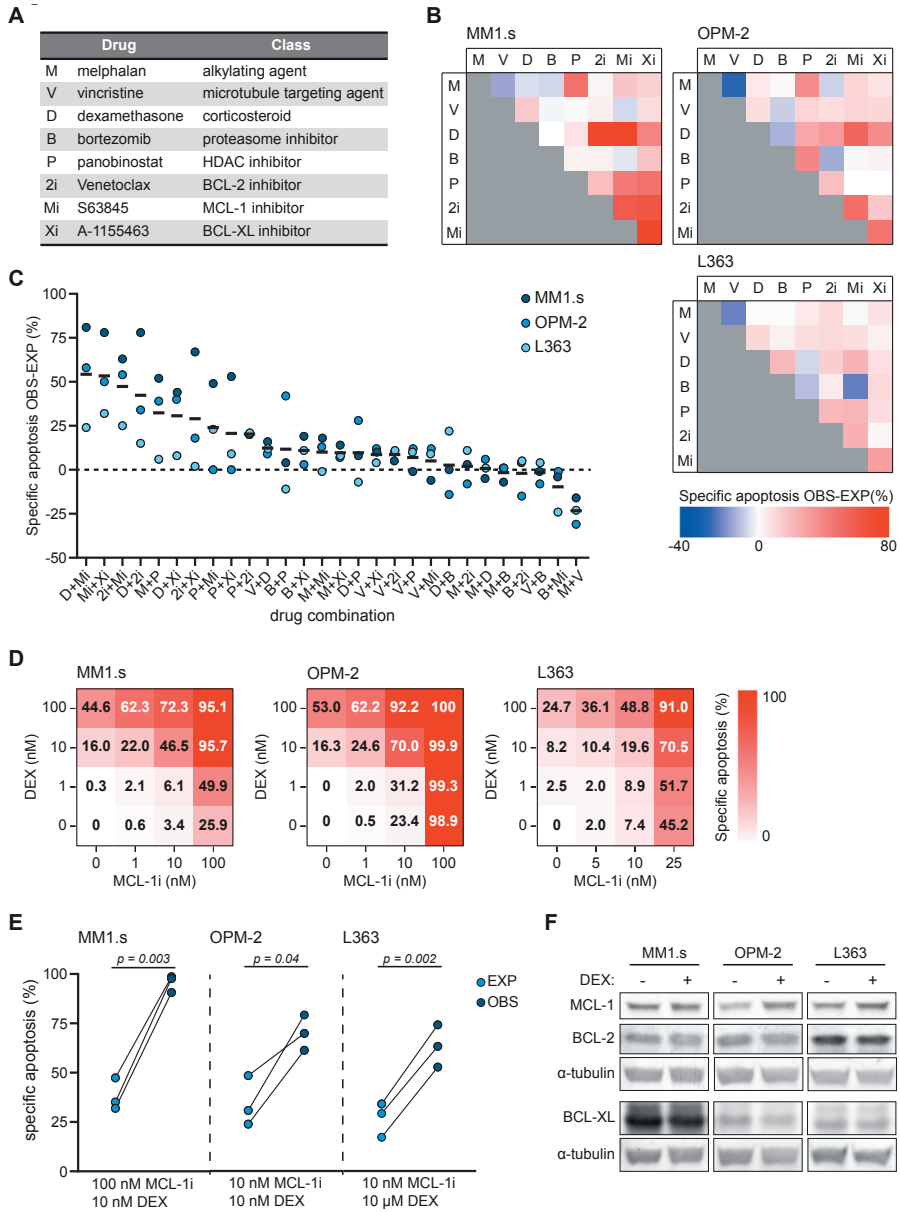
## 3.1 | Dexamethasone synergizes with MCL-1 inhibitor S63845 to induce apoptosis

Eight drugs representing 5 drug classes (Figure 1A), that are available or in clinical trials for (RR) MM and have a direct effect on apoptosis induction *in vitro*, were tested in combinations of 2 for synergistic apoptosis of HMCLs. Of the resulting 28 drug combinations, 13 combinations showed a more-than-additive effect on apoptosis of all 3 HMCLs (Figure 1B-C). The most potent drug combinations included combinations of BH3-mimetics and combinations of a BH3-mimetic with dexamethasone (Figure 1C). The drug combination with the most potent synergistic response was dexamethasone with MCL-1i. The average specific apoptosis induced by this combination was more than 50% higher compared to the sum of the individual drugs.

To verify this result, the HMCLs were exposed to dilution series of dexamethasone and MCL-1i, individual and combined (Figure 1D and Supplemental Figure 2). Specific apoptosis at the optimal drug concentrations was significantly increased compared to an additive effect of the two drugs (Figure 1E). In addition, average CIs below 0.2 (MM1s.), 0.6 (OPM-2) and 0.4 (L363) confirmed synergy between dexamethasone and MCL-1i in HMCLs with varying sensitivity to the single drugs (Supplemental Figure 3).

Expression of pro-survival BCL-2 family members has been shown to influence sensitivity to MCL-1 inhibition [26], and thus potentially also affects synergy between dexamethasone and MCL-1i. Therefore we measured their expression in dexamethasone-treated HMCLs. Exposure of HMCLs to dexamethasone did not reduce protein levels of MCL-1, BCL-2 or BCL-XL (Figure 1F). This excludes direct reduction of pro-survival proteins by dexamethasone as a general underlying mechanism of synergy in combination with MCL-1i.

**►Figure 1 | Dexamethasone synergizes with MCL-1 inhibition to induce apoptosis of HMCLs.** (A) Overview of the drugs that were implemented in the *in vitro* lethality screen, including their abbreviations and representing drug class. (B) Matrices showing the combined effect of 2 drugs in inducing specific apoptosis of HMCLs MM1s, OPM-2 and L363. Observed (OBS) specific apoptosis is compared to expected (EXP) specific apoptosis and represented by a color scale in which blue indicates an antagonistic effect, white an exact additive response and red a synergistic effect. Drug abbreviations as represented in panel A. Drug concentrations are described in Supplemental Table 1. Viability is analyzed after 48 hours of drug exposure. (C) Data as shown in panel B, ranked by the average effect of the drug combinations on OBS-EXP specific apoptosis of the 3 HMCLs. Mean values are indicated by solid black lines. The dashed line indicates an exact additive effect. (D) Heatmaps showing specific apoptosis of indicated HMCLs induced by serial dilution of dexamethasone (DEX) and MCL-1i, individual or combined. Viability was analyzed after 48 hours of drug exposure, values represent the mean of 3 individual experiments. (E) Plots comparing EXP to OBS specific apoptosis induced by DEX and MCL-1i combinations. Per HMCL the drug combination that resulted in the highest average OBS-EXP ratio was selected from the data obtained in panel D. The 3 connected datapoints show the data obtained from 3 individual experiments. Statistical analysis was performed by paired *t*-tests. (F) Representative western blot showing MCL-1, BCL-2 and BCL-XL protein expression of indicated HMCLs after 24 hours of exposure to 1  $\mu$ M dexamethasone or negative control. Alpha-tubulin was used as a loading control.



### **3.2 | Kinome analysis reveals dexamethasone-mediated reduction of Akt signaling as potential underlying mechanism of synergy with MCL-1i**

To further investigate the mechanism underlying synergy between dexamethasone and MCL-1i, kinome analysis on dexamethasone-treated HMCLs was performed. A comprehensive decrease in STK phosphorylation was observed in dexamethasone-treated samples compared to their paired controls (Figure 2A). Statistical analysis revealed 11 peptides with significantly reduced phosphorylation in both HMCLs, 25 unique peptides for MM1.s and 26 for OPM-2 (Supplemental Figure 4). More than 30% of these peptides belong to established Akt targets: 7 unique Akt targets in MM1.s and 5 in OPM-2, and 7 Akt targets, including the well-established downstream mediator mTOR, S6 and Bad, were identified in both HMCLs (Figure 2B). Additional analysis of the significant peptides by database-driven software predicted a reduction in Akt1 kinase activity as the single significant effect of dexamethasone shared between both HMCLs (Figure 2C).

### **3.3 | Dexamethasone exposure does not affect FOXO and GSK3 activity**

Two potent downstream mechanisms by which Akt regulates survival and apoptosis are inactivation of FOXO and GSK3 [19]. Western blot analysis showed that HMCLs either express FOXO1 (L363), FOXO3a (MM1.s) or a combination of both (OPM-2) (Supplemental Figure 5). To test if the predicted dexamethasone-mediated reduction in Akt1 activity also results in nuclear translocation and thus re-activation of FOXO, the 3 HMCLs were exposed to dexamethasone or copanlisib, a pan-class I PI3K inhibitor that strongly reduces Akt activity and downstream signaling [31]. Exposure of the HMCLs to dexamethasone did not alter nuclear FOXO1 or FOXO3a levels (Figure 3A). Visualization and quantification of FOXO expression relative to nuclear positions by image-based flow cytometry showed a predominant cytosolic localization of FOXO in untreated HMCLs, characteristic of FOXO inhibition by active Akt (Figure 3B-C). Exposure to dexamethasone did not alter these FOXO localization patterns. Only copanlisib exposure increased nuclear FOXO localization in the 3 HMCLs.

In addition to FOXO activation, we investigated if dexamethasone could reduce Akt-mediated inhibition of GSK3. Hereto the phosphorylation status of the GSK3 $\beta$  isoform on inhibitory serine 9 residue was assessed. Exposure to dexamethasone did not alter GSK3 $\beta$  phosphorylation in the 3 HMCLs (Figure 3D and Supplemental Figure 6). This in contrast to copanlisib, which reduced pGSK3 $\beta$  S9 expression



by more than 40%. Combined, this indicates that dexamethasone does not alter FOXO and GSK3 activity downstream of Akt.

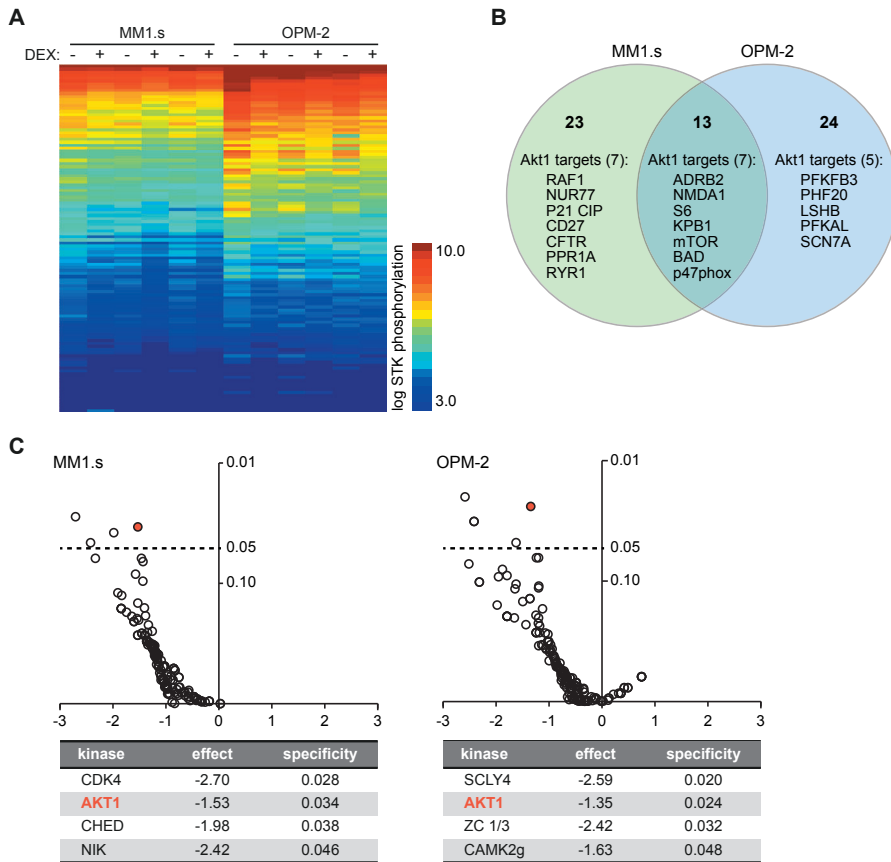


**Figure 2 | Exposure of HMCLs to dexamethasone reduces phosphorylation of Akt1 substrates.** (A) Heatmap showing serine/threonine kinase (STK) phosphorylation of peptides in lysates of MM1.s and OPM-2 exposed to 1  $\mu$ M dexamethasone (DEX) or DMSO control for 4 hours. Columns represent 3 technical triplicates per HMCL and treatment condition. Every row represents a unique peptide motif. The log STK phosphorylation is indicated by a color scale in which low phosphorylated peptides are indicated by blue and high phosphorylated peptides by orange/red. (B) Venn diagram depicting total number of peptides with statistically significant reduced phosphorylation in dexamethasone-treated MM1.s (23 unique hits) and OPM-2 (24 unique hits; 13 hits shared between both HMCLs), compared to control cells. Significant hits belonging to Akt1 downstream substrates are specified per HMCL (7/23 unique hits for MM1s; 5/24 unique hits for OPM-2; 7/13 hits shared between both HMCLs). For original data see Supplemental Figure 4. (C) Volcano plot of predicted STK activity based on statistically significant dexamethasone-mediated reduction of peptide phosphorylation as shown in Supplemental Figure 4, showing fold-difference (x-axis) and specificity (y-axis). Statistical significance with a  $p$ -value < 0.05 is indicated by the dashed line. Details are provided for the significant STKs per HMCL, Akt1 is indicated by the red mark.

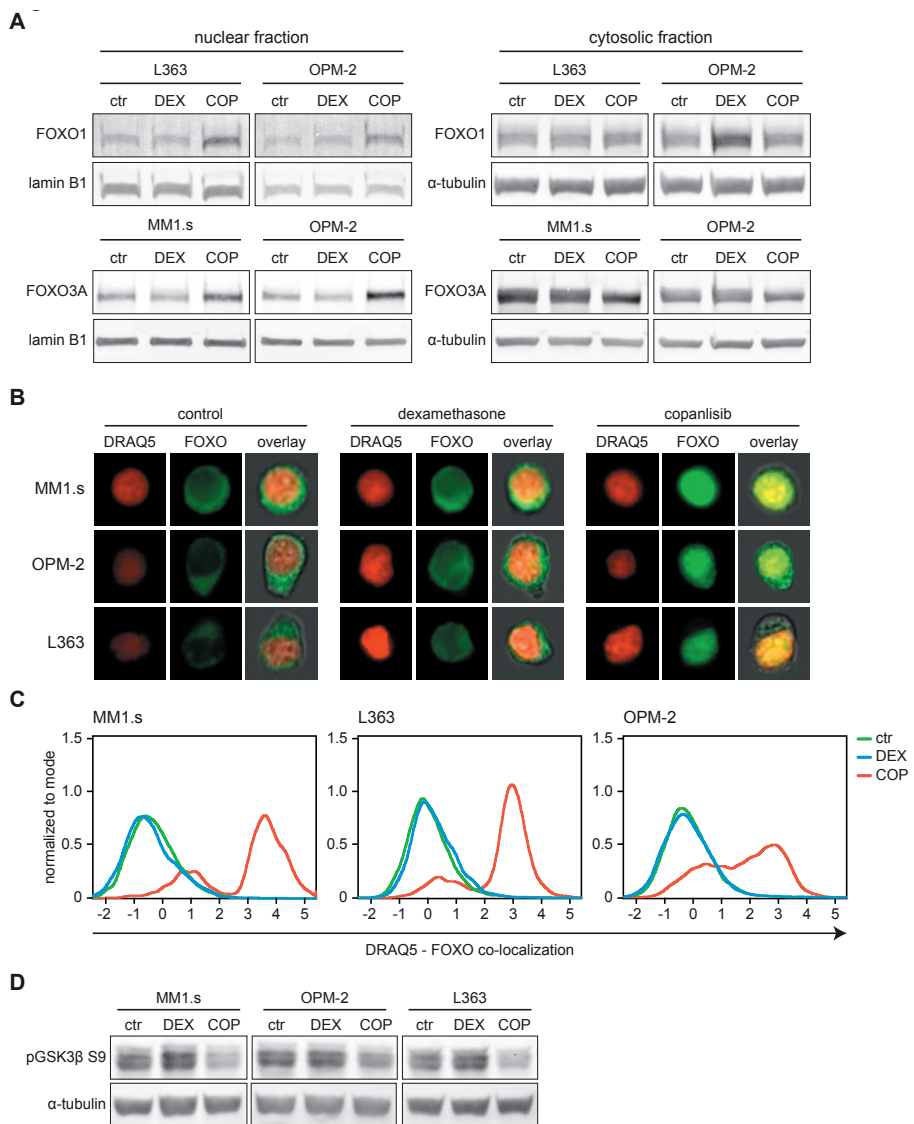


**Figure 3 | Exposure to dexamethasone does not alter FOXO or GSK3β activity in HMCLs.** (A) Representative western blot showing FOXO1 and FOXO3a protein expression in nuclear and cytosolic fractions of the indicated HMCLs after 4 hours of exposure to 1 μM dexamethasone (DEX), 100 nM copanlisib (COP) or negative control (ctr). Alpha-tubulin and lamin B1 were used as loading controls for cytosolic and nuclear fractions, respectively. (B) Representative image-based flow cytometry image captures by ImageStream at original 60x magnification from indicated HMCLs exposed for 4 hours to 1 μM dexamethasone, 100 nM copanlisib or negative control. Single images were taken for nuclear dye DRAQ5 and FOXO (FOXO3a for MM1.s and OPM-2 and FOXO1 for L363) and overlaid with bright-field images. (C) Histograms showing co-localization between DRAQ5 and FOXO of ImageStream data as

obtained in panel B. A positive value indicates similar pixel occupancy, and therefore colocalization, between DRAQ5 and FOXO, while a negative value indicates no similarity in pixel occupancy between both signals. (D) Representative western blot showing expression of GSK3 $\beta$  phosphorylated on serine residue 9 (pGSK3 $\beta$  S9) in indicated HMCLs after 4 hours of exposure to 1  $\mu$ M DEX, 100 nM COP or control. Alpha-tubulin was used as a loading control. For quantification see Supplemental Figure 6.

### 3.4 | Dexamethasone inhibits the mTORC1-P70S6K axis which underlies its synergistic effects with MCL-1 inhibition

An alternative for Akt-mediated inhibition of FOXO and GSK3 to regulate cell death and survival is Akt-mediated activation of mTORC1 [19]. To determine the activity of this complex, the phosphorylation status of its 2 direct targets, 4E-BP1 threonine 37/46 and P70S6K threonine 389, was assessed. Although dexamethasone did not alter 4E-BP1 phosphorylation, it reduced P70S6K phosphorylation by approximately 50% in all 3 HMCLs (Figure 4A and Supplemental Figure 7). To assess whether P70S6K activity is indeed inhibited, we measured phosphorylation of its direct substrate ribosomal protein S6. As expected, the dexamethasone-treated HMCLs showed a clear reduction in S6 phosphorylation on both serine 235/236 and 240/244 residues (Figure 4B). This data is in concordance with the reduction in mTOR and S6 phosphorylation that was observed in the kinome analysis of dexamethasone-treated HMCLs (Figure 2B). Furthermore, prednisolone, the active metabolite of the GC prednisone, recapitulated dexamethasone effects. In combination with MCL-1i, prednisolone induced synergistic apoptosis of the HMCLs MM1.s and L363 (Supplemental Figure 8A-C) and reduced S6 phosphorylation on serine 235/236 and serine 240/244 residues to a similar extent as dexamethasone (Supplemental Figure 8D).

To determine if the dexamethasone-mediated reduction in mTORC1 signaling could be the molecular mechanism responsible for synergy with MCL-1i, dexamethasone was replaced by the allosteric mTORC1 inhibitor rapamycin. Although sensitivity to rapamycin varied, the combination with MCL-1i substantially increased apoptosis of the 3 HMCLs (Figure 4C and Supplemental Figure 9). Specific apoptosis induced by this drug combination was significantly higher than could be expected by an additive effect of the two drugs in MM1.s and L363 (Figure 4D). A similar trend was observed for OPM-2, even though this HMCL was sensitive to single-agent rapamycin. Taken together, these data indicate that dexamethasone inhibits the mTORC1-P70S6K axis downstream of Akt and that this inhibition could explain the synergy with MCL-1i.

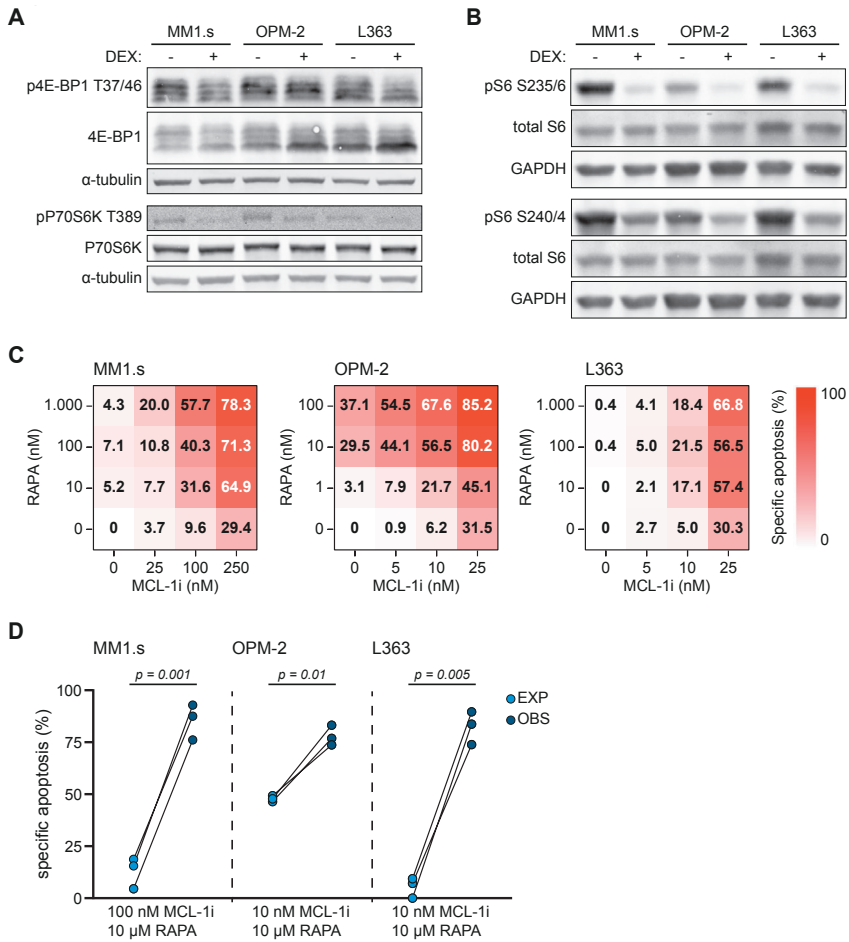


**Figure 4 | Dexamethasone reduces mTORC1 signaling and mTORC1 inhibitor rapamycin synergizes with MCL-1i.** (A) Representative western blot showing total 4E-BP1 and 4E-BP1 phosphorylation on threonine residue 37/46 (p4E-BP1 T37/46), and total P70S6K and P70S6K phosphorylation on threonine residue 389 (pP70S6K T389) in indicated HMCLs after 4 hours of exposure to 1  $\mu$ M dexamethasone (DEX) or negative control. Alpha-tubulin was used as a loading control. For quantification see Supplemental Figure 7 (B) Representative western blot showing total S6 and S6 phosphorylation on serine residues 235/236 (pS6 S235/6) and 240/244 (pS6 S240/4) in indicated HMCLs after 4 hours of exposure to 1  $\mu$ M DEX or negative control. GAPDH was used as a loading control. (C) Heatmaps showing specific apoptosis of indicated HMCLs induced by serial dilution of rapamycin (RAPA) and MCL-1i, individual or combined. Viability was analyzed after 48 hours of drug exposure, values show the mean of 3 individual experiments. (D) Plots comparing expected (EXP) specific apoptosis to observed (OBS) specific apoptosis induced by RAPA and MCL-1i combinations. Per HMCL the drug combination that resulted in the highest average OBS-EXP ratio was selected from the data obtained in panel C. The 3 connected datapoints show the data obtained from 3 individual experiments. Statistical analysis was performed by paired *t*-tests.

### 3.5 | Specific P70S6K1 inhibitor PF-4708671 can replace dexamethasone in the synergistic combination with MCL-1 inhibition

To further assess the role of the P70S6K signaling axis as a mechanism of synergy between dexamethasone and MCL-1i we investigated the effects of the specific P70S6K1 isoform inhibitor PF-4708671 (S6K1i). Titration of S6K1i on MM1.s showed that it reduces phosphorylation of S6 in a dose-dependent manner, with an optimal effect at a dosage of 10  $\mu$ M, similar to what was previously described (Figure 5A) [32]. This was comparable to inhibition mediated by 1  $\mu$ M dexamethasone (Figure 5B). Similar to dexamethasone, S6K1i exposure resulted in a dose-dependent induction of apoptosis of the 3 HMCLs (Figure 5C and Supplemental Figure 10). Combination of S6K1i with MCL-1i significantly increased specific apoptosis of MM1.s and L363 compared to the additive effect of the individual drugs (Figure 5D). In addition, average CIs below 0.6 (MM1.s), 0.7 (OPM-2) and 0.8 (L363) confirmed synergy between S6K1i and MCL-1i for all 3 HMCLs (Supplemental Figure 11). Together, these data show that dexamethasone could be replaced by S6K1i in the combination with MCL-1i to synergistically induce apoptosis of HMCLs. A potential pitfall of inhibiting molecules downstream in the Akt pathway is release of the negative feedback loop between S6K and IRS1, which can result in hyperactivation of Akt [33], and could therefore reverse anti-myeloma effects of S6K1i. Therefore, we compared the effects of dexamethasone and S6K1i on Akt kinase activity by assessing the phosphorylation status at the activating serine 473 residue (Supplemental Figure S12A-B). S6K1i exposure, single or in combination with MCL-1i, did not result in increased phosphorylation of Akt S473 compared to dexamethasone and therefore poses no increased risk of Akt hyperactivation.

One mechanism by which dexamethasone and other GCs induce apoptosis of MM and other hematopoietic cancers is by induction of the pro-apoptotic BH3-only protein BIM [10,34]. As expected, exposure to dexamethasone induced a dose-dependent increase in BIM expression in all 3 HMCLs (Supplemental Figure 13A-B). However, exposure to S6K1i only resulted in an increase in BIM expression in MM1.s, but not in the other HMCLs (Figure 5E). BIM expression in S6K1i-treated OPM-2 and L363 remained stable or even decreased compared to untreated control cells. Statistical analysis showed that expression of all 3 main BIM isoforms was significantly lower in S6K1i-treated OPM-2 and L363, compared to their dexamethasone-treated counterparts (Figure 5F). Combined, this indicates that BIM induction is not required for S6K1i-induced apoptosis of HMCLs or its synergistic effect in combination with MCL-1i. In addition, we assessed expression of pro-survival proteins MCL-1, BCL-2 and BCL-XL and of the pro-apoptotic BH-3 only protein NOXA, that was also identified to play an important role in MM treatment [35].

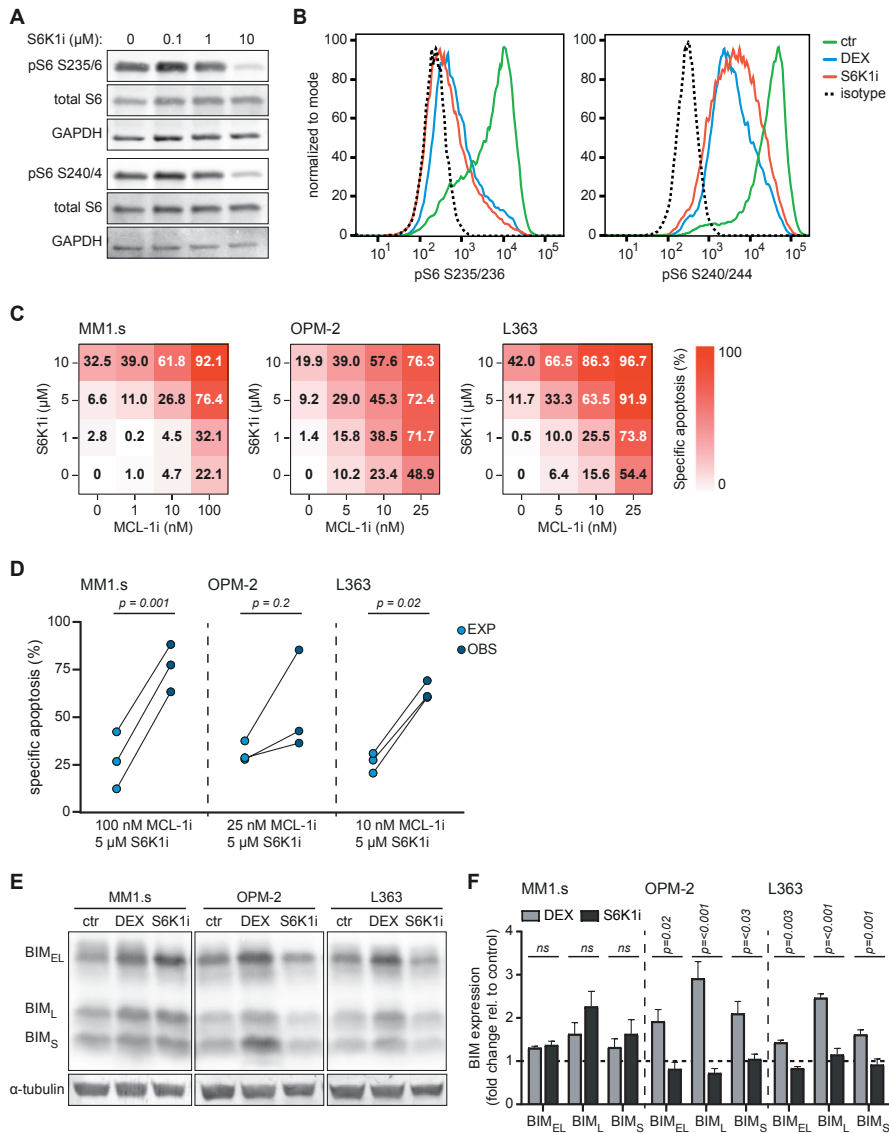


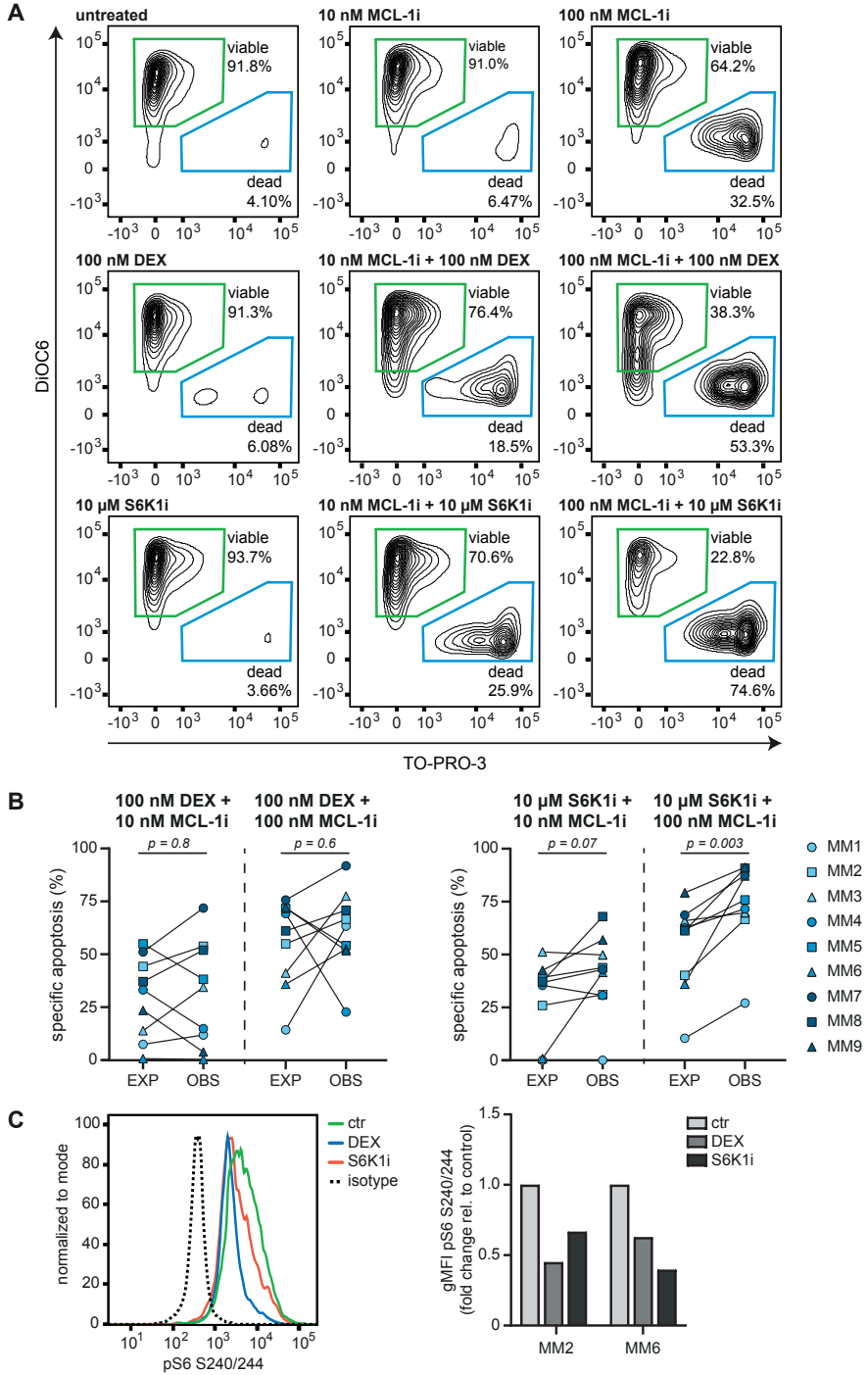
**Figure 5 | S6K1i inhibits S6 phosphorylation and synergizes with MCL-1i in apoptosis induction of HMCLs, independent of BIM protein induction.** (A) Western blot showing total S6 and S6 phosphorylation on serine residues 235/236 (pS6 S235/6) and 240/244 (pS6 S240/4) in MM1.s after 4 hours of exposure to indicated concentrations of S6K1i. GAPDH was used as a loading control. (B) Histograms comparing expression of S6 phosphorylation on serine residues 235/236 (pS6 S235/236) and 240/244 (pS6 S240/244) in MM1.s after 4 hours of exposure to 1 μM dexamethasone (DEX) or 10 μM S6K1i, determined by flow cytometric analysis. Expression was relative to medium-treated control cells (ctr) and corrected for isotype control, indicated by the dashed line. (C) Heatmaps showing specific apoptosis of indicated HMCLs induced by serial dilution of S6K1i and MCL-1i, individual or combined. Viability was analyzed after 48 hours of drug exposure, values show the mean of

3 individual experiments. (D) Plots comparing expected (EXP) specific apoptosis to observed (OBS) specific apoptosis induced by S6K1i and MCL-1i combinations. Per HMCL the drug combination that resulted in the highest average OBS-EXP ratio was selected from the data obtained in panel C. The 3 connected datapoints show the data obtained from 3 individual experiments. Statistical analysis was performed by paired *t*-tests. (E) Representative western blot showing expression of 3 BIM isoforms in indicated HMCLs after 24 hours of exposure to 1  $\mu$ M DEX, 10  $\mu$ M S6K1i or negative control (ctr). Alpha-tubulin was used as a loading control. (F) Comparison of BIM isoform expression in HMCLs treated with 1  $\mu$ M DEX or 10  $\mu$ M S6K1i. Values show the mean quantification of 3 individual western blot experiments, normalized to  $\alpha$ -tubulin and relative to untreated control cells, indicated by the dashed line. Statistical analysis was performed by 2-way ANOVA using Sidak correction for multiple testing; ns, not significant.

Interestingly, no consistent alterations in protein expression were observed when HMCLs were exposed to dexamethasone or S6K1i as single agents, or in combination with MCL-1i (Supplemental Figure 14A-B). Also, activity of the pro-apoptotic BH-3-only protein Bad, as assessed by phosphorylation on the serine 136 residue that has previously been linked to P70S6K-mediated regulation of cell survival [36], showed no consistent decrease in these conditions (Supplemental Figure 15A-B). Together, these data provide no indication for a conserved mechanism of apoptosis induction in HMCLs exposed to dexamethasone or S6K1i.

### 3.6 | S6K1i and MCL-1i synergistically induce apoptosis of primary MM plasma cells with minimal toxicity on stem and progenitor cells

Next, we investigated the apoptosis-inducing effects of the dexamethasone-MCL-1i and S6K1i-MCL-1i drug combinations on *ex vivo* cultured plasma cells from 9 untreated MM patients. MNC isolated from BM aspirates were exposed to dexamethasone, S6K1i, and MCL-1i, individual and combined, and specific apoptosis of CD38<sup>+</sup> plasma cells was assessed. Exposure to MCL-1i resulted in a dose-dependent increase of specific apoptosis ranging from 0% - 37% (average 22%) at 10 nM, and 10% - 72% (average 49%) at 100 nM (Figure 6A and Supplemental Figure 16). For single dosages of dexamethasone and S6K1i, specific apoptosis varied between 0%-37% (average 10%) and 0% - 25% (average 9%) respectively. In 5/9 MM samples, combination of dexamethasone with low-dose MCL-1i resulted in an increase of specific apoptosis that was higher than could be expected from an additive response (Figure 6B). A similar effect was observed for 6/9 MM samples when dexamethasone was combined with high-dose MCL-1i. Importantly, in all 9 MM samples S6K1i resulted in an additive or more-than-additive effect on apoptosis in combination with low-dose MCL-1i. In combination with high-dose MCL-1i a significant more-than-additive effect on apoptosis was reached in all examined MM samples.





◀**Figure 6 | S6K1i and MCL-1i synergistically induce apoptosis of *ex vivo* cultured primary MM plasma cells.** (A) Representative plots of flow cytometric analysis of apoptosis induction in CD38<sup>+</sup> primary MM cells after 48 hours of exposure to the indicated concentrations MCL-1, dexamethasone (DEX) or S6K1i. Gates represent viable (DiOC6<sup>+</sup>/TO-PRO-3<sup>-</sup>) and dead (DiOC6<sup>-</sup>/TO-PRO-3<sup>+</sup>) cells. (B) Plots comparing expected (EXP) specific apoptosis to observed (OBS) specific apoptosis induced by 48 hours of exposure to 100 nM DEX or 10 μM S6K1i, in combination with 10 nM or 100 nM MCL-1i in CD38<sup>+</sup> primary MM cells as indicated in panel A. Statistical analysis was performed by paired *t*-tests. (C) Representative histogram and quantification plot showing S6 phosphorylation on serine residues 240/244 (pS6 S240/244) in CD38<sup>+</sup> primary MM cells exposed to 100 nM DEX or 10 μM S6K1i for 8 hours, assessed by flow cytometry. The geometric mean fluorescent intensity (gMFI) was normalized to IgG isotype control and relative to untreated control cells (ctr).

Three of the included MM samples (MM1, MM3 and MM4) were subjected to a more extensive range of drug concentrations (Supplemental Figure 17A). With average CI of 0.4-0.7 for dexamethasone-MCL-1i combinations and CI of 0.6-0.7 for S6K1i-MCL1i combinations, synergy in primary MM was confirmed for both drug combinations.

We also analyzed S6 phosphorylation in 2 of the MM samples, since this was reduced in HMCLs after dexamethasone or S6K1i treatment. Exposure of both MM2 and MM6 to single dexamethasone or S6K1i reduced S6 phosphorylation by 30%-60%, compared to untreated control cells (Figure 6C). These results underline the molecular mechanism-of-action shared between dexamethasone and S6K1i to reduce P70S6K activity.

To explore a potential therapeutic window for the S6K1i-MCL-1i drug combination we assessed its toxicity compared to the dexamethasone-MCL-1i drug combination in CD34<sup>+</sup> stem and progenitor cells that were isolated from umbilical cord blood MNC of 2 healthy donors. Exposure of CD34<sup>+</sup> cells to S6K1i in combination with low dose MCL-1i resulted in 8% average specific apoptosis (Supplemental Figure 18). In combination with high dose MCL-1i toxicity increased to 33%, which was similar to specific apoptosis induced by combination of dexamethasone with low dose MCL-1i. To compare the apoptosis-inducing effects on myeloma cells to potential toxic side-effects on microenvironment stem and progenitor cells we assessed both S6K1i-MCL-1i and dexamethasone-MCL-1i drug combinations in a pre-clinical 3D MM model that was previously published by Braham *et al.* [28]. S6K1i in combination with high dose MCL-1i diminished the viable OPM-2 population, while no reduction of the viable EPC or MSC population could be observed. (Supplemental Figure 19A) Importantly, quantification of specific apoptosis showed near-complete killing of OPM-2 cells (97%) with only limited toxic effects on EPC and MSC populations (10% and 14% respectively; Supplemental Figure 19B). This was similar to the effects of dexamethasone in combination with high dose MCL-1i. Since these combinatorial dosages of S6K1i and MCL-1i were sufficient to induce synergistic apoptosis of primary MM cells, this indicates a potential therapeutic window for intervention by the S6K1i-MCL-1i drug combination.

## 4 | DISCUSSION

The rapid development of new drugs for the treatment of MM holds a promising outlook for patient survival and quality of life. However, for these novel drugs to be effectively incorporated in MM treatment regimens, it is essential to investigate which drugs act in synergy, by which mechanisms, and how this affects toxicity. In this study we performed a lethality screen to assess synergy between 2 drugs, both new and conventional, and reported MCL-1i and dexamethasone as the most potent synergistic combination. The successful combination of dexamethasone and MCL-1 inhibition in MM has recently been recognized by *in vitro* studies [7,8], and might be explained by their converging effects on intrinsic apoptosis activation. However, although dexamethasone and other GCs are a cornerstone of MM therapy, the mechanism(s) by which they induce apoptosis have been a long standing question. Dexamethasone treatment of MM1.s cells has been shown to reduce transcription and expression of pro-survival proteins [8,37], but we observed no dexamethasone-induced reduction in MCL-1, BCL-2 or BCL-XL protein levels. A central role has also been assigned to dexamethasone-induced expression of pro-apoptotic BIM [10,38]. Indeed, we observed increased BIM expression in HMCLs after dexamethasone exposure, but direct transcriptional regulation by the dexamethasone-GR complex seems unlikely due to lack of GREs in the BIM promoter region [39].

By direct transcriptional modulation via GREs and (in)direct interaction with multiple additional transcription factors, dexamethasone and other GCs can impact various cellular signaling systems [40]. By kinome analysis of dexamethasone-treated HMCLs we observed that 30% of the peptides with significantly reduced STK phosphorylation belong to known Akt substrates. By regulating both pro-apoptotic and pro-survival molecules, the PI3K-Akt pathway is one of the major signaling pathways balancing cell survival and apoptosis [17]. FOXO transcription factors can regulate BIM transcription in a variety of cell types, including lymphocytes [41]. In addition, GSK3 can regulate BIM activation [42], and the GSK3 $\beta$  isoform was also shown capable of regulating MCL-1 protein stability [43,44]. Our data, however, shows no dexamethasone-induced downstream Akt effects on FOXO or GSK3 $\beta$  activation, and the molecular mechanism of BIM induction therefore remains unclear.

Aberrant Akt-mTORC1 signaling is a common feature in many malignancies, including MM [45]. Although the predicted dexamethasone-mediated reduction in Akt activity was not accompanied by effects on FOXO or GSK3 $\beta$ , we could confirm a potent reduction in mTORC1 signaling. Dexamethasone could be replaced by rapamycin to mimic the synergistic effects on apoptosis in combination with MCL-

1i. Interestingly, MM1.s and L363 were insensitive to single-agent rapamycin, while the combination with MCL-1i resulted in up to 5.5-fold more apoptosis compared to single-agent MCL-1i. The potentiating effects of rapamycin to induce cell death and overcome drug resistance in combination with other agents, including bortezomib and dexamethasone, have previously been recognized in clinical trials for MM [45]. Downstream of mTORC1 we observed a 50% reduction of P70S6K phosphorylation, but only a 10% reduction in phosphorylation of 4E-BP1. This suggests that dexamethasone, similar to rapamycin and rapalogues, most strongly reduces activity of rapamycin-sensitive mTORC1 substrates (i.e. P70S6K) but less of rapamycin-insensitive mTORC1 substrates (i.e. 4E-BP1) [46].

The mTORC1-P70S6K1 axis is an important regulator of cell death and survival. It controls protein biosynthesis, an essential process required for cell growth and proliferation, and thereby indirectly affects cell survival [24]. In addition, P70S6K1 is capable of binding to mitochondrial membranes and subsequent phosphorylation of Bad, phosphorylation of Mdm2 upstream of p53, and phosphorylation of GSK3, thereby inhibiting the activity of these mediators in senescence and apoptosis [36,47,48]. Together, this makes P70S6K1 an interesting anticancer target, which resulted in the development of the first specific P70S6K1 inhibitor PF-4708671 [32]. We found that 10  $\mu\text{M}$  S6K1i was equally potent as 1  $\mu\text{M}$  dexamethasone in inhibiting P70S6K activity. In addition, dexamethasone could be replaced by S6K1i to induce synergistic apoptosis of HMCLs in combination with MCL-1i, although not to the extent of the dexamethasone-MCL-1i combination. This discrepancy might be explained by differences in apoptosis activation by both agents. Exposure of HMCLs to S6K1i did not result in BIM induction as was observed for dexamethasone, suggesting that BIM induction is not required for the synergistic killing of HMCLs in combination with MCL-1i. More likely, one or multiple P70S6K1-dependent mechanisms are responsible for the synergistic effect observed with MCL-1i. Dexamethasone-induced BIM could, however, still contribute to the overall apoptotic process, explaining the observed difference in potency between dexamethasone and S6K1i.

Although the synergistic S6K1i-MCL-1i combination was found to be somewhat less potent than the dexamethasone-MCL-1i combination in HMCLs, S6K1i did outperform dexamethasone in inducing apoptosis in a subset of primary MM cells in combination with MCL-1i. Interestingly, MM samples that showed no synergistic effect upon exposure to the dexamethasone-MCL-1i combination, did show more-than-additive apoptosis upon exposure to the S6K1i-MCL-1i combination. This effect was significant in combinations with high dose MCL-1i. A possible explanation for this difference is the more direct mechanism of action of S6K1i. Whereas dexamethasone is likely dependent on a transcription-

mediated inhibition of P70S6K, S6K1i can directly block kinase activity. This is of particular interest in the light of GC resistance. A significant subpopulation of patients experience resistance to dexamethasone and other GCs, due to a variety of molecular mechanisms resulting in altered GR function and/or GR-mediated transcription [49]. S6K1i could potentially circumvent this GC resistance and induce synergy with MCL-1i. This could also be of interest for other hematological malignancies that are treated with GCs, such as acute lymphoblastic leukemia (ALL) and non-Hodgkin lymphoma [50]. In addition, many of the GC-induced toxic side-effects are suggested to be the result of GR transactivation [51]. By replacing GCs by S6K1i in the synergistic combination with MCL-1i, GR-associated toxicity would be diminished.

Clinical studies combining MCL-1i and S6K1i could be a next step to prove the relevance of our findings. MCL-1 inhibitors, both single-agent and in combination with dexamethasone, are currently in clinical trials for MM [6]. Also, the first clinical trials using the ATP-competitive pan P70S6K inhibitor LY2584702 tosylate for treatment of patients with advanced solid tumors were completed [52,53]. A recently reported single dose study in healthy participants showed that this pan P70S6K inhibitor causes no serious adverse events (ClinicalTrials.gov Identifier: NCT01372085). The P70S6K 1 isoform inhibitor used in this study has proven to be specific with no identified off-target effects at 10  $\mu$ M dosages [32]. In addition, two studies with mouse solid tumor xenograft models reported no signs of toxicity or suffering at therapeutic dosages [54,55]. We also observed limited toxicity of healthy donor stem and progenitor cells in combination with MCL-1i at dosages that caused significant synergistic apoptosis of primary MM cells. Observed toxicity by the S6K1i-MCL-1i combination did not exceed the effects induced by the dexamethasone-MCL-1i combination. Combined, our findings provide a strong rationale to combine MCL-1 inhibitors and P70S6K(1) inhibitors in the treatment of MM to induce synergistic apoptosis of MM cells, with limited toxicity to stem and progenitor cells, and devoid of GR-induced toxicity and resistance.

## ACKNOWLEDGEMENTS

The authors thank the support facilities of the University Medical Center Utrecht (UMCU) and the Dutch Parelsnoer Institute for providing primary patient and donor samples. We are grateful to Servier for providing the MCL-1-specific inhibitor S63845. We thank M. Plantinga for umbilical cord blood CD34<sup>+</sup> samples and Z. Sebestyen for endothelial progenitor cells. In addition, we thank S. Rangarajan for support with kinome analyses. This work was supported in part by a Bas Mulder Award from the Dutch Cancer Foundation (KWF)/Alped'HuZes foundation (No. UU 2015-7663) (V.P.) and a project grant from the Dutch Cancer Foundation (KWF)/Alped'HuZes foundation (No. 11108) (V.P.).

## REFERENCES

1. Naymagon, L.; Abdul-Hay, M. Novel agents in the treatment of multiple myeloma: a review about the future. *J Hematol Oncol* 2016, *9*, 52.
2. Slomp, A.; Peperzak, V. Role and Regulation of Pro-survival BCL-2 Proteins in Multiple Myeloma. *Front Oncol* 2018, *8*, 533.
3. Delbridge, A.R.; Grabow, S.; Strasser, A.; Vaux, D.L. Thirty years of BCL-2: translating cell death discoveries into novel cancer therapies. *Nat Rev Cancer* 2016, *16*, 99-109.
4. Wuillème-Toumi, S.; Robillard, N.; Gomez, P.; Moreau, P.; Le Gouill, S.; Avet-Loiseau, H.; Harousseau, J.L.; Amiot, M.; Bataille, R. Mcl-1 is overexpressed in multiple myeloma and associated with relapse and shorter survival. *Leukemia* 2005, *19*, 1248-1252.
5. Nijhof, I.S.; van de Donk, N.; Zweegman, S.; Lokhorst, H.M. Current and New Therapeutic Strategies for Relapsed and Refractory Multiple Myeloma: An Update. *Drugs* 2018, *78*, 19-37.
6. Kotschy, A.; Szlavik, Z.; Murray, J.; Davidson, J.; Maragno, A.L.; Le Toumelin-Braizat, G.; Chanrion, M.; Kelly, G.L.; Gong, J.N.; Moujalled, D.M.; et al. The MCL1 inhibitor S63845 is tolerable and effective in diverse cancer models. *Nature* 2016, *538*, 477-482.
7. Caenepeel, S.; Brown, S.P.; Belmontes, B.; Moody, G.; Keegan, K.S.; Chui, D.; Whittington, D.A.; Huang, X.; Poppe, L.; Cheng, A.C.; et al. AMG 176, a Selective MCL1 Inhibitor, Is Effective in Hematologic Cancer Models Alone and in Combination with Established Therapies. *Cancer Discov* 2018, *8*, 1582-1597.
8. Teh, C.E.; Gong, J.N.; Segal, D.; Tan, T.; Vandenberg, C.J.; Fedele, P.L.; Low, M.S.Y.; Grigoriadis, G.; Harrison, S.J.; Strasser, A.; et al. Deep profiling of apoptotic pathways with mass cytometry identifies a synergistic drug combination for killing myeloma cells. *Cell Death Differ* 2020.
9. Dimopoulos, M.A.; Jakubowiak, A.J.; McCarthy, P.L.; Orlowski, R.Z.; Attal, M.; Bladé, J.; Goldschmidt, H.; Weisel, K.C.; Ramasamy, K.; Zweegman, S.; et al. Developments in continuous therapy and maintenance treatment approaches for patients with newly diagnosed multiple myeloma. *Blood Cancer J* 2020, *10*, 17.
10. Kfir-Erenfeld, S.; Sionov, R.V.; Spokoini, R.; Cohen, O.; Yefenof, E. Protein kinase networks regulating glucocorticoid-induced apoptosis of hematopoietic cancer cells: fundamental aspects and practical considerations. *Leuk Lymphoma* 2010, *51*, 1968-2005.
11. Greenstein, S.; Ghias, K.; Krett, N.L.; Rosen, S.T. Mechanisms of glucocorticoid-mediated apoptosis in hematological malignancies. *Clin Cancer Res* 2002, *8*, 1681-1694.
12. Chauhan, D.; Hideshima, T.; Rosen, S.; Reed, J.C.; Kharbanda, S.; Anderson, K.C. Apaf-1/cytochrome c-independent and Smac-dependent induction of apoptosis in multiple myeloma (MM) cells. *J Biol Chem* 2001, *276*, 24453-24456.
13. Rajkumar, S.V.; Blood, E.; Vesole, D.; Fonseca, R.; Greipp, P.R. Phase III clinical trial of thalidomide plus dexamethasone compared with dexamethasone alone in newly diagnosed multiple myeloma: a clinical trial coordinated by the Eastern Cooperative Oncology Group. *J Clin Oncol* 2006, *24*, 431-436.
14. Larocca, A.; Palumbo, A. How I treat fragile myeloma patients. *Blood* 2015, *126*, 2179-2185.

15. Burwick, N.; Sharma, S. Glucocorticoids in multiple myeloma: past, present, and future. *Ann Hematol* 2019, *98*, 19-28.
16. Mehta, J.; Cavo, M.; Singhal, S. How I treat elderly patients with myeloma. *Blood* 2010, *116*, 2215-2223.
17. Hoxhaj, G.; Manning, B.D. The PI3K-AKT network at the interface of oncogenic signalling and cancer metabolism. *Nat Rev Cancer* 2020, *20*, 74-88.
18. Hsu, J.H.; Shi, Y.; Hu, L.; Fisher, M.; Franke, T.F.; Lichtenstein, A. Role of the AKT kinase in expansion of multiple myeloma clones: effects on cytokine-dependent proliferative and survival responses. *Oncogene* 2002, *21*, 1391-1400.
19. Manning, B.D.; Toker, A. AKT/PKB Signaling: Navigating the Network. *Cell* 2017, *169*, 381-405.
20. Shariati, M.; Meric-Bernstam, F. Targeting AKT for cancer therapy. *Expert Opin Investig Drugs* 2019, *28*, 977-988.
21. van der Vos, K.E.; Coffey, P.J. The extending network of FOXO transcriptional target genes. *Antioxid Redox Signal* 2011, *14*, 579-592.
22. Maurer, U.; Charvet, C.; Wagman, A.S.; Dejardin, E.; Green, D.R. Glycogen synthase kinase-3 regulates mitochondrial outer membrane permeabilization and apoptosis by destabilization of MCL-1. *Mol Cell* 2006, *21*, 749-760.
23. Zoncu, R.; Efeyan, A.; Sabatini, D.M. mTOR: from growth signal integration to cancer, diabetes and ageing. *Nat Rev Mol Cell Biol* 2011, *12*, 21-35.
24. Magnuson, B.; Ekim, B.; Fingar, D.C. Regulation and function of ribosomal protein S6 kinase (S6K) within mTOR signalling networks. *Biochem J* 2012, *441*, 1-21.
25. Szalat, R.; Munshi, N.C. Novel Agents in Multiple Myeloma. *Cancer J* 2019, *25*, 45-53.
26. Slomp, A.; Moesbergen, L.M.; Gong, J.N.; Cuenca, M.; von dem Borne, P.A.; Sonneveld, P.; Huang, D.C.S.; Minnema, M.C.; Peperzak, V. Multiple myeloma with 1q21 amplification is highly sensitive to MCL-1 targeting. *Blood Adv* 2019, *3*, 4202-4214.
27. de Haar, C.; Plantinga, M.; Blokland, N.J.; van Til, N.P.; Flinsenberg, T.W.; Van Tendeloo, V.F.; Smits, E.L.; Boon, L.; Spel, L.; Boes, M.; et al. Generation of a cord blood-derived Wilms Tumor 1 dendritic cell vaccine for AML patients treated with allogeneic cord blood transplantation. *Oncoimmunology* 2015, *4*, e1023973.
28. Braham, M.V.J.; Minnema, M.C.; Aarts, T.; Sebestyen, Z.; Straetmans, T.; Vyborova, A.; Kuball, J.; Öner, F.C.; Robin, C.; Alblas, J. Cellular immunotherapy on primary multiple myeloma expanded in a 3D bone marrow niche model. *Oncoimmunology* 2018, *7*, e1434465.
29. Nijhof, I.S.; Lammerts van Bueren, J.J.; van Kessel, B.; Andre, P.; Morel, Y.; Lokhorst, H.M.; van de Donk, N.W.; Parren, P.W.; Mutis, T. Daratumumab-mediated lysis of primary multiple myeloma cells is enhanced in combination with the human anti-KIR antibody IPH2102 and lenalidomide. *Haematologica* 2015, *100*, 263-268.
30. Chou, T.C. Drug combination studies and their synergy quantification using the Chou-Talalay method. *Cancer Res* 2010, *70*, 440-446.
31. Markham, A. Copanlisib: First Global Approval. *Drugs* 2017, *77*, 2057-2062.
32. Pearce, L.R.; Alton, G.R.; Richter, D.T.; Kath, J.C.; Lingardo, L.; Chapman, J.; Hwang, C.; Alessi, D.R. Characterization of PF-4708671, a novel and highly specific inhibitor of p70

- ribosomal S6 kinase (S6K1). *Biochem J* 2010, 431, 245-255.
33. O'Reilly, K.E.; Rojo, F.; She, Q.B.; Solit, D.; Mills, G.B.; Smith, D.; Lane, H.; Hofmann, F.; Hicklin, D.J.; Ludwig, D.L.; et al. mTOR inhibition induces upstream receptor tyrosine kinase signaling and activates Akt. *Cancer Res* 2006, 66, 1500-1508.
  34. López-Royuela, N.; Balsas, P.; Galán-Malo, P.; Anel, A.; Marzo, I.; Naval, J. Bim is the key mediator of glucocorticoid-induced apoptosis and of its potentiation by rapamycin in human myeloma cells. *Biochim Biophys Acta* 2010, 1803, 311-322.
  35. Matulis, S.M.; Gupta, V.A.; Nooka, A.K.; Hollen, H.V.; Kaufman, J.L.; Lonial, S.; Boise, L.H. Dexamethasone treatment promotes Bcl-2 dependence in multiple myeloma resulting in sensitivity to venetoclax. *Leukemia* 2016, 30, 1086-1093.
  36. Harada, H.; Andersen, J.S.; Mann, M.; Terada, N.; Korsmeyer, S.J. p70S6 kinase signals cell survival as well as growth, inactivating the pro-apoptotic molecule BAD. *Proc Natl Acad Sci U S A* 2001, 98, 9666-9670.
  37. Chauhan, D.; Auclair, D.; Robinson, E.K.; Hideshima, T.; Li, G.; Podar, K.; Gupta, D.; Richardson, P.; Schlossman, R.L.; Krett, N.; et al. Identification of genes regulated by dexamethasone in multiple myeloma cells using oligonucleotide arrays. *Oncogene* 2002, 21, 1346-1358.
  38. Dong, L.; Vaux, D.L. Glucocorticoids can induce BIM to trigger apoptosis in the absence of BAX and BAK1. *Cell Death Dis* 2020, 11, 442.
  39. Wang, Z.; Malone, M.H.; He, H.; McColl, K.S.; Distelhorst, C.W. Microarray analysis uncovers the induction of the proapoptotic BH3-only protein Bim in multiple models of glucocorticoid-induced apoptosis. *J Biol Chem* 2003, 278, 23861-23867.
  40. Scheschowitsch, K.; Leite, J.A.; Assreuy, J. New Insights in Glucocorticoid Receptor Signaling-More Than Just a Ligand-Binding Receptor. *Front Endocrinol (Lausanne)* 2017, 8, 16.
  41. Dijkers, P.F.; Medema, R.H.; Lammers, J.W.; Koenderman, L.; Coffey, P.J. Expression of the pro-apoptotic Bcl-2 family member Bim is regulated by the forkhead transcription factor FKHR-L1. *Curr Biol* 2000, 10, 1201-1204.
  42. Spokoini, R.; Kfir-Erenfeld, S.; Yefenof, E.; Sionov, R.V. Glycogen synthase kinase-3 plays a central role in mediating glucocorticoid-induced apoptosis. *Mol Endocrinol* 2010, 24, 1136-1150.
  43. Ding, Q.; He, X.; Xia, W.; Hsu, J.M.; Chen, C.T.; Li, L.Y.; Lee, D.F.; Yang, J.Y.; Xie, X.; Liu, J.C.; et al. Myeloid cell leukemia-1 inversely correlates with glycogen synthase kinase-3beta activity and associates with poor prognosis in human breast cancer. *Cancer Res* 2007, 67, 4564-4571.
  44. Wang, R.; Xia, L.; Gabilove, J.; Waxman, S.; Jing, Y. Downregulation of Mcl-1 through GSK-3 $\beta$  activation contributes to arsenic trioxide-induced apoptosis in acute myeloid leukemia cells. *Leukemia* 2013, 27, 315-324.
  45. Ramakrishnan, V.; Kumar, S. PI3K/AKT/mTOR pathway in multiple myeloma: from basic biology to clinical promise. *Leuk Lymphoma* 2018, 59, 2524-2534.
  46. Choo, A.Y.; Blenis, J. Not all substrates are treated equally: implications for mTOR, rapamycin-resistance and cancer therapy. *Cell Cycle* 2009, 8, 567-572.
  47. Lai, K.P.; Leong, W.F.; Chau, J.F.; Jia, D.; Zeng, L.; Liu, H.; He, L.; Hao, A.; Zhang, H.; Meek, D.; et al. S6K1 is a multifaceted regulator of Mdm2 that connects nutrient status and DNA damage response. *Embo j* 2010, 29, 2994-3006.



48. Zhang, H.H.; Lipovsky, A.I.; Dibble, C.C.; Sahin, M.; Manning, B.D. S6K1 regulates GSK3 under conditions of mTOR-dependent feedback inhibition of Akt. *Mol Cell* 2006, 24, 185-197.
49. Scheijen, B. Molecular mechanisms contributing to glucocorticoid resistance in lymphoid malignancies. *Cancer Drug Resist* 2019, 2, 647-664.
50. Pufall, M.A. Glucocorticoids and Cancer. *Adv Exp Med Biol* 2015, 872, 315-333.
51. Schäcke, H.; Döcke, W.D.; Asadullah, K. Mechanisms involved in the side effects of glucocorticoids. *Pharmacol Ther* 2002, 96, 23-43.
52. Hollebecque, A.; Houédé, N.; Cohen, E.E.; Massard, C.; Italiano, A.; Westwood, P.; Bumgardner, W.; Miller, J.; Brail, L.H.; Benhadji, K.A.; et al. A phase Ib trial of LY2584702 tosylate, a p70 S6 inhibitor, in combination with erlotinib or everolimus in patients with solid tumours. *Eur J Cancer* 2014, 50, 876-884.
53. Tolcher, A.; Goldman, J.; Patnaik, A.; Papadopoulos, K.P.; Westwood, P.; Kelly, C.S.; Bumgardner, W.; Sams, L.; Geeganage, S.; Wang, T.; et al. A phase I trial of LY2584702 tosylate, a p70 S6 kinase inhibitor, in patients with advanced solid tumours. *Eur J Cancer* 2014, 50, 867-875.
54. Qiu, Z.X.; Sun, R.F.; Mo, X.M.; Li, W.M. The p70S6K Specific Inhibitor PF-4708671 Impedes Non-Small Cell Lung Cancer Growth. *PLoS One* 2016, 11, e0147185.
55. Segatto, I.; Berton, S.; Sonogo, M.; Massarut, S.; Fabris, L.; Armenia, J.; Mileto, M.; Colombatti, A.; Vecchione, A.; Baldassarre, G.; et al. p70S6 kinase mediates breast cancer cell survival in response to surgical wound fluid stimulation. *Mol Oncol* 2014, 8, 766-780.

## SUPPLEMENTAL TABLES

**Supplemental Table 1 | Overview of drugs.**

Drugs	Manufacturer	Concentrations		
		MM1.s	OPM-2	L363
<b>Drugs in screen</b>				
Melphalan	Sigma-Aldrich	2.5 µM	5 µM	10 µM
Vincristine	Selleck Chemicals	20 nM	3 nM	3 nM
Dexamethasone	Sigma-Aldrich	100 nM	12.5 nM	100 nM
Bortezomib	Tebu Bio	4 nM	4 nM	8 nM
Panobinostat (LBH589)	Selleck Chemicals	5 nM	5 nM	20 nM
BCL-2i ABT-199 / Venetoclax	LKT Laboratories	100 nM	100 nM	100 nM
MCL-1i S63845	Servier	100 nM	10 nM	10 nM
BCL-XLi A-1155463	MedChemExpress	100 nM	100 nM	100 nM
<b>Other drugs in study</b>				
Rapamycin (Sunitinib)	Selleck Chemicals			
P70S6K1 inhibitor (PF-4708671)	Selleck Chemicals			
Copanlisib (BAY 80-6946)	Selleck Chemicals			
Prednisolone	Sigma-Aldrich			

**Supplemental Table 2 | Overview of clinical characteristics and cytogenetics of MM patients.**

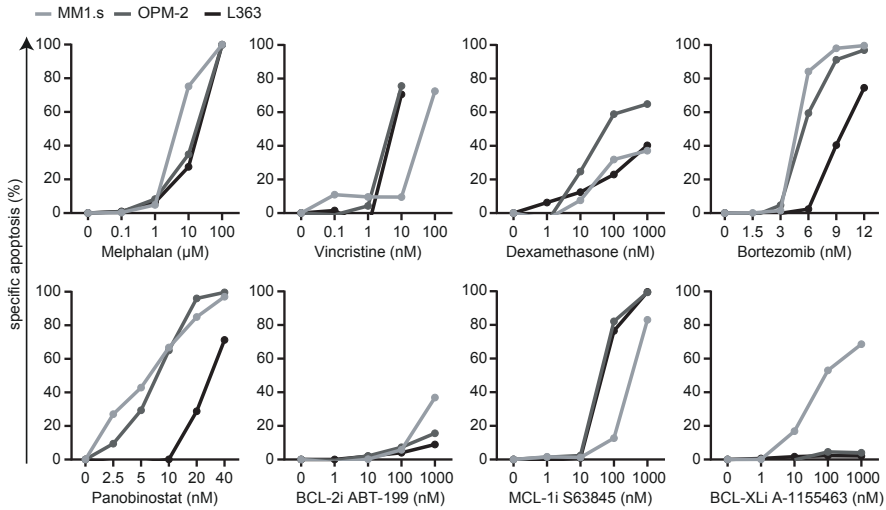
Characteristics	MM1	MM2	MM3	MM4	MM5	MM6	MM7	MM8	MM9
Age at diagnosis, y	53	52	59	66	80	55	51	68	48
Sex	female	male	male	male	male	male	male	male	male
Plasma cells, %	38	70	67	70	20	75	34	36	37
Immunoglobulin type	IgG	IgG	nd	IgG	IgA	IgA	IgG	nd	IgG
Light chain type	lambda	kappa	lambda	lambda	kappa	lambda	kappa	lambda	lambda
ISS stage at diagnosis	1	1	3	1	1	2	3	1	3
<b>Cytogenetics</b>									
hyperdiploidy	no	yes	no	yes	yes	nd	no	no	no
amplifications / deletions	1q <sup>+</sup> , 13q <sup>-</sup>	no	1q <sup>+</sup> , 13q <sup>-</sup>	no	13q <sup>-</sup>	1q <sup>+</sup> , 13q <sup>-</sup>	13q <sup>-</sup>	no	no
translocations	t(14;20)	no	no	no	no	t(4;14)	t(14;16)	no	no

ISS, international staging system; y, year; nd, no data.

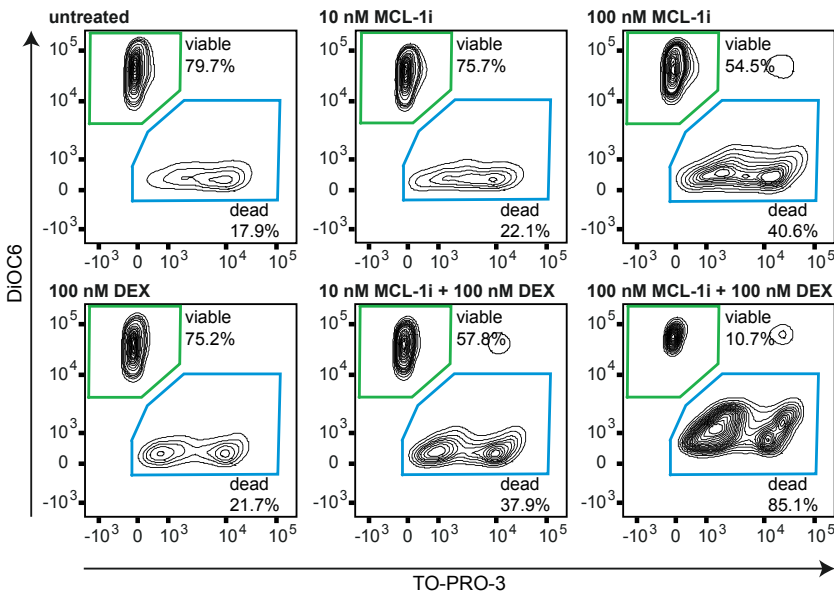
**Supplemental Table 3 | Overview of primary antibodies used for western blots in the study.**

Antibody	Clone	Manufacturer
rabbit anti-MCL-1	Y37	Abcam
mouse anti-BCL-2	124	Cell Signaling
rabbit anti-BCL-XL	54H6	Cell Signaling
rabbit anti-FOXO1	C29H4	Cell Signaling
rabbit anti-FOXO3a	D19A7	Cell Signaling
rabbit anti-pGSK3 $\beta$ Ser9	D85E12	Cell Signaling
rabbit anti-4E-BP1	53H11	Cell Signaling
rabbit anti-p4E-BP1 Thr37/46	236B4	Cell Signaling
rabbit anti-P70S6K	49D7	Cell Signaling
rabbit anti-pP70S6K Thr389	108D2	Cell Signaling
mouse anti-S6	54D2	Cell Signaling
rabbit anti-pS6 Ser235/236	D57.2.2E	Cell Signaling
rabbit anti-pS6 Ser240/244	D68F8	Cell Signaling
rabbit anti-pAkt Ser473	D9E	Cell Signaling
mouse anti-Akt	40D4	Cell Signaling
rabbit anti-BIM	C34C5	Cell Signaling
rabbit anti-pBad Ser136	D25H8	Cell Signaling
mouse anti-NOXA	114C307,1	Novus Bio
mouse anti- $\alpha$ -tubulin	DM1A	Cell Signaling
mouse anti-lamin B1		Cusabio
mouse anti-GAPDH	GA1R	Invitrogen

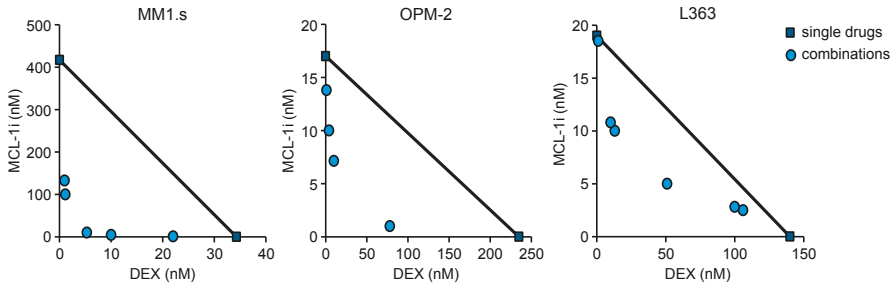
## SUPPLEMENTAL FIGURES



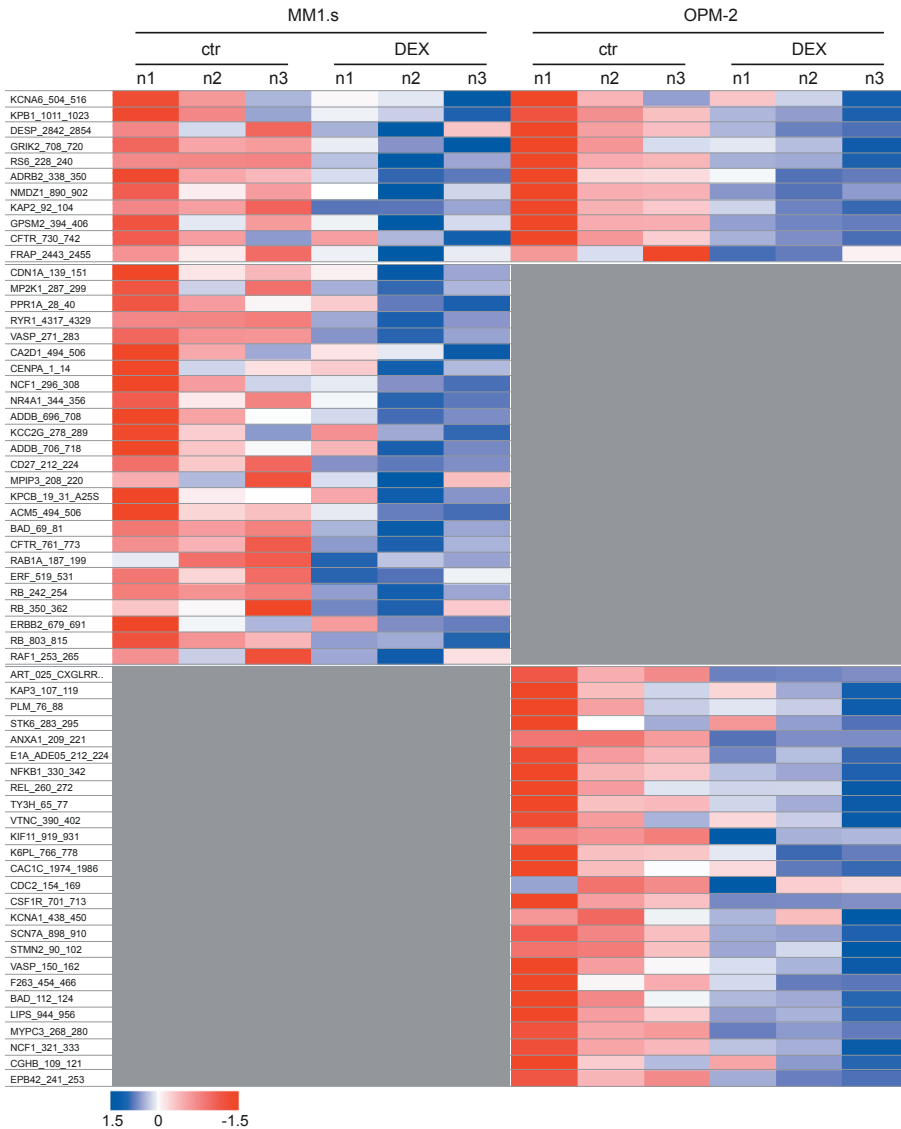
**Supplemental Figure 1 | Specific apoptosis induced by increasing concentrations of indicated drugs in HMCLs.** The HMCLs MM1.s, OPM-2 and L363 were exposed to indicated concentrations of melphalan, vincristine, dexamethasone, bortezomib and panobinostat for 48 hours. In addition, HMCLs were exposed to indicated concentrations of BH-3 mimetics BCL-2 inhibitor ABT199, MCL-1 inhibitor S63845 and BCL-XL inhibitor A1155463 for 24 hours.



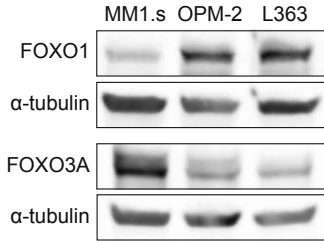
**Supplemental Figure 2 | Induction of apoptosis by dexamethasone and MCL-1i.** Representative flow cytometric analysis plots of apoptosis induction in HMCLs after 48 hours of exposure to the indicated concentrations of dexamethasone (DEX) or MCL-1i. Gates represent viable (DiOC6<sup>+</sup>/TO-PRO3<sup>-</sup>) and dead (DiOC6<sup>-</sup>/TO-PRO3<sup>+</sup>) MM1.s cells.



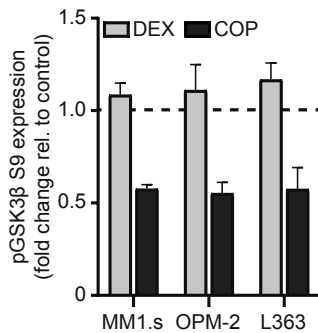
**Supplemental Figure 3 | Dexamethasone synergizes with MCL-1i to induce apoptosis of HMCLs.** Representative isobolograms of indicated HMCLs exposed to combinations of dexamethasone (DEX) and MCL-1i for 48 hours. Blue dots indicate the drug combination that induced 50% specific apoptosis (IC<sub>50</sub>) for MM1.s and OPM-2 or 25% specific apoptosis (IC<sub>25</sub>) for L363. The blue squares indicate the IC<sub>50</sub> (MM1.s and OPM-2) or IC<sub>25</sub> (L363) of the single drugs. The black lines connecting both single drug datapoints indicate an exact additive effect with a combination index (CI) of 1. All datapoints to the left of this line have a CI < 1, indicating synergy for the drug combination.



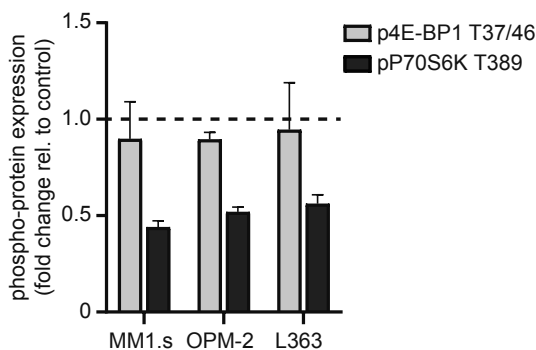
**Supplemental Figure 4 | Dexamethasone significantly reduces peptide phosphorylation by STKs in HMCLs.** Heatmap showing peptides with significantly reduced phosphorylation by serine/threonine kinases (STK) in MM1.s and OPM-2 exposed for 4 hours to 1  $\mu$ M dexamethasone (DEX) or DMSO control (ctr). Per treatment group 3 technical replicates were included. Statistical analysis was performed by paired *t*-tests. Grey fields indicate no statistically significant results for the specific peptides in the indicated HMCL.



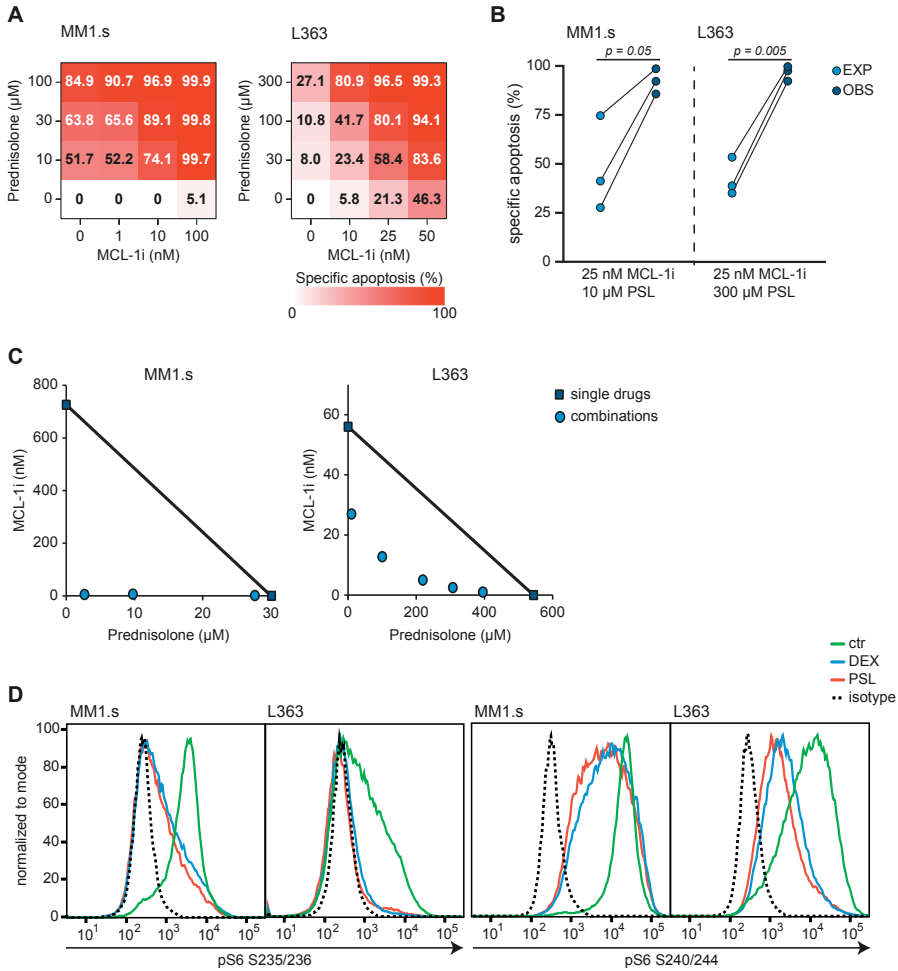
**Supplemental Figure 5 | FOXO protein expression in HMCLs.** Western blot showing FOXO1 and FOXO3a protein expression in untreated HMCLs. Alpha-tubulin was used as a loading control.



**Supplemental Figure 6 | Exposure of HMCLs to dexamethasone does not reduce inhibitory GSK3β phosphorylation.** Quantification of GSK3β phosphorylation on serine residue 9 (p GSK3β S9) in indicated HMCLs exposed to 1 μM dexamethasone (DEX) or 100 nM copanlisib (COP) for 4 hours. Quantification was performed on Western blots of 2 individual experiments, normalized to α-tubulin for loading control and relative to untreated control cells, indicated by the dashed line



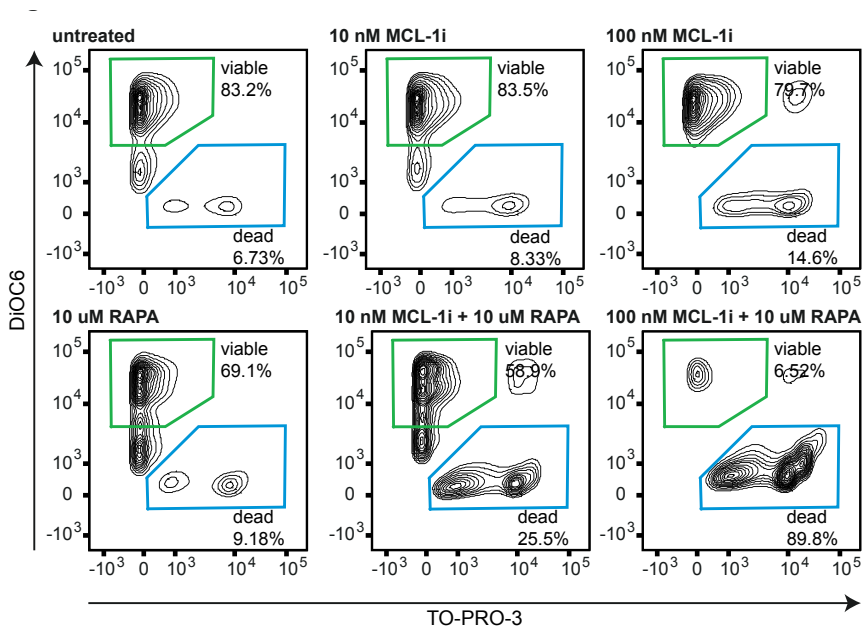
**Supplemental Figure 7 | Dexamethasone reduces phosphorylation of mTORC1 substrates 4E-BP1 and P70S6K.** Quantification of 4E-BP1 phosphorylation on threonine 37/46 residues (p4E-BP1 T37/46) and P70S6K phosphorylation on threonine residue 389 (pP70S6K T389) in indicated HMCLs exposed to 1 μM dexamethasone for 4 hours. Quantification was performed on western blots of 2 individual experiments, normalized to total 4E-BP1 or total P70S6K protein expression for loading control and relative to untreated control cells, indicated by the dashed line.



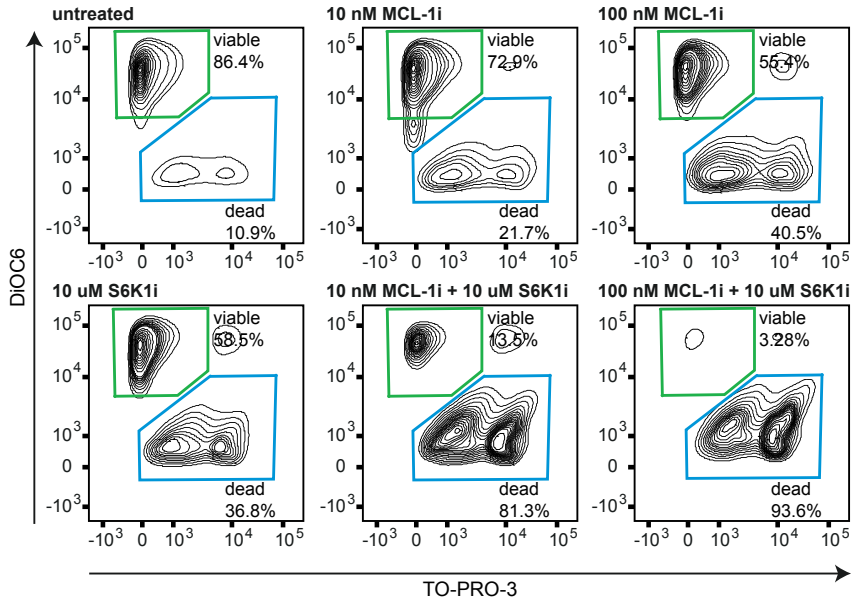
**Supplemental Figure 8 | Prednisolone synergizes with MCL-1i to induce apoptosis of HMCLs and reduces phosphorylation of S6.**

(A) Heatmaps showing specific apoptosis of indicated HMCLs induced by serial dilutions of prednisolone and MCL-1i, individual or combined. Viability was analyzed after 48 hours of drug exposure, values represent the mean of 3 individual experiments. (B) Plots comparing EXP to OBS specific apoptosis induced by prednisolone (PSL) and MCL-1i combinations. Per HMCL the drug combination that resulted in the highest average OBS-EXP ratio was selected from the data obtained in panel A. The 3 connected datapoints show the data obtained from 3 individual experiments. Statistical analysis was performed by paired t-tests. (C) Representative isobolograms of indicated HMCLs exposed to combinations of prednisolone and MCL-1i for 48 hours. Blue dots indicate the drug combination that induced 50% specific apoptosis ( $IC_{50}$ ), the blue squares indicate the  $IC_{50}$  of the single drugs. The black lines connecting both single drug datapoints indicate an exact additive effect with a CI of 1. All datapoints to the left of this line have a CI < 1, indicating synergy for the drug combination. (D) Histograms comparing expression of S6 phosphorylation on serine residues 235/236 (pS6 S235/236) and 240/244 (pS6 S240/244) in indicated HMCLs after 4 hours of exposure to 1 μM dexamethasone (DEX), 100 μM PSL for MM1.s or 300 μM PSL for L363, determined by flow cytometric analysis. Expression was relative to untreated control cells (ctr) and corrected for isotype control, indicated by the dashed line.

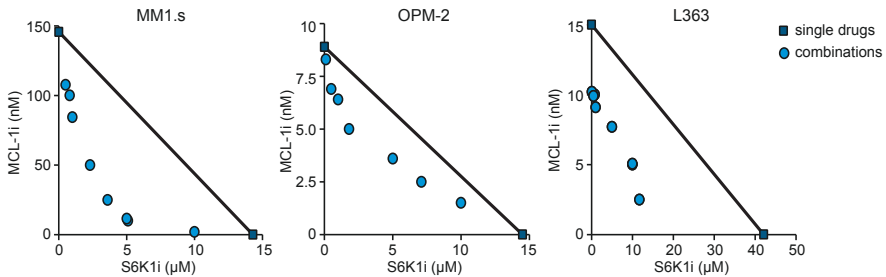




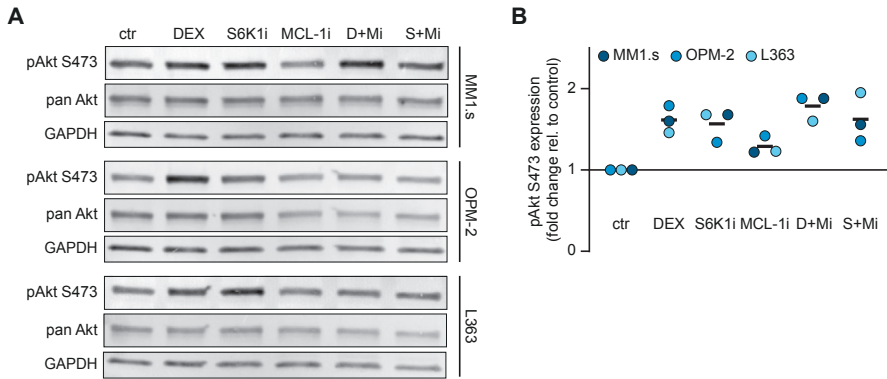
**Supplemental Figure 9 | Induction of apoptosis by rapamycin and MCL-1i.** Representative flow cytometric analysis plots of apoptosis induction in HMCLs after 48 hours of exposure to the indicated concentrations of rapamycin (RAPA) and MCL-1i. Gates represent viable (DiOC6<sup>+</sup>/TO-PRO3<sup>-</sup>) and dead (DiOC6<sup>+</sup>/TO-PRO3<sup>+</sup>) MM1.s cells.



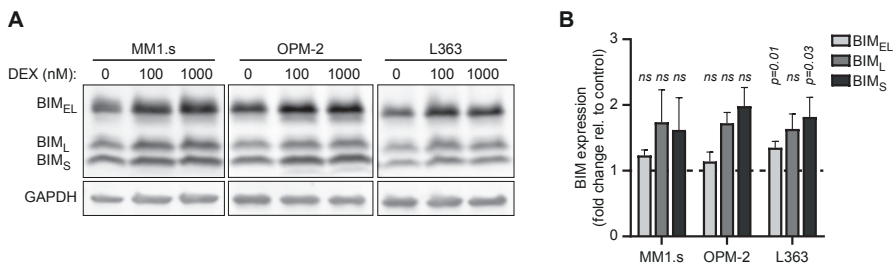
**Supplemental Figure 10 | Induction of apoptosis by S6K1i and MCL-1i.** Representative flow cytometric analysis plots of apoptosis induction in HMCLs after 48 hours of exposure to the indicated concentrations of S6K1i and MCL-1i. Gates represent viable (DiOC6<sup>+</sup>/TO-PRO3<sup>-</sup>) and dead (DiOC6<sup>+</sup>/TO-PRO3<sup>+</sup>) MM1.s cells.



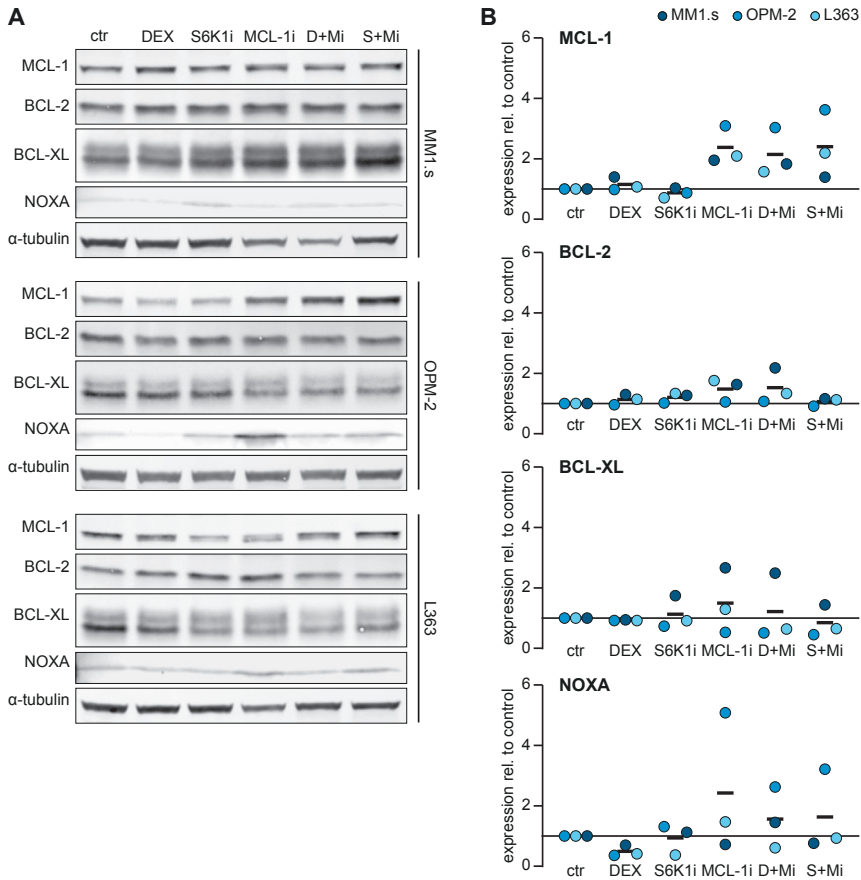
**Supplemental Figure 11 | S6K1i synergizes with MCL-1i to induce apoptosis of HMCLs.** Representative isobolograms of indicated HMCLs exposed to combinations of S6K1i and MCL-1i for 48 hours. Blue dots indicate the drug combinations that induced 50% specific apoptosis ( $IC_{50}$ ). The blue squares indicate the  $IC_{50}$  of the single drugs. The black lines connecting both single drug datapoints indicate an exact additive effect with a CI of 1. All datapoints to the left of this line have a CI < 1, indicating synergy for the drug combination.



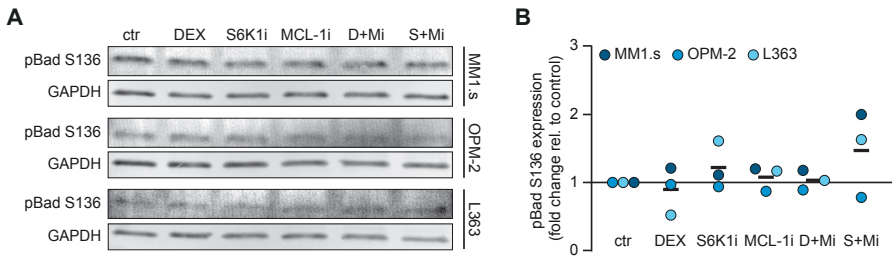
**Supplemental Figure 12 | Dexamethasone and S6K1i have similar effects on Akt kinase activity.** (A) Representative western blot showing phosphorylation of Akt on the activating serine 473 residue (pAkt S473) in indicated HMCLs after 4 hours of exposure to 100 nM dexamethasone (DEX; D), 1  $\mu$ M S6K1i (S), MCL-1i (Mi); 100 nM for MM1.s and 25 nM for OPM-2 and L363) and combinations thereof, relative to pan Akt and GAPDH as a loading control. Ctr indicates untreated control cells. (B) Quantification of pAkt S473 expression, normalized to pan Akt protein expression and relative to untreated control cells (ctr). All datapoints show the mean quantification that was performed on western blots of 2 individual experiments as described for panel A. The black lines indicate the mean value of the 3 indicated HMCLs.



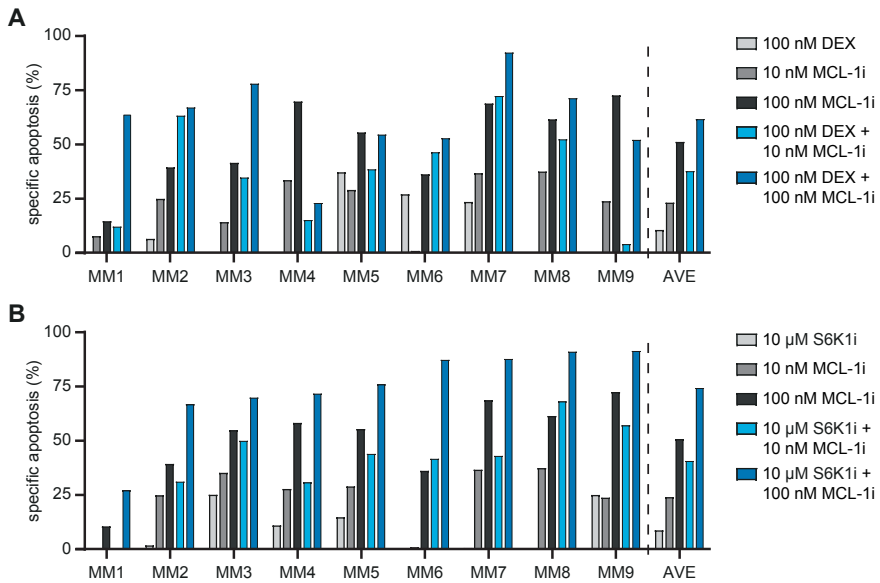
**Supplemental Figure 13 | Exposure of HMCLs to dexamethasone increases BIM protein expression in a dose-dependent manner.** (A) Representative western blot showing protein expression of 3 BIM isoforms in indicated HMCLs exposed to indicated concentrations of dexamethasone (DEX) for 24 hours. (B) Quantification of 3 BIM isoforms protein expression in indicated HMCLs exposed to 1  $\mu$ M dexamethasone for 24 hours. Quantification was performed on western blots of 3 individual experiments, normalized to GAPDH for loading control and relative to untreated control cells, indicated by the dashed line. Statistical analysis was performed by paired *t*-tests; ns, not significant.



**Supplemental Figure 14 | Exposure of HCMLs to dexamethasone, S6K1i, and MCL-1i do not consistently alter protein expression of BCL-2 family members.** (A) Representative western blot showing protein expression of pro-survival proteins MCL-1, BCL-2 and BCL-XL and BH-3-only pro-apoptotic protein NOXA in indicated HCMLs exposed for 24 hours to 100 nM dexamethasone (DEX; D), 1  $\mu$ M S6K1i (S), MCL-1i (Mi); 100 nM for MM1.s and 25 nM for OPM-2 and L363) and combinations thereof in the presence of 10  $\mu$ M pan caspase inhibitor Q-VD, relative to  $\alpha$ -tubulin as a loading control. Ctr indicates untreated control cells. (B) Quantification of MCL-1, BCL-2, BCL-XL and NOXA protein expression, normalized to  $\alpha$ -tubulin protein expression and relative to untreated control cells (ctr). All datapoints show the mean quantification that was performed on western blots of 2 individual experiments as described for panel A. The black lines indicate the mean value of the 3 indicated HCMLs.

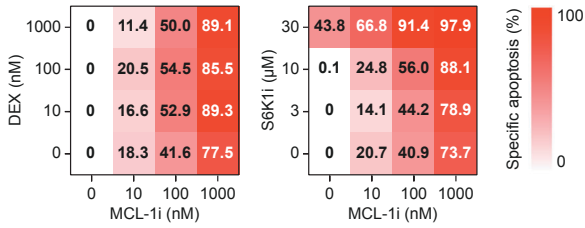


**Supplemental Figure 15 | Exposure of HCMLs to dexamethasone, S6K1i, and MCL-1i do not consistently alter pro-apoptotic Bad activity.** (A) Representative western blot showing phosphorylation of Bad on the activating serine 136 residue (pBad S136) in indicated HCMLs exposed for 4 hours to 100 nM dexamethasone (DEX; D), 1  $\mu$ M S6K1i (S), MCL-1i (Mi); 100 nM for MM1.s and 25 nM for OPM-2 and L363) and combinations thereof, relative to GAPDH as a loading control. Ctr indicates untreated control cells. (B) Quantification of pBad S136 protein expression, normalized to GAPDH protein expression and relative to untreated control cells. All datapoints show the mean quantification that was performed on western blots of 2 individual experiments as described for panel A. The black lines indicate the mean value of the 3 indicated HCMLs.

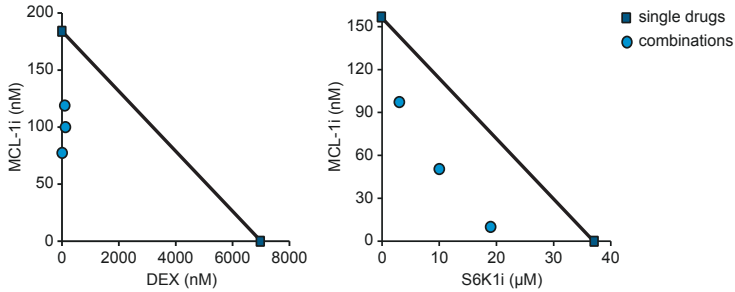


**Supplemental Figure 16 | Induction of apoptosis by dexamethasone, S6K1i and MCL-1i in individual primary MM samples.** Specific apoptosis of CD38<sup>+</sup> primary MM cells after 48 hours of drug exposure. (A) Treatment with 100 nM dexamethasone (DEX), 10 nM MCL-1i, 100 nM MCL-1i or DEX-MCL-1i drug combinations. (B) Treatment with 10  $\mu$ M S6K1i, 10 nM MCL-1i, 100 nM MCL-1i or S6K1i-MCL-1i drug combinations. Mean values of the 9 primary MM patient samples (AVE) are represented by bars separated by the dashed line.

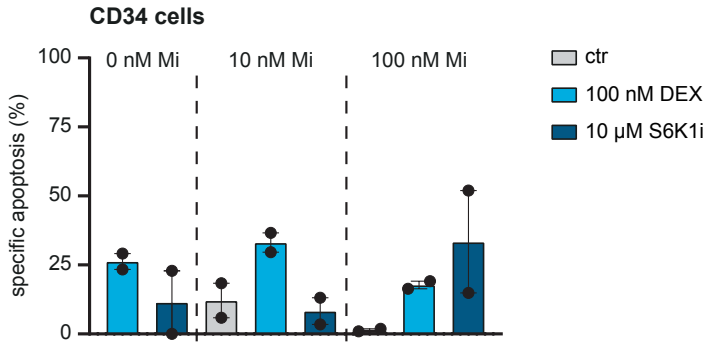
A



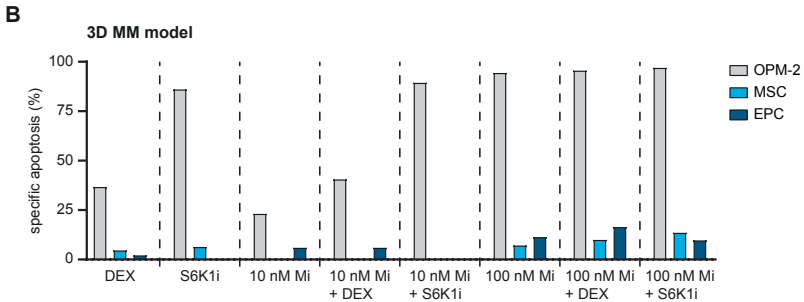
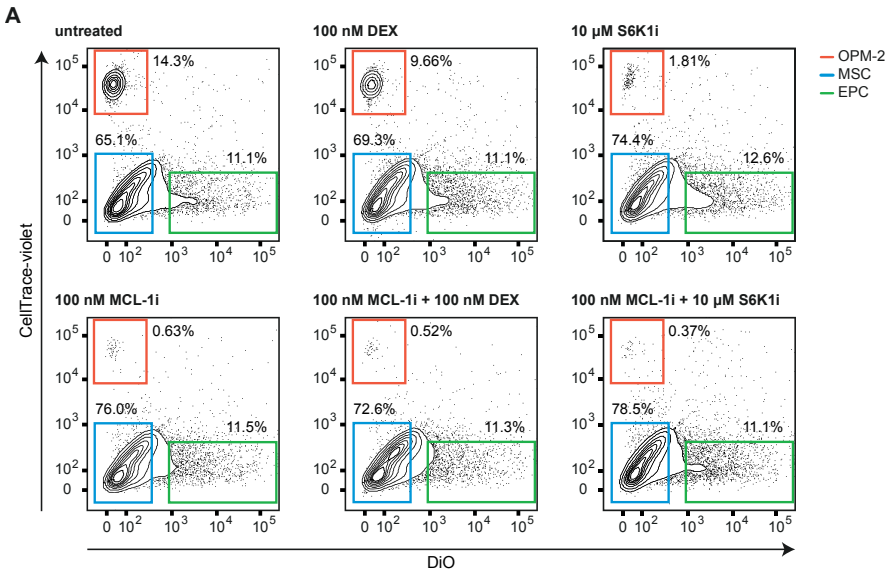
B



**Supplemental Figure 17 | Dexamethasone and S6K1i synergize with MCL-1i to induce apoptosis of primary MM cells.** A) Heatmaps showing specific apoptosis induced by single and combined serial dilutions of dexamethasone (DEX) and MCL-1i (left) or single and combined serial dilutions of S6K1i and MCL-1i (right). Viability of CD38<sup>+</sup> primary MM cells was analyzed after 48 hours of drug exposure, values represent the mean of 3 unique MM patient samples. (B) Isobolograms of the indicated drug combinations as described for panel A. Blue dots indicate the drug combination that induced 50% specific apoptosis ( $IC_{50}$ ), the blue squares indicate the  $IC_{50}$  of the single drugs. For dexamethasone the  $IC_{50}$  was > 7000 nM, but it was set to 7000 nM to be able to calculate CI values. The resulting CI (<1) therefore underestimates the synergistic effect with MCL-1i. All datapoints show the mean values of the 3 unique MM patient samples included, as in panel A.



**Supplemental Figure 18 | Dexamethasone and S6K1i induce limited toxicity in combination with MCL-1i in healthy donor CD34<sup>+</sup> precursor cells.** Specific apoptosis induced by 100 nM dexamethasone (DEX) or 10 μM S6K1i as single drug dosages or in combination with 10 nM and 100 nM MCL-1i (Mi), relative to untreated control cells. Viability of CD34<sup>+</sup> cells was analyzed after 48 hours of drug exposure by negative TO-PRO3 staining. The bars show the mean of the 2 unique healthy donor umbilical CB samples that were included, represented by the individual datapoints.



**Supplemental Figure 19 | Dexamethasone-MCL-1i and S6K1i-MCL-1i combinations kill myeloma cells but induce minimal toxicity of progenitor cells in a pre-clinical MM model.** (A) Representative flow cytometric analysis plots showing relative contribution of OPM-2 (labeled with CellTrace-violet), EPC (labeled with DiO) and MSC (unlabeled) to the viable population of cells (pre-gated on TO-PRO3 negative cells) after 48 hours of exposure to 100 nM dexamethasone (DEX), 10  $\mu$ M S6K1i, and 100 nM MCL-1i as single drug dosages or combinations thereof. (B) Quantification of specific apoptosis induced in OPM-2, MSC and EPC analyzed as described for panel A after 48 hours of exposure to DEX, S6K1i, and 10 nM or 100 nM MCL-1i (Mi), relative to untreated control cells. The plot combines the results of 2 individual experiments.







# Chapter six

## **Multiple myeloma relapse is associated with increased NFκB pathway activation and upregulation of the pro-survival BCL-2 protein BFL-1**

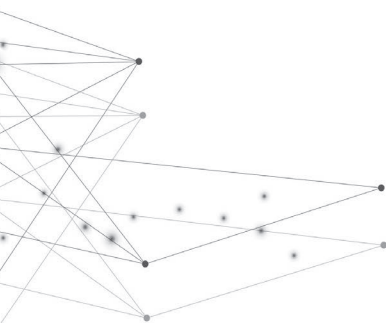
Ingrid Spaan<sup>1</sup>, Anja van de Stolpe<sup>2</sup>,  
Reinier Raymakers<sup>3</sup>, and Victor Peperzak<sup>1</sup>

<sup>1</sup> Laboratory of Translational Immunology,  
University Medical Center Utrecht,  
Utrecht, the Netherlands

<sup>2</sup> Precision Diagnostics, Philips Research,  
Eindhoven, the Netherlands

<sup>3</sup> Department of Hematology,  
University Medical Center Utrecht,  
Utrecht, the Netherlands

*Cancers (Basel)*, 2021; 13(18):4668



## ABSTRACT

Multiple myeloma (MM) is a hematological malignancy that is still considered incurable due to development of therapy resistance and subsequent relapse of disease. MM plasma cells (PC) use NF $\kappa$ B signaling to stimulate cell growth, disease progression, and for protection against therapy-induced apoptosis. Amongst its diverse array of target genes, NF $\kappa$ B regulates expression of pro-survival BCL-2 proteins BCL-XL, BFL-1 and BCL-2. A possible role for BFL-1 in MM is controversial, since BFL-1, encoded by BCL2A1, is downregulated when mature B-cells differentiate into antibody-secreting PC. NF $\kappa$ B signaling can be activated by many factors in the bone marrow microenvironment and/or induced by genetic lesions in MM PC. We used the novel signal transduction pathway activity (STA) computational model to quantify functional NF $\kappa$ B pathway output in primary MM PC from diverse patient subsets at multiple stages of disease. We found that NF $\kappa$ B pathway activity is not altered during disease development, is irrespective of patient prognosis, and does not predict therapy outcome. However, disease relapse after treatment resulted in increased NF $\kappa$ B pathway activity in surviving MM PC, which correlated with increased BCL2A1 expression in a subset of patients. This suggests that BFL-1 upregulation, in addition to BCL-XL and BCL-2, may render MM PC resistant to therapy-induced apoptosis, and that BFL-1 targeting could provide a new approach to reduce therapy resistance in a subset of relapsed-refractory MM patients.

## 1 | INTRODUCTION

Multiple myeloma (MM) is a hematological malignancy that is characterized by clonal proliferation of antibody-secreting plasma cells (PC) that typically reside in the bone marrow (BM) [1]. The clonal evolution that underlies malignant transformation in MM results in extensive intra- and interpatient heterogeneity. Gene expression profiling identified 10 distinct molecular clusters in newly diagnosed MM. These include 4 translocation clusters (CD-1, CD-2, MS, MF), a hyperdiploid cluster (HY), a cluster with proliferation-associated genes (PR), a cancer testis antigens overexpressing cluster (CTA), and a cluster that is characterized by high expression of genes involved in the NF $\kappa$ B pathway [2]. Mutations in NF $\kappa$ B genes are reported to be most prevalent in MM compared to all other human malignancies [3]. Two studies by Keats *et al.* and Annunziata *et al.* demonstrated that approximately 20% of MM patients and 40% of MM cell lines harbor at least one genetic lesion in MM PC that results in increased or constitutive NF $\kappa$ B pathway activation [4,5]. Two more recent studies, using next-generation sequencing, confirmed recurrent mutations in MM PC that either result in down-regulation or loss-of-function of NF $\kappa$ B negative regulators, or over-expression or gain-of-

function of positive NFκB regulators [6,7]. The majority of mutations in NFκB genes exhibit low individual frequency, indicating that NFκB pathway activating mechanisms are heterogeneous between patients [8].

In addition to clonal evolution of MM PC, disease progression is accompanied by development of a permissive BM microenvironment. Various BM components physically bind to MM PC or secrete cytokines and growth factors to promote NFκB signaling. These include APRIL and BAFF, which are important survival factors for healthy and malignant PC [9,10]. In MM PC, NFκB signaling regulates cell proliferation via cell cycle regulators, immortalization via telomerase, angiogenesis via VEGF, and intrinsic apoptosis resistance via pro-survival proteins. In addition, NFκB-mediated upregulation of adhesion molecules and matrix proteases intensifies the interaction with the BM microenvironment, thereby promoting malignant transformation, disease progression, and therapy resistance [11]. Vice versa, MM PC stimulate NFκB signaling in cellular components of the BM microenvironment to promote a MM-permissive niche. This results in increased pro-survival IL-6 expression by BM stromal cells, promotion of osteolytic bone disease by osteoclasts, and facilitates immune evasion by activation of myeloid-derived suppressor cells [8].

The numerous processes that contribute to aberrant NFκB signaling in MM and the pivotal role of NFκB signaling on various aspects of disease emphasizes the need to target this pathway for MM treatment. Current therapeutic regimens generally consist of multiple cycles of triple-drug combinations that include a proteasome inhibitor (PI), a glucocorticoid, and an immunomodulatory drug (IMiD) or chemotherapy. This is combined with high-dose melphalan and an autologous stem cell transplant (ASCT) for eligible patients [12]. Many of the effective anti-myeloma drugs that are included in this therapeutic armamentarium affect NFκB signaling as their primary or secondary target. The frequently administered PI bortezomib and IMiD thalidomide were both reported to inhibit NFκB signaling in MM [13,14]. Although these treatment regimens improved the life expectancy of MM patients during the last decades, the majority of patients gradually develop resistance to all available agents, relapse, and eventually become refractory to therapy [15].

Development of therapy resistance is a continuous threat in MM treatment, with sub-clonal heterogeneity that evolves during disease progression through selection of drug-resistant clones [16]. One mechanism to promote MM PC survival is by developing resistance to the intrinsic apoptosis pathway. This can be accomplished by overexpressing pro-survival BCL-2 proteins, of which the members BCL-XL (BCL2L1), BFL-1 (BCL2A1), and possibly BCL-2 (BCL2) are direct NFκB target genes [17]. BCL-XL and BCL-2 are known to contribute to apoptosis

resistance in MM, but a role for BFL-1 in MM PC is far more controversial. Several studies have demonstrated BFL-1 in development and activation of B-lymphocytes, and reported BFL-1/BCL2A1 overexpression in B-cell malignancies [18]. However, the transcriptional repressor Blimp-1, that is required for differentiation of B-cells into antibody-secreting PC, inhibits BFL-1/BCL2A1 expression [19].

To gain more insight into the role of NF $\kappa$ B signaling and its pro-survival BCL-2 target genes in MM, we used the novel signal transduction pathway activity (STA) model that was described by Verhaegh *et al.* and Van de Stolpe *et al.* [20,21]. This Bayesian computational model infers NF $\kappa$ B pathway activity from measurements of mRNA encoding direct target genes of the NF $\kappa$ B transcription factors. This model thus allows for quantification of functional NF $\kappa$ B pathway activity, irrespective of the mode of pathway activation, which could vary from increased signaling at the receptor level, intrinsic pathway mutations, or activation by cross-talk with additional signaling pathways. Using this STA model we determined NF $\kappa$ B pathway activity in Affymetrix microarray datasets that include purified PC at multiple stages of disease and from diverse MM subsets, and correlated NF $\kappa$ B pathway activity to mRNA expression encoding pro-survival BCL-2 family members.

## 2 | MATERIALS AND METHODS

### 2.1 | NF $\kappa$ B Signal Transduction pathway Activity (STA) analysis

The development of Bayesian network models to measure signal transduction pathway activity (STA), and development and validation of the STA test to measure activity of the NF $\kappa$ B signaling pathway have been described in detail previously [20,21]. In brief, the computational network model for signaling pathways is constructed to infer the probability that the pathway-driving transcription factor is actively transcribing mRNA of its target genes. The Bayesian network describes the causal relation that the measured intensity of micro-array probesets is dependent on the activity of target gene transcription, which is in turn causally related to the activity of the transcription complex. These relations are probabilistic in nature. Selection of target genes of the pathway-driving transcription factors have been based on literature insights from *in vitro* and *in vivo* studies assessing if the gene promotor region contains a transcription factor response element, if the transcription factor binds to this response or enhancer element, the promotor functionality, and differential expression upon pathway activation [21]. The NF $\kappa$ B STA contains 50 probesets representing 29 unique target genes and was calibrated on Affymetrix HG-U133Plus2.0 data of samples with ground-truth information about their pathway activity state [20].

## 2.2 | Micro-array datasets

We used the Gene Expression Omnibus (GEO; <https://www.ncbi.nlm.nih.gov/geo/>) for publicly available datasets containing Affymetrix HG-U133Plus2.0 microarray data of gene expression in PC samples from specified donor/patient subsets at various disease stages. In all datasets, samples were enriched for PC by anti-CD138 immuno-magnetic bead selection, resulting in a purity of >80% PC. All samples were subjected to extensive quality control before the data was used as input for the STA model to calculate the probability of the NFκB pathway to be active, as previously described [20]. Details of the datasets and included samples are summarized in Table 1.

**Table 1 | Samples included in STA NFκB analysis per dataset**

Dataset	Reference	Description	Included samples
GSE5900	Zhan et al. [22]	Untreated samples from healthy donors, MGUS, and SMM patients	hd PC n = 18 MGUS n = 40 SMM n = 12
GSE19784	Broyl et al. [2]	Newly diagnosed MM with specified ISS stage defining clinical prognosis	ISS 1 n = 71 ISS 2 n = 36 ISS 3 n = 41
		Newly diagnosed MM with specified molecular clusters <sup>1</sup>	CD-1 n = 7 CD-2 n = 18 MF n = 14 MS n = 21 PR n = 6 HY n = 37 NFκB n = 22 CTA n = 11
GSE68871	Terragna et al. [23]	Newly diagnosed MM with clinical response to subsequent first-line VTD induction therapy	CR n = 14 nCR n = 13 VGPR n = 38 PR n = 39 SD n = 5
GSE19554	Zhou et al. [24]	Longitudinal MM samples during first-line and second-line total therapy including ASCT	diagnosis n = 19 1st-line induction n = 17 2nd-line induction n = 8 maintenance n = 7
GSE82307	Weinhold et al. [25]	Matched MM samples at diagnosis and after progression/relapse to first-line total therapy <sup>2</sup>	diagnosis n = 33 relapse n = 33

<sup>1</sup> The SOCS3/PRL3 cluster contained only 3 samples and was therefore not included. The previously reported contaminated myeloid cluster was excluded from further analysis. <sup>2</sup> Samples were not analyzed by STA but on individual probeset intensity. MGUS, monoclonal gammopathy of undetermined significance; SMM, smoldering multiple myeloma; hd, healthy donor; MM multiple myeloma; ISS, international staging system; VTD bortezomib-thalidomide-dexamethasone; CR, complete response; nCR, near complete response; VGPR, very good partial response; PR, partial response; SD, stable disease; ASCT autologous stem cell transplant

## 2.3 | Statistical analysis

The STA pathway activity score was normalized to a score ranging from 0 to 100, which can be used in a quantitative manner to identify differences in NF $\kappa$ B pathway activity between samples, and visualized in violin plots. All included samples are represented by individual datapoints, solid red lines indicate the median, and dashed lines indicate the quartiles of the population. Statistical analysis was performed by GraphPad Prism 8. Multiple groups within one dataset were compared using one-way ANOVA using Tukey's correction for multiple comparison. Correlation was determined by linear regression analysis and reported as correlation coefficient (R) values. For all tests, a P value  $<.05$  was considered statistically significant.

## 3 | RESULTS

### 3.1 | NF $\kappa$ B pathway activity is stable during MM development and prognosis, but is significantly higher in a subgroup of MM patients with a molecular NF $\kappa$ B signature

MM is consistently preceded by a pre-malignant phase that is referred to as monoclonal gammopathy of undetermined significance (MGUS) [26], and a subset of patients also go through a still asymptomatic phase called smoldering MM (SMM) [27]. Since NF $\kappa$ B signaling activation is one of the events associated with MGUS-to-MM progression [28], we quantified NF $\kappa$ B signaling activity during MM development. We performed NF $\kappa$ B STA analysis on dataset GSE5900 that contains CD138-purified samples of healthy donors, MGUS, and SMM patients. The SMM samples showed a median NF $\kappa$ B activity score of 29.2 (range 14.0-57.9), which did not significantly differ from NF $\kappa$ B activity scores in MGUS samples (median 31.4, range 16.2-55.5) and healthy donor PC (median 29.6, range 17.0-49.6; Figure 1A). This indicates that functional NF $\kappa$ B pathway activity remains stable during early phases of disease development from healthy PC to malignant MM PC.

Symptomatic MM patients can be stratified into 3 risk groups using the international staging system (ISS), varying between a median survival of 62 months in stage 1 to a median survival of only 29 months in stage 3 [29]. We analyzed NF $\kappa$ B STA on dataset GSE19784 that contains CD138-purified samples of newly diagnosed MM patients with a specified ISS stage. Samples in the poor prognosis ISS 3 stage showed a median NF $\kappa$ B activity score of 37.4 (range 18.8-60.5), which did not significantly differ from NF $\kappa$ B activity scores in ISS 2 (median 35.1, range



24.4-56.2) and ISS 1 (median 36.0, range 17.0-60.4; Figure 1B). This indicates that functional NFκB pathway activity in MM PC from newly diagnosed patients is stable, irrespective of patient prognosis.

The samples of newly diagnosed MM patients from dataset GSE19784 could also be stratified based on molecular clusters as performed by Broyl *et al.* The NFκB molecular cluster identified in this study is defined by high expression of genes involved in the NFκB pathway, and was reported to have significantly greater NFκB indexes as reported by Keats *et al.* and Annunziata *et al.*, compared to the other molecular clusters [2]. STA analysis of samples in the NFκB cluster showed a median NFκB activity score of 44.0 (range 36.6-60.5; Figure 1C). This was significantly higher than NFκB activity scores in clusters HY (median 37.4, range 22.7-56.9), MS (median 33.0, range 25.9-51.5), PR (median 31.6, range 18.8-44.1), MF (median 31.4, range 17.0-48.2), and CD-1 (median 31.2, range 22.1-44.0). This data shows that high expression of NFκB-associated genes is accompanied by high functional activity of the NFκB pathway. In addition, when NFκB scores were compared between all included molecular clusters, no statistical differences could be observed, except for the increase in the NFκB cluster compared to clusters CD-1, MF, MS, HY, and PR (Supplemental Figure 1). However, the NFκB activity score in the NFκB molecular cluster was not significantly higher compared to clusters CD-2 (median 37.2, range 24.4-60.4), and CTA (median 35.6, range 26.7-53.9). This further underlines the significance of measuring functional pathway output by STA, on the target gene expression level, to allow identification of all patient samples with high NFκB signaling activity.

### **3.2 | NFκB pathway activity does not predict therapy response, but is significantly increased after MM relapse**

We hypothesized that the heterogeneity in NFκB signaling activity that was observed in MM PC of newly diagnosed patient samples in GSE19784, could also be reflected in the heterogeneous clinical response of MM patients to treatment. We therefore performed NFκB STA analysis on dataset GSE68871, that contains CD138-purified samples of newly diagnosed MM patients which were subsequently treated with first-line VTD (bortezomib-thalidomide-dexamethasone) induction therapy. MM PC from patients with a complete response (CR) had a median NFκB activity score of 50.8 (range 27.0-79.0) before start of therapy (Figure 2A). This was not significantly different from patients with a near clinical response (nCR; median 57.0, range 32.8-74.0), very good partial response (VGPR; median 56.4, range 33.4-79.3), partial response (PR; median 55.5, range 27.8-82.3), or stable disease (SD; median 61.8, range 46.4-71.7).

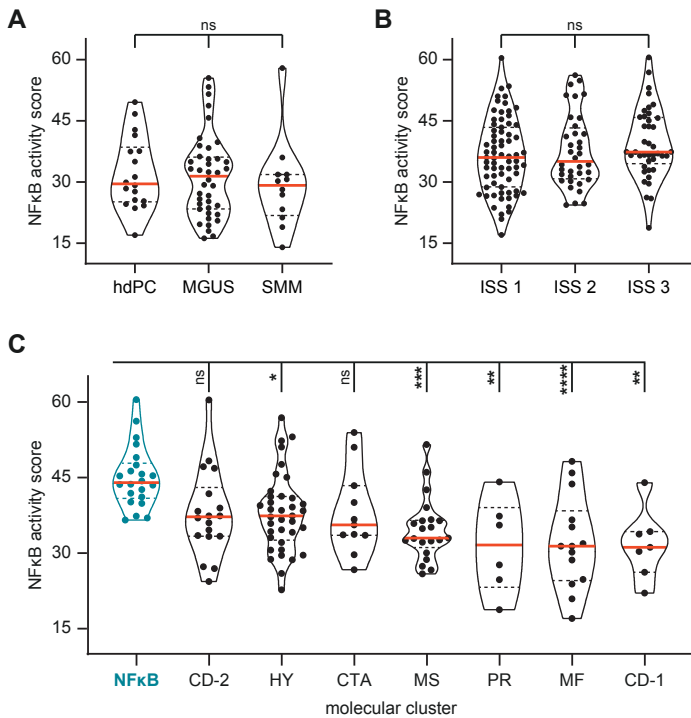


**Figure 1** | Violin plots showing NFκB activity score as analyzed by signal transduction pathway activity (STA) analysis in plasma cells (PC) from (A) healthy donors (hdPC), pre-malignant monoclonal gammopathy of undetermined significance (MGUS) patients, and asymptomatic smoldering multiple myeloma (SMM) patients, as incorporated in dataset GSE5900; (B) newly diagnosed MM patients, stratified by the international staging system (ISS) into good-prognosis ISS 1, intermediate-prognosis ISS 2, and poor-prognosis ISS 3, as incorporated in dataset GSE19784; (C) newly diagnosed MM patients, stratified by molecular clusters, as incorporated in dataset GSE19784. Included samples are represented by individual datapoints, solid red lines indicate the median, and dashed lines the quartiles of the population. ns, not significant, \* $P < .05$ , \*\* $P < .01$ , \*\*\* $P < .001$ , \*\*\*\* $P < .0001$ .

The observation that the NFκB pathway activity has no significant impact on response to first-line therapy was validated by analysis of a second dataset, GSE19554. This dataset includes CD138-purified longitudinal samples that were isolated from MM patients undergoing total therapy, consisting of chemotherapy-based induction therapy, ASCT, and maintenance/consolidation therapy. For all included patients, samples were taken at diagnosis, and after induction therapy prior to the first ASCT. A subgroup of patients relapsed after the first ASCT, and extra samples were taken after second-line induction therapy, and after the second ASCT before starting maintenance/consolidation therapy. STA analysis showed no

significant difference in NFκB activity score between patients undergoing 1 ASCT and patients requiring 2 ASCT when samples were taken at diagnosis (1 ASCT: median 36.0, range 27.0-61.1; 2 ASCT: median 38.4, range 28.3-57.7), or after first-line induction therapy (1 ASCT: median 50.8, range 35.1-57.4; 2 ASCT: median 45.5, range 27.0-62.7; Figure 2B).

For the subgroup of patients that relapsed after first-line total therapy, extra samples were taken after administration of second-line induction therapy. STA analysis of these samples showed a significant increase in NFκB activity score with a median score of 69.8 (range 54.5-75.0), compared to samples taken at diagnosis (median 38.8, range 27.0-63.8), or samples taken after first-line induction therapy prior to the first ASCT (median 45.7, range 27.0-62.7; Figure 2C). This elevated NFκB activity score remained high after the second ASCT prior to administration of maintenance/consolidation therapy (median 69.5, range 59.4-77.3).

By analyzing the longitudinal samples per individual patient, we observed a consistent increase in NFκB activity score after second-line induction therapy, irrespective of the NFκB activity score at diagnosis or after first-line induction therapy before the first ASCT (Figure 2D).

Combined, these data show that NFκB pathway activity at diagnosis has no impact on the effectivity of first-line treatment and can therefore not be used as a prediction marker for therapy response. However, after relapse to first-line total therapy and administration of second-line induction therapy, NFκB pathway activity was significantly increased in the surviving MM PC, and this activity remained high after second ASCT. This indicates that MM PC with high NFκB pathway activity have a survival advantage over MM PC with low NFκB pathway activity.

### **3.3 | BCL2A1 is the most frequently increased pro-survival BCL-2 member after MM relapse**

Increased expression of pro-survival BCL-2 proteins, of which BCL-XL (BCL2L1), BFL-1 (BCL2A1) and possibly BCL-2 (BCL2) are direct NFκB target genes, is a frequently used mechanism to overcome therapy-induced apoptosis [17]. We therefore analyzed gene transcript expression of these three BCL-2 family members in samples of the 8 MM patients that relapsed after first-line total therapy, as included in dataset GSE19554. Per individual patient we compared the difference in transcript expression between the sample taken at diagnosis (timepoint 1) to the sample taken after second-line induction therapy (timepoint 3). We observed that in all samples at least one of the three analyzed transcripts was increased, suggesting that relapse is accompanied by increased expression of pro-survival BCL-2 members (Figure 3A).

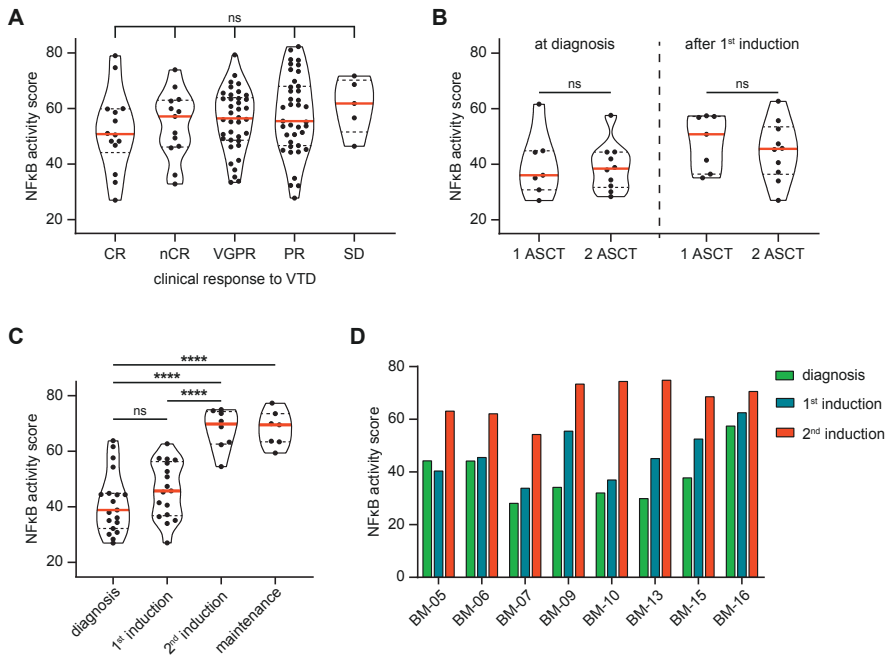


**Figure 2** | Violin plots showing NFκB activity score as analyzed by STA analysis in PC from (A) newly diagnosed MM patients with a quantified clinical response to subsequently administered first-line VTD (dexamethasone-thalidomide-bortezomib) induction therapy: complete response (CR), near-complete response (nCR), very good partial response (VGPR), partial response (PR), and stable disease (SD), as incorporated in dataset GSE68871; (B) MM patients at diagnosis, and after first-line chemotherapy-based induction therapy, that were stratified into two groups based on clinical response to subsequent total therapy: patients that required 1 ASCT, and patients that relapsed after the first ASCT and required a second ASCT (2 ASCT), as incorporated in dataset GSE19554; (C) MM patients at diagnosis, after first-line chemotherapy-based induction therapy prior to the first ASCT (1<sup>st</sup> induction), after second-line chemotherapy-based induction therapy prior to the second ASCT (2<sup>nd</sup> induction), and after the second ASCT before start of maintenance/consolidation therapy (maintenance), as incorporated in dataset GSE19554. Included samples are represented by individual datapoints, solid red lines indicate the median, and dashed lines the quartiles of the population. ns, not significant, \*\*\*\* $P < .0001$ . (D) Bar graph showing NFκB activity score as analyzed by STA analysis in longitudinal PC samples of 8 individual MM patients at diagnosis, after first-line chemotherapy-based induction therapy prior to the first ASCT (1<sup>st</sup> induction), and after second-line chemotherapy-based induction therapy prior to the second ASCT (2<sup>nd</sup> induction), as incorporated in dataset GSE19554. BM, bone marrow.

To assess if increased pro-survival BCL-2 expression was specific for members that are direct NFκB target genes, we also analyzed transcript expression of pro-survival BCL-2 members that are not directly regulated by NFκB: BCL-B (BCL2L10), MCL-1 (MCL1), and BCL-W (BCL2L2). In dataset GSE19554, relapse was associated

with >2-fold increased expression of NFκB targets BCL2A1 in 62.5% of samples, and BCL2L1 and BCL2 each in 25% of samples (Figure 3B). For NFκB-independent BCL-2 members a >2-fold increased transcript expression was observed for BCL2L10 in 25% samples, MCL1 in 0% of samples and BCL2L2 in 12.5% of samples. These results were verified in a second dataset GSE82307, that contains CD138-purified longitudinal samples of MM patients at diagnosis, and after relapse or progression to first-line total therapy, but before receiving second-line treatment. Also in samples of this second dataset, relapse/progression was more often associated with a >2-fold increased expression of NFκB-mediated pro-survival BCL-2 members, than with NFκB-independent pro-survival BCL-2 members. This suggests that MM therapy resistance is associated with increased NFκB pathway activity, and increased expression of pro-survival BCL-2 members that are direct NFκB target genes.

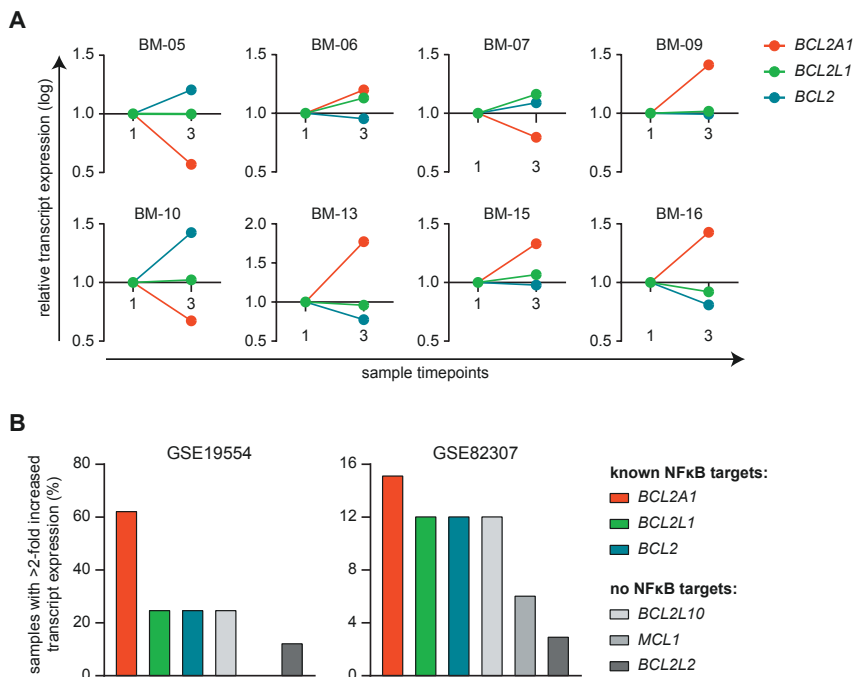


**Figure 3 |** (A) Plots showing relative mRNA transcript expression of BCL2A1 (BFL-1), BCL2L1 (BCL-XL), and BCL2 (BCL-2), in PC taken at diagnosis (timepoint 1), and after second-line chemotherapy-based induction therapy after relapse to first-line total therapy (timepoint 3), from 8 individual MM patients, as included in dataset GSE19554. (B) Bar graphs showing the percentage of MM PC patient samples that showed >2-fold increased mRNA transcript expression of NFκB-regulated pro-survival targets BCL2A1, BCL2L1, and BCL2, and NFκB-independent pro-survival members BCL2L10 (encoding BCL-B), MCL1 (encoding MCL-1), and BCL2L2 (encoding BCL-W), after relapse to first-line total therapy, with (dataset GSE19554) or without (GSE82307) subsequent administration of second-line induction therapy, in comparison to mRNA transcript expression at diagnosis.

### 3.4 | Increased BCL2A1 expression correlates with increased NFκB target gene expression after relapse

Although mRNA expression encoding for pro-survival BCL-2 family members is heterogeneous, in both datasets with longitudinal samples GSE19554 and GSE82307, BCL2A1 (BFL-1) was the most frequently upregulated pro-survival BCL-2 member after MM relapse/progression. Since a role for BFL-1 in MM is still under debate, we tested if differential BCL2A1 expression after relapse is associated with differential expression of NFκB target genes at this timepoint. In GSE19554 we observed a significant correlation between differential BCL2A1 expression and differential expression of 16 NFκB target genes that were incorporated in the STA model (Figure 4A). Eight of these 16 significantly correlating NFκB target genes were also identified in GSE82307, as well as 3 additional NFκB target genes of which differential expression after relapse significantly correlated with differential BCL2A1.

The NFκB molecular cluster in newly diagnosed MM patients included in dataset GSE19784 (Figure 1C), also showed significantly higher expression of BCL2A1, compared to 3 out of 5 additional molecular clusters that did not have a significantly increased NFκB activity score (Figure 4B). We observed no such relation between increased NFκB pathway activity and increased BCL2L1 expression, and even an inverse relation with BCL2 transcript expression. Since intrinsic apoptosis is not only mediated by pro-survival BCL-2 family members, but also by intricate interactions with pro-apoptotic BCL-2 family members, we analyzed the expression of pro-apoptotic effector proteins Bak and Bax [17]. Expression of mRNA encoding for Bak and Bax did not significantly differ between the NFκB molecular clusters and the 5 additional molecular clusters with significantly lower NFκB pathway activity (Supplemental Figure 2).

Taken together, this data indicates that increased NFκB target gene expression is correlated with increased BCL2A1 (BFL-1) expression. In addition to BCL-XL and BCL-2, BFL-1 induction could be a potential mechanism by which NFκB signaling protects MM PC from therapy-induced apoptosis, resulting in disease re-lapse. Direct or indirect targeting of BFL-1 could therefore provide a novel approach to reduce therapy resistance in a subset of relapsed-refractory (RR)-MM patients.

## 4 | DISCUSSION

In this study we used the novel STA model, that allows for quantification of functional NFκB pathway activity on individual sample gene expression data. We applied this computational model to Affymetrix gene expression microarray datasets containing MM PC samples from diverse patient subsets at multiple stages of disease. Our analysis shows that NFκB pathway activity is very heterogeneous.

This is observed in PC from MM patients, and is also visible in asymptomatic SMM or pre-malignant MGUS patients, and in PC from healthy donors. By comparing samples from these donor/patient populations, we observed no significant increase in NFκB pathway activity during early stages of disease development. Although activation of NFκB signaling has been suggested in MGUS-to-MM progression [28], our observations confirm results of an earlier publication by Annunziata, who showed that an 11-gene NFκB signature was similar in healthy PC, MGUS, and MM samples [4]. These results potentially reflect the dependency on NFκB-activating stimuli from the BM microenvironment that are required for survival of both healthy PC and early-phase (pre)-malignant MM PC [30].

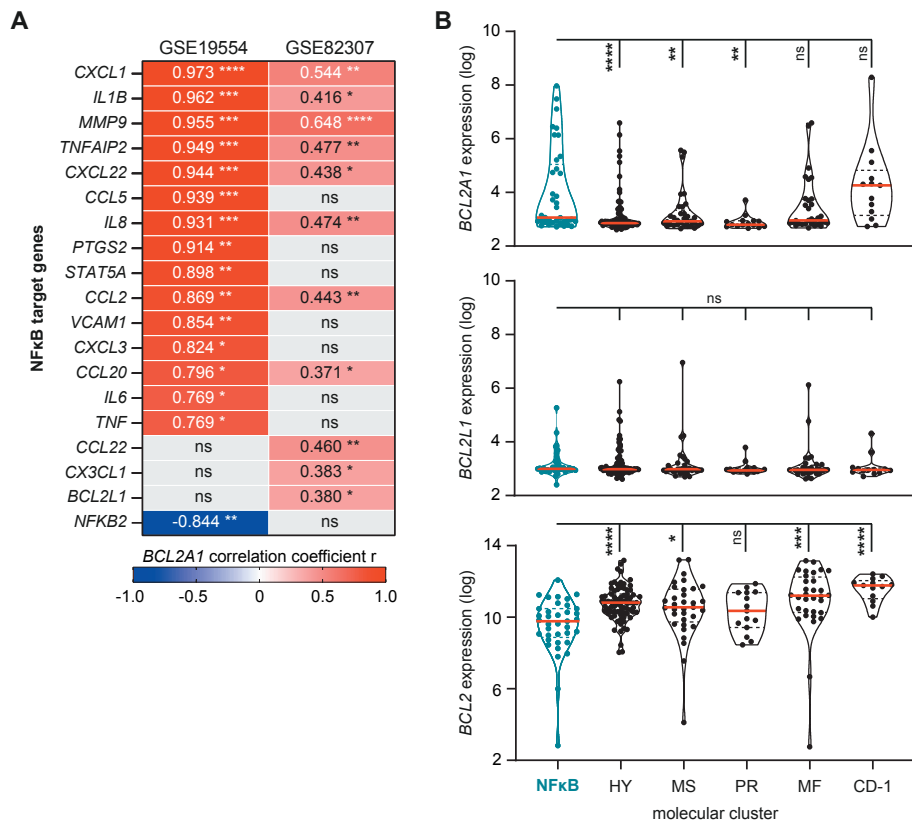


**Figure 4** | (A) Heatmap showing correlation coefficient (R value) between differential BCL2A1 expression and differential expression of NFκB target genes included in the STA analysis, as determined by mRNA transcript expression in PC from MM patients at diagnosis versus mRNA transcript expression after relapse to first-line total therapy, with (dataset GSE19554) or without (GSE82307) subsequent administration of second-line induction therapy. (B) Violin plots showing BCL2A1, BCL2L1, and BCL2 mRNA transcript expression in PC of newly diagnosed MM patients, as incorporated in dataset GSE19784, in molecular cluster NFκB, and molecular clusters HY, MS, PR, MF, and CD-1 that all showed a significant lower STA NFκB activity score compared to molecular cluster NFκB in Figure 1C. Included samples are represented by individual datapoints, solid red lines indicate the median, and dashed lines the quartiles of the population. ns, not significant, \* $P < .05$ , \*\* $P < .01$ , \*\*\* $P < .001$ , \*\*\*\* $P < .0001$ .

By stratification of newly diagnosed MM samples based on molecular clusters we could confirm that the NF $\kappa$ B molecular cluster, which is defined by high expression of genes involved in the NF $\kappa$ B pathway, also showed the highest STA NF $\kappa$ B pathway activity with a median score of 44.0, compared to a combined median score of 35.2 in the other molecular clusters. The NF $\kappa$ B molecular cluster is characterized by hyperdiploidy in 66% of cases [2], but NF $\kappa$ B pathway activity in the NF $\kappa$ B molecular cluster was significantly higher compared to NF $\kappa$ B pathway activity in the HY hyperdiploidy molecular cluster, confirming the discriminatory potential of functional NF $\kappa$ B pathway activity scores. In the TC classification by Bergsagel *et al.*, which discriminates 8 TC (translocation/cyclin D) groups, the majority of samples in the NF $\kappa$ B molecular cluster are assigned to the D1 group [2]. This D1 group is characterized by overexpression of cyclin D1 compared to healthy PC, without presence of the 5 recurrent immunoglobulin translocations that are associated with increased cyclin D expression. Patients within the D1 group showed extensive osteolytic bone disease, but were underrepresented in relapsed versus untreated MM and extramedullary PC leukemia, and were suggested to be particularly dependent on BM microenvironment interactions [31]. This favorable prognosis is in accordance with our results, showing that the NF $\kappa$ B activity score is not significantly altered in newly diagnosed MM samples with poor prognosis, or with a poor response to first-line induction therapy.

By analyzing longitudinal samples of MM patients undergoing total therapy we identified a significant increase in NF $\kappa$ B pathway activity in MM PC that survived first-line total therapy, and second-line chemo-therapy-based induction therapy after relapse. The median NF $\kappa$ B score in this group was increased by 80% compared to samples taken at diagnosis, and 53% compared to samples taken after first-line induction therapy. This increase in NF $\kappa$ B pathway activity during treatment was observed in samples from all individual MM patients included. Based on our analyses we cannot conclude if this increase is due to therapy-mediated positive selection of MM PC with high NF $\kappa$ B signaling, or if NF $\kappa$ B signaling is increased in all surviving MM PC due to treatment-induced activation of the BM microenvironment. Data of previous studies are more in accordance with the first clonal selection hypothesis. Mutations resulting in constitutive NF $\kappa$ B pathway activation that render MM PC less dependent on the BM microenvironment for survival are more common in MM cell lines, which often represent more advanced disease, than in primary MM PC [30]. In addition, the PI bortezomib was shown to result in activation, rather than inhibition of NF $\kappa$ B signaling, at late timepoints of exposure in MM PC from cell lines and primary patient samples [32].

Irrespective of the mechanism underlying increased NF $\kappa$ B pathway activity at relapse, MM PC surviving first-line total therapy and second-line induction therapy



are likely to be more resistant to therapy-induced cell death. We observed that the increase in NFκB pathway activity during therapy progression was accompanied by increased mRNA expression encoding for at least one member of the pro-survival BCL-2 protein family. Upregulation of these pro-survival BCL-2 transcripts was confirmed but less pronounced in a second dataset containing paired samples of MM patients at diagnosis and after progression/relapse to first-line total therapy. As these patients did not receive second-line therapy before sampling, this may indicate additional therapy-induced clonal selection by increasing selective pressure. In both datasets, increased expression of the direct NFκB target genes (encoding BCL-XL, BFL-1, and BCL-2) was more frequent compared to the NFκB-independent pro-survival BCL-2 members (encoding BCL-B, MCL-1, and BCL-W). Although expression levels were heterogeneous, BCL2A1 (BFL-1) was most frequently upregulated in samples taken after relapse, and this significantly correlated with differential expression of NFκB target genes included in the STA NFκB model.

BCL-XL and BCL-2 are known for their contribution to intrinsic apoptosis resistance in MM, and the BCL-2 targeting BH3-mimetic Venetoclax was shown to have clinical efficacy in RR-MM patients harboring a t(11;14) translocation [33]. A potential role for BFL-1 in MM is less clear, since BFL-1 expression is down-regulated by transcriptional repressor Blimp-1, which is required for differentiation of B-cells into anti-body-secreting PC [19]. Indeed, a study by Tarte *et al.* showed that BCL2A1 is strongly repressed in both healthy PC and MM PC purified from patient BM biopsies and cell lines, as compared to peripheral blood and tonsil B-cells. In addition, stimulation of an IL-6-dependent MM cell line with NFκB stimulating cytokines APRIL and BAFF did not result in BCL2A1 upregulation [34]. On the other hand, two studies by Mitsiades *et al.* reported contradictory results. Exposure of a MM cell line to the cytokine IGF-1 stimulated NFκB signaling, which was accompanied by upregulation of anti-apoptotic proteins including BFL-1 [35]. In addition, a specific NFκB inhibitor induced apoptosis in MM PC isolated from patients and cell lines. In at least one cell line this was the result of down-regulated NFκB signaling and subsequent reduction of apoptosis inhibitors including BFL-1 [36]. As MM cell lines are known to harbor more mutations in the NFκB pathway and are able to rapidly proliferate without presence of a BM microenvironment, these studies further underline the importance of primary patient samples to study potential effects of NFκB-induced BFL-1 expression in MM.

If BFL-1 expression is indeed a significant mediator of NFκB-induced therapy resistance in MM, (in)direct inhibition of BFL-1 could have therapeutic potential for treatment of RR-MM patients. Especially since direct and selective targeting of NFκB signaling upstream of BFL-1 has been proven challenging. The NFκB

transcription factor dimers lack accessible hydrophobic pockets that could be exploited for direct inhibition by small molecule inhibitors. Alternative strategies therefore focused on interfering with upstream pathway regulation by IKK and NIK, or even at the receptor signaling level by BCMA and TACI [8]. Despite these efforts, constitutive blocking of NF $\kappa$ B signaling resulted in dose-limiting side-effects, including severe infections due to silencing of the immune system [3]. It is hypothesized that inhibiting one of the canonical or non-canonical NF $\kappa$ B pathways is safer, but clinical studies using IKK $\beta$  inhibitors, which are expected to specifically block canonical signaling, also showed severe adverse effects [3]. In addition, blocking a signaling pathway can result in unwanted inhibition of the pathway negative feedback-loop(s), resulting in increased upstream signaling and additional downstream activation of associated pathways [8]. Blocking the downstream effect of active NF $\kappa$ B signaling by inhibition of BFL-1 could therefore be a preferred option, and this might induce less systemic toxicity compared to general NF $\kappa$ B pathway targeting. Development of BFL-1 inhibitors is still in a pre-clinical phase [37], and additional research is required to prove the efficacy and safety of BFL-1 targeting in MM.

## 4.1 | Future Perspectives

In the current study we utilized an *in silico* approach and revealed an increase in NF $\kappa$ B signaling after MM relapse to first-line therapy. In addition, we demonstrated that this was accompanied by increased expression of pro-survival BCL-2 family members BFL-1, BCL-XL, and BCL-2, which are also targets of the NF $\kappa$ B pathway. Future studies should focus on the molecular mechanism to validate the relevance of elevated NF $\kappa$ B signaling and BFL-1 expression in MM relapse, and to demonstrate a potential correlation between these observations. It would be of interest to isolate longitudinal samples of MM patients at diagnosis and after consecutive lines of therapy, to be able to analyze NF $\kappa$ B pathway activity using the STA model over a longer disease course. This could be combined by BH3-profiling, to determine the level of mitochondrial apoptotic priming, and to analyze the dependence on pro-survival BFL1, BCL-XL, and BCL-2 expression to resist apoptosis [38]. In addition, pharmaceutical inhibition of the NF $\kappa$ B pathway by targeted drugs in relapsed primary MM samples *ex vivo* could be used to assess potential changes in BCL2A1/BFL-1, BCL2L1/BCL-XL, and BCL2/BCL-2 mRNA and protein expression.

The STA model for diverse signal transduction pathways are currently being investigated in a multitude of solid tumors and hematological malignancies. Previous publications have already shown that the STA model is a useful tool to discriminate cancer cells from healthy tissue [20,21], and to discriminate cancer

patient populations with diverse prognostic outlooks [39]. For multiple signaling pathways this assay is now adapted for use by quantitative PCR, and commercially available. One of the great advantages of the STA model is that it is not only able to identify aberrant pathway activity, but that these pathways can also be clinically targeted by therapy. This resulted in the implementation of the STA model in a phase 3 clinical trial for recurrent ovarian carcinoma (NCT03458221). In this clinical study STA analysis will be performed on histological tumor biopsies, and patients will be treated with targeted drugs to inhibit the pre-dominant pathway. Future studies will have to indicate if the STA model can also be implicated in clinical diagnosis and treatment of MM.

## 5 | CONCLUSIONS

In this study we quantified functional NFκB pathway activity in healthy PC or (pre-)malignant MM PC from specific patient subgroups at various stages of disease using the computational STA model. We found that the NFκB pathway activity was higher in MM PC from newly diagnosed patients in the NFκB cluster compared to other molecular clusters, but observed no additional differences in NFκB pathway activity in relation to early disease development, patient prognosis, or response to first-line therapy. However, MM PC that survived first-line total therapy showed significantly increased NFκB pathway activity at relapse, compared to the MM PC from samples taken in the pre-treatment phase. In a subset of relapsed samples, this increase in NFκB pathway activity was accompanied by increased expression of the BCL2A1 transcript encoding pro-survival BFL-1. We hypothesize that upregulation of BFL-1, in addition to NFκB targets BCL-XL and BCL-2, could contribute to therapy resistance of MM PC, and propose that (in)direct targeting of BFL-1 may provide a new approach for a subset of RR-MM patients.

## ACKNOWLEDGEMENTS

This research was funded in part by a Bas Mulder Award from the Dutch Cancer Foundation (KWF)/Alped'HuZes foundation, grant number UU 2015-7663 (V.P.) and a project grant from the Dutch Cancer Foundation (KWF)/Alped'HuZes foundation, grant number 11108 (V.P.).

## REFERENCES

1. Kumar, S.K.; Rajkumar, V.; Kyle, R.A.; van Duin, M.; Sonneveld, P.; Mateos, M.V.; Gay, F.; Anderson, K.C. Multiple myeloma. *Nat Rev Dis Primers* 2017, 3, 17046.
2. Broyl, A.; Hose, D.; Lokhorst, H.; de Knecht, Y.; Peeters, J.; Jauch, A.; Bertsch, U.; Buijs, A.; Stevens-Kroef, M.; Beverloo, H.B.; et al. Gene expression profiling for molecular classification of multiple myeloma in newly diagnosed patients. *Blood* 2010, 116, 2543-2553.
3. Wong, A.H.; Shin, E.M.; Tergaonkar, V.; Chng, W.J. Targeting NF- $\kappa$ B Signaling for Multiple Myeloma. *Cancers (Basel)* 2020.
4. Annunziata, C.M.; Davis, R.E.; Demchenko, Y.; Bellamy, W.; Gabrea, A.; Zhan, F.; Lenz, G.; Hanamura, I.; Wright, G.; Xiao, W.; et al. Frequent engagement of the classical and alternative NF-kappaB pathways by diverse genetic abnormalities in multiple myeloma. *Cancer Cell* 2007, 12, 115-130.
5. Keats, J.J.; Fonseca, R.; Chesi, M.; Schop, R.; Baker, A.; Chng, W.J.; Van Wier, S.; Tiedemann, R.; Shi, C.X.; Sebag, M.; et al. Promiscuous mutations activate the noncanonical NF-kappaB pathway in multiple myeloma. *Cancer Cell* 2007, 12, 131-144.
6. Bolli, N.; Avet-Loiseau, H.; Wedge, D.C.; Van Loo, P.; Alexandrov, L.B.; Martincorena, I.; Dawson, K.J.; Iorio, F.; Nik-Zainal, S.; Bignell, G.R.; et al. Heterogeneity of genomic evolution and mutational profiles in multiple myeloma. *Nat Commun* 2014, 5, 2997.
7. Chapman, M.A.; Lawrence, M.S.; Keats, J.J.; Cibulskis, K.; Sougnez, C.; Schinzel, A.C.; Harview, C.L.; Brunet, J.P.; Ahmann, G.J.; Adli, M.; et al. Initial genome sequencing and analysis of multiple myeloma. *Nature* 2011, 471, 467-472.
8. Matthews, G.M.; de Matos Simoes, R.; Dhimolea, E.; Sheffer, M.; Gandolfi, S.; Dashevsky, O.; Sorrell, J.D.; Mitsiades, C.S. NF- $\kappa$ B dysregulation in multiple myeloma. *Semin Cancer Biol* 2016, 39, 68-76.
9. Bossen, C.; Schneider, P. BAFF, APRIL and their receptors: structure, function and signaling. *Semin Immunol* 2006, 18, 263-275.
10. Moreaux, J.; Legouffe, E.; Jourdan, E.; Quittet, P.; Rème, T.; Lugagne, C.; Moine, P.; Rossi, J.F.; Klein, B.; Tarte, K. BAFF and APRIL protect myeloma cells from apoptosis induced by interleukin 6 deprivation and dexamethasone. *Blood* 2004, 103, 3148-3157.
11. Li, Z.W.; Chen, H.; Campbell, R.A.; Bonavida, B.; Berenson, J.R. NF-kappaB in the pathogenesis and treatment of multiple myeloma. *Curr Opin Hematol* 2008, 15, 391-399.
12. Rajkumar, S.V. Multiple myeloma: Every year a new standard? *Hematol Oncol* 2019, 37 Suppl 1, 62-65.
13. Keifer, J.A.; Guttridge, D.C.; Ashburner, B.P.; Baldwin, A.S., Jr. Inhibition of NF-kappa B activity by thalidomide through suppression of I kappa B kinase activity. *J Biol Chem* 2001, 276, 22382-22387..
14. Traenckner, E.B.; Wilk, S.; Baeuerle, P.A. A proteasome inhibitor prevents activation of NF-kappa B and stabilizes a newly phosphorylated form of I kappa B-alpha that is still bound to NF-kappa B. *Embo j* 1994, 13, 5433-5441.
15. Nijhof, I.S.; van de Donk, N.; Zweegman, S.; Lokhorst, H.M. Current and New Therapeutic Strategies for Relapsed and Refractory Multiple Myeloma: An Update. *Drugs* 2018, 78, 19-37.

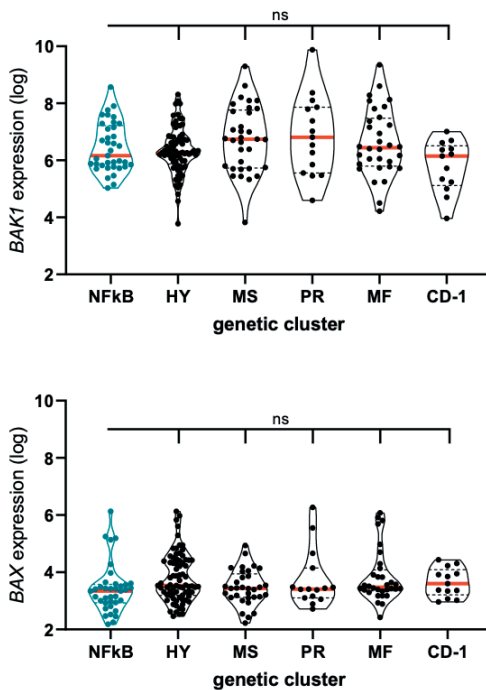
16. Davis, L.N.; Sherbenou, D.W. Emerging Therapeutic Strategies to Overcome Drug Resistance in Multiple Myeloma. *Cancers (Basel)* 2021, 13.
17. Slomp, A.; Peperzak, V. Role and Regulation of Pro-survival BCL-2 Proteins in Multiple Myeloma. *Front Oncol* 2018, 8, 533.
18. Vogler, M. BCL2A1: the underdog in the BCL2 family. *Cell Death Differ* 2012, 19, 67-74.
19. Shaffer, A.L.; Lin, K.I.; Kuo, T.C.; Yu, X.; Hurt, E.M.; Rosenwald, A.; Giltman, J.M.; Yang, L.; Zhao, H.; Calame, K.; et al. Blimp-1 orchestrates plasma cell differentiation by extinguishing the mature B cell gene expression program. *Immunity* 2002, 17, 51-62.
20. van de Stolpe, A.; Holtzer, L.; van Ooijen, H.; Inda, M.A.; Verhaegh, W. Enabling precision medicine by unravelling disease pathophysiology: quantifying signal transduction pathway activity across cell and tissue types. *Sci Rep* 2019, 9, 1603.
21. Verhaegh, W.; van Ooijen, H.; Inda, M.A.; Hatzis, P.; Versteeg, R.; Smid, M.; Martens, J.; Foekens, J.; van de Wiel, P.; Clevers, H.; et al. Selection of personalized patient therapy through the use of knowledge-based computational models that identify tumor-driving signal transduction pathways. *Cancer Res* 2014, 74, 2936-2945.
22. Zhan, F.; Barlogie, B.; Arzoumanian, V.; Huang, Y.; Williams, D.R.; Hollmig, K.; Pineda-Roman, M.; Tricot, G.; van Rhee, F.; Zangari, M.; et al. Gene-expression signature of benign monoclonal gammopathy evident in multiple myeloma is linked to good prognosis. *Blood* 2007, 109, 1692-1700.
23. Terragna, C.; Remondini, D.; Martello, M.; Zamagni, E.; Pantani, L.; Patriarca, F.; Pezzi, A.; Levi, G.; Offidani, M.; Proserpio, I.; et al. The genetic and genomic background of multiple myeloma patients achieving complete response after induction therapy with bortezomib, thalidomide and dexamethasone (VTD). *Oncotarget* 2016, 7, 9666-9679.
24. Zhou, W.; Yang, Y.; Xia, J.; Wang, H.; Salama, M.E.; Xiong, W.; Xu, H.; Shetty, S.; Chen, T.; Zeng, Z.; et al. NEK2 induces drug resistance mainly through activation of efflux drug pumps and is associated with poor prognosis in myeloma and other cancers. *Cancer Cell* 2013, 23, 48-62.
25. Weinhold, N.; Ashby, C.; Rasche, L.; Chavan, S.S.; Stein, C.; Stephens, O.W.; Tytarenko, R.; Bauer, M.A.; Meissner, T.; Deshpande, S.; et al. Clonal selection and double-hit events involving tumor suppressor genes underlie relapse in myeloma. *Blood* 2016, 128, 1735-1744.
26. Landgren, O.; Kyle, R.A.; Pfeiffer, R.M.; Katzmann, J.A.; Caporaso, N.E.; Hayes, R.B.; Dispenzieri, A.; Kumar, S.; Clark, R.J.; Baris, D.; et al. Monoclonal gammopathy of undetermined significance (MGUS) consistently precedes multiple myeloma: a prospective study. *Blood* 2009, 113, 5412-5417.
27. Rajkumar, S.V.; Landgren, O.; Mateos, M.V. Smoldering multiple myeloma. *Blood* 2015, 125, 3069-3075.
28. Vrabel, D.; Pour, L.; Ševčíková, S. The impact of NF-κB signaling on pathogenesis and current treatment strategies in multiple myeloma. *Blood Rev* 2019, 34, 56-66.
29. Kyle, R.A.; Rajkumar, S.V. Criteria for diagnosis, staging, risk stratification and response assessment of multiple myeloma. *Leukemia* 2009, 23, 3-9.
30. Demchenko, Y.N.; Kuehl, W.M. A critical role for the NFκB pathway in multiple myeloma. *Oncotarget* 2010, 1, 59-68.

31. Bergsagel, P.L.; Kuehl, W.M.; Zhan, F.; Sawyer, J.; Barlogie, B.; Shaughnessy, J., Jr. Cyclin D dysregulation: an early and unifying pathogenic event in multiple myeloma. *Blood* 2005, 106, 296-303.
32. Hideshima, T.; Ikeda, H.; Chauhan, D.; Okawa, Y.; Raje, N.; Podar, K.; Mitsiades, C.; Munshi, N.C.; Richardson, P.G.; Carrasco, R.D.; et al. Bortezomib induces canonical nuclear factor-kappaB activation in multiple myeloma cells. *Blood* 2009, 114, 1046-1052.
33. Kaufman, J.L.; Gasparetto, C.; Schjesvold, F.H.; Moreau, P.; Touzeau, C.; Facon, T.; Boise, L.H.; Jiang, Y.; Yang, X.; Dunbar, F.; et al. Targeting BCL-2 with venetoclax and dexamethasone in patients with relapsed/refractory t(11;14) multiple myeloma. *Am J Hematol* 2021, 96, 418-427.
34. Tarte, K.; Jourdan, M.; Veyrune, J.L.; Berberich, I.; Fiol, G.; Redal, N.; Shaughnessy, J., Jr.; Klein, B. The Bcl-2 family member Bfl-1/A1 is strongly repressed in normal and malignant plasma cells but is a potent anti-apoptotic factor for myeloma cells. *Br J Haematol* 2004, 125, 373-382.
35. Mitsiades, C.S.; Mitsiades, N.; Poulaki, V.; Schlossman, R.; Akiyama, M.; Chauhan, D.; Hideshima, T.; Treon, S.P.; Munshi, N.C.; Richardson, P.G.; et al. Activation of NF-kappaB and upregulation of intracellular anti-apoptotic proteins via the IGF-1/Akt signaling in human multiple myeloma cells: therapeutic implications. *Oncogene* 2002, 21, 5673-5683.
36. Mitsiades, N.; Mitsiades, C.S.; Poulaki, V.; Chauhan, D.; Richardson, P.G.; Hideshima, T.; Munshi, N.; Treon, S.P.; Anderson, K.C. Biologic sequelae of nuclear factor-kappaB blockade in multiple myeloma: therapeutic applications. *Blood* 2002, 99, 4079-4086.
37. Harvey, E.P.; Hauseman, Z.J.; Cohen, D.T.; Rettenmaier, T.J.; Lee, S.; Huhn, A.J.; Wales, T.E.; Seo, H.S.; Luccarelli, J.; Newman, C.E.; et al. Identification of a Covalent Molecular Inhibitor of Anti-apoptotic BFL-1 by Disulfide Tethering. *Cell Chem Biol* 2020, 27, 647-656.e646.
38. Touzeau, C.; Ryan, J.; Guerriero, J.; Moreau, P.; Chonghaile, T.N.; Le Gouill, S.; Richardson, P.; Anderson, K.; Amiot, M.; Le-tai, A. BH3 profiling identifies heterogeneous dependency on Bcl-2 family members in multiple myeloma and predicts sensitivity to BH3 mimetics. *Leukemia* 2016, 30, 761-764.
39. van Lieshout, L.; van de Stolpe, A.; van der Ploeg, P.; Bowtell, D.; de Hullu, J.; Piek, J. Signal Transduction Pathway Activity in High-Grade, Serous Ovarian Carcinoma Reveals a More Favorable Prognosis in Tumors with Low PI3K and High NF-κB Pathway Activity: A Novel Approach to a Long-Standing Enigma. *Cancers (Basel)* 2020, 12.

## SUPPLEMENTAL FIGURES

	CD-1	CD-2	MF	MS	HY	PR	NFkB	CTA
CD-1		ns	ns	ns	ns	ns	**	ns
CD-2			ns	ns	ns	ns	ns	ns
MF				ns	ns	ns	****	ns
MS					ns	ns	***	ns
HY						ns	*	ns
PR							**	ns
NFkB								ns
CTA								

**Supplemental Figure 1** | Matrix showing statistical significant differences in NFkB activity score as analyzed by signal transduction pathway activity (STA) analysis in plasma cells (PC) from newly diagnosed MM patients, stratified by molecular clusters, as incorporated in dataset GSE19784. ns, not significant, \* $P < .05$ , \*\* $P < .01$ , \*\*\* $P < .001$ , \*\*\*\* $P < .0001$ .



**Supplemental Figure 2** | Violin plots showing BAK1 and BAX mRNA transcript expression in PC of newly diagnosed MM patients, as incorporated in dataset GSE19784, in molecular cluster NFkB, and molecular clusters HY, MS, PR, MF, and CD-1 that all showed a significant lower STA NFkB activity score compared to molecular cluster NFkB in Figure 1C. Included samples are represented by individual datapoints, solid red lines indicate the median, and dashed lines the quartiles of the population. ns, not significant.







# Chapter seven

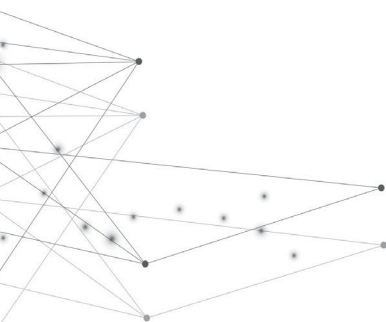
## **Bortezomib resistance in multiple myeloma is independent of PIM kinases**

Ingrid Spaan<sup>1</sup>, Laura Moesbergen<sup>1</sup>,  
Saskia Vijver<sup>1</sup>, Reinier Raymakers<sup>2</sup>,  
and Victor Peperzak<sup>1</sup>

<sup>1</sup> Laboratory of Translational Immunology,  
University Medical Center Utrecht,  
Utrecht, the Netherlands

<sup>2</sup> Department of Hematology,  
University Medical Center Utrecht,  
Utrecht, the Netherlands

*Manuscript in preparation*



## ABSTRACT

Proteasome inhibitors (PI), including bortezomib, have become a cornerstone in the treatment of multiple myeloma (MM), and significantly contributed to the improvement of patient survival in the past two decades. However, a sustained effect of PI treatment in MM is hampered by acquired drug resistance. PI induce cellular stress responses by continuous inhibition of proteasomal degradation, that ultimately promote apoptosis of MM cells. Importantly, proteasome inhibition can also lead to accumulation of pro-survival mediators in MM cells that escape from PI-induced apoptosis. The aim of this study is to uncover and potentially target PI-induced mediators of pro-survival signaling, and to assess if inhibition of these pro-survival pathways could re-sensitize resistant cells to PI. Using kinome analysis of PI-naïve MM cell lines, we identified a bortezomib-induced increase of constitutively active pro-survival PIM kinases. Targeting PIM kinases in these MM cells by the small-molecule pan-PIM inhibitor PIM447 resulted in an additive effect on apoptosis induction in combination with bortezomib. However, after acquiring bortezomib resistance, MM cell lines lost sensitivity to PIM447, both as a single agent and in combination with PI. To conclude, we demonstrate that bortezomib-resistant cells cannot be re-sensitized to bortezomib by PIM inhibition, and that targeting PIM kinases would be ineffective in PI-refractory MM patients.

## 1 | INTRODUCTION

Multiple myeloma (MM) is a genetically heterogeneous malignancy of clonal plasma cells (PC) that primarily proliferate in the bone marrow. The malignant MM-PC are characterized by production and secretion of monoclonal immunoglobulins, which are referred to as M-protein [1]. This high intracellular protein production is inevitably accompanied by the presence of misfolded and unfolded proteins. MM-PC therefore particularly rely on the proteasome for degradation of these unwanted protein products [2]. The proteasome is a large multi-protein complex that contains three catalytic core units: the  $\beta 5$  subunits with chymotrypsin-like activity, the  $\beta 1$  subunits with caspase-like activity, and the  $\beta 2$  subunits with trypsin-like activity [3]. By recognizing proteins that are marked for degradation, the proteasome degrades proteins that are misfolded, damaged, redundant, or that are tightly regulated due to their role in critical cellular processes, like cell cycle control and apoptosis [4].

Bortezomib is the first-in-class proteasome inhibitor (PI) approved for treatment of both newly diagnosed and relapsed-refractory MM patients [5]. Bortezomib is a boronic acid dipeptide that selectively and reversibly inhibits the  $\beta 5$  subunit

and, to a lesser extent, the  $\beta 1$  subunit of the proteasome. Two additional second-generation PI, the irreversible PI carfilzomib and the oral PI ixazomib, have been approved for second-line therapy and beyond [6]. By inhibition of proteasomal activity, PI induce the accumulation of undegraded proteins. This leads to a plethora of cellular stress responses, including endoplasmic reticulum stress, production of reactive oxygen species, activation of JNK and p53, inhibition of cyclin-dependent kinases, and induction of pro-apoptotic proteins, that ultimately result in MM cell death [7]. In addition, bortezomib inhibits the NF $\kappa$ B signaling pathway, thereby preventing expression of NF $\kappa$ B target genes that are involved in cell proliferation, immortalization, angiogenesis, intrinsic apoptosis resistance, and interaction with the MM-permissive bone marrow microenvironment [8].

The combination of PI with an immunomodulatory drug and dexamethasone are among the most active current triplet regimens, and resulted in the significant improvement of MM patient survival during the last two decades [9]. Despite the effective initial response, MM relapses after PI treatment are frequent, and acquired resistance hampers sustained PI effects [10]. A plethora of PI resistance mechanisms have been described in literature, and include *de novo* mutations in the PI binding pocket of the  $\beta 5$  proteasome subunit, overexpression of proteasomal subunits, increased autophagy, reduced cellular stress responses, activation of drug efflux pumps and nuclear export proteins, metabolic adaptation, and increased adhesion to components of the protective bone marrow microenvironment [11,12].

We hypothesize that escape from PI-induced apoptosis after prolonged proteasome inhibition may result in accumulation of proteins involved in pro-survival signaling in MM-PC. This pro-survival signaling potentially contributes to acquired therapy resistance of MM-PC. In the current study, we performed kinome analysis to identify PI-induced mediators of pro-survival signaling, analyzed the therapeutic targetability of these mediators to improve the PI response, and assessed if inhibition of these pro-survival pathways could re-sensitize resistant MM-PC to PI.

## 2 | METHODS

### 2.1 | Cell culture and reagents

All human multiple myeloma cell lines (HMCL) were cultured in RPMI 1640 GlutaMAX HEPES (Life Technologies), containing 100 µg/ml penicillin-streptomycin (Life Technologies). MM1.s and L363 cultures were supplemented with 10% fetal bovine serum (FBS; Biowest). NCI-H929 cultures were supplemented with 20% FBS, 1 mM sodium pyruvate (Thermo Fisher Scientific), and 50 µM β-mercaptoethanol (Life Technologies). RPMI-8226 cells were obtained and cultured as previously published by Franke *et al.* and Zaal *et al.* [13,14]. In brief, cells were maintained at a density of  $3 \times 10^5$  cells/ml twice weekly. Bortezomib-resistant cells were continuously cultured in the presence of 7 nM bortezomib (Tebu bio) for BTZ7, and 100 nM bortezomib for BTZ100, which was removed from cultures 4-6 days prior to the experiments. All cells were maintained at 37 °C and 5% CO<sub>2</sub>.

### 2.2 | Kinome analysis

For kinomic profiling HMCL were lysed in M-PER mammalian protein extraction reagent containing Halt protease and Halt phosphatase inhibitor cocktails (all Thermo Fisher Scientific). Analysis of serine/threonine kinase (STK) activity was performed using the high-throughput peptide microarray system of the PamStation 12 platform (PamGene), according to the manufacturer's instructions. Initial sample and array processing and image captures were performed using Evolve software (PamGene). Raw data processing, quantification, and statistical analysis of peptide phosphorylation was performed using BioNavigator software (PamGene). Prediction of upstream kinases was performed on peptides with bortezomib-induced statistically significant altered phosphorylation using the Kinexus Kinase Predictor ([www.phosphonet.ca](http://www.phosphonet.ca)) and identified by scoring kinase prevalence in the top10 list per peptide.

### 2.3 | Datasets

PIM transcript expression was assessed in samples from newly diagnosed MM patients using publicly available datasets GSE2658 [15] and GSE87900 [16] from the Gene Expression Omnibus, and analyzed using the R2 Genomics Analysis and Visualization Platform.

## 2.4 | Apoptosis assays

Cell viability of HMCL was determined after 48 hours of exposure to bortezomib and/or PIM447 (LGH447; SelleckChem) by staining with 15 nM DiOC6 and 20 nM TO-PRO-3 (both Thermo Fisher Scientific) and measured by flow cytometry (FACS Canto II, BD Biosciences) using FACSDiva software (BD Biosciences). Data was analyzed using FlowJo software (BD). Specific apoptosis was calculated by relating the reduced percentage of viable cells (DiOC6<sup>+</sup>/TO-PRO-3<sup>-</sup>) upon drug exposure to the percentage of viable control cells, as follows:  $([\% \text{ cell death in treated cells} - \% \text{ cell death in control}] / \% \text{ viable cells control}) \times 100\%$ . The drug combination effects were determined by comparing observed (OBS) specific apoptosis to hypothetical expected (EXP) specific apoptosis that assumes an additive effect of the two combined drugs. This was calculated as previously published by Nijhof *et al.*:  $([\text{apoptosis drug A} + \text{apoptosis drug B}] - (\text{apoptosis drug A} \times \text{apoptosis drug B}))$  [17]. Synergy was assessed using isobolograms showing drug combinations that caused 25% specific apoptosis (IC<sub>25</sub>). Combination indexes (CI) were calculated using the Chou-Talalay method [18].

## 2.5 | Statistical analysis

Data bars are represented as mean and error bars indicate standard error of the mean. Data of drug combination experiments visualized as heatmaps show the mean of multiple individual experiments. Datapoints of experiments comparing expected and observed specific apoptosis, and datapoints included in the isobolograms are obtained from the same individual experiments. Statistical analysis was performed using GraphPad Prism8 (GraphPad software Inc.). Sets of two groups were compared using paired t-tests and comparison of multiple groups was performed by one-way ANOVA using Dunnett correction for multiple comparison. For all tests a *P*-value of < 0.05 was considered statistically significant.

# 3 | RESULTS AND DISCUSSION

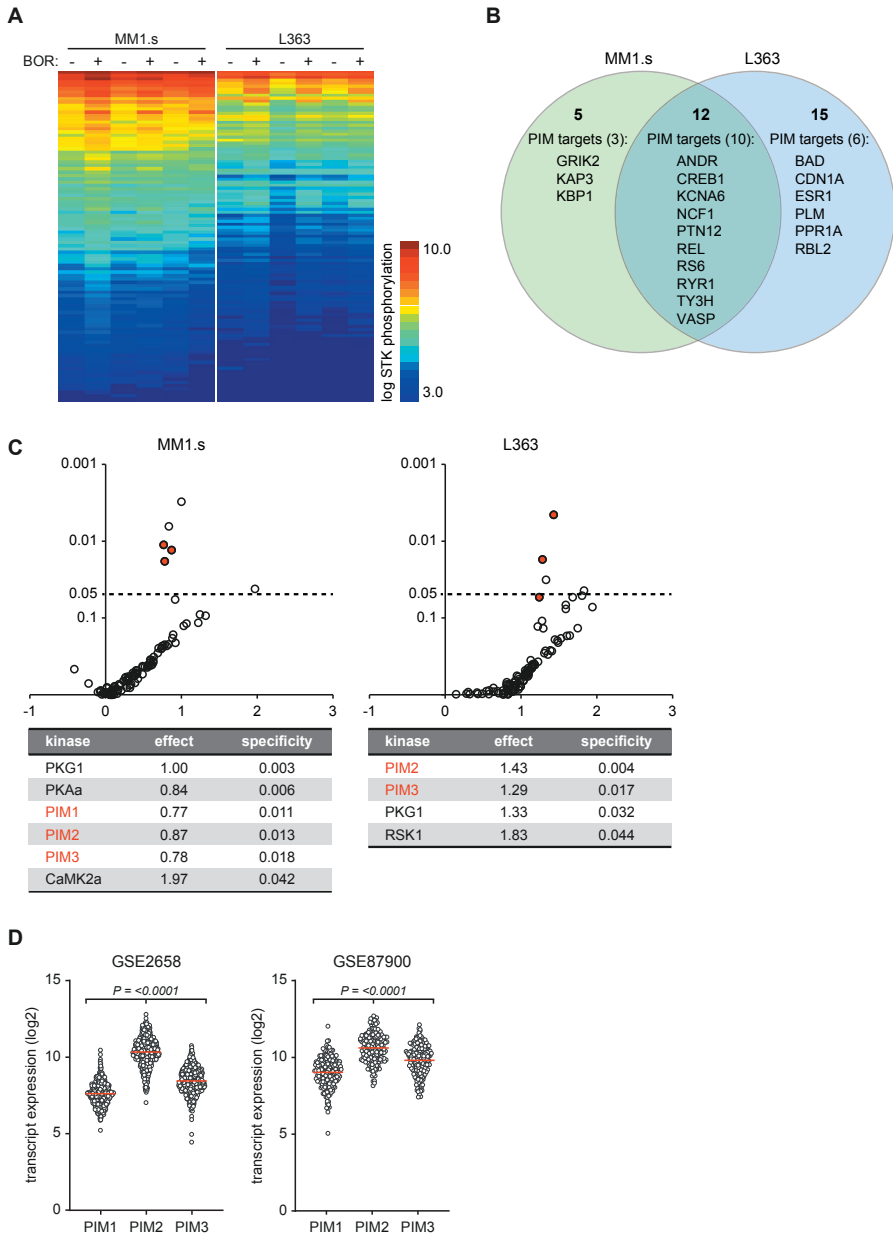
## 3.1 | Proteasome inhibition by bortezomib induces PIM kinase activity in human myeloma cell lines

To assess if proteasome inhibition by PI induces accumulation of active mediators that could contribute to pro-survival signaling in MM, we performed kinome analysis of PI-naïve HMCL that were exposed to bortezomib for 6 hours, at concentrations known to induce apoptosis at prolonged 24 hour exposure.

A comprehensive increase in peptide phosphorylation by STK was observed in bortezomib-treated HMCL MM1.s and L363, compared to their paired DMSO control samples (Figure 1A). Statistical analysis identified 12 peptides with significantly increased phosphorylation in both HMCL, 5 peptides unique for MM1.s, and 15 peptides unique for L363 (Supplemental Figure 1). Interestingly, nearly 60% of the peptides with significant bortezomib-induced phosphorylation are substrates of PIM kinases; 3/5 peptides unique for MM1.s, 6/15 peptides unique for L363, and 10/12 peptides that were identified in both HMCL (Figure 1B). These peptides include mediators of the PI3K/Akt pathway (RS6), NF $\kappa$ B pathway (REL), and intrinsic apoptosis pathway (BAD), that are associated with PIM kinase signaling [19]. Additional analysis of the peptides with significant bortezomib-induced phosphorylation by database-driven software predicted a statistically significant increase in PIM1, PIM2, and PIM3 isoforms in MM1.s, and PIM2 and PIM3 in L363 (Figure 1C).

PIM kinases are a family of three isoforms with oncogenic potential that play a critical role in cell cycle progression, cell survival, and tumorigenesis [20]. PIM kinases are constitutively active and require no post-translational modifications to achieve an active conformation. Their activity is therefore primarily regulated by balancing its synthesis and degradation by the proteasome [19]. PIM2 is significantly increased in MM-PC isolated from newly diagnosed multiple myeloma patients (Figure 1D) [21], and proteasome inhibition by bortezomib has previously been demonstrated to result in accumulation of catalytically active PIM2 *in vitro* [22].

**►Figure 1 | Exposure of HMCLs to bortezomib induces phosphorylation of PIM substrates.** (A) Heatmap showing serine/threonine kinase (STK) phosphorylation of peptides in lysates of MM1.s exposed to 12 nM bortezomib (BOR; left panel), and L363 exposed to 24 nM BOR (right panel), or DMSO control for 6 hours. Columns represent 3 technical triplicates per HMCL and treatment condition. Every row represents a unique peptide motif. The log STK phosphorylation is indicated by a color scale in which low phosphorylated peptides are indicated by blue and high phosphorylated peptides by orange/red. (B) Venn diagram depicting total number of peptides with statistically significant increased phosphorylation in bortezomib-treated MM1.s (5 unique hits) and L363 (15 unique hits; 12 hits shared between both HMCLs), compared to control cells. Significant hits belonging to PIM downstream substrates are specified per HMCL (3/5 unique hits for MM1s; 6/15 unique hits for L363; 10/12 hits shared between both HMCLs). For original data see Supplemental Figure 1. (C) Volcano plot of predicted STK activity based on statistically significant bortezomib-induced peptide phosphorylation as shown in Supplemental Figure 1, showing fold-difference (x-axis) and specificity (y-axis). Statistical significance with a P-value <0.05 is indicated by the dashed line. Details are provided for the significant STK per HMCL, PIM isoforms are indicated by the red marks. (D) Scatter plots showing transcript expression of PIM1, PIM2, and PIM3 isoforms in two publicly available datasets GSE2658 and GSE87900 containing 542 and 180 samples of newly diagnosed MM patients, respectively. All samples are represented by individual datapoints, solid red lines indicate the mean of the population.



In addition to the PIM isoforms, kinome analysis of dexamethasone-exposed HMCL also predicted a statistically significant increase in PKG1 activity (Figure 1C). PKG1 is a member of the protein kinase G family that is regulated by the nitric oxide (NO)-cyclic GMP pathway. PKG has previously been identified as a positive regulator of proteasome-mediated degradation of misfolded proteins in cardiomyocytes [23]. In addition, the NO-cyclic GMP-PKG pathway is recognized as an endogenous apoptotic pathway with anti-neoplastic properties in several solid cancers [24]. Further studies should reveal if PKG activation is a compensatory mechanism for proteasome inhibition by bortezomib, and indicate clinical significance of PKG activation in MM.

### **3.2 | Pan-PIM inhibition by PIM447 increases bortezomib-induced apoptosis in PI-naïve HMCLs**

PIM447 is a potent and highly selective small molecule inhibitor of all three PIM isoforms. Pan-PIM inhibition by PIM447 was well tolerated and showed single-agent anti-tumor activity in relapsed/refractory MM patients, with a clinical benefit rate of 25% and median progression-free survival of 10.9 months at the recommended dose [25]. To test the combinatorial effect of PI and pan-PIM inhibition, PI-naïve HMCL were exposed to dilution series of PIM447 and bortezomib, both as single-agents and combined. Exposure to these drugs resulted in a dose-dependent induction of apoptosis in all three HMCL, with NCI-H929 as the most sensitive cell line for both agents (Figure 2A). Combinations of PIM447 and bortezomib increased specific apoptosis compared to their single-agent activity, resulting in average combination indexes (CI) of 0.98 (range 0.81-1.28) for MM1.s, 1.05 (range 0.93-1.13) for L363, and 0.99 (range 0.85-1.22) for NCI-H929 (Figure 2B), indicating an additive effect of PIM447 and bortezomib. This data is in accordance with previous *in vitro* studies showing that pan-PIM inhibition by AZD1208 and PIM447 improves efficiency of standard-of-care drugs for MM, including bortezomib [22,26].



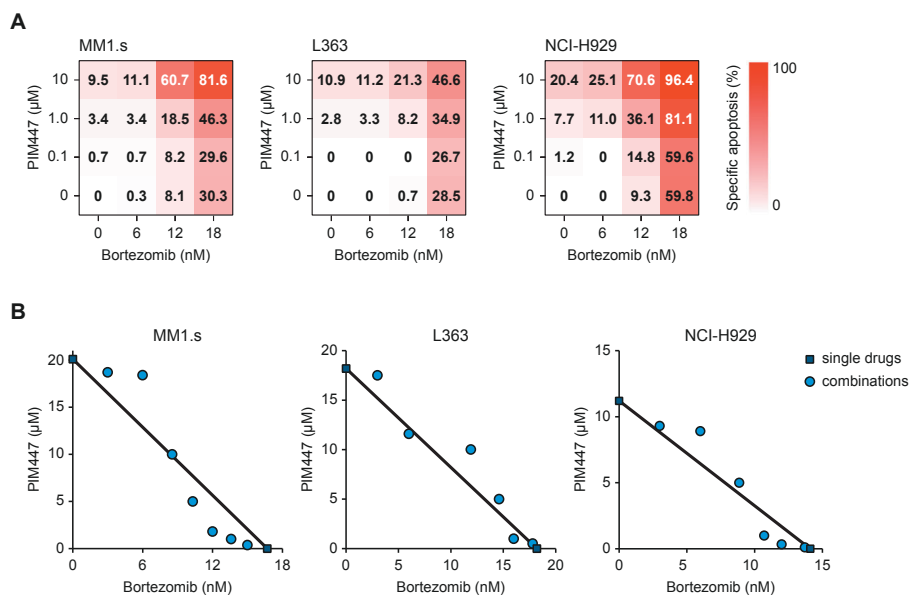


**Figure 2 | Combination of bortezomib and PIM inhibitor induces additive apoptosis in HMCL naïve to proteasome inhibition.** (A) Heatmaps showing specific apoptosis of indicated HMCL induced by serial dilution of bortezomib and PIM447, individual or combined. Viability was analyzed after 48 hours of drug exposure, values represent the mean of 2 individual experiments. (B) Isobolograms of indicated HMCL exposed to combinations of bortezomib and PIM447 for 48 hours. Blue dots indicate the drug combination that induced 25% specific apoptosis (IC<sub>25</sub>), the blue squares indicate the IC<sub>25</sub> concentrations of the single drugs. The black lines connecting both single drug datapoints indicate an exact additive effect with a combination index (CI) of 1. All values represent the mean of 2 individual experiments.

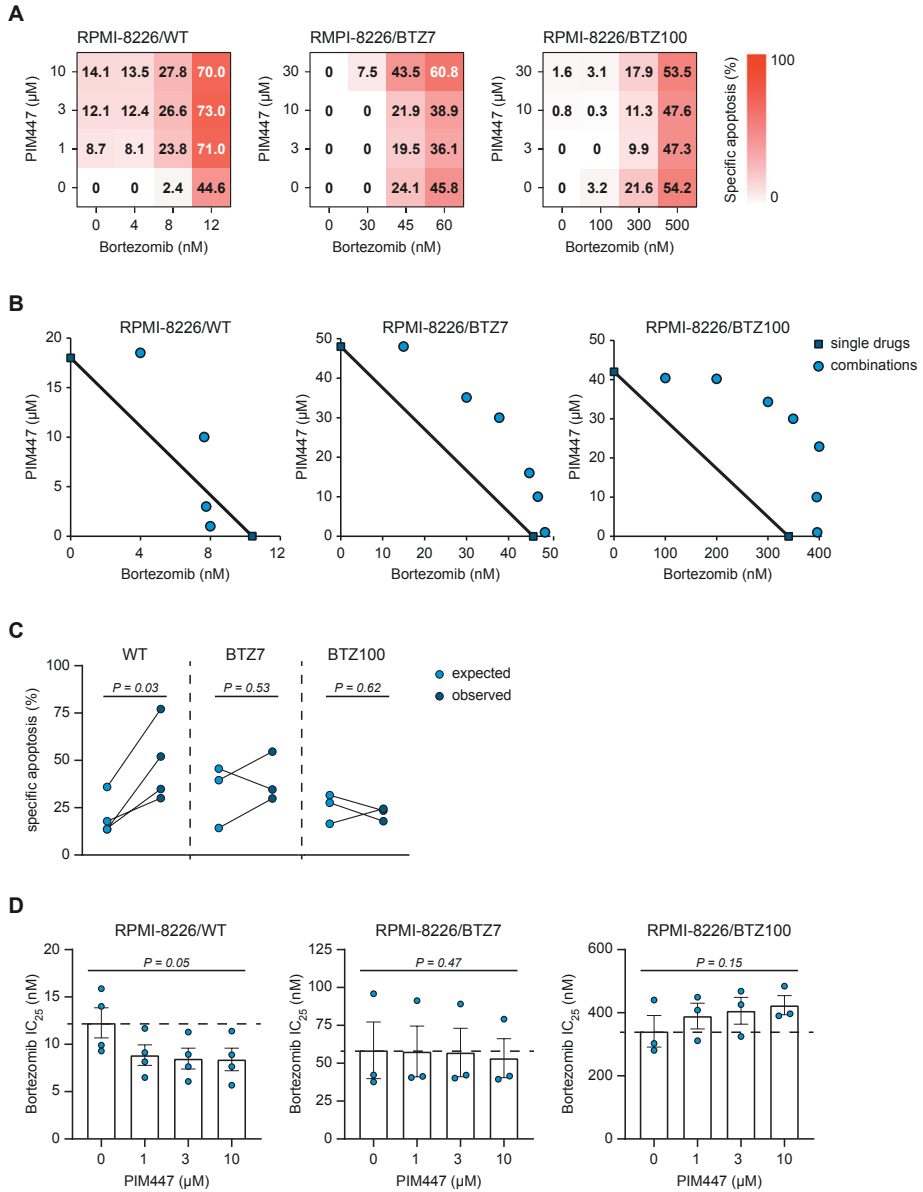
### 3.3 | Sensitivity to PIM447 in HMCL is lost after acquired bortezomib resistance

To determine if PIM kinases contribute to PI resistance, and to assess if PIM targeting improves PI responses in PI-resistant MM-PC, we compared the effects of PIM447 in HMCL RPMI-8226 that are either naïve or resistant to bortezomib. Previous publications by Franke *et al.* and Zaal *et al.* demonstrated that RPMI-8226 resistant ton7 nM bortezomib (BTZ7) and 100 nM bortezomib (BTZ100) utilize at least two complementary resistance mechanisms. First, they harbor mutations in the PSMB5 gene that map to the bortezomib-binding pocket of the proteasomal  $\beta 5$  subunit, thereby hindering bortezomib binding to the proteasome and resulting in reduced proteasomal activity [13]. Secondly, the bortezomib-resistant cells showed rewired glucose metabolism, ultimately resulting in increased antioxidant capacity as a coping mechanism to survive despite continuous proteasome inhibition [14].

Exposure of the bortezomib-naïve RPMI-8226 (wild-type, WT) to PIM447 and bortezomib resulted in a dose-dependent induction of apoptosis (Figure 3A). This was similar to the effect that was previously observed in PI-naïve HMCL MM1.s, L363, and NCI-H929 (Figure 2A). As expected, BTZ7 and BTZ100 were less sensitive to bortezomib-induced apoptosis (Figure 3A). However, in addition to bortezomib resistance, sensitivity to single-agent PIM447 was also lost in BTZ7 and BTZ100 cell lines, with a maximum of < 2% specific apoptosis at a dose of 30  $\mu$ M PIM447. In RPMI-8226/WT, combinations of PIM447 and bortezomib increased specific apoptosis compared to their single-agent activity, resulting in an average CI of 1.1 (range 0.83-1.41; Figure 3B). This additive drug effect was no longer observed in the bortezomib-resistant cells, in which average CI increased to 1.27 (range 1.08-1.45) for BTZ7, and 1.48 (range 1.19-1.74) for BTZ100. The observed specific apoptosis induced by the optimal PIM447-bortezomib combination was significantly higher than the expected additive specific apoptosis in RPMI-8226/WT, but not in BTZ7 and BTZ100 (Figure 3C). In addition, PIM447 significantly reduced bortezomib IC<sub>25</sub> values in RPMI-8226/WT, which was lost in BTZ7 and BTZ100 (Figure 3D). Taken together, this data indicates that the apoptosis-inducing effects of PIM447, both as a single agent and in combination with bortezomib, is lost in bortezomib-resistant cells.

► **Figure 3 | Bortezomib resistance disrupts apoptosis-inducing effects of PIM inhibition.**

(A) Heatmaps showing specific apoptosis induced by serial dilution of bortezomib and PIM447, individual or combined, in HMCL RPMI-8226 sensitive to bortezomib (wild-type, WT), resistant to 7 nM bortezomib (BTZ7), or resistant to 100 nM bortezomib (BTZ100). Viability was analyzed after 48 hours of drug exposure, values represent the mean of 4 (WT) or 3 (BTZ7 and BTZ100) individual experiments. (B) Isobolograms of indicated RPMI-8226 variant exposed to combinations of bortezomib and PIM447 for 48 hours. Blue dots indicate the drug combination that induced 25% specific apoptosis (IC<sub>25</sub>), the blue squares indicate the IC<sub>25</sub> concentrations of the single drugs. The black lines connecting both single drug datapoints indicate an exact additive effect with a combination index (CI) of 1. All values represent the mean of 4 (WT) or 3 (BTZ7 and BTZ100) individual experiments. (C) Plots comparing expected (EXP) to observed (OBS) specific apoptosis induced by 48 hours of exposure to bortezomib and PIM447 combinations in RPMI-8226 variants. The connected datapoints show the data obtained from 4 (WT) or 3 (BTZ7 and BTZ100) individual experiments. For bortezomib the concentration nearest to the IC<sub>25</sub> was selected per experiment, which was combined with 3  $\mu$ M PIM447 for WT, 10  $\mu$ M PIM447 for BTZ7, and 30  $\mu$ M PIM447 for BTZ100. Statistical analysis was performed by paired t-tests. (D) Plots comparing bortezomib IC<sub>25</sub> concentrations in RPMI-8226 variants in combination with increasing concentrations of PIM447. All bars show the mean and individual datapoints of 4 (WT) or 3 (BTZ7 and BTZ100) individual experiments after 48 hours of drug exposure. Bortezomib single IC<sub>25</sub> concentrations are indicated by the dashed lines. Statistical analysis was performed by one-way ANOVA using Dunnett correction for multiple comparison.



The reduced effect of the PIM447-bortezomib combination in bortezomib-resistant RPMI-8226 cells could be explained by insensitivity to proteasome inhibition. In turn, this would result in reduced accumulation of constitutively active PIM kinases, and thereby reduced sensitivity to PIM447. This hypothesis could be tested by comparing PIM protein expression in bortezomib-exposed RPMI-8226/WT, BTZ7, and BTZ100. In addition, other HMCL with acquired PI resistance should be generated and tested in a similar manner to examine whether this observation is common between different HMCL.

Future experiments should focus on the mechanism underlying loss of sensitivity to single-agent PIM447 upon PI resistance. Previous studies suggest proteasome subunit overexpression as a compensatory mechanism for impaired proteasomal activity, either due to mutations or continuous PI exposure [11,13]. Additional experiments should verify if this potential compensatory mechanism leads to more efficient proteasomal function in the absence of PI, resulting in increased PIM kinase degradation. Furthermore, the efficacy of PIM447 in PI-refractory MM patient samples should be studied, as PSMB5 mutations are expected to occur only in a subset of MM patients [27], and therefore additional mechanism of PI resistance should also be taken into account.

## 4 | CONCLUSIONS

In this study we demonstrated that bortezomib exposure in PI-naïve HMCL results in increased activity of pro-survival PIM kinases. Inhibition of PIM kinases by the pan-PIM inhibitor PIM447 in combination with bortezomib resulted in an additive effect on apoptosis induction. However, when the HMCL RPMI8226 acquired bortezomib resistance, sensitivity to PIM447 was lost, both as a single agent and in combination with bortezomib. Our data indicate that PIM inhibition cannot re-sensitize bortezomib-resistant cells to PI-mediated cell death (Figure 4), and suggests that PIM targeting would be mostly ineffective in PI-refractory MM patients.

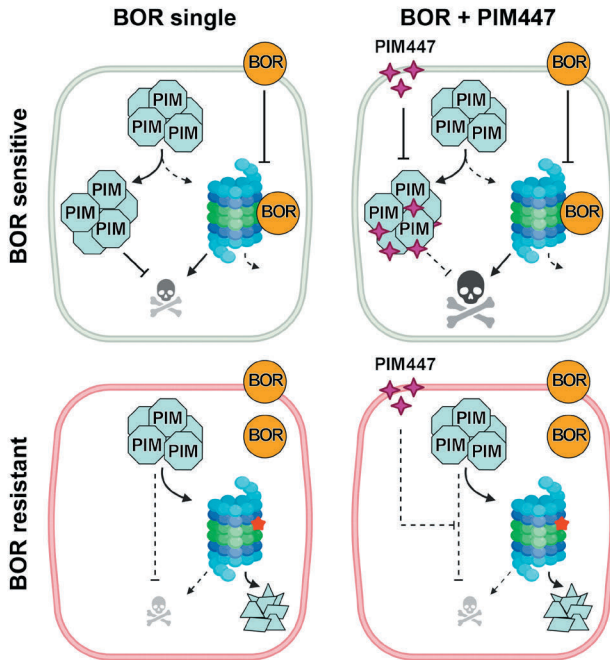


**Figure 4 | Sensitivity to pan-PIM inhibitor PIM447 is lost when HMCL become resistant to PI.** Proposed model of the relation between bortezomib (BOR) and PIM447 sensitivity in HMCL RPMI-8226. When BOR-naïve cells are exposed to single agent BOR (left upper panel), BOR inhibits the proteasome, resulting in accumulation of pro-survival PIM kinases. If the pro-apoptotic effects of PI exposure are balanced by the pro-survival effects of PIM kinases, the cell can escape PI-induced apoptosis. When BOR-naïve cells are exposed to a combination of BOR and PIM447 (right upper panel), the accumulated PIM kinases are inhibited by PIM447 and the pro-survival signal is inhibited, resulting in PI-induced apoptosis. When cells become resistant to BOR (lower panels), PIM kinases are continuously degraded by the active proteasome. As a result, there is no pro-survival signaling via PIM, but also no PI-induced cell stress, and the cell remains viable. Adding PIM447 to BOR-resistant cells has no additive effect, since there is no accumulation of PIM kinases to be inhibited.

## **ACKNOWLEDGEMENTS**

The authors thank the support facilities of the University Medical Center Utrecht and are grateful to Jaqueline Cloos for the RPMI-8226 bortezomib-resistant cell lines. This research was funded in part by a Bas Mulder Award from the Dutch Cancer Foundation (KWF)/Alped'HuZes foundation, grant number UU 2015-7663 (V.P.) and a project grant from the Dutch Cancer Foundation (KWF)/Alped'HuZes foundation, grant number 11108 (V.P.).

## REFERENCES

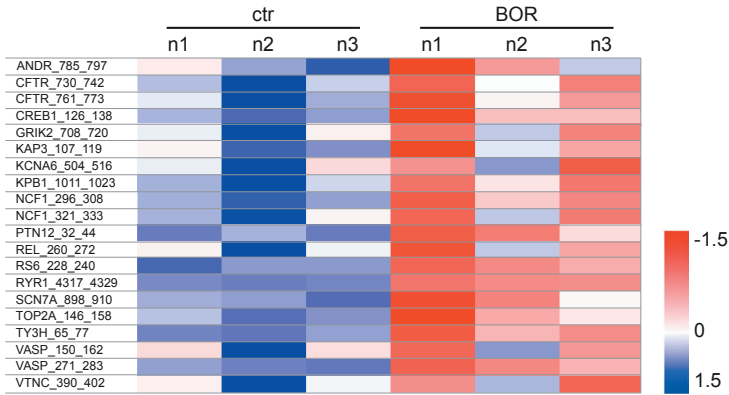
1. van de Donk, N.; Pawlyn, C.; Yong, K.L. Multiple myeloma. *Lancet* 2021, *397*, 410-427.
2. Nikesitch, N.; Lee, J.M.; Ling, S.; Roberts, T.L. Endoplasmic reticulum stress in the development of multiple myeloma and drug resistance. *Clin Transl Immunology* 2018, *7*, e1007.
3. Adams, J. The proteasome: a suitable antineoplastic target. *Nat Rev Cancer* 2004, *4*, 349-360.
4. Burger, A.M.; Seth, A.K. The ubiquitin-mediated protein degradation pathway in cancer: therapeutic implications. *Eur J Cancer* 2004, *40*, 2217-2229.
5. Guerrero-Garcia, T.A.; Gandolfi, S.; Laubach, J.P.; Hideshima, T.; Chauhan, D.; Mitsiades, C.; Anderson, K.C.; Richardson, P.G. The power of proteasome inhibition in multiple myeloma. *Expert Rev Proteomics* 2018, *15*, 1033-1052.
6. Besse, A.; Besse, L.; Kraus, M.; Mendez-Lopez, M.; Bader, J.; Xin, B.T.; de Bruin, G.; Maurits, E.; Overkleeft, H.S.; Driessen, C. Proteasome Inhibition in Multiple Myeloma: Head-to-Head Comparison of Currently Available Proteasome Inhibitors. *Cell Chem Biol* 2019, *26*, 340-351.e343.
7. Ito, S. Proteasome Inhibitors for the Treatment of Multiple Myeloma. *Cancers (Basel)* 2020, *12*.
8. Traenckner, E.B.; Wilk, S.; Baeuerle, P.A. A proteasome inhibitor prevents activation of NF-kappa B and stabilizes a newly phosphorylated form of I kappa B-alpha that is still bound to NF-kappa B. *Embo j* 1994, *13*, 5433-5441.
9. Gandolfi, S.; Laubach, J.P.; Hideshima, T.; Chauhan, D.; Anderson, K.C.; Richardson, P.G. The proteasome and proteasome inhibitors in multiple myeloma. *Cancer Metastasis Rev* 2017, *36*, 561-584.
10. Gonzalez-Santamarta, M.; Quinet, G.; Reyes-Garau, D.; Sola, B.; Roué, G.; Rodriguez, M.S. Resistance to the Proteasome Inhibitors: Lessons from Multiple Myeloma and Mantle Cell Lymphoma. *Adv Exp Med Biol* 2020, *1233*, 153-174.
11. Bai, Y.; Su, X. Updates to the drug-resistant mechanism of proteasome inhibitors in multiple myeloma. *Asia Pac J Clin Oncol* 2021, *17*, 29-35.
12. Wallington-Beddoe, C.T.; Sobieraj-Teague, M.; Kuss, B.J.; Pitson, S.M. Resistance to proteasome inhibitors and other targeted therapies in myeloma. *Br J Haematol* 2018, *182*, 11-28.
13. Franke, N.E.; Niewerth, D.; Assaraf, Y.G.; van Meerloo, J.; Vojtekova, K.; van Zantwijk, C.H.; Zweegman, S.; Chan, E.T.; Kirk, C.J.; Geerke, D.P.; et al. Impaired bortezomib binding to mutant  $\beta 5$  subunit of the proteasome is the underlying basis for bortezomib resistance in leukemia cells. *Leukemia* 2012, *26*, 757-768.
14. Zaal, E.A.; Wu, W.; Jansen, G.; Zweegman, S.; Cloos, J.; Berkers, C.R. Bortezomib resistance in multiple myeloma is associated with increased serine synthesis. *Cancer Metab* 2017, *5*, 7.
15. Hanamura, I.; Huang, Y.; Zhan, F.; Barlogie, B.; Shaughnessy, J. Prognostic value of cyclin D2 mRNA expression in newly diagnosed multiple myeloma treated with high-dose chemotherapy and tandem autologous stem cell transplantations. *Leukemia* 2006, *20*, 1288-1290.

16. Kuiper, R.; Zweegman, S.; van Duin, M.; van Vliet, M.H.; van Beers, E.H.; Dumeé, B.; Vermeulen, M.; Koenders, J.; van der Holt, B.; Visser-Wisselaar, H.; et al. Prognostic and predictive performance of R-ISS with SKY92 in older patients with multiple myeloma: the HOVON-87/NMSG-18 trial. *Blood Adv* 2020, *4*, 6298-6309.
17. Nijhof, I.S.; Lammerts van Bueren, J.J.; van Kessel, B.; Andre, P.; Morel, Y.; Lokhorst, H.M.; van de Donk, N.W.; Parren, P.W.; Mutis, T. Daratumumab-mediated lysis of primary multiple myeloma cells is enhanced in combination with the human anti-KIR antibody IPH2102 and lenalidomide. *Haematologica* 2015, *100*, 263-268.
18. Chou, T.C. Drug combination studies and their synergy quantification using the Chou-Talalay method. *Cancer Res* 2010, *70*, 440-446.
19. Brault, L.; Gasser, C.; Bracher, F.; Huber, K.; Knapp, S.; Schwaller, J. PIM serine/threonine kinases in the pathogenesis and therapy of hematologic malignancies and solid cancers. *Haematologica* 2010, *95*, 1004-1015.
20. Nawijn, M.C.; Alendar, A.; Berns, A. For better or for worse: the role of Pim oncogenes in tumorigenesis. *Nat Rev Cancer* 2011, *11*, 23-34.
21. Keane, N.A.; Reidy, M.; Natoni, A.; Raab, M.S.; O'Dwyer, M. Targeting the Pim kinases in multiple myeloma. *Blood Cancer J* 2015, *5*, e325.
22. Adam, K.; Lambert, M.; Lestang, E.; Champenois, G.; Dusanter-Fourt, I.; Tamburini, J.; Bouscary, D.; Lacombe, C.; Zermati, Y.; Mayeux, P. Control of Pim2 kinase stability and expression in transformed human haematopoietic cells. *Biosci Rep* 2015, *35*.
23. Ranek, M.J.; Terpstra, E.J.; Li, J.; Kass, D.A.; Wang, X. Protein kinase g positively regulates proteasome-mediated degradation of misfolded proteins. *Circulation* 2013, *128*, 365-376.
24. Tuttle, T.R.; Mierzwa, M.L.; Wells, S.I.; Fox, S.R.; Ben-Jonathan, N. The cyclic GMP/protein kinase G pathway as a therapeutic target in head and neck squamous cell carcinoma. *Cancer Lett* 2016, *370*, 279-285.
25. Raab, M.S.; Thomas, S.K.; Ocio, E.M.; Guenther, A.; Goh, Y.T.; Talpaz, M.; Hohmann, N.; Zhao, S.; Xiang, F.; Simon, C.; et al. The first-in-human study of the pan-PIM kinase inhibitor PIM447 in patients with relapsed and/or refractory multiple myeloma. *Leukemia* 2019, *33*, 2924-2933.
26. Paíno, T.; Garcia-Gomez, A.; González-Méndez, L.; San-Segundo, L.; Hernández-García, S.; López-Iglesias, A.A.; Algarín, E.M.; Martín-Sánchez, M.; Corbacho, D.; Ortiz-de-Solorzano, C.; et al. The Novel Pan-PIM Kinase Inhibitor, PIM447, Displays Dual Antimyeloma and Bone-Protective Effects, and Potently Synergizes with Current Standards of Care. *Clin Cancer Res* 2017, *23*, 225-238.
27. Barrio, S.; Stühmer, T.; Da-Viá, M.; Barrio-García, C.; Lehnert, N.; Besse, A.; Cuenca, I.; Garitano-Trojaola, A.; Fink, S.; Leich, E.; et al. Spectrum and functional validation of PSMB5 mutations in multiple myeloma. *Leukemia* 2019, *33*, 447-456.

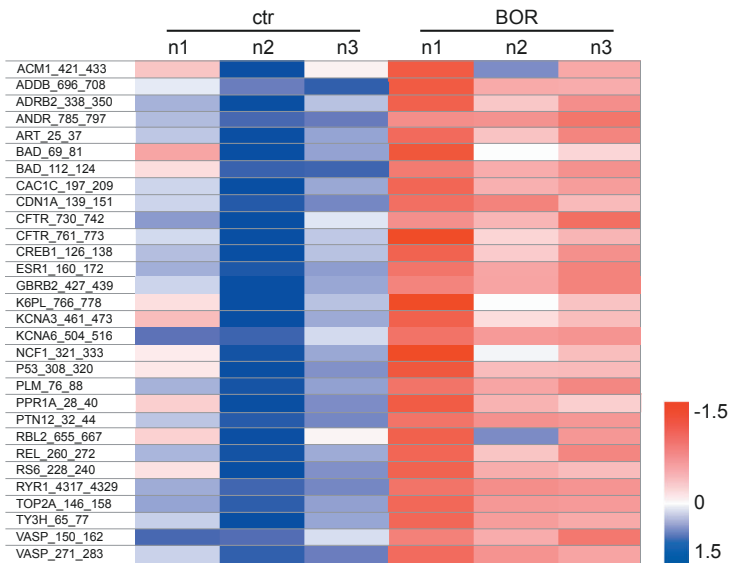


## SUPPLEMENTAL FIGURES

A



B



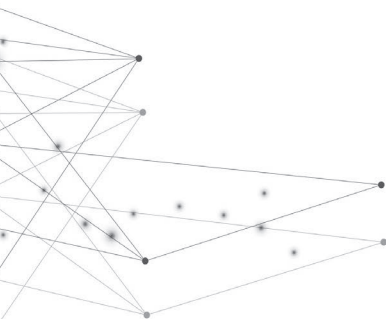
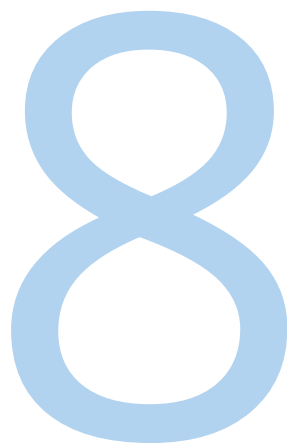
**Supplemental Figure 1 | Bortezomib significantly increases peptide phosphorylation by STK in HMCL.** Heatmaps showing peptides with significantly increased phosphorylation by serine/threonine kinases (STK) after 6 hours exposure to (A) 12 nM bortezomib (BOR) in MM1.s, or (B) 24 nM bortezomib in L363, or DMSO control (ctr). Per treatment group 3 technical replicates (n1-3) were included. Statistical analysis was performed by paired t-test.



# Chapter eight

## Targeting pro-survival cell signaling pathways as personalized treatment for multiple myeloma

Summary and future perspectives



# **1 | TARGETING PRO-SURVIVAL SIGNALING PATHWAYS AS PERSONALIZED TREATMENT FOR MULTIPLE MYELOMA**

Therapeutic options for multiple myeloma (MM) have rapidly evolved over the past years. For decades, MM treatment consisted of chemotherapy and corticosteroids, which were combined with an autologous stem cell transplantation for eligible patients. Since 2006, the therapeutic armamentarium gradually expanded with the approval of immunomodulatory drugs (thalidomide, lenalidomide, pomalidomide), proteasome inhibitors (bortezomib, carfilzomib, ixazomib), monoclonal antibodies targeting CD38 (daratumumab, isatuximab) and SLAMF7 (elotuzumab), an antibody-drug conjugate targeting BCMA (belantamab-mafodotin), and small-molecule inhibitors for histone deacetylase (panobinostat) and nuclear exportin-1 (selinexor). Conventional therapies are nowadays combined with these novel agents, resulting in therapeutic regimens that combine two, three, or even four drug classes at a time [1]. Despite the high initial efficacy of these combination treatments, the majority of MM patients relapse. As a result, most patients receive on average five or more lines of sequential therapy over several years, often leading to gradual development of drug resistance to multiple agents or drug classes [2]. Relapsed refractory disease not only limits further therapeutic options, but also patient prognosis. Especially MM patients that are triple-class refractory to immunomodulatory drugs, proteasome inhibitors, and anti-CD38 monoclonal antibodies, show a median overall survival of only 5.6 months [3]. This highlights the need for novel and more effective therapies. The translational research described in this thesis shows opportunities for targeting pro-survival signaling pathways in MM. In this chapter, I will summarize the main findings of these studies and discuss the future perspectives for targeting pro-survival signaling pathways as personalized treatment for newly-diagnosed (ND) and relapsed-refractory (RR) MM.

## **1.1 | Targeted therapy as a new era in treatment of hematological malignancies**

Targeting pro-survival signaling pathways that drive or support oncogenic behavior of cancer cells is a promising therapeutic strategy that gained a lot of interest since the approval of imatinib for treatment of chronic myeloid leukemia (CML) by the FDA in 2001. Imatinib was one of the first tyrosine kinase inhibitors (TKI) developed, and specifically targets the BCR-ABL fusion gene t(9;22), also known as the Philadelphia chromosome, that is characteristic for CML. By inducing a spectacular complete hematologic response in 98% of chronic-phase CML

patients, imatinib converted CML from a fatal cancer to a manageable chronic condition [4]. To date, additional TKI have been approved for frontline treatment of chronic-phase CML, and second and third generation TKI are available for CML after first-line treatment failure [5]. Even in patients with a cytogenetic relapse after failure on second and third generation TKI, these TKI continue to contribute to long-term survival.

Since the successful use of imatinib in CML, more hematological malignancies were treated with targeted therapy of pro-survival signaling pathways. Well-known examples include vemurafenib for hairy cell leukemia (HCL), which targets the BRAF V600E mutation that drives HCL pathogenesis. As monotherapy, vemurafenib induced a response in 91% of patients, of which 35% showed a complete response [6]. Because single agent vemurafenib could not prevent post-therapeutic early-relapse due to persisting residual disease, recent clinical trials investigated its clinical effects in combination with rituximab. This monoclonal antibody targets CD20 surface molecules that are highly expressed by the malignant B-cells, and in combination with vemurafenib improved the depth and duration of response to a relapse-free survival of 85% at median follow-up of 34 months [7].

A final example worth mentioning in the context of successful integration of targeted therapies is that of BTK inhibitors for B-cell malignancies. BTK is a non-receptor tyrosine kinase that signals downstream of the B-cell receptor (BCR) and is crucial for survival of both healthy and malignant B-cells. In addition, BTK is involved in signaling pathways that regulate proliferation and retention in supportive microenvironmental niches [8]. Ibrutinib is the first available BTK inhibitor, and was approved by the FDA in 2013 for treatment of chronic lymphocytic leukemia (CLL). As monotherapy, ibrutinib improved progression-free and overall survival compared to conventional chemo-immunotherapy in newly diagnosed CLL patients [9]. In addition to CLL, ibrutinib and second-generation BTK inhibitors are approved for treatment of mantle cell lymphoma and Waldenström macroglobulinemia, and are in clinical trials for follicular lymphoma, marginal zone lymphoma, and diffuse large B-cell lymphoma. In order to manage ibrutinib resistance, additional clinical trials focus on combination therapies with BTK inhibitors to achieve deeper remissions within a shorter treatment time [8].

## 1.2 | Multiple myeloma heterogeneity warrants personalized treatment

The above examples of targeted therapies that inhibit pro-survival signaling pathways in cancer cells, and thereby improve the outcome of patients with a variety of hematological malignancies, shows an optimistic perspective for MM

treatment. The foremost complexity in applying similar strategies for the treatment of MM is the heterogeneity of this disease. Compared to CML and HCL, MM is not characterized by a dominant genetic lesion that is responsible for pathogenesis and that can be targeted by a specific inhibitor. In addition, MM plasma cells (PC) are not addicted to one dominant pathway for survival.

As described in **chapter 2** of this thesis, MM is characterized by extensive heterogeneity. The pre-malignant MGUS phase is not initiated by a single driver lesion, but in the vast majority of patients is either due to hyperdiploidy, characterized by extra copies of the odd-numbered chromosomes 3, 5, 7, 9, 11, 15, 19, and 21; or the result of one of six recurrent translocations that juxtapose the potent immunoglobulin heavy chain enhancer near a diverse set of (proto) oncogenes. MGUS progression to overt MM is frequently accompanied by secondary genetic events, including extra gains and/or deletions of chromosomes or chromosomal arms, secondary translocations, and increased activation of pro-survival signaling pathways by genomic lesions and/or altered epigenetics. In contrast to MGUS-initiation events, secondary and subsequent driver lesions often occur in a sub-clone of cells, which are subjected to evolution-based selective pressure. As a result, there are only a few genetic lesions that are shared among a significant fraction of patients. In a recent study by Walker *et al.*, sequencing of 1273 newly-diagnosed MM patient samples and combined frequency-based and functional-based analysis identified 63 unique driver genes [10]. Only 8 of the 63 driver lesions were frequent enough to occur in >5% of the samples, and while most samples contained 2 or more driver lesions, 16% of samples did not contain any of the identified mutated driver genes.

In addition to the complex mutational landscape, the oncogenic behavior of MM PC is affected by reciprocal interactions with the bone marrow microenvironment. By both secretory and adhesive interactions, the various components of this dynamic niche impact a plethora of cellular processes and signaling pathways. The bone marrow microenvironment derived signals are indispensable for MM PC survival and also significantly contribute to the heterogeneity between MM patients.

The heterogeneity of MM is reflected by the outcome of early-phase clinical trials that analyzed MM patient response to kinase inhibitors. Several small molecule inhibitors for pro-survival signaling kinases have been tested in phase I and II clinical trials for RR-MM, including multi-kinase inhibitors like sorafenib [11], and more targeted kinase inhibitors like the c-MET inhibitor tivantinib and the mTORC inhibitor TAK-228/MLN0128 [12,13]. Unfortunately, the results of kinase inhibitors, either as monotherapy or in combination with the conventional corticosteroid dexamethasone, were limited. A recent meta-analysis showed that the 95%

confidence interval (CI) of the overall response rate (ORR) for kinase inhibitors was 2.9-13.7% for phase I trials, and 1.6-7.2% for phase II trials in MM [14]. These results are especially disappointing when compared to currently approved and implemented drug classes, like proteasome inhibitors (95% CI ORR 15.6-44.6% for phase I, 21.1-45.9% for phase II), and immunomodulatory drugs (95% CI ORR 10.9-36.8% for phase I, 23.7-35.8% for phase II). Rather than incorporating these targeted therapies into pre-existing combination regimens for unselected RR-MM patients to assess their added value, as is often suggested for kinase inhibitors with acceptable tolerability but limited single-agent activity, the potential of these targeted drugs should be re-evaluated in the context of personalized medicine. This strategy should aim to identify the pre-dominant pro-survival pathway(s) per subgroup of patients, irrespective if this results from genetic lesions or interactions with the bone marrow microenvironment, and match the targeted therapy that specifically interferes with this pathway.

### **1.3 | Personalized targeting of multiple myeloma pro-survival pathways**

Determining the optimal treatment for individual patients with a disease that is characterized by heterogeneity and for which increasing numbers of therapeutic options are available, often relies on the identification of biomarkers. Several studies have aimed to link biomarkers, varying from metabolites to molecular subtypes, to treatment responses, in order to predict the individual chances of benefit from a specific therapy. A recent example is the use of venetoclax, a BCL-2-mimetic that inhibits the pro-survival BCL-2 protein, for RR-MM patients. In the randomized and double-blinded phase 3 BELLINI trial, standard-of-care agents bortezomib and dexamethasone were combined with either venetoclax or placebo [15]. Although the addition of venetoclax significantly improved the response rate and progression-free survival in the triple treatment-group, the mortality rate was also increased in comparison to the placebo-group and resulted in an unfavorable risk-benefit ratio in unselected RR-MM patients. Additional subset analysis showed that patients with a t(11;14) translocation were an exception to this observation. These patients showed improved response and progression-free survival without increased mortality, and venetoclax was therefore suggested as potentially the first biomarker-driven therapy for RR-MM [15]. Although the t(11;14) translocation indeed enriches for venetoclax-sensitive MM, not all patients with this translocation respond well, while there are also patients negative for t(11;14) that do show a response benefit. Ongoing research is now focusing on the downstream mechanisms that determine venetoclax sensitivity. Multiple studies reported that the ratio between BCL-2 expression and other members of the

BCL-2 family, especially pro-survival BCL-XL, is of importance [16]. Another recent *ex vivo* study suggested that a molecular B-cell signature of the MM PC predicts venetoclax sensitivity, independent of the t(11;14) translocation status [17].

The applicability of a biomarker to predict therapy response is for a large part dependent on how closely this readout parameter is linked to the druggable target of interest. In **chapter 7** of this thesis we used a human myeloma cell line (HMCL) with acquired multi-modal resistance to proteasome inhibitors (PI) [18,19], and identified that PI resistance is associated with additional resistance to the pro-apoptotic effects of PIM447, an inhibitor of all three pro-survival PIM isoforms [20]. We hypothesize that these two events are directly related, since the proteasome is required for degradation of the otherwise constitutively active PIM kinases [21]. In these types of direct cause-consequence interactions, the biomarker can predict the response to a specific targeted therapy. When confirmed by additional *in vivo* data, this means that patients refractory to PI should not be treated with PIM447, because of predicted lack of clinical benefit. However, there is additional merit in mapping these types of interactions when it comes to predicting the effectiveness of newly developed therapies. The RR-MM patients included in the PIM447 phase I trial were heavily pre-treated, of which 89.9% had received prior therapy with at least one PI, and at minimum 34% of patients were refractory to multiple PI [22]. In the entire study population, a clinical benefit rate of 25.3% and an overall response rate of 8.9% were observed, with a median progression-free survival at the recommended drug dose of 10.9 months [22]. The benefit seems rather modest, but if these results are indeed negatively influenced by the patient group refractory to PI, the chances of benefit from PIM447 treatment for the PI-sensitive population would increase, and perhaps provide a new perspective on the administration of PIM447 for (RR)-MM.

Another factor that should be taken into account when analyzing potential biomarkers for predicting therapy response, is that not all patients respond in a similar way to comparable molecular events. In **chapter 6** of this thesis we used an *in silico* approach to quantify NF $\kappa$ B pathway activity [23,24], and showed that pro-survival NF $\kappa$ B pathway activity in MM PC significantly increases when patients relapsed to first-line total therapy, independent of the NF $\kappa$ B activity status at diagnosis. The downstream mechanisms of NF $\kappa$ B-mediated survival, however, is less uniform. Even in these small datasets, we observed that increased pro-survival NF $\kappa$ B activity after relapse can be associated with increased BCL-XL, BCL-2, or BFL-1 expression. Although all three proteins are NF $\kappa$ B target genes and members of the pro-survival BCL-2 family, targeting these anti-apoptotic mediators requires different BH-3 mimetics [25]. Since constitutive inhibition of the NF $\kappa$ B pathway results in dose-limiting side effects, more specific downstream inhibition would



be preferable [26]. In this instance, quantification of NF $\kappa$ B pathway activity should be combined with analysis of the different BCL-2 protein ratios as described for predicting venetoclax sensitivity, BH3-profiling [27], or BH3-mimetic profiling [28], in order to determine the most effective downstream target per patient.

The superiority of selecting downstream over upstream pro-survival pathway mediators for therapeutic targeting, as described above in the context of the NF $\kappa$ B pathway, was also highlighted in **chapter 5**. In this study we demonstrated that the glucocorticoid dexamethasone inhibits the constitutively active pro-survival mTORC1/P70S6K pathway in HMCL, and that this mechanism underlies synergy with S63845, a BH3-mimetic that inhibits pro-survival MCL-1 [29]. When applied to *ex vivo* cultured ND-MM patient samples, the dexamethasone and S63845 drug combination indeed induced synergistic apoptosis in a subset of samples. We then replaced dexamethasone by PF-4708671, a direct small-molecule inhibitor of the P70S6K1 kinase that is located downstream in the dexamethasone-inhibited pro-survival pathway [30]. Interestingly, the more specifically downstream targeting PF-4708671 and S63845 drug combination showed synergy in all patient samples tested. Based on these results we hypothesize that replacement of dexamethasone by the P70S6K1 inhibitor can reduce the vast amount of toxic side effects that are associated with glucocorticoid treatment [31,32]. In addition, this more specific downstream targeted approach can potentially be used to treat patients with glucocorticoid resistance that are insensitive to dexamethasone administration due to altered glucocorticoid receptor (GR) function and/or GR-mediated transcription [33].

The differential response of treatment-naïve ND-MM samples to upstream inhibitors of pro-survival signaling, as was seen for the previous dexamethasone and S63845 drug combination, was also observed in **chapter 4**. In this study, *ex vivo* cultured ND-MM samples were either exposed to tankyrase inhibitor XAV939, to inhibit the canonical  $\beta$ -catenin mediated Wnt pathway at the intracellular level [34], or to porcupine inhibitor C59, to inhibit the secretion of Wnt ligands that have the potential to activate both the canonical and non-canonical Wnt pathway receptors [35]. However, even when the MM PC were insensitive to both single agents, the combination of both tankyrase and porcupine inhibitors resulted in an uniform response of reduced long-term survival. Single-cell sequencing of the MM PC transcriptome after combinatorial drug exposure showed that this response was associated with a reduced capacity of the unfolded protein response (UPR) pathway. As the UPR pathway is crucial for cellular functionality of healthy and MM PC, due to their high protein production load [36], we hypothesize that combinatorial inhibition of the UPR pathway by XAV939 and C59, together with a PI, could be successful to target an universal MM mechanism of survival.

## 2 | CHALLENGES AND OPPURTUNITIES IN MM PERSONALIZED THERAPY

Personalized treatment has gained a lot of interest from researchers during the last decades, with citations increasing from approximately 75,000 in 1990 to almost 268,000 in 2020. To date, the research community is making progress in tackling some of the most significant obstacles in personalized targeted therapy, including the availability of tumor material, mapping of signaling activity in this material, and targeting these signaling pathways for therapeutic benefit. In light of these new advancements, future perspectives for personalized targeted treatment of MM are encouraging.

### 2.1 Availability of tumor material

Up until today, the retrieval of MM tumor material for all diagnostic and prognostic purposes is dependent on bone marrow aspirates and biopsies. These techniques suffice to confirm presence of disease, and provide some additional prognostic information based on the status of recurrent genetic lesions in combination with high-risk disease features. However, in the context of personalized targeted treatment, extra data is required. As described in **chapter 2** of this thesis, MM heterogeneity is not only observed between patients, but also between different clones within one patient. A study by Rasche *et al.* reported spatial genomic heterogeneity in >75% of patients, which included the activation status of tumor-suppressor TP53 and the pro-survival MAPK pathway [37]. In addition, the *in silico* quantification of NFκB pathway activity in MM samples taken at diagnosis and after relapse to first-line total therapy, as described in **chapter 6**, emphasizes the merit of longitudinal sample analysis. Unfortunately, bone marrow examination does not readily allow for analysis of spatiotemporal clonality, due to the invasive nature of these techniques.

A potential solution in this context may come from recent advancements in liquid biopsy testing, in which circulating tumor components are analyzed in body effluents, e.g. blood or urine, and thereby provide a far less invasive, safer, and real-time method to study disease. The biological material that can serve as a template for this type of analysis comprises circulating tumor cells, cell-free nucleic acids including DNA (cfNDA) and (micro)-RNA, and secreted extracellular vesicles / exosomes [38]. Since 2016, the FDA approved the use of liquid biopsies for cfDNA analysis in several solid cancers, including non-small cell lung cancer [39]. Currently, multiple clinical trials are evaluating the use of liquid biopsies for MM, in regards to diagnostic and prognostic information, treatment response, and

disease progression (NCT03702309 and NCT03657251) and to monitor minimal residual disease (NCT04108624). Increased availability of these samples will not only provide more complete information about the real-time disease status of patients, but can also facilitate the analysis of active pro-survival signaling, including the identification of relevant biomarkers.

## 2.2 Mapping pro-survival signaling activity

Our knowledge of signaling pathways that can drive or contribute to oncogenic behavior of cancer cells is increasing, and so is the number of available agents to target these pathways. Now the availability of patient tumor material is expected to improve, another important interconnecting factor is to accurately map which pathways are active, and therefore targetable, in the malignant cells. As described previously in this chapter, many studies have aimed to link biomarkers to treatment responses. However, due to the complex nature of most signaling pathways, biomarkers that are associated with events upstream in a signaling pathway (e.g. receptor amplification status), are not necessarily accompanied by a matching downstream signaling response. An increasing number of platforms are therefore exploring the opportunities for downstream pathway activation mapping. Two of those techniques have been utilized in the conducted research of this thesis. The PamStation 12 platform of PamGene (**chapter 5** and **chapter 7**) allows for kinomic profiling by applying cell lysates to microarrays with immobilized peptides that contain specified tyrosine or serine/threonine phosphorylation motifs. The signal transduction pathway activity (STA) model of Philips (**chapter 6**) uses an *in silico* model to quantify pathway activity and is based on transcription of a defined set of downstream pathway target genes. For multiple signaling pathways, the STA model is now adapted for use by quantitative PCR and commercially available, and the clinical application of the NF $\kappa$ B STA is currently being evaluated in a phase 3 clinical trial for recurrent ovarian carcinoma (NCT03458221). In addition to these two techniques, transcriptome sequencing (bulk or single cell, as applied in **chapter 4**) also becomes more readily available, and allows for a complete analysis without the need to anticipate for specific pathways.

The most important factor that should be taken into account when using either of these techniques to map signaling pathway activity is crosstalk within a pathway and between multiple pathways. Most peptides incorporated in the PamStation microarrays can be phosphorylated by a multitude of kinases that function in multiple pathways. A software prediction tool therefore estimates which kinases are most likely responsible for the total phosphorylation pattern that was quantified. Additional variables in this case include the activity of phosphatase that can counteract kinase activity, and the subcellular localization that is prerequisite

for some kinases to activate downstream signaling but that is lost during cell lysis. Similar considerations apply to the STA model, in which multiple downstream target genes can be activated by multiple upstream pathways, and a pre-defined selection has been made to distinguish between those. Defining this selection of target genes is required for practical feasibility, but makes it challenging to apply the same model to various heterogeneous diseases. In addition, not all relevant pro-survival pathways have a transcriptional output, as for example the mTORC-P70S6K pathway described in **chapter 5**. If MM PC are manipulated *ex vivo* before pathway analysis is performed, the loss of microenvironmental context should also be considered, as both the reciprocal adhesive and soluble interactions impact the cell signaling profile. Of interest in this regard is the improvement of MM PC *ex vivo* culturing techniques, which mimic the microenvironment and thereby promote cellular persistence, and allow for prediction of treatment responses with increasing accuracy [40,41].

## 2.3 Direct targeting of pro-survival pathways as the Achilles heel of MM

Based on the average number of genetic aberrations in MM PC, and the extensive interactions with the bone marrow microenvironment, mapping of pro-survival pathways likely results in identification of multiple concurrently active signaling pathways. Targeting of these pathways would therefore most probably also require a combinatorial approach. As seen in the research conducted in **chapter 4**, **chapter 5**, and **chapter 7**, such a combinatorial treatment approach can result in a more-than-additive or synergistic drug effect. This allows for reduced dosing of the individual drugs, while their combination remains therapeutically effective, and can be of particular interest when considering dose-limiting toxicities of individual agents.

An additional attempt to reduce toxicity while maintaining therapeutic effectivity can be made by inhibiting the active pro-survival pathways on a downstream level, rather than an upstream level. As discussed in paragraph 1.3 and **chapter 6**, the pro-survival NF $\kappa$ B pathway is a relevant therapeutic target for (RR)-MM. However, constitutive inhibition results in dose-limiting side effects, including severe infections due to silencing of the immune system [26]. In addition, many oncogenic transcription factors that are relevant for MM, including NF $\kappa$ B dimers, are difficult to target due to their lack of targetable hydrophobic pockets [42]. Targeting the key downstream pro-survival mechanisms could therefore be an approach to circumvent both practical limitations.

As was also discussed in paragraph 1.3 and **chapter 5**, downstream inhibition of the pro-survival mTORC1/P70S6K pathway by PF-4708671, a small-molecule inhibitor of P70S6K1, is also preferred over upstream pathway inhibition by dexamethasone. Although dexamethasone is an integral component of MM therapeutic regimens, its effectiveness is accompanied by serious side-effects, including muscle weakness, increased infection rate, cardiovascular problems, and mental health problems [32]. High grade toxicity might require dose reduction, especially in the elderly and frail patients, and limits its therapeutic potential [31]. In addition, a subset of MM patients suffers from intrinsic or acquired dexamethasone resistance, due to altered GR function and/or GR-mediated transcription [33]. Replacing dexamethasone by the specific and downstream P70S6K1 inhibitor, in combination with MCL-1 inhibition by S63845, may therefore provide a solution for patients ineligible or insensitive to dexamethasone or other glucocorticoids. A potential pitfall that should be taken into account when targeting pro-survival pathways by inhibition of downstream mediators, is the release of negative feedback loops that can result in unwanted upstream pathway stimulation. This also accounts for the negative feedback loop between P70S6K1 and IRS1, which can result in hyperactivation of Akt, and could therefore reverse the anti-myeloma effects of PF-4708671 [43]. However, comparison of upstream pathway inhibition by dexamethasone and downstream pathway inhibition by PF-4708671, as single agents or in combination with S63845, showed no increase in Akt phosphorylation status and therefore poses no increased risk of Akt hyperactivation.

### 3 | CONCLUDING REMARKS

The translational research described in this thesis shows the relevance of mapping active pro-survival signaling pathways during diagnosis and treatment, and after resistance and relapse of MM. Comparable to other hematological malignancies, there are increasing opportunities to successfully target these pro-survival signaling pathways in MM, but due to heterogeneity of disease this will have to be conducted in a personalized approach. As the *ex vivo* analysis techniques are improving, future research should focus on assessing the clinical effects of pro-survival inhibitors in a pre-selected group of MM patients, that are predicted to benefit from therapy based on their pro-survival signaling profile. In my hypothesis, incorporation of more directed downstream targeting of pro-survival signaling pathways into current and future treatment combinations will improve patient outcome and reduce toxic side-effects.

## REFERENCES

1. Rajkumar, S.V. Sequencing of myeloma therapy: Finding the right path among many standards. *Hematol Oncol* 2021, *39 Suppl 1*, 68-72.
2. Davis, L.N.; Sherbenou, D.W. Emerging Therapeutic Strategies to Overcome Drug Resistance in Multiple Myeloma. *Cancers (Basel)* 2021, *13*.
3. Gandhi, U.H.; Cornell, R.F.; Lakshman, A.; Gahvari, Z.J.; McGehee, E.; Jagosky, M.H.; Gupta, R.; Varnado, W.; Fiala, M.A.; Chhabra, S.; et al. Outcomes of patients with multiple myeloma refractory to CD38-targeted monoclonal antibody therapy. *Leukemia* 2019, *33*, 2266-2275.
4. Iqbal, N.; Iqbal, N. Imatinib: a breakthrough of targeted therapy in cancer. *Chemother Res Pract* 2014, *2014*, 357027.
5. Jabbour, E.; Kantarjian, H. Chronic myeloid leukemia: 2020 update on diagnosis, therapy and monitoring. *Am J Hematol* 2020, *95*, 691-709.
6. Falini, B.; Martelli, M.P.; Tiacci, E. BRAF V600E mutation in hairy cell leukemia: from bench to bedside. *Blood* 2016, *128*, 1918-1927.
7. Tiacci, E.; De Carolis, L.; Simonetti, E.; Capponi, M.; Ambrosetti, A.; Lucia, E.; Antolino, A.; Pulsoni, A.; Ferrari, S.; Zinzani, P.L.; et al. Vemurafenib plus Rituximab in Refractory or Relapsed Hairy-Cell Leukemia. *N Engl J Med* 2021, *384*, 1810-1823.
8. Pal Singh, S.; Dammeijer, F.; Hendriks, R.W. Role of Bruton's tyrosine kinase in B cells and malignancies. *Mol Cancer* 2018, *17*, 57.
9. Ahn, I.E.; Brown, J.R. Targeting Bruton's Tyrosine Kinase in CLL. *Front Immunol* 2021, *12*, 687458.
10. Walker, B.A.; Mavrommatis, K.; Wardell, C.P.; Ashby, T.C.; Bauer, M.; Davies, F.E.; Rosenthal, A.; Wang, H.; Qu, P.; Hoering, A.; et al. Identification of novel mutational drivers reveals oncogene dependencies in multiple myeloma. *Blood* 2018, *132*, 587-597.
11. Adnane, L.; Trail, P.A.; Taylor, I.; Wilhelm, S.M. Sorafenib (BAY 43-9006, Nexavar), a dual-action inhibitor that targets RAF/MEK/ERK pathway in tumor cells and tyrosine kinases VEGFR/PDGFR in tumor vasculature. *Methods Enzymol* 2006, *407*, 597-612.
12. Baljevic, M.; Zaman, S.; Baladandayuthapani, V.; Lin, Y.H.; de Partovi, C.M.; Berkova, Z.; Amini, B.; Thomas, S.K.; Shah, J.J.; Weber, D.M.; et al. Phase II study of the c-MET inhibitor tivantinib (ARQ 197) in patients with relapsed or relapsed/refractory multiple myeloma. *Ann Hematol* 2017, *96*, 977-985.
13. Ghobrial, I.M.; Siegel, D.S.; Vij, R.; Berdeja, J.G.; Richardson, P.G.; Neuwirth, R.; Patel, C.G.; Zohren, F.; Wolf, J.L. TAK-228 (formerly MLN0128), an investigational oral dual TORC1/2 inhibitor: A phase I dose escalation study in patients with relapsed or refractory multiple myeloma, non-Hodgkin lymphoma, or Waldenström's macroglobulinemia. *Am J Hematol* 2016, *91*, 400-405.
14. van Nieuwenhuijzen, N.; Frunt, R.; May, A.M.; Minnema, M.C. Therapeutic outcome of early-phase clinical trials in multiple myeloma: a meta-analysis. *Blood Cancer J* 2021, *11*, 44.
15. Kumar, S.K.; Harrison, S.J.; Cavo, M.; de la Rubia, J.; Popat, R.; Gasparetto, C.; Hungria, V.; Salwender, H.; Suzuki, K.; Kim, I.; et al. Venetoclax or placebo in combination with

- bortezomib and dexamethasone in patients with relapsed or refractory multiple myeloma (BELLINI): a randomised, double-blind, multicentre, phase 3 trial. *Lancet Oncol* 2020, *21*, 1630-1642.
16. Gupta, V.A.; Ackley, J.; Kaufman, J.L.; Boise, L.H. BCL2 Family Inhibitors in the Biology and Treatment of Multiple Myeloma. *Blood Lymphat Cancer* 2021, *11*, 11-24.
  17. Gupta, V.A.; Barwick, B.G.; Matulis, S.M.; Shirasaki, R.; Jaye, D.L.; Keats, J.J.; Oberlton, B.; Joseph, N.S.; Hofmeister, C.C.; Heffner, L.T.; et al. Venetoclax sensitivity in multiple myeloma is associated with B-cell gene expression. *Blood* 2021, *137*, 3604-3615.
  18. Franke, N.E.; Niewerth, D.; Assaraf, Y.G.; van Meerloo, J.; Vojtekova, K.; van Zantwijk, C.H.; Zweegman, S.; Chan, E.T.; Kirk, C.J.; Geerke, D.P.; et al. Impaired bortezomib binding to mutant  $\beta 5$  subunit of the proteasome is the underlying basis for bortezomib resistance in leukemia cells. *Leukemia* 2012, *26*, 757-768.
  19. Zaal, E.A.; Wu, W.; Jansen, G.; Zweegman, S.; Cloos, J.; Berkers, C.R. Bortezomib resistance in multiple myeloma is associated with increased serine synthesis. *Cancer Metab* 2017, *5*, 7.
  20. Paíno, T.; Garcia-Gomez, A.; González-Méndez, L.; San-Segundo, L.; Hernández-García, S.; López-Iglesias, A.A.; Algarín, E.M.; Martín-Sánchez, M.; Corbacho, D.; Ortiz-de-Solorzano, C.; et al. The Novel Pan-PIM Kinase Inhibitor, PIM447, Displays Dual Antimyeloma and Bone-Protective Effects, and Potently Synergizes with Current Standards of Care. *Clin Cancer Res* 2017, *23*, 225-238.
  21. Brault, L.; Gasser, C.; Bracher, F.; Huber, K.; Knapp, S.; Schwaller, J. PIM serine/threonine kinases in the pathogenesis and therapy of hematologic malignancies and solid cancers. *Haematologica* 2010, *95*, 1004-1015.
  22. Raab, M.S.; Thomas, S.K.; Ocio, E.M.; Guenther, A.; Goh, Y.T.; Talpaz, M.; Hohmann, N.; Zhao, S.; Xiang, F.; Simon, C.; et al. The first-in-human study of the pan-PIM kinase inhibitor PIM447 in patients with relapsed and/or refractory multiple myeloma. *Leukemia* 2019, *33*, 2924-2933.
  23. van de Stolpe, A.; Holtzer, L.; van Ooijen, H.; Inda, M.A.; Verhaegh, W. Enabling precision medicine by unravelling disease pathophysiology: quantifying signal transduction pathway activity across cell and tissue types. *Sci Rep* 2019, *9*, 1603.
  24. Verhaegh, W.; van Ooijen, H.; Inda, M.A.; Hatzis, P.; Versteeg, R.; Smid, M.; Martens, J.; Foekens, J.; van de Wiel, P.; Clevers, H.; et al. Selection of personalized patient therapy through the use of knowledge-based computational models that identify tumor-driving signal transduction pathways. *Cancer Res* 2014, *74*, 2936-2945.
  25. Slomp, A.; Peperzak, V. Role and Regulation of Pro-survival BCL-2 Proteins in Multiple Myeloma. *Front Oncol* 2018, *8*, 533.
  26. Wong, A.H.; Shin, E.M.; Tergaonkar, V.; Chng, W.J. Targeting NF- $\kappa$ B Signaling for Multiple Myeloma. *Cancers (Basel)* 2020, *12*.
  27. Del Gaizo Moore, V.; Letai, A. BH3 profiling--measuring integrated function of the mitochondrial apoptotic pathway to predict cell fate decisions. *Cancer Lett* 2013, *332*, 202-205.
  28. Peperzak, V.; Slinger, E.; Ter Burg, J.; Eldering, E. Functional disparities among BCL-2 members in tonsillar and leukemic B-cell subsets assessed by BH3-mimetic profiling. *Cell Death Differ* 2017, *24*, 111-119.

29. Kotschy, A.; Szlavik, Z.; Murray, J.; Davidson, J.; Maragno, A.L.; Le Toumelin-Braizat, G.; Chanrion, M.; Kelly, G.L.; Gong, J.N.; Moujalled, D.M.; et al. The MCL1 inhibitor S63845 is tolerable and effective in diverse cancer models. *Nature* 2016, *538*, 477-482.
30. Pearce, L.R.; Alton, G.R.; Richter, D.T.; Kath, J.C.; Lingardo, L.; Chapman, J.; Hwang, C.; Alessi, D.R. Characterization of PF-4708671, a novel and highly specific inhibitor of p70 ribosomal S6 kinase (S6K1). *Biochem J* 2010, *431*, 245-255.
31. Larocca, A.; Palumbo, A. How I treat fragile myeloma patients. *Blood* 2015, *126*, 2179-2185.
32. Rajkumar, S.V.; Blood, E.; Vesole, D.; Fonseca, R.; Greipp, P.R. Phase III clinical trial of thalidomide plus dexamethasone compared with dexamethasone alone in newly diagnosed multiple myeloma: a clinical trial coordinated by the Eastern Cooperative Oncology Group. *J Clin Oncol* 2006, *24*, 431-436.
33. Scheijen, B. Molecular mechanisms contributing to glucocorticoid resistance in lymphoid malignancies. *Cancer Drug Resistance* 2019, *2*, 647-664.
34. Huang, S.M.; Mishina, Y.M.; Liu, S.; Cheung, A.; Stegmeier, F.; Michaud, G.A.; Charlat, O.; Wiелlette, E.; Zhang, Y.; Wiessner, S.; et al. Tankyrase inhibition stabilizes axin and antagonizes Wnt signalling. *Nature* 2009, *461*, 614-620.
35. Proffitt, K.D.; Madan, B.; Ke, Z.; Pendharkar, V.; Ding, L.; Lee, M.A.; Hannoush, R.N.; Virshup, D.M. Pharmacological inhibition of the Wnt acyltransferase PORCN prevents growth of WNT-driven mammary cancer. *Cancer Res* 2013, *73*, 502-507.
36. Vincenz, L.; Jäger, R.; O'Dwyer, M.; Samali, A. Endoplasmic reticulum stress and the unfolded protein response: targeting the Achilles heel of multiple myeloma. *Mol Cancer Ther* 2013, *12*, 831-843.
37. Rasche, L.; Chavan, S.S.; Stephens, O.W.; Patel, P.H.; Tytarenko, R.; Ashby, C.; Bauer, M.; Stein, C.; Deshpande, S.; Wardell, C.; et al. Spatial genomic heterogeneity in multiple myeloma revealed by multi-region sequencing. *Nat Commun* 2017, *8*, 268.
38. Ferreira, B.; Caetano, J.; Barahona, F.; Lopes, R.; Carneiro, E.; Costa-Silva, B.; João, C. Liquid biopsies for multiple myeloma in a time of precision medicine. *J Mol Med (Berl)* 2020, *98*, 513-525.
39. Kwapisz, D. The first liquid biopsy test approved. Is it a new era of mutation testing for non-small cell lung cancer? *Ann Transl Med* 2017, *5*, 46.
40. Alhallak, K.; Jeske, A.; de la Puente, P.; Sun, J.; Fiala, M.; Azab, F.; Muz, B.; Sahin, I.; Vij, R.; DiPersio, J.F.; et al. A pilot study of 3D tissue-engineered bone marrow culture as a tool to predict patient response to therapy in multiple myeloma. *Sci Rep* 2021, *11*, 19343.
41. Papadimitriou, K.; Kostopoulos, I.V.; Tsopanidou, A.; Orologas-Stavrou, N.; Kastritis, E.; Tsitsilonis, O.; Dimopoulos, M.A.; Terpos, E. Ex Vivo Models Simulating the Bone Marrow Environment and Predicting Response to Therapy in Multiple Myeloma. *Cancers (Basel)* 2020, *12*.
42. Matthews, G.M.; de Matos Simoes, R.; Dhimolea, E.; Sheffer, M.; Gandolfi, S.; Dashevsky, O.; Sorrell, J.D.; Mitsiades, C.S. NF- $\kappa$ B dysregulation in multiple myeloma. *Semin Cancer Biol* 2016, *39*, 68-76.
43. O'Reilly, K.E.; Rojo, F.; She, Q.B.; Solit, D.; Mills, G.B.; Smith, D.; Lane, H.; Hofmann, F.; Hicklin, D.J.; Ludwig, D.L.; et al. mTOR inhibition induces upstream receptor tyrosine kinase signaling and activates Akt. *Cancer Res* 2006, *66*, 1500-1508.







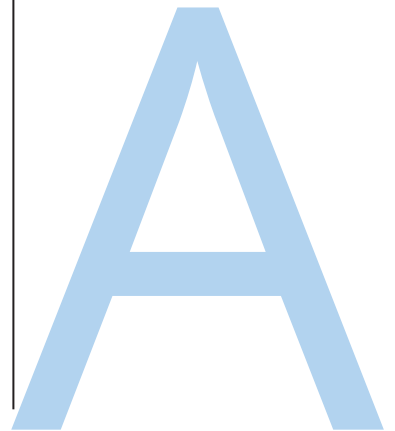
# Appendices

**Nederlandse samenvatting**

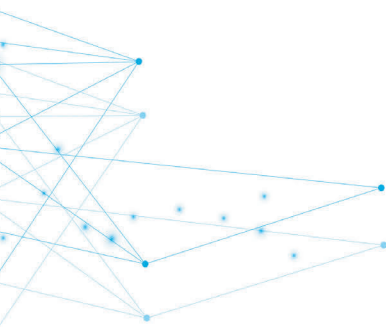
**Dankwoord**

**Curriculum vitae**

**List of publications**



A large, light blue letter 'A' is positioned on the right side of the page, partially overlapping a vertical black line that runs from the top of the 'Appendices' header down to the bottom of the page.



## NEDERLANDSE SAMENVATTING

In meercellige organismen communiceren lichaamcellen via een moleculair mechanisme dat cellulaire signalering wordt genoemd. Dit mechanisme stelt de cellen in staat om informatie te ontvangen vanuit hun omgeving, deze informatie door te geven, en om op relevante informatie te reageren door hun fysiologie aan te passen. Alle belangrijke processen in de cel worden gereguleerd middels deze signaleringsroutes. Denk hierbij aan vermeerdering door celdeling, het ontwikkelen van gespecialiseerde functies door differentiatie, en geprogrammeerde celdood door apoptose. Al deze verschillende signaleringsroutes zijn noodzakelijk voor het goed laten functioneren van een meercellig organisme. Als deze regulatie niet goed verloopt, dan kan dat leiden tot diverse ziektebeelden, zoals degeneratieve aandoeningen of allerlei vormen van kanker.

### Cellulaire communicatie via signaleringsroutes

Cellulaire signaleringsroutes kunnen worden verdeeld in drie verschillende stadia: de ontvangst van het initiërende signaal vanuit de omgeving, de intracellulaire cascade om deze informatie binnen de cel te verwerken, en de response waarbij de cellulaire fysiologie wordt aangepast naar aanleiding van de verwerkte informatie. Informatie wordt door cellen ontvangen wanneer een signaalmolecuul als ligand bindt aan een bijbehorende receptor. Deze receptoren bevinden zich hoofdzakelijk in de celmembraan aan de oppervlakte van een cel, maar kunnen in specifieke gevallen ook intracellulair aanwezig zijn. Binding van het betreffende ligand leidt tot een vormverandering in de receptor, ook wel conformatieverandering genoemd. Deze verandering is de start van een intracellulaire cascade, waarbij de geactiveerde receptor één of meerdere vervolgmoleculen, mediators genoemd, activeert. Na conformatieverandering activeren deze mediators op hun beurt ook weer een set van één of meerdere mediators, waardoor een soort domino-effect ontstaat. Tijdens deze cascade wordt de informatie niet alleen doorgegeven, maar ook bewerkt. Bijvoorbeeld door het signaal te versterken, of om te zetten naar een ander type signaal. Ook kunnen signalen vanuit meerdere signaleringsroutes worden geïntegreerd in één informatiestroom, of andersom, waarbij één signaal verschillende cascades activeert. Een belangrijke groep van mediators in deze cascades zijn de kinases. Deze eiwitten met een enzymatische functie hebben een snel functionerende schakelcapaciteit, welke noodzakelijk is voor een efficiënte signaaloverdracht. De signaleringcascades bereiken hun eindpunt bij de intracellulaire effectoren. Dit zijn de eiwitten die het gedrag van de ontvangende cel aanpassen op basis van het verkregen signaal. Afhankelijk van de aard van het signaal en de bijbehorende respons, kunnen deze aanpassingen al na enkele seconden plaatsvinden, of meerdere uren in beslag nemen.

## Verstoorde cellulaire signalering in kanker en therapie

In een gezond meercellig organisme zorgt de communicatie via signaleringsroutes ervoor dat cellen hun gedrag op elkaar kunnen afstemmen. De cellen delen, differentiëren, en sterven af in een gecoördineerd proces waarbij homeostase wordt gehandhaafd. Zodra een gezonde cel muteert tot een kankercel raken deze processen verstoort. De kankercel concurreert met gezonde cellen om te overleven, en verspreidt zich middels metastasering buiten het eigen leefgebied, of niche, om zich te vestigen in het territorium van andere cellen en weefsels. De transformatie van een gezonde cel tot een kankercel wordt tumorgenese genoemd. Dit proces bestaat uit meerdere stappen, waarvoor mutaties in het DNA de grondslag vormen. Als deze genetische schade in het voordeel van de kankercel is, dan bevordert het de onafhankelijke celdeling en vaak verminderde apoptose. De getransformeerde cel beïnvloedt ook niet-maligne cellen die in de niche aanwezig zijn, en kunnen deze cellen instrueren om bij te dragen aan processen die de verdere ontwikkeling van kankercellen stimuleren.

De transformaties die in de gemuteerde kankercel plaatsvinden beïnvloeden de signaleringsroutes die normaal de homeostase handhaven. De kankercel is afhankelijk van deze veranderende cellulaire signaleringsroutes, die dan ook steeds vaker gezien worden als een mogelijk doel voor anti-kanker therapie. Deze zogenaamde "targeted" therapieën richten zich op de signaleringsroutes waarvan de kankercellen het meest afhankelijk zijn, met als doel om deze maligne cellen hun groei- en overlevingsvoordeel te ontnemen, terwijl de gezonde cellen zoveel mogelijk gespaard blijven. De beschikbare "targeted" therapieën zijn op basis van hun molecuulgrootte in te delen in twee categorieën. De macromoleculen, waaronder antistoffen, zijn erg groot en binden aan extracellulaire onderdelen van de signaleringsroutes, zoals de receptoren, om deze te inactiveren. De zogenaamde "small-molecule" remmers zijn klein genoeg om de cellen binnen te dringen, en binden aan de intracellulaire mediators van de cascades, zoals de kinases. Deze "small-molecule" remmers hebben een revolutie teweeggebracht in de behandeling van kanker. Sinds de eerste goedkeuring van imatinib voor chronisch myeloïde leukemie in 2001, zijn tenminste 89 van deze remmers geregistreerd voor de behandeling van verschillende type tumoren.

## Behandeling van multipel myeloom

Multipel myeloom, in Nederland ook wel bekend als de ziekte van Kahler, is een kanker die ontstaat door mutaties in de antistof-producerende plasmacellen van het immuunsysteem. Tijdens het proces van tumorgenese hebben deze cellen opnieuw de capaciteit tot celdeling verworven, en zijn daardoor vaak in meerdere

haarden in het beenmerg te vinden. Door hun ongereguleerde groei verstoren de myeloomcellen de aanmaak van gezonde immuun- en bloedcellen, die normaal ook in het beenmerg plaatsvindt. Bloedarmoede is daardoor een vaak voorkomend symptoom van deze ziekte. Daarnaast stimuleren de myeloomcellen de osteoclasten (verantwoordelijk voor botafbraak), en remmen myeloomcellen de osteoblasten (verantwoordelijk voor botaanmaak), waardoor het botweefsel wordt aangetast. Dit kan leiden tot botbreuken op alle plaatsen waar beenmergaanmaak plaatsvindt, zoals het centrale skelet, de ruggenwervels, ribben, het bekken, de schedel, en de bovenarmen en benen. Door het bij de botafbraak vrijkomende calcium kan er ook nierschade ontstaan.

In de afgelopen decennia zijn de behandelmogelijkheden voor multipel myeloom sterk verbeterd. Voor lange tijd bestond deze slechts uit systemisch gegeven chemotherapie en corticosteroiden, eventueel in combinatie met een hoge dosis melfalan en autologe stamceltransplantatie bij de jongere niet-fragiele patiënten. Sinds 2006 zijn de beschikbare therapieën gestaag uitgebreid met onder andere de goedkeuring van immunomodulatoire middelen, proteasoomremmers, en monoclonale antistoffen tegen verschillende extracellulaire antigenen. De eerdergenoemde behandelingen worden tegenwoordig vaak gecombineerd met deze nieuwe therapieën, wat resulteert in combinatiebehandelingen met twee, drie, of zelfs vier middelen tegelijkertijd. Patiënten krijgen gemiddeld vijf of meer lijnen van deze combinatietherapieën over meerdere jaren verspreid. De prognose is hierdoor sterk verbeterd, maar de ziekte wordt zelden genezen. Gedurende het behandeltraject treedt vaak resistentie tegen verschillende middelen op, voornamelijk door nieuwe mutaties en selectie van resistente myeloomsubklonen. De terugkeer van resistente ziekte beperkt niet alleen de beschikbare behandelmogelijkheden, maar ook de prognose voor de patiënt. Met name patiënten waarvan de myeloomcellen resistent zijn tegen immunomodulatoire middelen, proteasoomremmers, en monoclonale CD38-antistoffen, hebben een zeer beperkte levensverwachting van slechts 5,6 maanden. Dit gegeven onderstreept de noodzaak voor nieuwe en meer effectieve therapieën. Het translationele onderzoek beschreven in dit proefschrift richt zich op het remmen van signaleringsroutes die belangrijk zijn voor de overleving van myeloomcellen, voor behandeling-op-maat van patiënten met nieuw gediagnosticeerde of terugkerende resistente multipel myeloom.

## **Samenvatting van de belangrijkste resultaten**

**Hoofdstuk 2** bestaat uit een review artikel waarin de verschillende processen staan beschreven die een rol spelen bij de transformatie van een gezonde tot een maligne plasmacel. Multipel myeloom wordt gekenmerkt door grote genetische

heterogeniteit, ook al in de premaligne MGUS fase. Vaak voorkomende mutaties zijn extra kopieën van de oneven chromosomen 3, 5, 7, 9, 11, 15, 19, en 21; of één van de zes meest voorkomende chromosomale translocaties, waarbij een moleculaire activator van de antistofproductie voor een gen wordt geplaatst dat de celdeling bevordert. Gedurende de ontwikkeling van de ziekte ontstaan er vaak secundaire mutaties. Deze secundaire mutaties kunnen variëren van het verkrijgen of verliezen van complete of gedeeltes van chromosomen, extra translocaties, en verhoogde activiteit van signaleringsroutes die de overleving van de myeloomcellen stimuleren als gevolg van DNA mutaties of veranderde epigenetica. Daarnaast is ook de interactie tussen de myeloomcellen en de niche van belang. De cellen en componenten uit deze niche stimuleren het gedrag van de myeloomcellen middels uitgescheiden factoren en directe interacties. Op basis van deze grote heterogeniteit verwacht ik dat er niet één vaststaande therapie beschikbaar komen die geschikt is voor iedere patiënt. Toekomstige behandelingen zullen daarom steeds meer op maat gemaakt moeten worden, afhankelijk van de precieze kenmerken van de gemuteerde plasmacel.

**Hoofdstuk 3** bestaat uit een uitgebreid review waarin het belang van de Wnt signaleringsroute voor multiple myeloom wordt beschreven. De Wnt signaleringsroute is onder andere betrokken bij de regulering van celdeling, differentiatie, migratie, en de vernieuwing van stamcellen. Het belang van deze cascade is met name erkent in de ontwikkelingsbiologie en verschillende vormen van kanker, zoals colorectale kanker en leukemie. In dit review is te lezen dat verstoring van de Wnt signaleringsroute ook een centrale rol speelt in multipel myeloom pathogenese. De myeloomcellen scheiden verschillende Wnt remmers uit, waardoor de Wnt signaleringsbalans in het beenmerg verstoort raakt. Dit heeft als gevolg dat er meer botweefsel wordt afgebroken dan dat er nieuw botweefsel wordt aangemaakt, wat leidt tot de botlaesies die zo karakteristiek zijn voor multipel myeloom. Naast de extracellulaire verstoring van Wnt door de myeloomcellen, is er ook steeds meer bewijs dat de Wnt signaleringsroute abnormale activiteit vertoont intracellulair in de myeloomcellen, en dat dit bijdraagt aan de overleving van deze maligne cellen. Daarnaast is de Wnt signaleringsroute geassocieerd met een toename in adhesie-gemedieerde resistentie van myeloomcellen tegen verschillende therapeutische middelen. Op basis hiervan verwacht ik dat de Wnt signaleringsroute een mogelijk effectief doel zou zijn voor “targeted” therapie in multiple myeloom.

In **hoofdstuk 4** wordt de bovenstaande hypothese in het laboratorium getest. We gebruiken hiervoor onsterfelijk gemaakte myeloomcellijnen, en primaire myeloomcellen die zich in de beenmergafnames van patiënten met nieuw gediagnosticeerde ziekte bevinden. Tijdens onze experimenten observeerden

we dat extra toevoeging van Wnt ligand, om de Wnt signaleringsroute te stimuleren, de overleving van primaire myeloomcellen verbeterd, als deze in de controles over verloop van tijd afneemt. Het behandelen van de cellen met een combinatie van tankyrase-remmer en porcupine-remmer blokkeerde de Wnt signaleringsroute in myeloomcellijnen, en zorgde voor een afname van overleving van primaire myeloomcellen. Analyse van het transcriptoom van deze behandelde myeloomcellen, door middel van sequenzen, leerde ons welk mechanisme hieraan ten grondslag ligt: afname van een stress-signaleringsroute die normalerwijs actief wordt bij grote hoeveelheden ongevouwen of verkeerd gevouwen eiwit. Deze stress-signaleringsroute is in gezonde en maligne plasmacellen van groot belang, om te kunnen omgaan met de hoge productie van antistoffen. Op basis van deze resultaten verwacht ik dat Wnt blokkering door de tankyrase- en porcupine-remmers goed gecombineerd kan worden met andere middelen die deze specifieke stress-signaleringsroute nog verder afremmen. Onder deze middelen vallen de proteasoomremmers, die nu al een vast onderdeel zijn van de combinatietherapieën voor multipel myeloom.

In **hoofdstuk 5** ga ik nader in op de remming van cellulaire signaleringcascades die de overleving van myeloomcellen stimuleren. Deze remming kan specifiek plaatsvinden door middel van de "targeted" remmers, maar deze signaleringsroutes kunnen ook worden geblokkeerd als onderdeel van het werkingsmechanisme van standaardtherapieën. Het artikel begint met een experiment waarbij we combinaties van nieuwe middelen en standaardmiddelen hebben beoordeeld op het vermogen om de overleving van myeloomcellijnen te verminderen. Onze analyse laat zien dat de combinatie van de corticosteroïde dexamethason met de MCL-1 remmer S63845 het meest succesvol was. Individueel hebben deze middelen een beperkt effect, maar gecombineerd is het effect vele malen groter. Dit versterkende effect wordt aangeduid als synergie. Van de MCL-1 remmer S63845 is bekend dat het apoptose, ofwel geprogrammeerde zelfdoding van cellen, stimuleert. Het onderliggende mechanisme van de synergie tussen S63845 en dexamethason werd duidelijk tijdens de vervollexperimenten. In myeloomcellijnen observeerden we dat dexamethason de mTORC1/P70S6K signaleringsroute blokkeert die normaal bijdraagt aan de overleving van myeloomcellen. Deze mTORC1/P70S6K signaleringsroute kan ook specifiek worden geblokkeerd met een "targeted small-molecule" remmer van het P70S6K1 kinase, genaamd PF-4708671. Wanneer we de synergie vergeleken tussen de dexamethason en S63845 combinatie, en de meer specifieke PF-4708671 en S63845 combinatie, observeerden we dat de specifieke PF-4708671 en S63845 combinatie zelfs effectiever was in het induceren van celdood van primaire myeloomcellen. De potentiële vervanging van dexamethason door PF-4708671, in



deze combinatietherapie met S63845, is mogelijk goed nieuws voor patiënten met multipel myeloom. Corticosteroiden geven door hun brede werkingsmechanisme vaak vele bijwerkingen, en een subgroep van de patiënten heeft te maken met resistentie tegen dexamethason.

In **hoofdstuk 6** richten we ons specifiek op de behandelopties voor patiënten waarbij de multipel myeloom terugkeert na eerstelijns totaal-therapie, welke bestaat uit inductietherapie, en een autologe stamceltransplantatie, gevolgd door onderhoudstherapie. In dit artikel gebruiken we een computermodel om de activiteit van bekende signaleringsroutes te kwantificeren, op verschillende tijdstippen tijdens de behandeling. We observeerden dat de activiteit van de NF $\kappa$ B signaleringsroute significant stijgt in myeloomcellen bij progressie van de ziekte na totaal-therapie, ongeacht de mate van activiteit voordat behandeling plaatsvond. Hoewel dit effect duidelijk zichtbaar was, observeerden we dat het onderliggende mechanisme dat verantwoordelijk is voor de toename in overleving van deze myeloomcellen meer divers was. Dit kon namelijk berusten op een toename in BCL-XL, BCL-2, of BFL-1. Hoewel deze drie eiwitten inderdaad geactiveerd kunnen worden door NF $\kappa$ B, en allen deel uitmaken van dezelfde familie van anti-apoptotische eiwitten, is deze informatie toch relevant. Voor het remmen van deze eiwitten zijn namelijk verschillende “targeted small-molecule” remmers noodzakelijk. Mijn advies is daarom om de NF $\kappa$ B analyse altijd te combineren met het opstellen van een profiel voor BCL-XL, BCL-2, en BFL-1 eiwitexpressie of remming.

**Hoofdstuk 7** bevat de beschrijving van een specifiek onderzoek naar myeloomcellijnen die resistent zijn geworden tegen proteasoomremmers, welke vaak onderdeel uitmaken van de huidige combinatietherapieën. In onze experimenten observeerden we dat resistentie tegen proteasoomremmers gepaard gaat met resistentie tegen de pan PIM kinase remmer PIM447. De PIM kinases dragen bij aan de signaleringsroutes die overleving van myeloomcellen stimuleren, en zijn constitutief actief. Dit betekent dat de activiteit afhankelijk is van hun concentratie, en wordt gereguleerd door aanmaak en afbraak van het kinase eiwit. Aangezien voor de afbraak van PIM een functioneel proteasoom vereist is, verwacht ik dat beide resistentiemechanismen direct met elkaar verbonden zijn. Als onze data wordt bevestigd, dan zou dit betekenen dat patiënten met multipel myeloom dat resistent is voor proteasoomremmers, niet behandeld zouden moeten worden met PIM447. Dit is mogelijk goed nieuws voor patiënten met multipel myeloom dat wel gevoelig is voor proteasoomremmers, aangezien de effectiviteit van PIM447 in een fase I klinische studie is bepaald op een patiëntenpopulatie waarvan tenminste 34% resistent was tegen meerdere proteasoomremmers. Ik verwacht daarom dat de patiënten met multipel

myeloom dat wel gevoelig is voor proteasoomremmers een betere response na behandeling met PIM447 zullen hebben dan de gerapporteerde totale response van 8,9%, met een gemiddelde progressie-vrije overleving van 10,9 maanden bij de geadviseerde dosis.

In **hoofdstuk 8** worden tot slot de bovenstaande resultaten bediscussieerd en in een breder perspectief geplaatst. Concluderend zie ik verschillende mogelijkheden voor het remmen van signaleringsroutes die bijdragen aan de overleving van multipel myeloomcellen, met behulp van “targeted small-molecule” remmers. Dit geldt zowel voor nieuw gediagnosticeerde ziekte, als bij terugkeer van resistente multipel myeloom. Gezien de grote heterogeniteit van de ziekte verwacht ik dat deze behandelingen zullen plaatsvinden in op-maat-gemaakte therapieën

## DANKWOORD

Na het schrijven van dit dankwoord is de inhoud van mijn proefschrift (eindelijk) compleet. Iets waar ik ontzettend blij mee ben, en trots op ben! De totstandkoming van dit proefschrift was niet mogelijk geweest zonder de steun van een heel aantal mensen die direct of indirect aan dit promotiewerk hebben bijgedragen.

Ik begin graag met een hartelijk woord van dank aan mijn begeleidingsteam.

Geachte dr. Peperzak, beste Victor, ik ben blij dat ik als tweede promovenda jouw onderzoeksgroep mocht komen versterken in 2016. Ondanks dat onze achtergronden nogal verschillend waren, denk ik dat er een aantal mooie projecten tot stand zijn gekomen waarin apoptose en celsignalering zijn verenigd. Ik heb je interesse altijd enorm gewaardeerd. Zo werden er niet alleen laat in de avond nog foto's gedeeld van net gescande western blots of nieuwe microarray analyses, maar vergat je ook nooit te informeren hoe het met mij ging. Bedankt ook voor je oneindige optimisme, waarbij jij altijd weer interessante aanwijzingen of mooie conclusies zag in data die ik als onbruikbaar beschouwde. Ik denk dat ik tot ons beider blijdschap kan mededelen dat dit het laatste epos van mijn hand is om te lezen.

Geachte dr. Raymakers, beste Reinier, zonder jouw herhaaldelijke voorstel om het literatuuronderzoek van mijn masterscriptie voort te zetten als promotieonderzoek was dit proefschrift er vermoedelijk nooit gekomen. Bedankt voor je vertrouwen en steun in de afgelopen jaren. Met jouw aanwezigheid was ik er altijd van verzekerd dat mijn belangen werden behartigd. Ook veel dank voor je interesse in mijn projecten, het geven van een klinisch perspectief op de uitkomsten hiervan, en je altijd snelle feedback. Ik vermoed dat je menig treinrit van Nijmegen naar Utrecht bezig bent geweest om mijn teksten van commentaar te voorzien, zodat ik die de volgende ochtend om 8 uur weer in mijn inbox vond.

Geachte prof. dr. Minnema, beste Monique, bedankt dat jij in 2018 mijn promotiecommissie als promotor bent komen versterken. Ik bewonder hoe jij al je kennis, van het lab tot de kliniek, samen laat komen en het enthousiasme waarmee je dit overdraagt. Ik kon altijd rekenen op nieuwe ideeën en suggesties tijdens de werkbesprekingen, en kritische opmerkingen op mijn manuscripten om ook de klinische relevantie van de projecten te bewaken. Ik prijs mezelf gelukkig dat onze samenwerking na dit proefschrift nog niet stopt, en ik hoop ook in de toekomst nog veel van je te mogen blijven leren.

Geachte prof. dr. Maurice, beste Madelon, toen duidelijk werd dat (Wnt) signalering een belangrijke plaats in mijn promotieonderzoek zou gaan innemen, was het een

grote wens om ook jou als promotor toe te mogen voegen aan mijn commissie. Tijdens mijn masterstage heb ik je leren kennen als een gedreven onderzoeker die, ondanks een drukke agenda, altijd tijd had voor één-op-één begeleiding van iedere (PhD-)student. Bedankt dat ik ook de afgelopen jaren op jouw kennis en begeleiding mocht vertrouwen.

Ookeen hartelijk woord van dank aan de leden van mijn AIO begeleidingscommissie, prof. dr. Jürgen Kuball, dr. Stefan Nierkens, en dr. Nieke Vrisekoop, voor al jullie input tijdens onze jaarlijkse gesprekken en voor het bewaken van de focus en de praktische uitvoerbaarheid van dit promotieonderzoek.

Ik vond het een voorrecht om mijn promotieonderzoek binnen de Peperzak-groep uit te mogen voeren. Zowel voor inhoudelijke en praktische hulp, als voor de nodige gezelligheid en uitjes kon ik op jullie rekenen.

Laura, ik heb jou altijd beschouwd als het opperhoofd van de uitvoerende tak van de Peperzak-groep. Jouw organisatorische skills en technische kennis maakten het lab-leven vaak net iets gemakkelijker. Dank ook voor alle uren die je met mij heb doorgebracht bij het cel-sorten van weer een setje platen.

Marta, I consider myself lucky that you joined the group shortly after I started. You were a tremendous help with flow cytometry, from difficult compensations to excellent FlowJo skills. Thank you for all our late-afternoon lunches, and for being my roomie at the last real-life DHC.

Anne, toen ik als PhD student bij de Peperzak-groep startte kende ik je alleen van naam. Wat een opluchting toen bleek dat het zo goed klikte! Je bent werkelijk mijn steun en toeverlaat geweest tijdens deze 5 jaar. Voor praktische zaken, maar vooral ook om successen mee te vieren en teleurstellingen mee te verwerken. Ik ben blij dat onze vriendschap is blijven bestaan, ondanks dat we inmiddels allebei een andere baan zijn gestart. Bedankt dat je me als paranimf wilt bijstaan tijdens de verdediging van dit proefschrift.

Thomas, met jouw entree kwam er altijd gezelligheid in het lab. Hoe complex of lang experimenten ook waren, jij neuriede je overal doorheen. Dank voor al je hulp rondom Akt, en de uitwisseling van microscopie-gedachten.

Laura, toen jij op het Dex project startte kreeg ik niet alleen praktische hulp, maar ook een goede vriendin erbij. Fijn dat we samen zowel hoogte- als diepte punten kunnen delen. Ik bewonder je doorzettingsvermogen en fanatieke instelling, en ik weet zeker dat je je doelen gaat bereiken. Ik hoop maar dat het winnen van elk bordspel dat we spelen niet tot één van die doelen behoort.

Niels, van masterstudent zonder pipetteerervaring tot gewaardeerde PhD-collega met ambitieuze projecten. Ik ben blij dat je onder mijn supervisie de interesse in het doen van onderzoek niet bent verloren. Ik laat de afronding van het Wnt project bij jou achter, en heb er het volste vertrouwen in dat je ook dit manuscript tot een goed einde weet te brengen.

Patrick, misschien hoor je eigenlijk meer bij de Boes-groep dan bij de Peperzak-groep, maar toch mag je in dit rijtje niet ontbreken. Veel succes met het vervolg van je PhD, en bedankt voor je essentiële bijdrage aan ons Kubb-team. Gelukkig is jouw richtingsgevoel beter ontwikkeld dan dat van mij.

Saskia, dank voor jouw hulp op het Pim project tijdens je bachelorstage. Jij bent misschien wel de meest gedreven student die ik in deze tijd ben tegengekomen. Veel succes met het afronden van je master, en bij al je toekomstige plannen.

Daarnaast wil ik nog een aantal anderen bedanken voor de prettige samenwerking. Anja van de Stolpe, hartelijk dank voor de nauwe samenwerking op het "signal transduction pathway activity" model. Margot Jak, dank voor alle input tijdens de werkbesprekingen. Ingrid Jordens, hartelijk dank voor alle ondersteuning op het Wnt project. Dank aan alle medewerkers van de Flow faciliteit voor de FACS ondersteuning. Dank aan Corlinda ten Brink voor de hulp bij de imaging faciliteit. Kris Reedquist, Savithri Rangarajan and Almar Willekes, thank you for your help on the Pamstation experiments.

Gedurende mijn promotieonderzoek was kantoor "G.02.wie weet het nummer?" mijn home-away-from-home. A big thank you to all my office roommates. Inez, it was much fun sharing a desk, as well as the PhD experience, with you. I'm sorry for each time that you walked into me eating apples in the office, while I thought you were at the mice facility. Eline, bedankt dat je me op één van mijn eerste werkdagen mee op sleeptouw nam om koffie te gaan drinken, en dat je mijn bunkie wou zijn op de van Kinsbergen. Succes met de laatste loodjes! Anna, zal ik dit in het Nederlands, in English, oder auf Deutsch sagen? Ik bewonder hoe snel en vloeiend jij de Nederlandse taal onder de knie hebt gekregen. Ik vind nog steeds dat wij één van de beste pompoenen hebben gemaakt tijdens de PhD retreat. Kim, dank voor de vele gezellige uitwisselingen, van microscopieprotocollen tot recepten en muziek. Froso, Angelo, Patricia, en alle kamergenootjes in de back-office, thank you as well for the nice time and all the fun we had together during our PhD/CTI/dinner-outings.

Het CTI bestaat uit een grote groep van fijne mensen. Daarom wil ik alle collega's die ik hier niet met naam en toenaam heb genoemd ook hartelijk danken voor de samenwerking, praktische hulp, wetenschappelijk input, en de gezellige tijd.

Daarnaast wil ik ook graag mijn nieuwe collega's bedanken, Frank, team Q4 en team B5, voor de tijd die jullie mij hebben gegund om dit proefschrift af te maken, en jullie bemoedigende woorden tijdens deze "laatste loodjes".

Tijdens mijn promotieonderzoek kon ik gelukkig ook rekenen op de onuitputtelijke steun van het thuisfront.

Manon, onze vriendschap stamt nog uit de tijd van de box. En al zijn onze levens misschien nu zo verschillend, onze band is altijd hecht gebleven. Jij hebt mijn hele studieperiode gevolgd, met interesse en soms ook verbazing. Ik bewonder jouw onbevagenheid, het vermogen om je aan te passen en in te leven, maar ook je eigen keuzes te blijven maken. Bedankt dat je me ook als paranimf bij wilt staan tijdens de verdediging van dit proefschrift. Daarnaast wil ik graag Hilda, Jos, Kirsten en Anouk bedanken. Ik heb me altijd erg welkom gevoeld in jullie gezin.

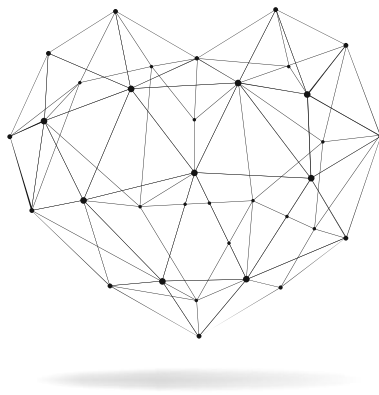
Wiebe, Claudia, Sharon, en de drie-eenheid Nadja, Niels en Matthijs. Samen als MLO'ers doorstromen naar het HLO scheidt een band. Dank voor alle gezelligheid, tijdens en buiten de colleges om, en de vele feesten & partijen, ook samen met Bas en Nima.

Ans en Edwin, Vincent, Sjoerd en Esther, Silas en Suzanne, en de nieuwe generatie: Luka, Noah, Annabel, Samuel en Jonathan. Met z'n allen bij elkaar staat altijd garant voor chaos en gezelligheid. Bedankt dat jullie me hebben opgenomen in jullie familie. Ik hoop dat ik voldoende uit heb kunnen leggen wat ik nou hele dagen deed. Hierbij ook nog een naslagwerk voor in de boekenkast.

Pap en mam, jullie hebben me altijd gestimuleerd om het beste uit mezelf te halen. Hoeveel vervolgstudies ik ook wilde doen, jullie hadden altijd vertrouwen in mij en in een goede afloop. Bedankt voor de steun en ondersteuning in de afgelopen jaren. Qua wetenschappelijke titels houdt het hier wel even op, maar ik denk dat jullie trots zullen zijn.

Lieve Niek, ik ben ontzettend blij dat we zo snel een goede band hebben kunnen opbouwen. Ik hoop dat dit boekje je kan laten inzien dat je met doorzettingsvermogen meer kunt bereiken dan je van tevoren had kunnen bedenken. Maar vooral ook dat het belangrijk is om je eigen keuzes te maken, en je in te zetten voor een doel waar je in gelooft. Je zal blij zijn om te lezen dat, nu het af is, het werken in weekenden en tijdens feestdagen voorbij is. Ik ben trots op je, en kijk er naar uit om je tijdens je verdere ontwikkeling te mogen bijstaan.

En tot slot, lieve Guido, jouw bijdrage aan dit traject is groter dan je zelf ooit zal toegeven, en misschien wel groter dan je zelf beseft. Jij voelt altijd feilloos aan wanneer ik een duwtje in de rug nodig heb om door te zetten, of juist afleiding en ontspanning kan gebruiken om op te laden voor de volgende piek. Bedankt voor het vertrouwen en de rust die je me geeft, je luisterende oor voor mijn dromen en ideeën, je sterke armen om in te schuilen voor mijn zorgen, en het geduld dat je altijd weer op weet te brengen terwijl ik me op mijn volgende project stort. Samen zijn wij een sterk team, en ik kijk uit naar alle avonturen die ons nog te wachten staan. Ik zal proberen om dan niet altijd voor de moeilijkste weg of de hoogst haalbare doelen te kiezen, beloofd!



## CURRICULUM VITAE

Ingrid Spaan was born on 24 May 1990 in Doetinchem, the Netherlands. She finished her secondary education in 2006, at Brewinc College in Doetinchem (mavo - theoretische leerweg). In the same year, she started her training to become a research technician, with a specialization in biotechnology and technical microbiology, at ROC Rijn IJssel College in Arnhem and Nijmegen (MLO). For this, she did an 8-month internship in the Laboratory of Virology at Wageningen University & Research (WUR), under supervision of prof. dr. Monique van Oers, to optimize the baculovirus expression system for stable recombinant hemagglutinin1 expression for the production of influenza vaccines.

After her graduation in 2010, Ingrid moved to Utrecht to start a bachelor in life sciences, with a specialization in biomolecular research, at the University of Applied Sciences in Utrecht (HLO). This included an 8-month internship, which she did in the research group of dr. Johan de Rooij at the Hubrecht Institute in Utrecht, to study the effects of physical force induction on E-cadherin mediated cell-cell adherens junctions. The resulting bachelor thesis was nominated for the NVML Zilveren Vlam award, and Ingrid graduated *cum laude* in 2013.

In 2013, after obtaining her BAsc degree, Ingrid enrolled in the biomedical master program Cancer, Stem cells, and Developmental biology, at Utrecht University. As part of this program, she did a 9-month internship in the research group of prof. dr. Madelon Maurice at the University Medical Center (UMC) in Utrecht, to study the role of Axin1 missense mutations in tumorigenesis. After this, she moved to Germany, to do a 7-month internship in the research group of prof. dr. Peter Angel at the DKFZ German Cancer Research Center in Heidelberg. There, she focused on *in vitro* characterization of transformed neuronal stem cells that were isolated from a novel murine glioma model. In addition, Ingrid was a member of the master program student committee.

After obtaining her MSc degree in 2016, Ingrid joined the PhD program Infection & Immunity, and started her research at the Center for Translational Immunology at UMC Utrecht, under supervision of co-promoters dr. Victor Peperzak and dr. Reinier Raymakers, and promoters prof. dr. Monique Minnema and prof. dr. Madelon Maurice. There, she focused on the identification of active pro-survival pathways in hematological malignancies, with a particular emphasis on multiple myeloma, and investigated the potential to target these pathways in a personalized approach. The results of this research are described in this thesis.

Currently, Ingrid is working as a clinical trial coordinator and data manager at the hematology research team of the UMC Utrecht Cancer Center.



## LIST OF PUBLICATIONS

Ingrid Spaan, Laura M. Timmerman, Thomas Kimman, Anne Slomp, Marta Cuenca, Niels van Nieuwenhuijzen, Laura M. Moesbergen, Monique C. Minnema, Reinier A. Raymakers, and Victor Peperzak. Direct P70S6K1 inhibition to replace dexamethasone in synergistic combination with MCL-1 inhibition in multiple myeloma. *Blood Adv.* 2021; 5(12): 2593-2607

Ingrid Spaan, Anja van de Stolpe, Reinier A. Raymakers, and Victor Peperzak. Multiple myeloma relapse is associated with increased NFκB pathway activation and upregulation of the pro-survival BCL-2 protein BFL-1. *Cancers (Basel)*. 2021; 13(18): 4668-4683

Ingrid Spaan, Reinier A. Raymakers, Anja van de Stolpe, and Victor Peperzak. Wnt signaling in multiple myeloma: a central player in disease with therapeutic potential. *J Hematol Oncol.* 2018; 11(1): 67-85

Niels van Nieuwenhuijzen, Ingrid Spaan, Reinier A. Raymakers, and Victor Peperzak. From MGUS to multiple myeloma, a paradigm for clonal evolution of premalignant cells. *Cancer Res.* 2018; 78(10): 2449-2456

Barbara Costa, Tanja Eisemann, Jens Strelau, Ingrid Spaan, Andrey Korshunov, Hai-Kun Liu, Peter Bugert, Peter Angel, and Heike Peterziel. Intratumoral platelet aggregate formation in a murine preclinical glioma model depends on podoplanin expression on tumor cells. *Blood Adv.* 2019; 3(7): 1092-1102

### In preparation:

Ingrid Spaan, Niels van Nieuwenhuijzen, Madelon M. Maurice, Monique C. Minnema, Reinier A. Raymakers, and Victor Peperzak. Dual targeting of Wnt signaling promotes cell death of primary multiple myeloma cells by inhibition of the unfolded protein response pathway. *Submitted 2021*



